Solidification/Stabilization of harbor sediments using GGBS-based hydraulic binders

Tetiana Gutsalenko

Thèse de doctorat

NNT : 2020UPAST058

université PARIS-SACLAY

Solidification/Stabilisation des sédiments portuaires à l'aide des liants hydrauliques à base de laitier de haut-fourneau

Solidification/Stabilization of harbor sediments using GGBS-based hydraulic binders

Thèse de doctorat de l'université Paris-Saclay

École doctorale n°579 : sciences mécaniques et énergétiques, matériaux et géosciences (SMEMAG)
Spécialité de doctorat : Génie Civil
Unité de recherche : Université Paris-Saclay, ENS Paris-Saclay, CNRS, LMT - Laboratoire de Mécanique et Technologie, 91190, Gif-sur-Yvette, France
Référent : ENS Paris-Saclay

Thèse présentée et soutenue à Paris-Saclay, le 1 décembre 2020, par

Tetiana GUTSALENKO

Composition du Jury

Cécile QUANTIN Professeur des Universités, Université Paris-Saclay	Présidente et Examinatrice
Dimitri DENEELE Directeur de Recherche CNRS (DR2), Université Gustave Eiffel	Rapporteur
Guillaume MORIN Directeur de Recherche CNRS, Sorbonne Université	Rapporteur
David BULTEEL Professeur des Universités, IMT Lille Douai	Examinateur

Direction de la thèse

Mohend CHAOUCHE Dirceteur de Recherche CNRS (DR2), ENS Paris-Saclay	Directeur de thèse
Alexandra BOURDOT Maître de conférences, ENS Paris-Saclay	Co-encadrante de thèse

Remerciements

Voici donc la fin de plusieurs années de travail sur la thèse. Il y a un étrange sentiment de vide, de joie et d'anticipation de quelque chose de nouveau. Ne connaissant pas du tout le système du Doctorat en France, j'ai eu cette envie de travailler dans le domaine de la recherche. Ma nature aventurière m'a amené jusqu'ici. Le chemin a été difficile, mais très gratifiant. Je ne pensais pas qu'il était possible de comprendre autant de choses sur moi-même, de mûrir après tout, pendant une période relativement courte.

Je voudrais tout d'abord adresser toute ma gratitude au directeur de la thèse, Mohend Chaouche, Directeur de recherche CNRS, pour sa disponibilité, ses conseils scientifiques, pour m'avoir encouragée à aller au-delà de l'habituel.
Je tiens à exprimer toute ma reconnaissance à mes co-encadrantes, Aveline Darquennes, Professeure des Universités, puis Alexandra Bourdot, Maître de conférences. Je les remercie de m'avoir encadrée, aidée et d'avoir guidé mes réflexions. Alexandra, merci de m'avoir encouragée autant et d'avoir cru en moi jusqu'au bout de ce chemin.

J'adresse ma profonde reconnaissance à tous les membres du jury qui ont accepté de juger ce travail et m'ont autorisée à soutenir pendant la période de crise sanitaire. Je suis très reconnaissante envers Guillaume Morin et Dimitri Deneele, Directeurs de recherche CNRS, d'avoir accepté d'être rapporteurs et d'avoir apporté des remarques pertinentes sur mon travail. Je remercie également le Professeur David Bulteel d'avoir examiné ma thèse. Je suis très touchée par l'honneur que m'a fait la Professeure Cécile Quantin en acceptant d'être la présidente du jury.

J'exprime mes sincères remerciements au groupe ECOCEM qui a soutenu financièrement ce travail de recherche.
Je tiens à remercier spécialement Laurent Frouin, Directeur de recherche Ecocem, pour sa confiance qui m'a été accordée et m'a permis de bénéficier de financement pour mon travail de thèse. Merci d'avoir apporté vos connaissances, votre esprit créatif et visionnaire. Je suis ravie de continuer mon parcours au sein d'Ecocem.
J'adresse également mes remerciements à Peter Seymour, le manager du projet, pour sa contribution à ce travail, pour ses conseils, son aide, sa disponibilité et sa gentillesse. Je voudrais également remercier Claude Musikas de m'avoir guidée dans le monde de la chimie, je me souviendrai toujours de nos discussions scientifiques passionnantes et si utiles pour la recherche.
Je voudrais exprimer ma gratitude à Thomas Wattez, mon encadrant côté entreprise, toujours avec moi pour me guider dans mes réflexions, à m'encourager, à me donner de l'espoir. Je suis heureuse de pouvoir continuer à travailler avec Thomas sur des sujets innovants et prometteurs.

Pendant ces années de thèse, j'ai eu une énorme chance de collaborer avec différents laboratoires. Je tiens à remercier vivement Valérie Montouillout, chercheur au laboratoire CEMHTI CNRS, d'avoir partagé son expérience de la RMN du solide et d'avoir apporté des données supplémentaires originales et enrichissantes à ce travail.
Mes remerciements vont également au laboratoire METIS, plus particulièrement à Sylvie Derenne, Directrice de recherche CNRS, et Christelle Anquetil, Ingénieure de recherche. Je suis très reconnaissante envers le Professeur Gabriel Billon,

responsable de l'équipe physico-chimie de l'environnement au LASIR ainsi que Véronique Alaimo, technicienne en chimie et sciences physiques, qui ont contribué à alimenter ce travail avec des idées et méthodes originales ainsi que des conseils précieux.

Je remercie de tout mon cœur l'ensemble du personnel du LMT, chercheurs, techniciens, personnel administratif, qui ont contribué à l'accomplissement et la réalisation de ce travail. J'ai éprouvé beaucoup de plaisir à partager ces années de travail avec vous. Je remercie Rémi Legroux pour l'aide apportée pour mes essais expérimentaux et pour la bonne ambiance en salle physico-chimie. Mes remerciements vont également à Olivier Rateau pour sa disponibilité et son aide avec mes essais au DGC. Je remercie Marc Bonnet pour les heures qu'il m'a accordé en essais de MEB et DRX.

J'adresse un grand merci à l'ensemble des doctorants que j'ai eu le plaisir de rencontrer au sein du laboratoire et d'avoir partagé de belles discussions lors des pauses cafés. Merci Artur de m'avoir aidée et initiée aux essais expérimentaux pendant mon stage. Merci Erisa et Yasmine, mes collègues de bureau et mes chères amies, pour votre soutien, votre bonne humeur et pour tous les moments durs où vous avez su trouver les mots pour me redonner des forces et m'encourager. Yasmine, je ne trouve pas assez de mots pour exprimer tous mes sentiments envers toi, mais saches que je serai toujours là pour toi comme tu l'as été pour moi. Merci Matthew pour ton énergie positive, je te remercie également pour ta relecture de mon manuscrit! Heureuse de continuer mon chemin avec vous.

Merci Maria, ton apparition dans ma vie a changé beaucoup de choses, m'a montré mes fausses croyances et m'a donné des forces pour continuer ma route.

Finalement, merci à ma famille, je vous aime tant (maman, papa, mamie et Julie). Malgré la distance physique je sais que vous êtes toujours là pour moi, vous croyez en moi et me soutenez énormément. Merci à mes amis ukrainiens, vous êtes une telle force pour moi, j'espère vous voir plus souvent (Olya, Katya, Sofia, Lena, Anton, Vlad). Je me rends compte à quel point je suis chanceuse de rencontrer des amis loin de mon pays, merci Anya et Apo. Enfin, il n'y aura jamais assez de mots pour remercier Mika, sans qui je n'en serais pas là aujourd'hui. Merci pour ton amour, ton soutien, ta patience, pour tous les repas que tu m'as cuisiné tous ces jours, merci de m'avoir inspirée et motivée. Merci également à ta famille (Pascale, Christian, Claire) qui a cru en moi…

Contents

Introduction

Sediments contain a range of fine particles that settle at the bottom of a body of water. They principally contain clay, sand, silt, and other fractions such as organic matter (OM) from the decomposition of plants and living organisms. Sedimentation induces a gradual decrease in the depth of navigation channels. The accumulation of sediments in large ports, especially in their berthing and manoeuvring areas, requires frequent dredging. Therefore, large quantities of sediment must be managed for the maintenance of waterways and harbour activities.

Nowadays, human interventions impact the natural dynamic of sedimentation, considerably affecting ecosystems. With the rapid growth of industry worldwide, the annual accumulation of sediments has grown to hundreds of millions of cubic metres per year and is expected to increase in the coming years. Historically, dredged sediments were subjected to disposal at sea or simply relocated on land. Over the last few decades, regulation has become increasingly strict (OSPAR Convention, 2009), (London Protocol, 1996) concerning the disposal of sediments at sea or storage on land because of an increased number of polluted sites, incidents of contamination, and the scarcity of usable land (Suman Raj et al., 2005). Industrial and urban activities are responsible for the emission of hazardous chemicals to waterways due to the waste produced from mining, chemical industries, municipal sewage, agriculture, etc. Sediments are known to be a sink for different types of contaminants (toxic heavy metals (HM), TBT, PCB, PHC, mineral oils compounds, and organochlorins (Apitz, 2010)). The pollutants tend to accumulate on the sediment particles. The disturbance or resuspension of sediments presents a source of toxic compounds to the environment and a risk for marine ecosystems and human health. Today, contaminated dredged sediment is considered as a waste and is classified in the European List of Waste by the Commission Decision 2000/532/EC. In Europe approximately 100-200 million m^3/year of contaminated sediment can be produced and it requires an appropriate management strategy from international and local authorities and regulators (SedNet, European Sediment Network).

Various remediation technologies are available for polluted sediments including both in-situ and ex-situ methods. Ex-situ applications include thermal treatments, washing, etc. In-situ applications include different capping solutions, the use of sorbents, solidification/stabilization (S/S), and biotechnological approaches (Akcil et al., 2015).

The current study focuses on the use of the S/S remediation technology using cementitious materials for the treatment of genuine contaminated sediment. The S/S method was demonstrated to be a cost-effective solution to achieve the necessary engineering properties for the reuse of the treated materials and to encapsulate contaminants. The most common binding agents in S/S practices are Ordinary Portland Cement (OPC) and lime (Spence & Shi, 2005). However, nowadays there is

a strong demand for the sustainable management of waste materials. The production of OPC requires a high consumption of raw materials, energy, and moreover it emits 1 tonne of carbon dioxide for each manufactured tonne of Portland cement. In order to reduce the carbon footprint of clinker production, there is a growing body of research that recognises the importance of the use of materials with a considerably lower emission factor. The current study investigates the application of ground granulated blast furnace slag (GGBS) for the treatment of a contaminated sediment. GGBS is a by-product of pig iron production in a blast furnace: the liquid molten slag is cooled and turned into a granulated material presenting latent hydraulic properties. It consists of a depolymerised calcium alumina-silicates amorphous structure with some low-crystallinity phases from the mellite group (Walkley & Provis, 2019).

It is now well established by a variety of studies that GGBS significantly improves the sulfate and chloride resistance of concrete, shows a significant reduction in permeability through reducing pore size and increasing density, as well as increases the ultimate strength with the replacement of OPC with GGBS (Mahedi et al., 2018; Özbay et al., 2016; Shi & Qian, 2000; Thomas et al., 2012). Moreover, GGBS can incorporate and retain heavy metals in hydration products such as C-S-H and hydrotalcite. However, despite the use of GGBS as a major supplementary cementitious material for more than a century (Yuksel, 2018), and growing research interest in alkali-activated GGBS within the past decade, there is little published research on the application of GGBS-based formulations in the field of Solidification/Stabilization of contaminated sediments.

In order to assess the effectiveness of GGBS-based binding agents in the solidification of sediment and stabilization of contaminants, a sediment originating from the Dublin Port, Ireland was used in this study. The Dublin port is situated on the estuary of the River Liffey which crosses the city of Dublin and between the Great Wall and the North Bull Wall before entering Dublin Bay (Fig. 1). A capital dredging campaign is planned as a part of the Alexandra Basin Redevelopment (ABR) Project in the area to improve ship navigation (from -7,8 m to -10 m). Different types of works are planned within the Alexandra Basin such as the construction of new quay walls and structures. It is therefore proposed by port authorities to improve the engineering properties of the dredged material from the Alexandra Basin through S/S treatment in order to reuse it to fill and seal Graving Dock N2 and to an extent Alexandra Quay West.

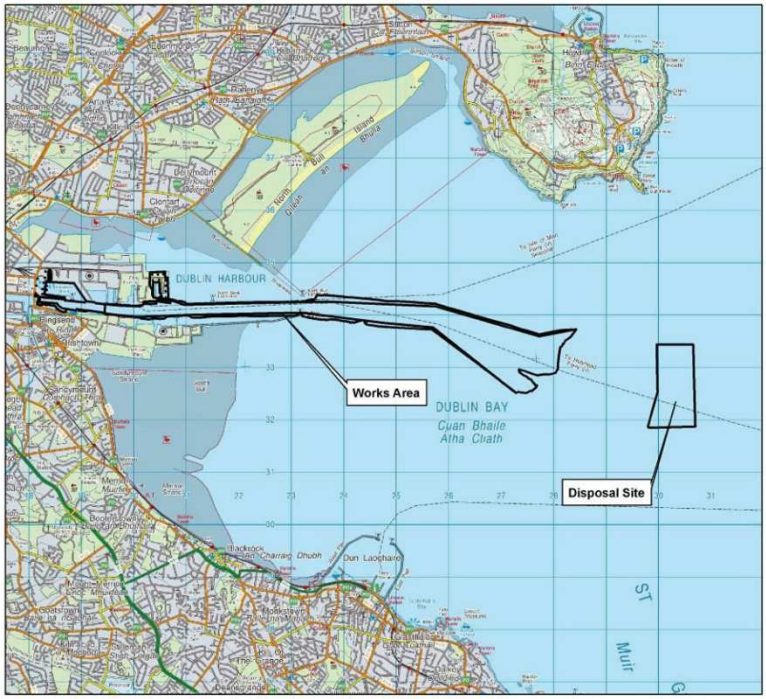

Fig. 1 Proposed works areas within the Alexandra Basin and Navigation Channel & Disposal Site *(www.housing.gov.ie)*

This study has several main objectives in order to valorise the contaminated sediment using S/S:

- to characterize the sediment matrix through the range of available techniques;
- to define an appropriate GGBS-based formulation, considering different types of activation, for the treatment of the Dublin Port sediment;
- to assess the engineering properties of the GGBS-based mixtures required for the project;
- to explore the mechanisms responsible for the mechanical performances of GGBS-treated sediments;
- to examine the mobility of trace elements from the treated sediment according to standardised leaching tests;
- to investigate the mechanisms of stabilization of heavy metals within GGBS-based formulations.

Outline of the dissertation

This dissertation is composed of five themed chapters.

This study first gives an overview of the relevance of the management of dredged material and focusses on European legislation. Then the sediment's geological origin and composition are discussed in general terms, revealing the complexity of the sediment matrix from the point of view of its potential treatment. Chapter I identifies the different toxic heavy metals occurring in sediments, their sources and chemical speciation, as well as factors affecting their mobility. The chapter reviews different remediation strategies for the treatment of contaminated sediments with particular focus on the Solidification/Stabilization method. The main properties of OPC and GGBS-based hydraulic binders are reviewed as well as their use as binding agents in recent S/S practices.

In Chapter II, the range of experimental tools applied in this study are presented to characterize the Dublin sediment and examine the material after S/S. The mineralogical composition and chemical properties of the Dublin sediment are compared to the sediment which originated from the Gothenburg Port, used in this study in order to investigate the effectiveness of binding agents applied to sediments having different natures. The total amount of major and trace elements is assessed through the total attack procedure. Standardized techniques used to estimate the effectiveness of binding agents are described in this chapter, and more sophisticated tools (XANES, NMR, etc.) are presented which were used to investigate the mechanisms of the S/S process using GGBS-based binders.

The third chapter is concerned with the solidification process of the treatment. First, different types of GGBS activation were applied in order to obtain the necessary strength. The choice of an appropriate binder for the Dublin sediment treatment was made based on the results of the strength evolution over 6 months of storage. Then the chosen GGBS-rich binder was compared to the OPC treatment through mineralogical, shrinkage, and microstructural analysis. In the sections that follow, the impact of different parameters on the compressive strength development was considered. Therefore, the next part of the chapter compares the compressive strength development of sediments having different origins. Further, the clay and organic fraction of the sediment were considered separately in order to get a deeper understanding of the mechanisms governing the solidification process. Finally, the role of the level of dispersion of the sediment and clay fabric on the evolution of compressive strength was examined with the help of rheological and zeta potential measurements.

After investigating the impact of major sediments constituents on the solidification

process of the sediment, the impact of heavy metals was examined. Chapter IV presents the study of the impact of Zn, Cu, Cd, and Ni on the early hydration kinetics of the Portland cement binder (OPC), ground granulated blast furnace slag binder (GGBS) activated by OPC, and the supersulfated cement (SSC). The heavy metals in the form of nitrate salts were used for the considered simplified model. Hydration heat evolution of the binders with and without HM was assessed through isothermal calorimetry. The main hydration products were analysed through XRD after 24 hours and 7 days. The NMR investigation was conducted at long term to assess the changes in the formation of amorphous products after the addition of HM.

Finally, the fifth chapter focuses on the effectiveness of GGBS-based binders to reduce the mobility of heavy metals after S/S treatment. The first part of the chapter provides the results of the batch leaching test evaluating the stability of the considered toxic elements within the matrix of the treated Dublin sediment. Moreover, an X-ray absorption spectroscopy (XAS) investigation was performed for the Dublin sediment and the sediment-binder system to observe changes in the speciation of Cu and Zn after treatment. The 4-step sequential extraction procedure was applied to the raw sediment and the sediment mixed with the OPC and GGBS-based binders to investigate the repartition of HM in different sediment fractions before and after S/S. A study on the speciation of Ni and Cd in the pure OPC and GGBS-rich binders was conducted using XAS.

Bibliography

Akcil, A., Erust, C., Ozdemiroglu, S., Fonti, V., & Beolchini, F. (2015). A review of approaches and techniques used in aquatic contaminated sediments: Metal removal and stabilization by chemical and biotechnological processes. *Journal of Cleaner Production*, *86*, 24–36. https://doi.org/10.1016/j.jclepro.2014.08.009

Apitz, S. E. (2010). Waste or resource? Classifying and scoring dredged material management strategies in terms of the waste hierarchy. *Journal of Soils and Sediments*, *10*(8), 1657–1668. https://doi.org/10.1007/s11368-010-0300-9

Couvidat, J., Benzaazoua, M., Chatain, V., & Bouzahzah, H. (2016). Environmental evaluation of dredged sediment submitted to a solidification stabilization process using hydraulic binders. *Environmental Science and Pollution Research*, *23*(17), 17142–17157. https://doi.org/10.1007/s11356-016-6869-9

London Protocol, 1996. (n.d.). *Convention on the Prevention of Marine Pollution by Dumping of Wastes and Other Matter*. Retrieved 10 August 2020, from http://www.imo.org/en/OurWork/Environment/LCLP/Pages/default.aspx

Mahedi, M., Cetin, B., & White, D. J. (2018). Performance Evaluation of Cement and Slag Stabilized Expansive Soils. *Transportation Research Record: Journal of the Transportation Research Board*, *2672*(52), 164–173. https://doi.org/10.1177/0361198118757439

OSPAR Convention. (2009). *Convention*. OSPAR Commission. https://www.ospar.org/convention

Özbay, E., Erdemir, M., & Durmuş, H. İ. (2016). Utilization and efficiency of ground granulated blast furnace slag on concrete properties – A review. *Construction and Building Materials*, *105*, 423–434. https://doi.org/10.1016/j.conbuildmat.2015.12.153

SedNet. (European Sediment Network). *SedNet | European Sediment Network*. https://sednet.org/, 08/07/2020

Shi, C., & Qian, J. (2000). High performance cementing materials from industrial slags—A review. *Resources, Conservation and Recycling*, *29*(3), 195–207. https://doi.org/10.1016/S0921-3449(99)00060-9

Spence & Shi. (2005). *Stabilization and Solidification of Hazardous, Radioactive, and Mixed Wastes*. CRC Press. https://www.routledge.com/Stabilization-and-Solidification-of-Hazardous-Radioactive-and-Mixed-Wastes/Spence-Shi/p/book/9780367393410

Suman Raj, D. S., Aparna, C., Rekha, P., Bindhu, V. H., & Anjaneyulu, Y. (2005). Stabilization and solidification technologies for the remediation of contaminated soils and sediments—An overview. *Land Contamination & Reclamation*, *13*(1), 23–48. https://doi.org/10.2462/09670513.645

Thomas, M. D. A., Hooton, R. D., Scott, A., & Zibara, H. (2012). The effect of supplementary cementitious materials on chloride binding in hardened cement paste. *Cement and Concrete Research*, *42*(1), 1–7. https://doi.org/10.1016/j.cemconres.2011.01.001

Walkley, B., & Provis, J. L. (2019). Solid-state nuclear magnetic resonance spectroscopy of cements. *Materials Today Advances*, *1*, 100007. https://doi.org/10.1016/j.mtadv.2019.100007

Yuksel, I. (2018). Blast-furnace slag. In *Waste and Supplementary Cementitious Materials in Concrete* (pp. 361–415). Elsevier. https://doi.org/10.1016/B978-0-08-102156-9.00012-2

Chapter I: Literature review

I.1 Introduction

The chapter aims to provide the bibliographic information necessary to understand the main mechanisms involved in the treatment of polluted marine sediments during the practice of Solidification/Stabilization (S/S). This literature review provides some important insights into the complex nature of multicomponent sediments as the main matrix for this study. The existing body of research on sediments suggests that their physicochemical characteristics are variable according to their origin, composition (such as clays minerals, organic matter, microbiota), etc., but they remain fairly stable in undisturbed environments.

Changes in the biophysicochemical parameters of sediments during dredging operations and the application of the S/S remediation method have been observed in several studies. The factors influencing the physicochemical parameters of sediments such as pH, redox potential, salinity, etc. have been reported in previous studies. Depending on the given environment, these factors may vary, which has a significant impact on the mobility of toxic trace elements.

This chapter provides an overview of the importance of dredging procedures and general information on the origin and composition of sediments, including the types of contaminants and their sources. Different types of remediation technologies are briefly presented in this chapter with special attention given to the S/S technique. Recent developments in the use of alternative binders for a range of applications have heightened the need to apply these materials as binding agents for S/S. The main properties of ordinary Portland cement and ground-granulated blast furnace slag as an alternative binder for the S/S method are reported in this chapter.

I.2 Management of harbor sediments

I.2.1 Defining dredging operations

The accumulation of sedimentary inorganic particles and organic matter arises from natural processes and anthropogenic activities. The latter may contribute considerably to the rate of accumulation of sediments and their contamination by organic and inorganic pollutants from industrial sources located near ports, stormwater runoff, effluents containing heavy metals, pesticides, oils, etc.

The term “dredging” describes the process of sediment disturbance by moving, extracting, transporting, or relocating the material from the bed of any waterway. This material is therefore specified as “dredged material” (DM). The dredging process can be divided between capital, maintenance, or remediation dredging.

The dredging procedure has a crucial importance for maintaining the operability and economical effectiveness of harbors and waterways. Therefore, dredging actions cover many purposes – the removal of surplus sediment resulting from the transit of boats, extension of existing harbors, construction of new navigation channels, etc.

(Dede, 2018). The dredged material presents direct or indirect impacts on the environment depending on its volume, physicochemical characteristics, toxicity, the dredging method and disposal, dredging procedure duration, etc.
The appropriate management of contaminated sediments becomes a big challenge for the port authorities because of an increase in polluted sites, and a range of complex political, economic, and technological issues.

I.2.2 European management of sediments. Legislation.

The total amount of dredged material in Europe can be estimated to be between 100 to 200 million m^3 per year (Subsed). In France, annual dredging reaches 40-50 million m^3 of dredged sediments per year (Hayet et al., 2017). The dredged material in France has been subjected to stricter regulation since 2000 due to the environmental control, therefore specific tests are carried out regularly on the material after dredging. In Ireland, the volumes of dredged materials are relatively small compared to other European countries, around 0.64 million dry tonnes per year (Harrington et al., 2013). However, the dredging procedure is indispensable from the economical point of view – Irish ports and harbors regulate 99% of Ireland's imports and exports by volume.
Regarding the international regulation of dredging activities, they are maintained by three legal documents:

- **The Convention for the Protection of the Marine Environment of the North-East Atlantic (OSPAR), 1992.** One of the main purposes of this convention, including its ecosystem approach, is described as follows: "the comprehensive integrated management of human activities based on the best available scientific knowledge about the ecosystem and its dynamics, in order to identify and take action on influences which are critical to the health of marine ecosystems, thereby achieving sustainable use of ecosystem goods and services and maintenance of ecosystem integrity" (*OSPAR Commission | Protecting and conserving the North-East Atlantic and its resources*, s. d.). In 2009 OSPAR published new guidelines for dredged sediments characterization and management.
- **The London Protocol, 1996** (updated London Convention - one of the first conventions that preserves the marine environment from anthropogenic activities). This protocol aimed to control and prevent marine pollution through regulating the dumping of waste material into the sea (adoption of "blacklist" approach – when dumping is prohibited due to environmental risks of hazardous material) (*Convention on the Prevention of Marine Pollution by Dumping of Wastes and Other Matter*, s. d.)
- **The Barcelona Convention for the Protection of the Marine Environment and the Coastal Region of the Mediterranean, 1995.** The main objective of the convention is to protect the marine environment through the sustainable

management of natural resources in order to reduce and control pollution (*Barcelona Convention - Marine - Environment - European Commission*, s. d.)

In terms of local regulation, different countries have their own relevant legislation and directives for the management of dredging procedures. Here is a brief list of some legislative framework in Ireland (Harrington et al., 2013), which is included considering that the sediment investigated in this study was dredged in the Dublin port:

- *Dredging/Dumping at Sea Legislation:*

- Foreshore Act (1933–2005) – manage dredged material from country owned foreshore, control its extraction and placement on the foreshore;
- Dumping at Sea Act (1996-2010) - under the responsibility of EPA (Environmental Protection Agency). This agency admits and allows the beneficial use of dredged materials as well as mandates the evaluation of alternatives to dumping at sea.

- *Beneficial Use/Treatment Legislation:*

- Waste Management Act (1996–2013) - under the responsibility of EPA. The license is applied to waste material >100,000 tonnes and is implemented to all land-based activities managing waste disposal;
- Article 5 of the EU Framework Directive 2008/98/EC on Waste - under the responsibility of EPA. This article permits to consider dredged material as by-product;
- EU Waste Acceptance Criteria for landfills 2003/33/EC - under the responsibility of EPA. These criteria summarize different values (e.g. leaching test) for landfill materials.

A) Regulation of dredged sediments in Ireland

The chemical composition of dredged material in Ireland is a decisive factor for the beneficial use of this material. The presence of heavy metals, organotin compounds (TBT, DBT), polychlorinated biphenyls (PCBs), polycyclic aromatic hydrocarbons (PAHs) should be quantified due to their high toxicity and risk of bioaccumulation. For this reason, based on the OSPAR requirements, Ireland established its own ‘Action List’ of contaminants with corresponding ‘Action Limits’ AL1 and AL2 (Table I.1). If the concentration of a listed contaminant is above the threshold values (AL2), they should be treated before further beneficial use.

Table I.1 Ireland Action List of contaminants with threshold values AL1 and AL2

Chemical Compound	Units (dry weight)	Lower level - AL1	Upper level - AL2
Heavy Metals			
Arsenic (As)	mg/kg	9	70
Cadmium (Cd)	mg/kg	0.7	4.2
Chromium (Cr)	mg/kg	120	370
Copper (Cu)	mg/kg	40	110
Lead (Pb)	mg/kg	60	218
Mercury (Hg)	mg/kg	0.2	0.7
Nickel (Ni)	mg/kg	21	60
Zinc (Zn)	mg/kg	160	410
Organic Contaminants			
PCB 28	µg/kg	1	180
PCB 52	µg/kg	1	180
PCB 101	µg/kg	1	180
PCB 118	µg/kg	1	180
PCB 138	µg/kg	1	180
PCB 153	µg/kg	1	180
PCB 180	µg/kg	1	180
Sum PCB 7	µg/kg	7	1260
Hexachlorcyclohexane	µg/kg	0.3	1
Hexachlorbenzene	µg/kg	0.3	1
TBT + DBT	µg/kg	0.1	0.5
Total Extractable Hydrocarbon	µg/kg	1000	-
PAH 16	µg/kg	4000	-

B) Regulation of dredged sediments in France

In France there are corresponding contamination thresholds named N1 (AL1) and N2 (AL2), that should be evaluated as a part of a complex physicochemical analysis before dredging operations begin. The *Circular No. 2000-62 of June 14, 2000* regulates the application of these threshold values – if the contamination level is <N1, the dredged material is allowed to be managed by disposal at sea; if the contaminants concentration is between N1 and N2, additional investigations are required (depends on the project risks); when contaminant concentrations exceed N2, land-based disposal is necessary (treatment or re-use of sediments) (Fig. I.1).

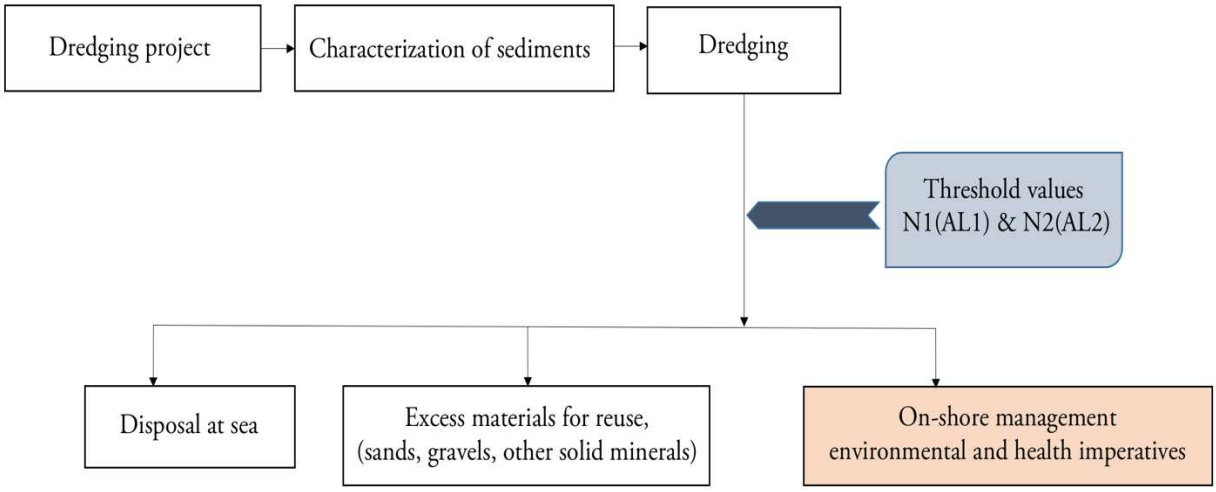

Fig. I.1 Management of dredged sediments in France, (Hayet et al., 2017)

The land-based disposal of dredged sediments is subject to *Decree No. 2002-540 of April 18, 2002*. First, it should be classified according to 'inert / non-hazardous / hazardous' material'. The sediment is considered as hazardous if it has at least one of the characteristics defined in the document (HP1-HP15, hazard criteria defined in Annex I of the Decree No. 2002-540). However, these criteria cannot always be considered appropriate in the case of sediment management in relation to the correct assessment of the sediment's ecotoxicity. Therefore, the Office of Geological and Mining Research of France proposed new ecotoxicological tests for continental and marine sediments (analysis of heavy metals, PCBs, PAHs, TBT according to N1 and N2 and then specific leaching tests of acute toxicity, chronic toxicity, etc.) (Hayet et al., 2017), (Kribi, 2005).
The *Decree of 12/12/2014* manages landscaping, coastal engineering and construction product applications of possible valorisations of sediments in France. These applications require a special examination of the physicochemical characteristics of a dredged material before and after treatment (e.g. leaching test according to (*NF EN 12457-2 - December 2002*, s. d.)). Laboratory investigations and field studies may be required.

C) Comparison to the regulation of some other European countries

Purposes fixed by international regulation of marine environment are common for all members (countries). At the same time, on the national level each country can proceed in its own way to achieve the sustainable management of dredging sediments, especially concerning waste and water legislation. For example, the threshold values of potential contaminants vary for some countries, based on local calculations and estimations of dangerousness. Table I.2 presents a comparison of threshold values for

dredged materials in different European countries. As can be seen from the table, Ireland and France present some of the most restrictive values for contaminant limits.

Table I.2 Threshold values of contaminants in different European countries, (Hayet et al., 2017)

	Allemagne		Belgique		Danemark		Espagne		Finlande		France		Irlande		RU		Norvège	
	N1	N2	N1	N2	N1	N2	N1	N2	N1	N2	N1	N2	N1	N2	N1	N2	N1	N2
Mercure	1	5	0,3	1,5	0,25	1	0,6	3	0,1	1	0,4	0,8	0,2	0,7	0,3	3	0,6	5
Cadmium	2,5	12,5	2,5	7	0,4	2,5	1	5	0,5	2,5	1,2	2,4	0,7	4,2	0,4	5	1	10
Chrome	150	750	60	220	50	270	200	1000	65	270	90	180	120	370	40	400	300	5 000
Cuivre	40	200	20	100	20	90	100	400	50	90	45	90	40	110	40	400	150	1 500
Plomb	100	500	70	350	40	200	120	600	40	200	100	200	60	218	50	500	120	1 500
Arsenic	30	150	20	100	20	60	80	200	15	60	25	50	9	70	20	100	80	1 000
Zinc	350	1750	160	500	130	500	500	3000	170	500	276	552	160	410	130	800	700	10 000
Nickel	50	250	70	280	30	60	100	400	45	60	37	74	21	60	20	200	130	1 500

Moreover, local legislation for the management of dredged materials which are classified as “hazardous waste” varies. In France there are no existing value-giving applications for hazardous materials compared for example to the Netherlands, where under certain conditions “hazardous” sediments can be valorised as a specific material based on the physicochemical characteristics of the dredged material and its final environmental impact after project realization. Furthermore, for some countries such as the Netherlands and Belgium, the most important contaminant values are the leached values rather than the total contaminant content in dredged sediments. This means that these countries are more focussed on the final material – if the contaminants are stable (leaching tests are required) in the material produced based on hazardous waste, this material can therefore change its status, meaning it is no longer classified as a hazardous material. (Hayet et al., 2017) and (Kribi, 2005) in their studies concluded that today in France there is a great demand and expectations concerning the relevant regulation of sediment valorisation (land managed sediments). Figure I.2 below shows a schematic representation of the French regulation of dredged material.

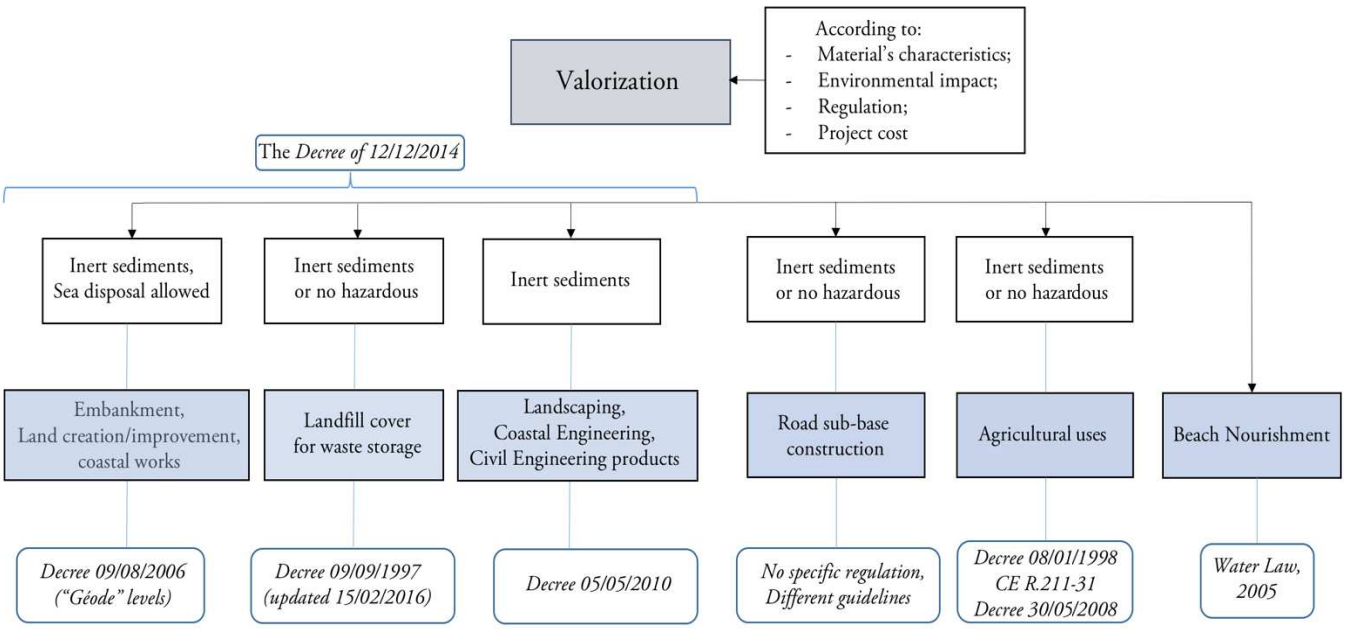

Fig. I.2 Sediments Land-based management in France (Regulation scope), (Hayet et al., 2017)

I.2.3 Existing projects and hierarchy for DM management

I.2.3.1 Projects for DM in France and Ireland

The most important dredging sites in France are Port of Nantes St-Nazaire (10 MM.m^3), Port of Bordeaux (7 MM.m^3), Port of Rouen (5 MM.m^3), Port of Le Havre (1,5 MM.m^3), Port of Dunkirk, and Port of Marseille. Different types of inland management of DM in France were carried out such as land improvement, filling material for forestry, landfill capping, and beach nourishment.
(Harrington et al., 2013) reported the different types of applications and practices performed to date in their guidance on the beneficial use of sediments in Ireland. Among them are beach nourishment projects, landfill cover (e.g. Dublin Royal Canal Dredging Project), coastal protection (e.g. breakwater constructions in Ireland), concrete manufacture (use as a raw material as aggregates for concrete manufacture, Caladh Mor), etc.

I.2.3.2 Hierarchy of dredged materials

(Apitz, 2010) in her article discusses the waste hierarchy of dredged materials (Fig. I.3) as an important factor to help decision makers adopt the most relevant waste treatment technology for sustainable management. She proposes the following definitions for the main classifications of the dredged materials hierarchy:

- *Pollution Prevention:* different strategies can be examined to prevent pollution in harbors – the reduction or refusal of dredging procedures as well as

controlling contaminant sources. Some approaches may help to avoid or reduce the dredging footprint, for example by using 2D or 3D site surveys in order to represent a more detailed contaminant distribution, to carry out more accurate and rigorous dredging procedures, or to reduce the volume of dredged material.

- *Re-use :* dredged material can be re-used depending on its contaminant concentration, therefore depending on the local or other level regulations. One of the main criteria is that sediments must stay in the same form as before treatment (e.g. sorting, cleaning). Dredged sediments may be relocated to maintain sediment balance in the environment without any risks, so this dredged material will be classified as re-used.

- *Recycling :* this strategy describes the use of dredged sediments in other forms than the original state – for example it can be used as a raw material for aggregate production, brick manufacturing, ceramics, etc. Recycling strategies are usually more expensive than disposal strategies, however contaminated sediments can present an attractive approach for construction materials production due to transport, energy, and resources economies.

- *Recovery :* the recovery strategy describes the beneficial use of contaminated or clean waste material if “biomass or energy is recovered” (e.g. materials that can be used as fuels).

- *Disposal :* this option is on the bottom of the waste hirarchy pyramid and is considered as the last resort for contaminated dredged material. Disposal of sediments may require additional monitoring due to possible release of contaminants over time as well as may be restricted by additional space needs. Among categories listed by (Apitz, 2010) are uncontrolled marine diposal (not for contaminated sediments), confined disposal facilities, disposal at sea with capping with clean sediment, disposal in special geotextile bags or in impermeable basins.

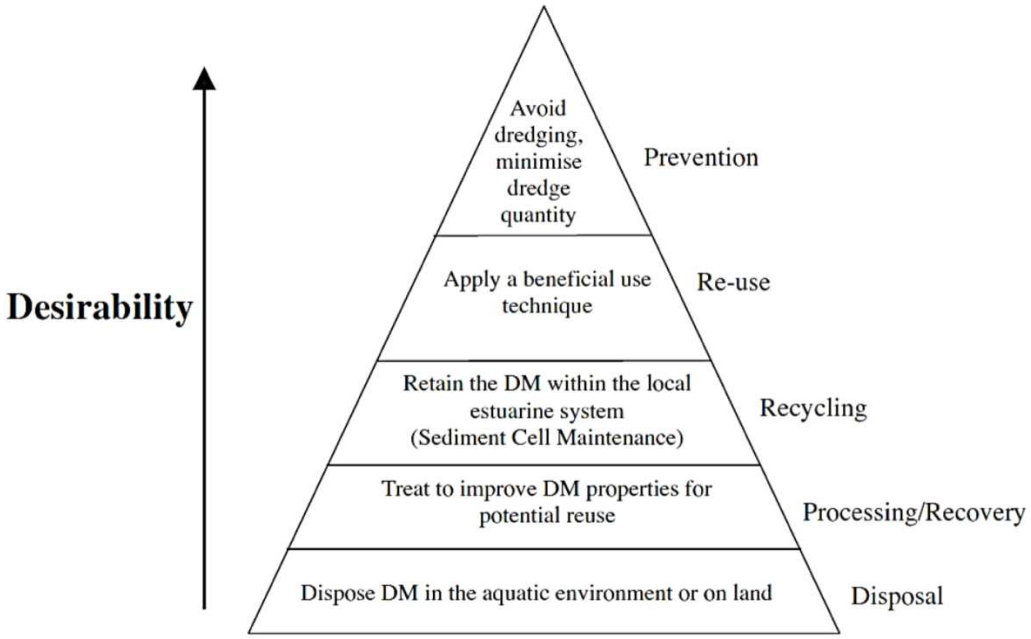

Fig. I.3 Hierarchy for Prioritising DM Management (adapted from (*Directive 2008/98/EC on waste (Waste Framework Directive) - Environment - European Commission*))

I.3 Origin and composition of sediments

I.3.1 Geological origin of sediments

The composition of sediments is highly dependent on the geology of the basin, topography, climate, and vegetation of a region. It is a highly dynamic and heterogeneous system (Schulz & Zabel, 2006). Regarding the geological provenance of sediments and their constituents' formation, there are four main groups that can be distinguished:

- *Lithogenous (terrigenous)* sediments that come from crushed and dissolved continental rocks (through chemical and physical weathering taking into account climatic changes, biological activity, etc.); the geographical location (relief, surface area, land-use) plays a considerable role in the particles transport and disposal; eolian transport plays a non-negligible role in the sediments' transport – the wind transports the fine fraction of sediments – clays and silts;
- *Biogenous sediment* – the part of sediment that consists mostly of calcareous, siliceous, or phosphatic minerals which were formed in the biosphere. Some compounds of iron, aluminium, manganese, calcite, Mg-Calcite, or aragonite were formed by different groups of marine organisms (plankton, benthos).
- *Hydrogenous (Authigenic) sediment* – represents the new formations by precipitation, alteration of particles in solution or within the sediment;
- *Anthropogenic sediments* are formed due to human activity – port activities and urban areas produce industrial (mining industry, chemical industry, construction

etc.), agricultural wastes containing the organic matter, pollutants from wastewater and sewage treatment.

I.3.2 Composition of sediments

A knowledge of a sediment's chemistry, meaning its organic and inorganic constituents, gives an understanding of the chemical reactions that may take place from the point of view of contamination of the environment. These reactions may alter the solubility, mobility, and bioavailability of pollutants in waters (Sparks, 2002).

A sediment's matrix consists of three main phases (Fig. I.4):

- Inorganic phase,
- Organic phase,
- Liquid phase.

Some amount of trapped air (hydrated gases) can be also found in sediments (Gamsonré, 2014).

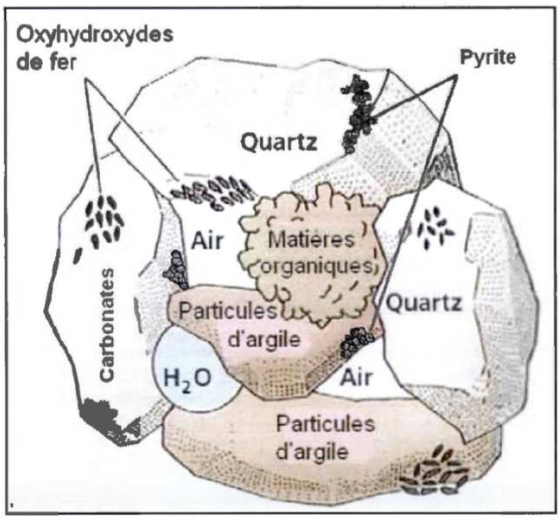

Fig. I.4 Main components of sediments (after (Cao et al., 2010))

I.3.2.1 Inorganic phase

The inorganic constituents of sediments possess different physical and chemical properties and can differ significantly in size – from clay's fine fraction (<2µm) to gravel (>2 mm) and rocks. (Sparks, 2002) distinguished primary and secondary minerals based on their formation – primary minerals were not transformed chemically since their deposition and crystallization from the liquid state (lava); these minerals are sands (particle diameters between 0.05 and 2 mm) and silts (particle diameters between 0.002 and 0.05 mm). When the primary mineral's structure was affected by weathering

(by dissolution), secondary minerals were formed. These minerals are commonly called aluminosilicates. They are clay minerals such as kaolinite, montmorillonite, oxides such as gibbsite, sulfurs, carbonate minerals, etc.

I.3.2.1.1 Clays

A large amount of chemical reactions are impacted by sediments' secondary minerals. Clay minerals present a complex structure of tetrahedral and octahedral sheets. The linkage of one octahedral and one tetrahedral sheet forms a 1:1 clay mineral with an ideal formula of $Si_4^{IV}Al_4^{VI}O_{10}(OH)_8$. A 2:1 clay mineral presents the structure when two tetrahedral sheets are coordinated to one octahedral sheet – the formula is $Si_8^{IV}Al_4^{VI}O_{20}(OH)_4$. In the interlayer space there are individual cations or cations octahedrally bound with hydroxyls (e.g. chlorites).

An isomorphous substitution phenomenon may take place during the formation of clay minerals. Depending on the cationic radius, different substitutions may occur. For example, in the octahedral sheet Fe^{2+}, Fe^{3+}, Mg^{2+}, Ni^{2+}, Zn^{2+}, or Cu^{2+} can substitute for Al^{3+}; or in the tetrahedral sheet Al^{3+} can substitute for Si^{4+} developing the charge imbalance compensated by cations (Sparks, 2002).

Figure I.5 shows the main structural schemes of secondary minerals. Here are some well-defined clay minerals and their properties:

1:1 Clay → Ex. Kaolinite. Its structure has a silica tetrahedral sheet bonded to an aluminium octahedral sheet assembled by hydrogen bonding; the ideal chemical formula is $Si_4^{IV}Al_4^{VI}O_{10}(OH)_8$; no interlayer bonding is possible for a 1:1 clay mineral.

2:1 Clay → Ex. Montmorillonite. The cations for the tetrahedral sheet are Si^{4+} and for the octahedral sheet the cations are Al^{3+}, Fe^{2+}, and Mg^{2+} with a chemical formula $M_{0.33}$, $H_2OAl_{1.67}(Fe^{2+}, Mg^{2+})_{0.33}\ Si_4O_{10}(OH)_2$ where M indicates a metal cation in the interlayer space between sheets, being either Na^+, Ca^{2+} or Mg^{2+} as the dominant cations. Montmorillonite clay is characterized by the presence of a big amount of water molecules between the sheets. This makes this type of clay mineral sensitive to swelling or shrinkage. Montmorillonite presents a high cation exchange capacity and high specific surface.

2:1 Clay → Ex. Illite. The chemical characteristics of illite are close to mica minerals and smectite minerals; one-fourth of the tetrahedral atoms are Al^{3+} and illite has more Si^{4+} and Mg^{2+} than muscovite. Therefore, the negative charge of the isomorphous substitution is balanced by the K^+ cations in the interlayer space, as well as by Ca^{2+}, Mg^{2+}, or NH_4^+, but less often. This type of clay is non-expanding and has a low CEC capacity (Sondi et al., 1996).

2:1:1 Clay → Ex. Chlorite. Chlorites are characterized by the non-expanding nature of 2:1 clays when the charge is compensated by brucite (Mg hydroxide) or gibbsite-like (Al hydroxide) minerals, that are often positively charged.

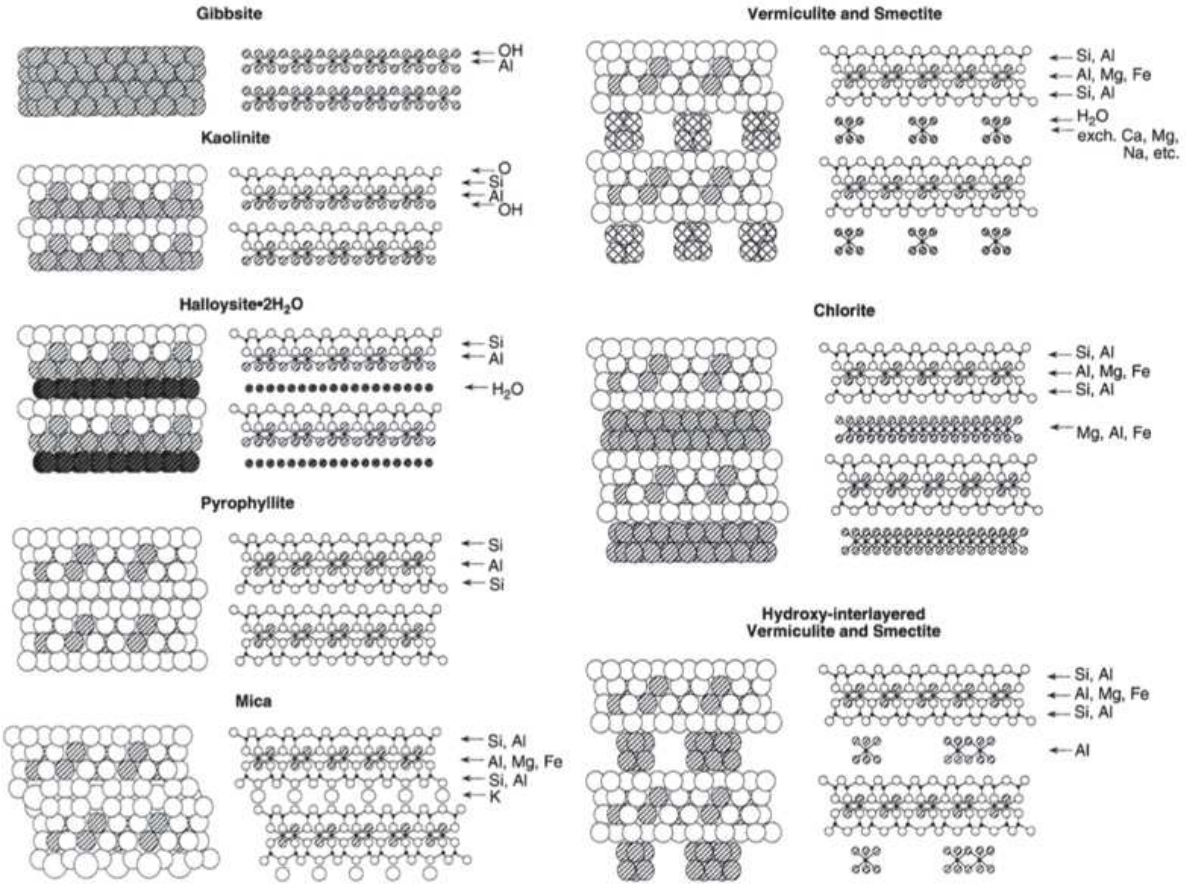

Fig. I.5 Structural scheme of soil minerals, (Schulz & Zabel, 2006)

I.3.2.1.2 Oxides, hydroxides, oxyhydroxides

Iron, aluminium, and manganese oxides play a crucial role in the chemistry of sediments regarding heavy metal mobility. Gibbsite ($Al(OH)_3$) and boehmite (γ-AlOOH) are the most common Al-oxides naturally present in soils and sediments. For Fe oxides, goethite (FeO(OH)) is one of the most prevalent and thermodynamically stable minerals and takes the form of needle-shaped crystals. The other common Fe oxide is hematite. Some heavy metal cations can be found in Fe oxides - Ni, Ti, Co, Cu, Zn or Fe can be isomorphically substituted by Al, Mn, and Cr (Sparks, 2002).

I.3.2.1.3 Carbonates

Carbonate minerals are much more soluble compared to siliceous minerals. The most often encountered carbonates in soils are calcite ($CaCO_3$) and magnesite ($MgCO_3$).

Due to their instability, they can be converted to dolomite ($CaMg(CO_3)_2$), ankerite ($(Ca,Fe,Mg)_2(CO3)_2$) or siderite ($FeCO_3$) (Sparks, 2002).
The solubility of carbonates partially controls the pH of the sediment's solution due to the buffer effect. Therefore, at some concentration of carbonates, the pH of the sediment can be slightly alkaline (~8) and some heavy metals may precipitate in the form of carbonates (hydroxycarbonates) – for example the zinc cation may precipitate in the form of $ZnCO_3$ or $Zn_5(OH)_6(CO3)_2$ species and copper in the form of malachite ($Cu_2(OH)_2CO_3$) or azurite ($Cu_3(OH)_2(CO_3)_2$) (Cazalet, 2012; Kribi, 2005).

I.3.2.1.4 Sulfurs

Sulfurs in sediments originate from the reduction process of sulfates ions in an anaerobic medium (Couvidat, 2016). The reduction reactions of sulfates in the sediment matrix are controlled biologically through the action of sulfate-reducing bacteria in the presence of reactive organic matter and without oxygen, (1) (Cazalet, 2012; Lesven, 2008):

$$2CH_2O_{(s)} + SO_4^{2-} \longrightarrow HS^- + 2HCO_3^- + H^+ \qquad (1)$$

The formation of sulfurs plays a key role in the mobility of some trace elements in sediments like Fe, Mn, Pb, Cd, Hg, Cu, As, and Zn. Depending on the chemical and microbiological environment within the sediment matrix, the different oxidation states for sulfur may occur - from sulfates (+VI) in the oxygenated water-sediment interface to sulfurs in the most reduced form (-II). According to (Lesven, 2008) the principal dissolved species of sulfur is HS^- in the natural environment. Subsequently, there are several reactions than can take place – the formation of organo-sulfur compounds, the precipitation of iron sulfide (pyrite) or the complexation of heavy metals, (2), (3) (Billon, 2001):

$$Fe^{2+} + HS^- \longrightarrow FeS + H^+ \qquad (2)$$
$$M^{2+} + HS^- \longrightarrow MS + H^+, \text{ (M-metals)} \qquad (3)$$

During the dredging and dewatering process, inorganic sulfurs may undergo oxidation and further sulfate formation. For example in the case of the reaction of pyrite with oxygen, the pH decreases due to the formation of sulfuric acid (4), (Gamsonré, 2014):

$$4FeS_2 + 14O_2 + 4H_2O \longrightarrow 4FeSO_4 + 4H_2SO_4 \qquad (4)$$

The formation of sulfuric acid can produce the reaction of this acid with carbonates. Consequently, gypsum formation occurs following reaction (5) (Gamsonré, 2014):

$$H_2SO_4 + CaCO_3 + 2H_2O \longrightarrow CaSO_4.2H_2O + H_2O + C_2O \qquad (5)$$

The further crystallization of gypsum may become an important issue for sediment recycling and the risks of swelling and expansion should be taken into account. In the case of the S/S method, an appropriate binder should be designed in order to avoid degradation over time due to volumetric changes.

I.3.2.2 Organic phase

The organic compounds of marine geochemistry present a complex environmental system that controls different important processes in sediments. The large structural variety of the organic compounds turns out to be an important challenge to be quantified and distinguished as different groups and components co-exist. Most of the molecules in organic matter (OM) form macromolecules, for example proteins and polysaccharides, that have to be disassembled into smaller structural units - amino acids and sugars (Emerson & Hedges, 2008).
The organic structure is built up of carbon-linked substructures of single molecules, such as hydrocarbons that have only carbon chains with hydrogen adjuncts and are considered as one of the simplest organic molecules.
Organic matter is divided into two main groups of substances: humic and non-humic. Non-humic material contains carbohydrates, proteins, peptides, amino acids, fats, waxes, and low-molecular-weight acids. These OM components are not very stable and can be easily transformed by microorganisms (Sparks, 2002). Humic substances (HS) are subdivided into humic acid (HA), fulvic acid (FA), and humin, which have different solubilities in different pH mediums. Fulvic acid and humic acid are soluble in alkaline media (characteristic of hydraulic binders) but not humin (Fig. I.6). Humic substances vary considerably in molecular weight as well as in size. According to (Piccolo, 1996; Stevenson, 1982) HS present as two- or three-dimensional macromolecules (Fig. I.7) that are interconnected and form a negatively charged surface from the ionization of acidic functional groups, for example carboxyls.

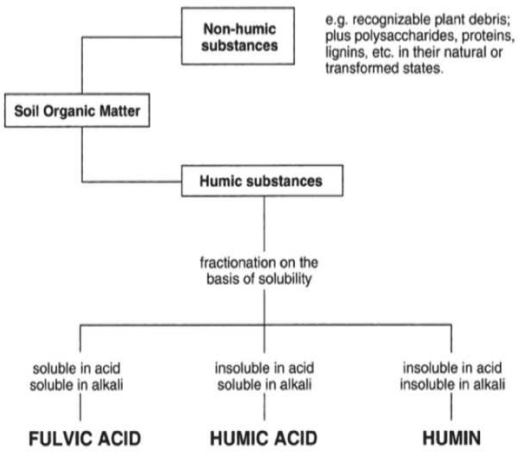

Fig. I.6 Fractionation of soil organic matter, (Sparks, 2002)

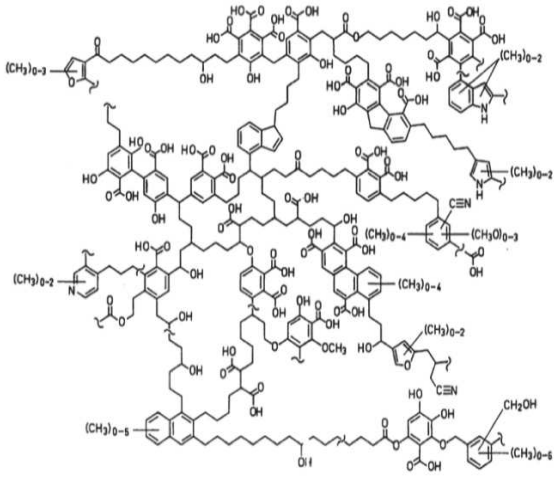

Fig. I.7 Two-dimensional HA model structure (Piccolo, 1996; Stevenson, 1982)

In geochemistry the “biomarkers” method is used to determine the properties and provenance of natural organic systems. Regarding organic carbon compounds, the main biomarkers are proteins, lipids and carbohydrates in living organisms, and other biopolymers such as lignin and tannin from plants (Emerson & Hedges, 2008).
Concerning the protein amino acids group, these compounds are some of the most abundant in marine biomass, having carboxyl (COOH), amino (CNH_2), hydrogen, and R groups. In the range of neutral pH, the amino acid group will present the ionized forms of COO^- and CNH^{3+}. The next most abundant biomarkers are carbohydrates with the general formula $(CH_2O)_n$. Carbon sugars are monomeric units of carbohydrates, combining in oligo- or polysaccharides. The next group of biomarkers consists of lipids, assembles hydrocarbons, fatty acids, sterols, and alkenones families. Lignins and tannins form the next group of biomarkers which represent the phenol biopolymer as products of vascular plants.
One of the types of marine organic matter is dissolved organic matter (DOM) which is a form of dissolved carbon in water. This phase contains mostly biopolymers and can be chemically or biologically degraded in the water column (Cazalet, 2012). As DOM presents a source of bioactive elements, it plays an important role in photochemical reactions, metals complexation, etc.

I.4 Contaminants in sediments and their sources

Toxic elements are widespread within coastal and estuarine sediments and make up part of the complex environmental chemistry of sediments nowadays. Heavy metals, polyaromatic hydrocarbons, organochlorines (such as PCBs), pesticides, etc. may present a considerable risk for aquatic life and human health. Due to industrialization processes developed through the last decades, the heavy metals level in sediments is more elevated than naturally occurring metals in sediment minerals.
Trace elements (<0.1% in natural materials) are considered as toxic if they exceed concentrations presenting risks for living organisms. They include trace and heavy metals, metalloids, micronutrients, and organic contaminants (Sparks, 2002). The source of these elements can originate from natural material as well as from anthropogenic activities – industrial discharges, mining activities, pesticides, agriculture, and harbor activities (e.g. boat painting).
Regarding the complexity and heterogeneity of sediment composition and chemistry, there is evidence of their strong impact on the bioavailability and fate of toxic elements in the environment. It can be found in the literature that the term “sink” is widely used to emphasize the great capacity of sediments to retain and stock metals. Pollutant mobility and bioavailability are strongly dependent on their chemical speciation. In this part of the literature review, some main pollutants and their chemical and mineral forms occurring in sediments will be considered. Unlike organic molecules, the main problem with inorganic contaminants is that they cannot be biodegraded, therefore heavy metals have a tendency to bioaccumulate (Couvidat, 2016). In this part of the review,

some toxic elements encountered in Dublin's sediment matrix are considered, specifically their sources and behaviour. The pe-pH (Pourbaix) diagrams were calculated at standard ambient temperature and pressure (25°C; 101.325 kPa).

I.4.1 Organic contaminants

The environmental risks related to organic contaminants increased sharply through the last decades. Anthropological activities generate a high rate of organic pollutants from different sources: industrial leaks and spills, improper application of pesticides, leaks from oil and chemical storage tanks, leaks from pipelines, accidents, spills during transportation, etc. (Snousy, 2017). The primary source of groundwater contamination is petroleum hydrocarbons from underground storage tanks. Different physical forms of organic contaminants are presented in Fig. I.8. Most organic molecules will be adsorbed to the soils and sediments surface due to their hydrophobic nature.

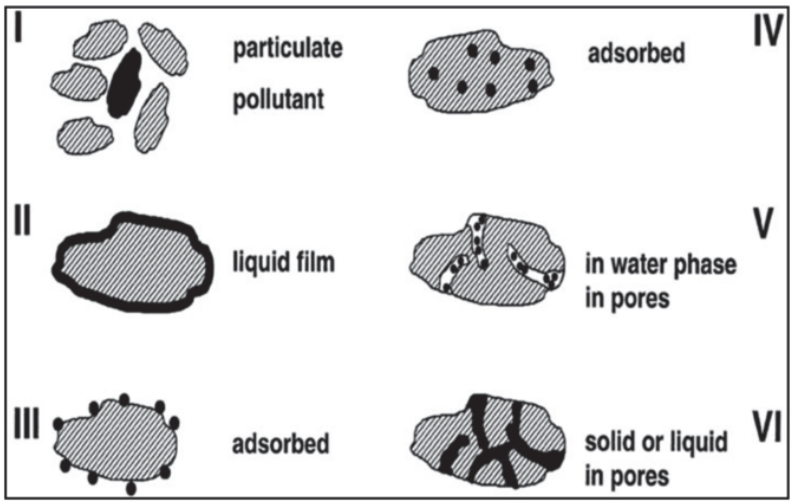

Fig. I.8 Different physical forms of organic pollutants in soil (Snousy, 2017)

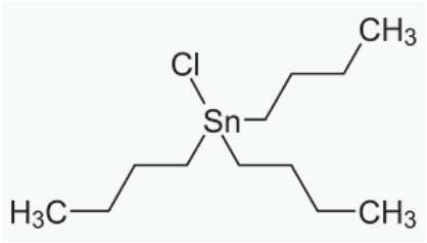

Fig. I.9 Chemical structure of TBT(Cl) molecule

In the aquatic medium, the most widespread organic contaminates are PAHs (polycyclic aromatic hydrocarbons), PCBs (polychlorinated biphenyls) and different organometallic compounds such as TBT (tributyltin chloride) (Fig. I.9). TBT compounds were accumulated in sediments due to their large use as anti-foulants until they were banned due to their high toxicity. They can induce disruption in the reproductive function in mammals, behave as hepatoxins, immunotoxins, neurotoxins, and

obesogens (Haydee & Dalma, 2017).

I.4.2 Inorganic contaminants

I.4.2.1 Zinc

Zinc is considered as an essential element for many metalloenzymes and it can be very toxic for plants at high concentrations. Zinc is found in sewage sludge at high concentrations. Its provenance is often associated with industrial waste and metal factories. In harbor areas, zinc is applied on the submerged parts of boats as an antifouling agent/paint (Alzieu, 1999).
Regarding the mineralogy of zinc in sediments, it is often combined with lead or copper, as well as cadmium (Burnol et al., 2006; Lesven, 2008). It can be readily adsorbed onto clay minerals, carbonites, or hydroxides which retards its desorption into the environment (Burnol et al., 2006). (Tessier, 1979) reported an important affinity of zinc to iron and manganese oxides according to the following order: FeO/MnOOH>carbonates> clays.
Zinc is found in nature in the oxidation state of +2. The most abundant mineral forms of zinc are zincite (ZnO), zinc carbonate (smithsonite, $ZnCO_3$), sphalerite, or zinc sulfide (ZnS), as well as silicates and mixed oxides of zinc and iron. Zinc sulfides are the main insoluble form of zinc precipitate that is formed in anaerobic conditions (Burnol et al., 2006). The different ionic species of zinc that can be found in soils are presented in Fig. I.10 (Burnol et al., 2006).

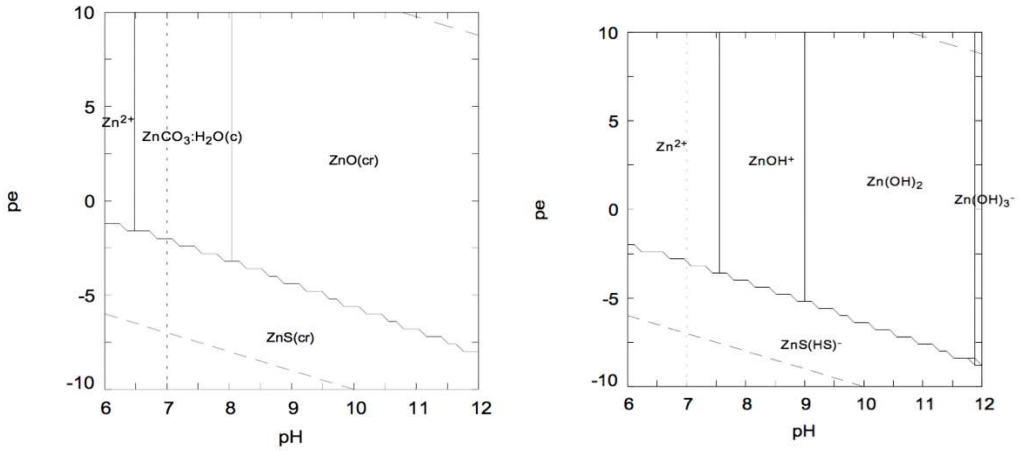

Fig. I.10 Zinc pe-pH diagram of solid (left) and aqueous phases

I.4.2.2 Nickel

Different types of nickel minerals are found in the geochemistry of soils and sediments. They can be found in the form of oxides, carbonates, and silicates and are particularly abundant in the form of sulfides (vaesite (NiS_2), millerite (NiS), and iron nickel sulfide (pentlandite, Fe,Ni_9S_8)) (Gamsonré, 2014). Nickel minerals are poorly soluble in

natural systems. Nickel salts can also occur in the natural environment and nickel chlorides, sulfates, and carbonates are more soluble than nickel oxide. The presence of nickel in the aquatic environment can be attributed to the natural phenomena of volcanism or forest fires, as well as to sources from human activities such as the metal industry and petroleum combustion (Alzieu, 1999), (Lesven, 2008).

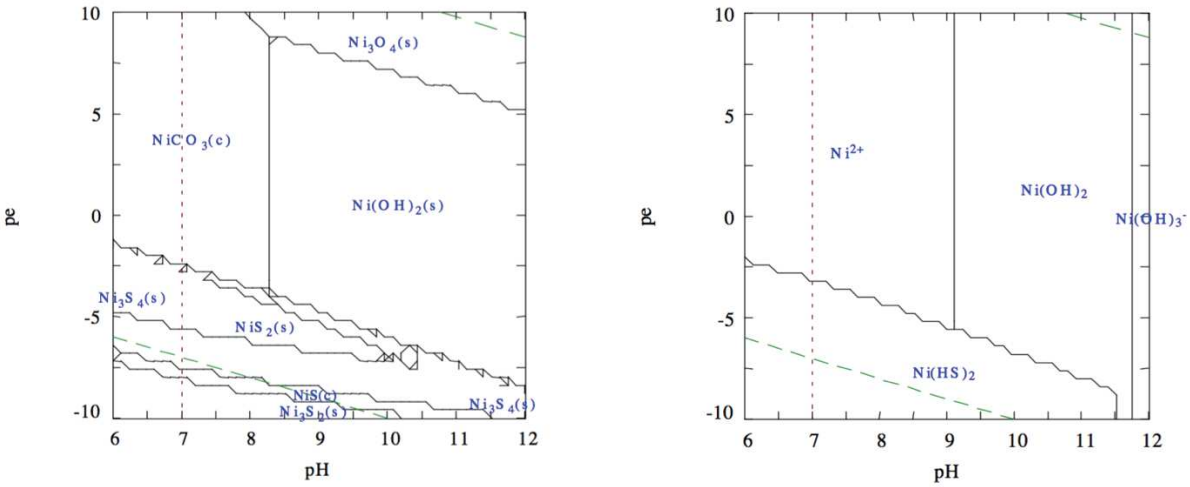

Fig. I.11 pe-pH diagram of predominance of solid nickel phase (left) and aqueous species of Ni (right)

Nickel has an important affinity to iron oxides via adsorption (e.g. goethite), kaolinite, and organic matter (Gamsonré, 2014). However, it is readily exchangeable because of the attached hydrated nickel species on the surfaces of inorganic or organic phases, governed by the electrostatic forces through hydrogen bonding (Rinklebe & Shaheen, 2017).

In aquatic media, nickel is present only in the oxidation state of +2. In anoxic sediments nickel will precipitate with HS^- to form nickel sulfides. In acidic or neutral conditions, the concentration of nickel is dependent on the solubility of solid carbonates (Fig. I.11).

I.4.2.3 Cadmium

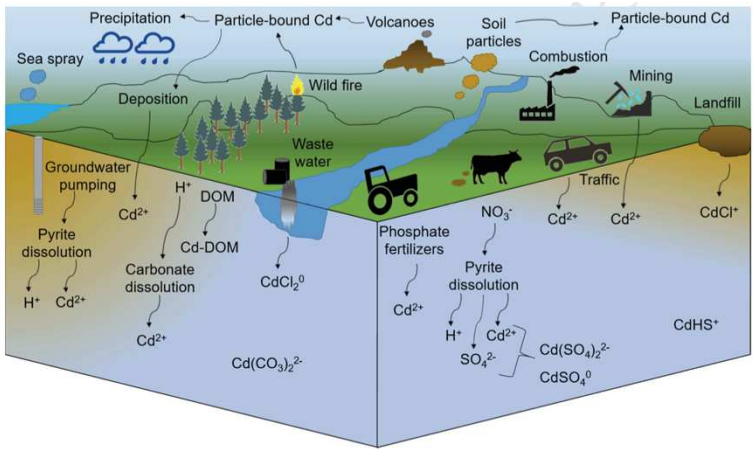

Fig. I.12 Origin of cadmium pollution in the environment

Cadmium is abundantly present in the environment and is both highly toxic and carcinogenic. (Kubier et al., 2019) reported in his review that cadmium is one of the most mobile toxic elements. It can easily replace calcium in minerals and consequently human bodies due to the similar ionic size and chemical behaviour. The anthropogenic sources of cadmium are mining, the metal industry, the petroleum industry, textiles, etc. (Fig. I.12).

Cadmium in nature is often associated with zinc and can substitute for Zn in sphalerite (ZnS) or smithsonite ($ZnCO_3$). Some other cations can also participate in isomorphous substitution with cadmium – Ca, Fe, Zn, and Pb (Kubier et al., 2019). In the anoxic sulfurs environment, cadmium can be present as the metal sulfide mineral greenockite (CdS). Adsorption is the main mechanism of cadmium immobilization/retention – it can be adsorbed onto the clay minerals, iron or manganese oxides, carbonates, or even associated with organic matter and sulfide complexes (Burnol et al., 2006). The most stable cadmium phase in reducible media is CdS.

When cadmium ions are present in oxidation conditions, the solubility will be controlled by cadmium carbonate ($CdCO_3$) at neutral pH, by sulfates/hydroxides at slightly more alkaline pH, and cadmium hydroxides will predominate in highly alkaline media (Fig. I.13). In the aquatic environment, the free ion Cd^{2+} is the most abundant form of the hydrolysable cation.

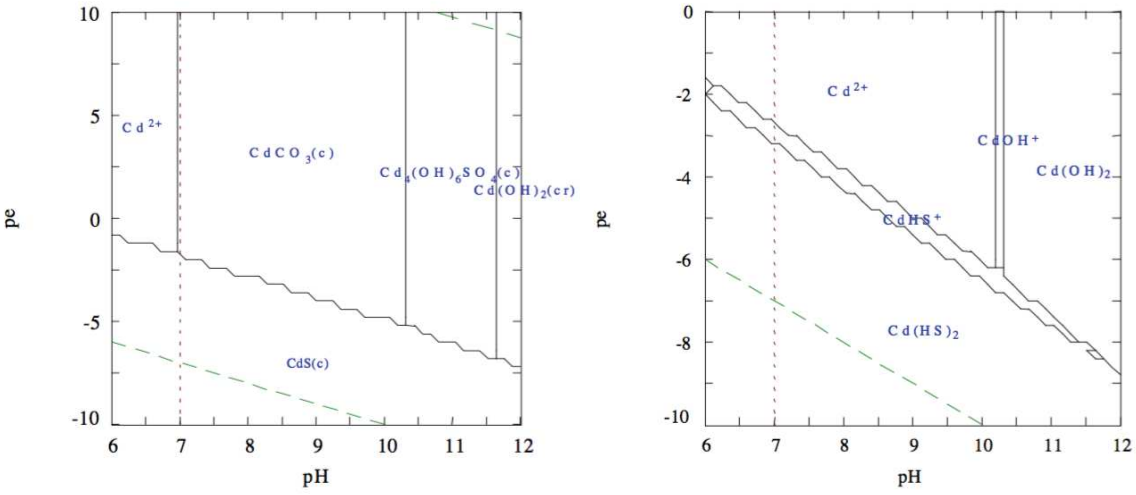

Fig. I.13 pe-pH diagram of predominance of solid cadmium phases (left) and Cd aqueous species of Cd (right)

I.4.2.4 Copper

According to the (OSPAR Commission, 2016), the main sources of copper in the environment are the mining industry (~18 million tonnes per year), chemical production (chlorides, sulfides, and oxides), and electronics production. In the marine environment copper originates from boat propellers or chemicals used for antifouling treatments. Once TBT compounds were forbidden as efficient antifouling agents due to their high toxicity, copper use in boat paints and biocides increased significantly. The main

copper minerals found in nature are chalcocite copper(I) sulfide (Cu_2S) and copper iron sulfide (chalcopyrite, $CuFeS_2$). Some oxide minerals such as cuprite (Cu_2O), tenorite (CuO), and carbonate minerals such as malachite ($Cu_2CO_3(OH)_2$) and azurite ($Cu_3(CO_3)_2(OH)_2$) can also be found (Cazalet, 2012).

Different sediment phases may adsorb copper in natural conditions – Cu ions have a great affinity for organic matter, iron and manganese oxides, clays, and organoclay complexes. In aquatic media the oxidation state of copper is +1 or +2 depending on the physicochemical conditions of the environment. When copper is in the oxidizing medium, the main phases controlling its availability are carbonites or oxides depending on the pH (Fig. I.15). Copper sulfides will precipitate in the reducing environment in the presence of sulfurs (Fig. I.14).

The toxicity of copper depends on its oxidation state and chemical form. According to (Alzieu, 1999) copper is more toxic in the oxidation state of +1. (Fairbrother et al., 2007) reported that for some marine species even 2μg/L of copper can be critical and, in some cases, lethal.

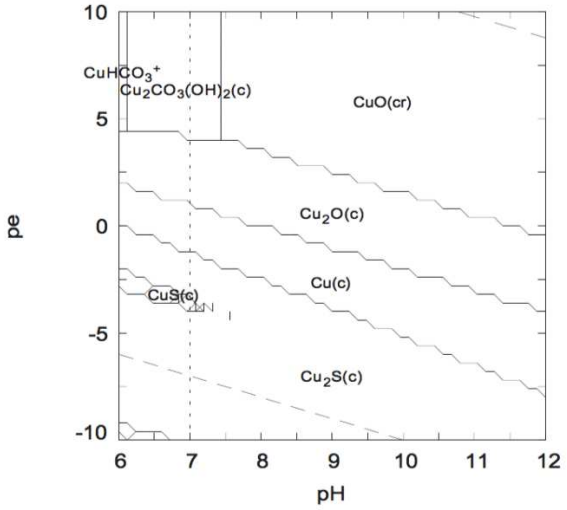

Fig. I.14 pe-pH diagram of predominance of solid phases of copper

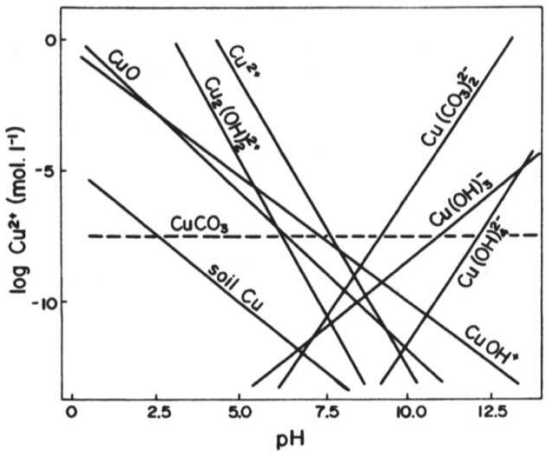

Fig. I.15 pH dependant copper species

I.4.2.5 Arsenic

Arsenic can be found in nature in different oxidation states (-3, 0, +3 and +5), meanwhile in the aquatic environment arsenic occurs mostly as oxyanions of trivalent arsenite (As(III)) or pentavalent arsenate (As(V)). Some organic forms can also be found in sediments when industrial pollution is high. Inorganic arsenic naturally occurs in groundwater; it is used in the processing of glass, pigments, textiles, paper, metal adhesives, wood preservatives, and ammunition (*Arsenic*). Inorganic arsenic compounds are considered to be highly toxic and carcinogenic.

More than 200 As minerals have been identified – among them elemental arsenic, arsenides, sulfides, oxides, arsenates and arsenites (Smedley, 2005). Arsenic in minerals is often found to be associated with other metals and one of the most abundant is arsenopyrite (FeAsS). Arsenic mobilization is controlled by its association with oxide minerals – many studies were conducted on the adsorption of arsenite and arsenate onto hydrous ferric oxides, aluminium and manganese oxides, and adsorption on clays minerals due to their oxide-like character of edges, e.g. kaolinite and montmorillonite (Burnol et al., 2006). The stabilization of As is a highly pH dependent process.

The reduction of iron oxides produced in anaerobic sediments is an important phenomenon for arsenic mobility - adsorbed or combined arsenic with hydrous iron oxides will be dissolved.

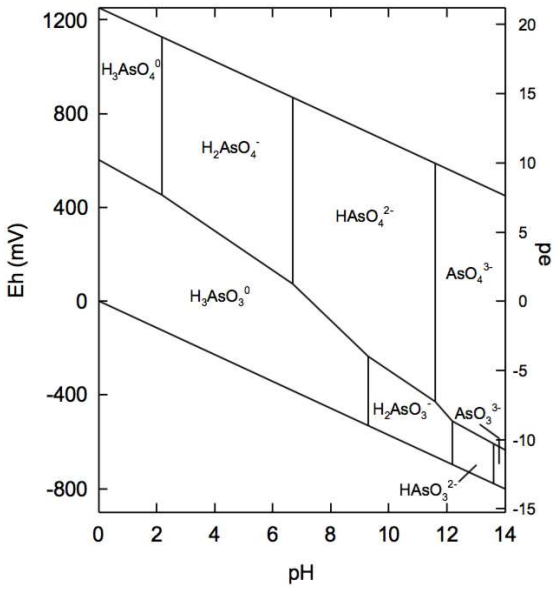

Fig. I.16 Eh-pH diagram of aqueous arsenic species in the system As–O_2–H_2O at 25°C

As speciation is highly impacted by the environmental conditions – pH and redox potential (Eh). As can be seen in Fig. I.16, the predominant species of As under oxidizing conditions and at high pH are $HAsO_4^{2-}$ and AsO_4^{3-}.

I.4.2.6 Chromium

Due to the ionic radii of trivalent chromium (Cr^{3+}), it can easily substitute for Al^{3+}, Fe^{3+}, Ti^{4+}, and Mg^{2+} in different minerals (e.g. peridotite, serpentinite, etc.) (Chrysochoou et al., 2016). Chromium (Cr) occurs in sediments from different anthropogenic activities, for example in wood preservation, cement production, leather treatment, and metal dipping. Two main chromium species are prevalent and stable in aquatic environments – trivalent Cr(III) and hexavalent Cr(VI). Cr(VI) pollution is an important issue due to its toxic and carcinogenic character. Moreover, hexavalent chromium is very mobile because it exists in the form of oxyanions $Cr_2O_7^{2-}$, $HCrO_4^-$, and CrO_4^{2-} and therefore the adsorption sites in sediments are limited (e.g. positive sites of iron and aluminium oxides at neutral pH) and they decrease with increasing pH (Alzieu, 1999; Billon, 2001; Gamsonré, 2014).

Fe(II), organic matter, bacteria, and HS^- may promote the reduction of Cr(VI) to Cr(III) in acidic environments. Conversely, the presence of manganese oxides as well as dissolved oxygen, nitrates, and sulfates favour the oxidation of Cr(III) to Cr(VI) (Gamsonré, 2014), (Burnol et al., 2006).

Trivalent chromium is less soluble and more stable due to the formation of hydroxyl complexes $Cr(OH)^{2+}$, $Cr(OH)_2^+$, $Cr(OH)_3$, and $Cr(OH)_4^-$ (Fig. I.17).

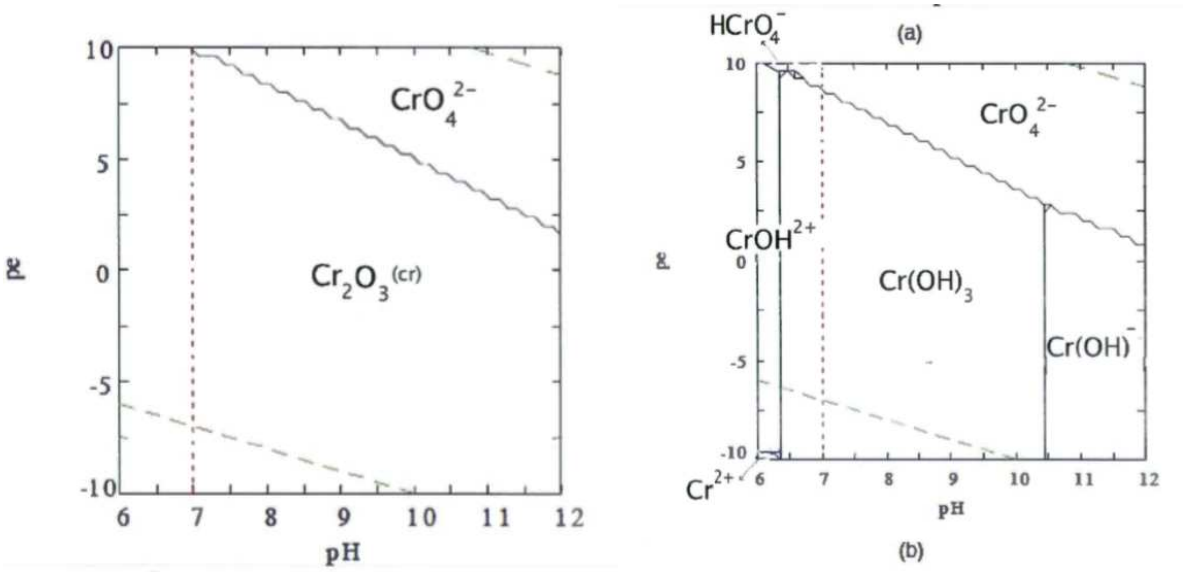

Fig. I.17 pH-potential diagram of predominance for chromium species

I.5 Factors affecting HM availability

Sediments present a heterogeneous system of solid fractions (minerals, e.g. clays, Fe, Mn and Al oxides), organic matter, and liquid phase, and thus the mobility of contaminants varies significantly depending on the sediment composition and its physicochemical properties.

Acting as a 'sink', sediments interact with contaminants according to different

mechanisms such as ion exchange, adsorption and desorption (Fig. I.18), complexation, precipitation and dissolution, oxidation-reduction, biological immobilization and mobilization, and plant uptake (Alamgir, 2016). The intermolecular interactions occurring between the solid and liquid phases in sediments can be summarized as follows (Kabata-Pendias & Pendias, 2001): van der Waals forces, ion-dipole forces, hydrophobic and hydrogen bonding, ion and ligand exchanges, chemisorption, etc.

According to (Kabata-Pendias & Pendias, 2001) the most important properties of soils influencing the release of trace elements and bioavailability are: E_h (redox potential)-pH profile, CEC (cation exchange capacity), salinity, organic matter type and content, water, temperature, and micro- and mezobiota activities. Each component of the sediment system can contribute to the accumulation of trace elements and reduce their mobility and toxicity for marine organisms. Consequently, when environmental changes or some sort of disturbance occurs in the system (e.g. dredging of harbor sediments), the remobilization of contaminants may occur as a result of desorption or chemical transformation of contaminants into more mobile and toxic forms (Eggleton & Thomas, 2004).

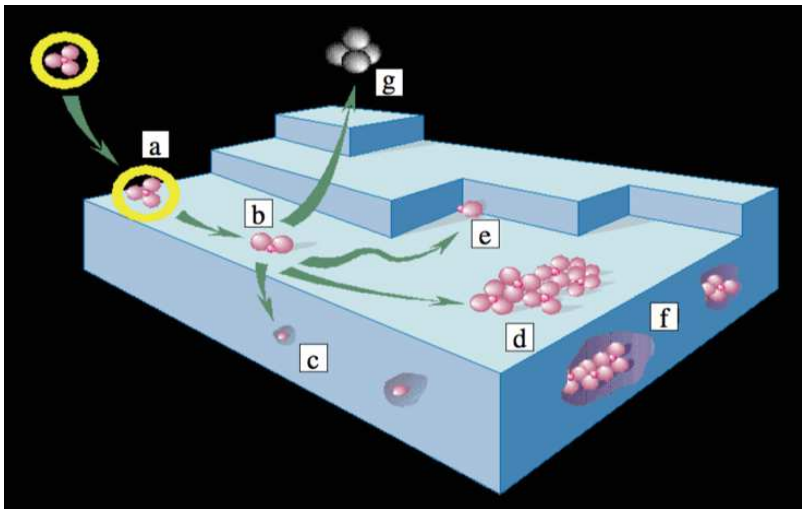

Fig. I.18 Various mechanisms of sorption of an ion at the mineral/water interface:
(a) adsorption of an ion via formation of an outer-sphere complex; (b) loss of hydration water and formation of an inner-sphere complex; (c) lattice diffusion and isomorphic substitution within the mineral lattice; (d) rapid lateral diffusion and formation either of a surface polymer, or adsorption on a ledge (which maximizes the number of bonds to the atom) (e). Upon particle growth, surface polymers end up embedded in the lattice structure (f); finally, the adsorbed ion can diffuse back in solution, either as a result of dynamic equilibrium or as a product of surface redox reactions (g); (Sparks, 2002).

I.5.1 Influence of pH

Previous research has demonstrated the impact of pH on the mobility of the inorganic contaminants in the sediment matrix. A sediment's pH is controlled by the biological activities and buffering capacities derived from the carbonate ion balance (CO_3^{2-} /HCO3$^-$..), exchangeable ions, clays, and oxy- hydroxides. The oxidation environment

can induce the transformation of sulfides into sulfates and a decrease in pH (Cazalet, 2012; Kribi, 2005).

The surfaces of sediment minerals react over different pH range by developing electrical charges at the surface. At acidic pH there are more H^+ ions that are available to saturate the metal vacant sites and therefore the mobility of trace elements may increase due to increased proton concentration (Alamgir, 2016). Typically, metal sorption by oxides surface increases with increasing pH.

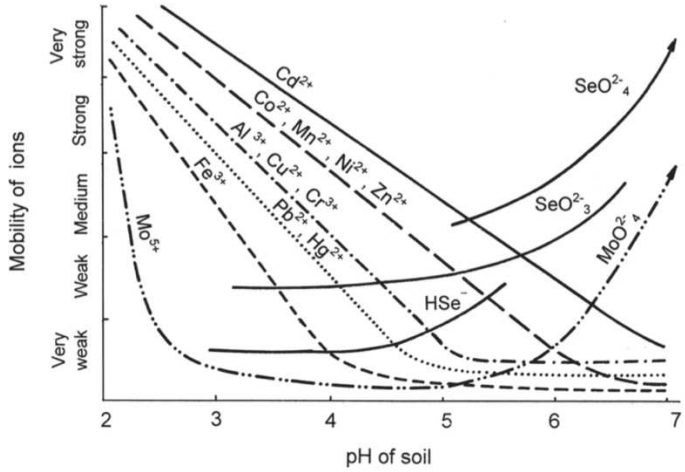

Fig. I.19 Schematic trends in the mobility of metals as influenced by soil pH.

Trace elements can be divided into two groups – the first includes cationic metals (Pb, Cu, Zn, Ni, Cd, Hg, Cr(III), and Co), and the second contains anionic metals (As, Se, Cr(VI), Mo, and B) (Fig. I.19). The metals of the first group occur at low pH as free cations, then at neutral pH they can precipitate as hydroxylated cations or uncharged species. Under alkaline conditions hydroxyl species are formed.

I.5.2 Oxidation-Reduction Potential

The crucial parameter that governs the processes affecting the mobility of heavy metals in sediments (dissolution, sorption, complexation, diffusion, binding by organic complexes etc.) is redox potential. Reduction / oxidation potential (E_h, measured in mV) provides information about the geochemical environment of sediments and soils and varies widely from aerated conditions (>400 mV) to the anaerobic environment (-300 mV).

Dredging of sediments induces changes in redox potential due to the transition from an anaerobic reducing medium to an oxidizing medium. These modifications in the chemical environment cause the oxidation of sulfides into sulfates and the oxidation of organic matter and therefore desorption and increased mobility of trace elements. It was demonstrated that heavy metal solubility, as a function of pH, increases in oxidizing media comparing to reducing media (Kribi, 2005; Tack et al., 1996).

I.5.3 Cation exchange capacity (CEC)

One of the predominant factors controlling heavy metal mobility is the cation exchange capacity (CEC) of sediment systems. CEC is expressed in centimoles per kg (cmol/kg) meaning the number of exchangeable cations that can adsorb onto a unit weight of soil (Alamgir, 2016). Typically, the specific surface of solid phases in a soil is directly related to its capacity to adsorb cations, therefore clay minerals and organic matter will control the CEC of the system (Kabata-Pendias & Pendias, 2001). The clayey fraction of sediments and soils exhibits higher CEC values than the sandy fraction. Moreover 2:1 clay structures have a larger capacity to adsorb cations than 1:1 clay structures. (Alamgir, 2016) presents that the following order for the CEC value of clay minerals (the higher the value, the more exchangeable sites) : montmorillonite, imogolite > vermiculite > illite, chlorite > halloysite > kaolinite.

Ca and Mg have an important effect on the adsorption of trace elements due to their high abundance in the soil matrix, and they may compete with each other. Some cations are more capable of replacing others due to their ionic charge and radius, their affinities for organic matter, and the surface of oxides.

According to (Sargent, 2015), soils with high CEC values arising from clays particles will undergo more important mechanical changes than those with low CEC. Figure I.20 (Sargent, 2015) indicates that the low CEC value is attributed to soils with low organic matter content, low clay content, and high sand content.

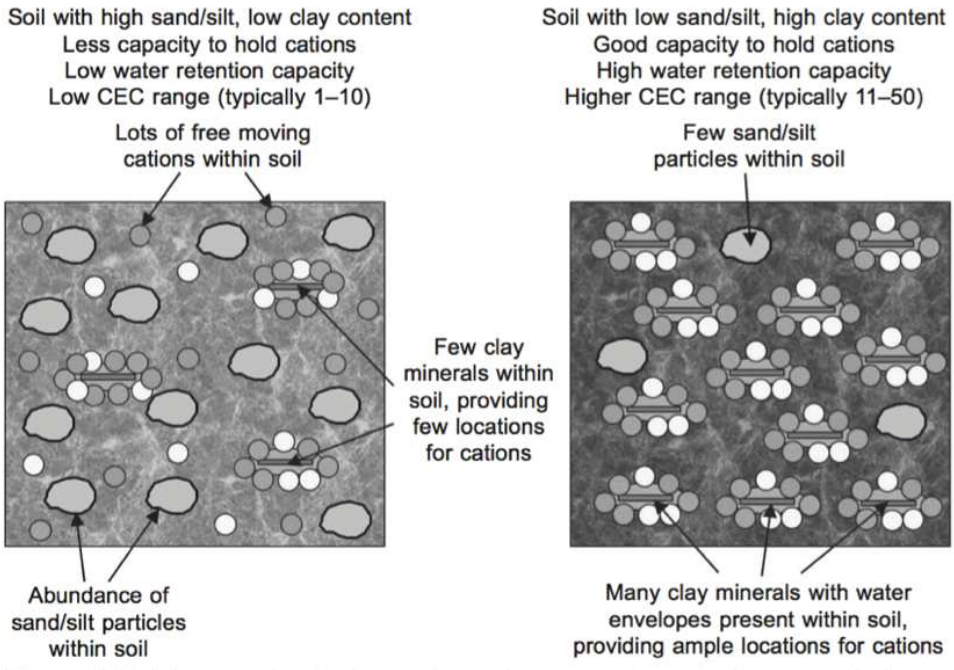

Fig. I.20 Variations of CEC according to the soil composition

The factors that can impact CEC are pH, salinity (ionic strength of a soil's solution), specific surface area, etc. (Robertson et al., 1999). The average CEC value of clays varies between 10-150 cmol(+)/kg, for organic matter 200-400 cmol(+)/kg, and for

sandy soils the CEC value is around 10 cmol(+)/kg (Botta et al., 2015).

I.5.4 Organic matter

The role of organic matter in the mobility of trace elements in sediment systems is extremely important. Humic substances in sediments participate in the sorption of heavy metals by forming strong complexes due to the large surface area of organic matter and its high reactivity arising from S-, O- and N- functional groups (Alamgir, 2016). Different types of interactions of heavy metals and organic substances in the marine environment are shown in Fig. I.21 – reactions with dissolved organic carbon and complexation reactions with suspended organic matter and bottom sediment. The complexation reaction can be described as follows (6), (Alamgir, 2016):

$$R - L^{1-} + M^{m+} \leftrightarrow R - L - M^{m-1} , \qquad (6)$$

where R - C-chain,
L - active group which actually binds,
M - metal,
m and 1 - valences of metal and ligand

There is a broad range of organic acid ligands in soils that may precipitate with heavy metals. Among them are oxalic, citric, formic, acetic, malic, succinic, malonic, maleic, lactic, aconitic, and fumeric acids (Alamgir, 2016). Many studies have focused on the specific role of the carboxyl and hydroxyl groups in the reactions between organic matter and trace elements.

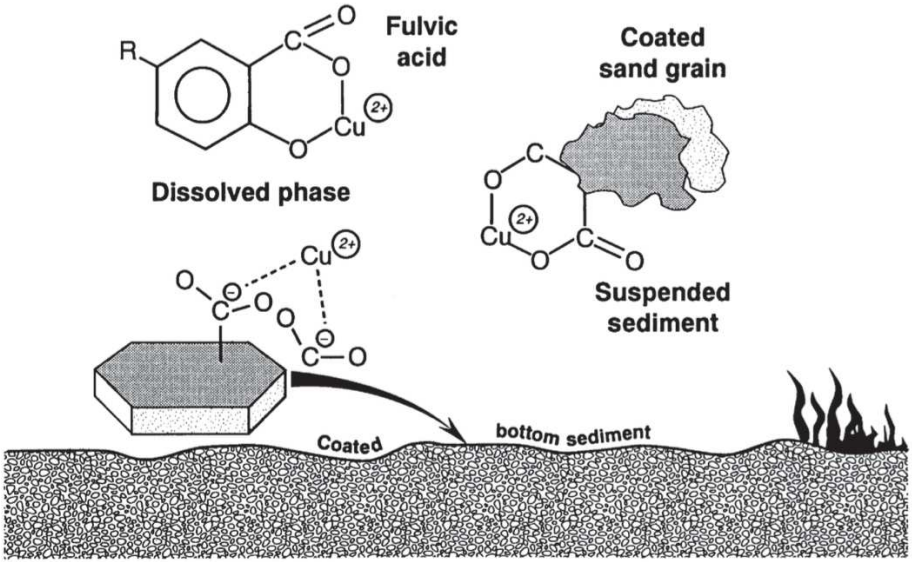

Fig. I.21 Complexation of metal ions by organic matter in suspended sediment, bottom sediment, colloidal, and dissolved phases

(Kabata-Pendias & Pendias, 2001) mentioned a correlation between pH and the binding capacity of the soil OM – with a pH increase from 3 to 7, the stability of heavy metals complexed by fulvic and humic OM fractions increased. Also some studies confirm that the binding capacity of fulvic acids are higher compared to humic acids. (Kodama & Schnitzer, 1980) presented the order of the affinity of some trace metal cations to form complexes with fulvic acids:

$$Fe = Cr = Al > Pb = Cu > Hg > Zn = Ni = Co = Cd = Mn$$

The amount of organic acid is important in the regulation of the mobility of heavy metals - when it is too low (<2%) the organic matter fraction cannot be considered as the main factor in controlling the sorption of trace elements, even if the metal sorption capacity on the organic matter fraction is significantly higher than that of the mineral fraction.

I.5.5 Salinity

Salinity is one of the important physicochemical parameters affecting heavy metal mobility and toxicity, especially in marine and estuarine environments where this parameter may vary considerably (Okoro & Fatoki, 2012). Major seawater ions such as Cl^- and SO_4^{2-} may compete with negatively charged particle surfaces and tend to stabilize heavy metals in solution. Several studies demonstrated the formation of chloro-complexes of cadmium, zinc, etc. (Mayer T. et al., 2008). Therefore, the mobilisation of heavy metals may increase through complexation phenomena with seawater anions.

I.6 Treatment technologies for dredged sediments

Different remediation technologies have been developed for the management of contaminated sediments. To provide the best approach and meet the objectives of dredging and remediation operations, the decision makers (harbor managers, local authorities, etc.) have to evaluate the engineering feasibility, efficiency, cost, and performance of a remediation system.

Contaminated sediment treatment options are numerous and some of them have proven their effectiveness on an industrial scale, while others were tested only at the laboratory or pilot scale. To design an optimal treatment technique, it is necessary to take into account the physicochemical characteristics of a sediment, the pollutants' association with the sediment matrix, the volume of sediment, as well as local environmental aspects (Kribi, 2005).

There are two main remediation technology groups – in-situ stabilization and ex-situ stabilization. In-situ stabilization includes one or more operations that do not require the displacement of contaminated sediment from its original location (Peng et al., 2009). Therefore, contaminants are destroyed, isolated, or immobilized through

different techniques in-situ. This group comprises in-place capping, chemical treatments, biological treatments, etc. Ex-situ management is applied when dredged material is too contaminated and cannot be deposited in open water systems. Dredging, transport, and disposal increase the cost of ex-situ management, and the types and amount of contaminants may complicate the choice of treatment method. Sometimes several procedures are required to manage ex-situ dredged material (Keener, 1998). Remediation techniques can combine in-situ and ex-situ treatments in order to select the best strategy for the clean-up of contaminated materials. Below are some examples of remediation technologies that will be discussed in more detail.

I.6.1 Pre-treatment

Large debris and water should be removed before the main treatment stage, therefore the pre-treatment phase is necessary immediately after dredging. The dredging technology will determine the dewatering rate. For hydraulic dredging, sediments require a subsequent dewatering procedure while mechanical and pneumatic dredges occasionally directly provide a satisfactory water level for treatment (Keener, 1998). Some tools can be used during the dewatering stage such as centrifuges, filter presses, plate or diaphragm-plate filters, and gravity thickening (Mulligan et al., 2001). It must be noted that these tools are not always suitable for silt and clay particles.

I.6.2 Physical separation

Physical separation aims to separate smaller particles from larger ones, considering that smaller particles are often more contaminated. Different technologies have been applied to carry out the separation procedure – centrifugation, flocculation, screening, hydrocylones, etc. (Mulligan et al., 2001). Some chemicals combined with an aeration process can make contaminants flow and therefore separate. Screening technology is widely used for particles >1mm. Gravity separation may be applied depending on the specific gravity of the considered contaminated fraction.
Physical separation is rarely economically advantageous and requires a high sand fraction (>25%). Overall, this procedure decreases the volume of contaminated material, reduces handling and disposal costs, but in any case, it always demands further treatment (e.g. chemical, thermal).

I.6.3 Washing

Washing processes present a comparably simple technique of transferring contaminants from dredged sediments into the wash solution. To perform a successful clean-up procedure, the extractant solution should be adapted to the contaminants and soil type. During the mixing of a sediment with the extractant solution, heavy metal contaminants may be transferred through different mechanisms – precipitation, ion

exchange, chelation, and adsorption (Khalid et al., 2017). Different chemical additives can be applied to modify the efficiency of the washing technology – acids (e.g. H_2SO_4, HNO_3), surfactants (e.g. biodegradable biosurfactants - surfactin, rhamnolipid, sophorolipid in oil contaminated material (Mulligan et al., 2001)), chelating agents (e.g. EDTA, DTPA and EDDS) (Peng et al., 2009), or organic acids. For washing cationic metals, the most effective chelating agent is EDTA, especially for Cd, Cu, Pb, and Zn (Khalid et al., 2017).

The washing efficiency largely depends on the heavy metal fraction in dredged sediments – the weaker the metals are bound, the more successful their removal. Hydroxides, reducible oxides, and carbonates are the most likely to be transferred from sediments to the washing solution. One of the technology's limitations, as noted by (Peng et al., 2009), is the granulometric variations meaning that this method is more relevant for sand and gravel fractions than for the fine grains. The degree of efficiency of the washing treatment can be improved by combining different chemical agents (Khalid et al., 2017).

I.6.4 Electrokinetic remediation

Electrokinetic remediation is a relatively new physical remediation technique which separates heavy metals through electrophoresis (charged particle movement), electro-osmosis (fluid movement), electric seepage or electromigration (charged chemicals movement) phenomena (Khalid et al., 2017). The low intensity electric field gradient between a cathode and an anode makes charged particles in sediments move and therefore heavy metals can be eliminated. Hydroxides, oxides, carbonates, as well as soluble heavy metal ions can be removed quite effectively. However, heavy metals with low conductivity (like sulfides or the metallic form of Hg) may demand additional treatment. More precisely, an appropriate electrolyte should be used. Parameters that should be controlled during the procedure are the pH and electrolyte conditions in order to maintain the efficiency of the remediation process (e.g. to avoid anode drying) (Mulligan et al., 2001).

In some cases, electrokinetic technology on its own is not sufficient to clean up the entire range of contaminants in a dredged material. Consequently, a combination of techniques can present an optimal solution. (Khalid et al., 2017) mentioned in his review the complementary processes to follow electrokinetic remediation: microbe remediation, oxidation/reduction technique, phytoremediation, and the use of permeable reactive barrier.

Low permeability soils can be more easily decontaminated via electrokinetic techniques. The main limiting factor of the treatment is soil pH control, which can be resolved by using buffer solutions, complexants or an ion exchange membrane (Khalid et al., 2017).

I.6.5 In-situ Capping

In-place capping is a suitable remediation strategy when a contaminated sediment is covered by a clean isolating material cap. The procedure is performed without disturbing the original location of a sediment and usually the sediment bed remains undisrupted (Keener, 1998). Materials that can be used for this type of remediation technique are natural sand, uncontaminated mud, and some geosynthetic materials (Keener, 1998). Caps present a natural barrier which protects the marine environment from coming into contact with the contaminants and from erosion.
The capping solution can be beneficial when sediment moving and disposal present a high cost and risks for the environment. For an effective capping procedure, it is necessary to consider appropriate materials (type and quantity, conformity to the physicochemical parameters of the sediment and aquatic environment), hydraulic conditions, etc. Capping can be an optimal solution in cases when the sediment must stay in its location of origin (no navigation dredging in the area of interest), so the contaminants may be isolated and their release noticeably retarded. However, the cost of the procedure may be significant when the area of concerns is large.
Figure I.22 below presents different concepts of remediation management and existing containment structures that can play a role in contaminated sediments management – containment approach, in-situ capping, and deep ocean dumping.

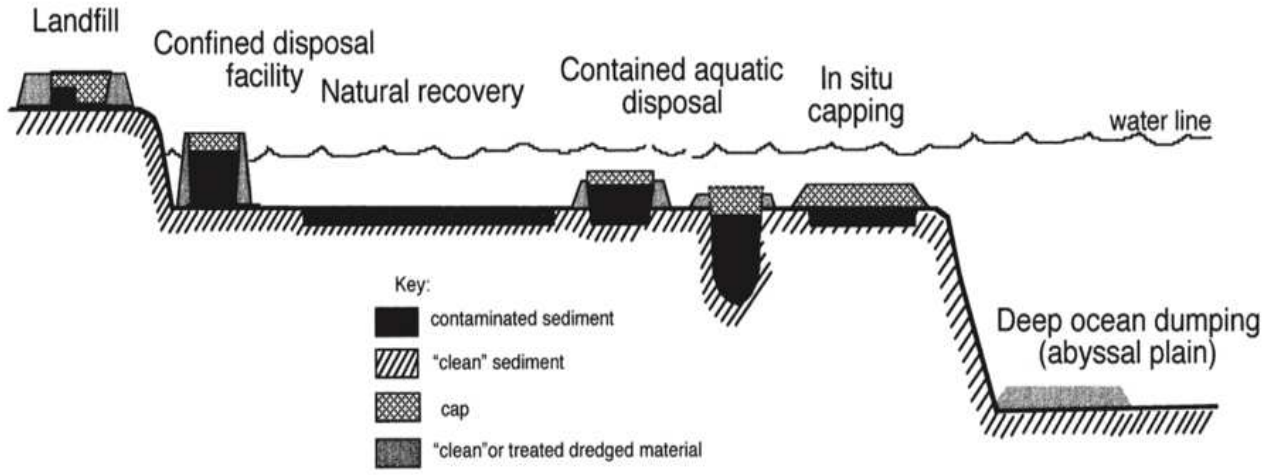

Fig. I.22 Recovery technologies of contaminated sediments

I.6.6 Biological remediation

Biological treatment of contaminated sites presents a viable strategy for the natural restoration of an ecosystem. Bioremediation involves microbial degradation or detoxification/removal of contaminants with the help of plants or microorganisms.

- *Phytoremediation*

This remediation strategy presents an ecological alternative to most of the other remediation solutions due to its environmentally friendly, low-cost, and energy-efficient technology used to extract/detoxify contaminants. Phytoremediation technology can be classified into three groups: phytostabilization, phytoextraction, and phytoevaporation (Khalid et al., 2017).

Phytovolatilization (phytoevaporation) decontaminates sediments through the transpiration phenomena of plants. Toxic trace elements from the sediment can be transformed into less toxic forms and then be evaporated into the atmosphere. Heavy metals such Se, Hg, and As can be converted into gaseous less toxic species. This transfer of heavy metals in plants is governed by enzymes and genes that are rarely present in natural plants. Therefore, genetically modified plants are widely used to improve the efficiency of phytovolatilization.

Another phytoremediation technology is phytostabilization – plants immobilize heavy metals and thus decrease their bioavailability. There are several mechanisms of phytostabilization – the leaching of heavy metals is lowered due to the upstream flow of sediments solution, as well as due to the role of plants roots in decreasing erosion. Plants change the physico-bio-chemical conditions of soils. In some cases, these changes near the root zone induce the immobilization of heavy metals – for example, cadmium forms sulfide species and lead reacts with phosphates.

The efficiency of phytoremediation techniques applied to contaminated sediments depends largely on the capacity of hydrophyte plants to detoxify polluted material. One study has indicated that the hydroremediation can be limited due to the low metals uptake by hydrophytes (Peng et al., 2009).

- *Microbial remediation*

Microorganisms can be used as a remediation solution in contaminated soils and sediments because of their capacities to promote heavy metal precipitation, adsorption, and oxidation/reduction. Different mechanisms may be responsible concerning metals remediation via microorganisms – biosorption, enzyme-catalysed transformation, biomineralization, and redox reactions (Khalid). The biodegradation due to the microbial remediation of a variety of organic compounds was observed (PCBs, diesel oils, petroleum products, pesticides, etc.).

However, microorganisms may also increase metals mobility, depending on the processes they induce. Before microbial remediation, different aspects should be evaluated such as sediment and pore water composition and benthic biology.

I.6.7 Thermal Extraction

Thermal treatment refers to the technology of exposing contaminants to high temperatures (Sharma et al., 2018). It is known that some heavy metals (arsenic, mercury, cadmium) and their compounds are evaporated when exposed to

temperatures in the range of 800°C. The efficiency of this procedure highly depends on the temperature range and time adjustment. For example, some volatile and semi-volatile organic contaminants can be eliminated from contaminated waste even at 200°C-300°C. Gases produced during desorption via thermal treatment should be treated to remove dust and cooled. However, the liquid produced from condensation of the gas stream should be additionally treated in order to be decontaminated (Keener, 1998). Thermal desorption treatment can be very costly in the case of dredged material with high water content as a significant amount of additional energy is needed.

The thermal destruction method is very effective for the elimination of contaminants. This method consists of combustion at >900°C in an oxidizing environment or reduction in non-flame reactor. Organic contaminants in combustion systems go through the contact with an oxidizing flame and are decomposed to carbon dioxide and water. Post-combustion treatment is required. Despite the effectiveness, this method remains very expensive.

I.6.8 Solidification/Stabilization (S/S)

Immobilization treatment presents an effective strategy to prevent the migration of contaminants in the environment. Different methods of waste contaminant immobilization reduces the mobility of pollutants by modifying the physicochemical properties of the waste matrix (e.g. dredged material). Among immobilization methods there are geopolymer based Solidification/Stabilization techniques, vitrification, carbonation (Li), NOVOSOL method (combustion plus phosphatation), cement based S/S process, etc. (Guo et al., 2017), (Kribi, 2005). An immobilization technique using cementitious materials is widely applied and is one of the most advantageous methods compared to other remediation strategies. The S/S method is relatively low-cost, simple to carry out, uses non-toxic materials, is easy to store long term due to physical and chemical stability, etc. (Paria & Yuet, 2006). According to the USEPA, the S/S method was reported to be effective in immobilizing a variety of inorganic contaminants: volatile and non-volatile metals, radioactive waste, asbestos, etc. Organic contaminants can also be treated with this method, but the challenge is more complicated, and therefore some additional additives can be needed. The reactions of hydrolysis, oxidation/reduction, and salt formation are likely to occur in cement-organic waste interactions (Bone et al., 2004).

I.6.8.1 Tests for the S/S evaluation

In order to assess the S/S mix design effectiveness, the treated material undergoes different tests to evaluate several main parameters – density, porosity, hydraulic conductivity, durability, CBR (California Bearing Ratio), but the principal and most essential parameters are the leachability of the contaminants and strength evolution.

The batch leaching test is applied to the crushed material, consequently the leachability may be overestimated regarding the increasing leaching potential. The tank leaching test analyses the diffusion processes in treated waste and can be considered as more real-life approach. The compressive strength criterion allows for an assessment of the hydration rate of the material. It is a key aspect regarding the durability and stability of the system (Kogbara, 2014).
After a successful Solidification/Stabilization treatment the waste, or in this case the dredged sediment, presents a hardened stable monolith in which contaminants are encapsulated due to physical and chemical fixation. Cementation of the treated material leads to the decrease of contact of contaminants with water by forming a low permeability matrix (Saeed et al., 2012). This phenomenon can be described as physical encapsulation when heavy metal migration is significantly reduced. Mechanical strength in term of contaminants embedding exhibits the integrity of the treated matrix (Guo et al., 2017). The more resistant material potentially better stabilizes the trace elements.

I.6.8.2 S/S main reactions mechanisms of HM fixation

Regarding the main mechanisms of contaminant immobilization using the Solidification/Stabilization method, there are different fixation processes: adsorption to the solid phase, pH-dependent precipitation, oxidation/reduction precipitation, and isomorphic substitution with cement matrix.
As was discussed previously regarding the importance of redox potential, some heavy metals exist in the form of stable sulfide compounds in reducing media. However, when the sediment is aerated during the drainage, dewatering and S/S procedures, sulfides of heavy metals may precipitate in the form of sulfates which are much more soluble (Kabata-Pendias & Pendias, 2001). Portland cement creates an oxidizing medium, because it possesses an E_h value between +100 and +200 mV due to dissolved oxygen (Taylor, 1997). Unlike Portland cement, GGBS creates a reducing environment – its redox potential is around -400 mV due to the presence of chemically reduced sulfurs in the slag glass structure. The reduced sulfurs may play an important role in decreasing the mobility of some toxic trace elements which precipitate in the form of highly stable sulfides (Glasser, 1997). It should be mentioned however that reducing conditions of GGBS may impact Fe/Mn oxides and therefore HM related to these phases.
The equilibrium of the sediment system may be considerably impacted by highly soluble sulfate, chloride, and nitrate compounds. Cations and anions from soluble species and the surface of sediments (clays, organic matter) interact due to the ion exchange process, which can be impacted by the incorporation of the binder's ions. The ion exchange describes the formation of electrostatic outer-sphere complexes arising from physical forces.
The adsorption mechanisms of heavy metals on mineral surfaces are quite complex

and depend on many factors. When mineral surfaces are in contact with water, they will attract water molecules that will then dissociate making the surface covered by hydroxyls (≡SOH). These hydroxides behave as proton acceptors or proton donors depending on the pH of the medium (7), (8):

$$\equiv SOH + H^+ \rightleftharpoons \equiv SOH^+ \qquad (7)$$
$$\equiv SOH \rightleftharpoons SO^- + H^+ \qquad (8)$$

Regarding the complexity of the sediment environment and binders chemistry, it is possible to believe that different types of linkages are formed on the mineral surface (≡SOH) in presence of ligands (L) and metal cations $M^{(Z+)}$. Ligands in sediment-binder systems that may complex metal ions vary noticeably: water molecules (H_2O), hydroxyls (OH-), carbonates (CO_3^{2-}), chlorides (Cl^-) and sulfates (SO_4^{2-}) as well as ligands from the organic matter (Taneez, 2016). Figure I.23 describes different adsorption mechanisms occurring between the solid's surface, a metal cation and different ligands:

- simple replacement of the surface proton;
- the metal can be bound on the ligand that previously replaced a surface OH group and also an adsorbed metal may bind a ligand;
- adsorption of metal or ligand to more than one surface site (called multidentate).

The sorption process can be considered as one of the most important mechanisms of the interaction between inorganic contaminants and binders, especially in the early stages.

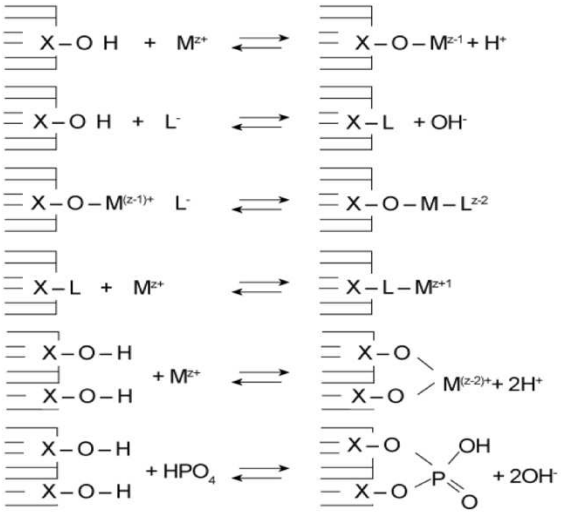

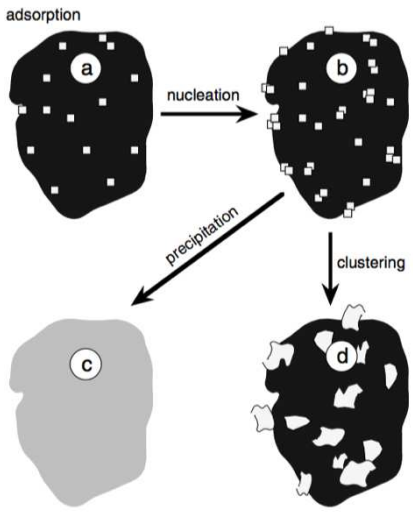

Fig. I.23 (left) (Adsorption mechanisms (X – surface, L – ligand, M – metal). Fig. I.24 (right) An illustration of metal ion sorption reactions on (hydr)oxide. (a) At low surface coverage, isolated site binding (adsorption) is the dominant sorption mechanism; (b) with increased metal loading, M hydroxide nucleation begins. Further increases in metal loadings results in (c) surface precipitation or (d) surface clusters

Another mechanism of immobilization is precipitation or co-precipitation, which is considered according to some studies (Saeed et al., 2012) as the most important mechanism of HM stabilization. Precipitation describes the process occurring after surface saturation – a new phase is formed, but its composition varies from the original solid. Figure I.24 shows the progressive surface saturation which leads to nucleation and further surface precipitation or cluster formation. When contaminants precipitate with other elements (e.g. elements dissolved from minerals) simultaneously, this process is called the co-precipitation and it depends largely on the minerals dissolution rate (Taneez, 2016).

When one of the atoms of the crystalline lattice is substituted by another without disrupting the crystalline structure, the process is called isomorphic substitution. (Sparks, 2002) gives an example of the adsorption of nickel on the phyllosilicates and aluminium oxides resulting in the co-precipitation of Ni-LDH (layered double hydroxides). The ionic radii play an important role in the fixation of HM in the LDH structure.

It should be mentioned that some trace elements can precipitate as metal salts from solution. The formation of metal salts is pH-dependent, therefore in the case of highly alkaline hydraulic binders the concentration of OH^- will play an important role in simple and complex salts precipitation. The formation of metal hydroxides in the case of cations often occurs during the application of the S/S method. In the pH range of 9-12 metal hydroxides remain insoluble, however with a pH increase the metal cations become much more mobile (Fig. I.25). It seems that oxyanions like arsenates, chromates, and molybdates are less soluble in the same pH range, however the other anions in sediment-binder solutions (sulfates, carbonates, chlorides) may impact the availability of these metals by competing with them.

In the case of sediment treatment, the pH, redox potential, organic matter, cation exchange capacity, and metal speciation will govern the potential salt formation and their solubility (Bone et al., 2004). For example, according to (Yousuf et al., 1995), Cd and Zn will be fixed in the cement matrix in the form of complex salts physically rather than chemically.

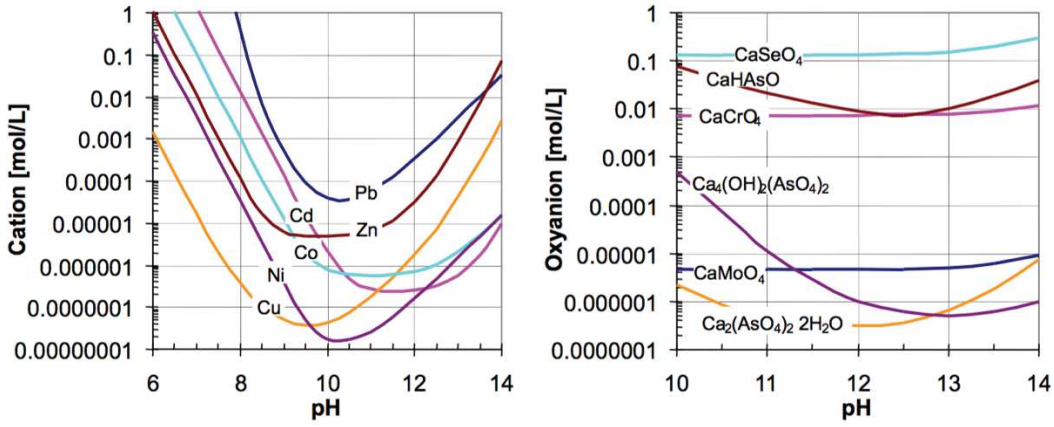

Fig. I.25 Solubility of cationic metals (hydroxides) and oxyanions (calcium salts) as a function of pH

Regarding the complexity of the interaction of contaminants with mineral surfaces, the choice of a suitable binder should be made before treatment. Also, some additional additives can be used to enhance S/S performance. The pH, being one of the most important parameters regarding trace element adsorption/desorption and precipitation, can be adjusted to the range where HM are less soluble (pH=9-12) by using alternative binders.

I.6.8.3 Stability of the treated matrix

Successful S/S treatment considers the ability of the treated material to remain functional based on key parameters such as leachability and strength immediately after the treatment operation as well as in the long term. Internal and external factors may impact the performance of the system and alter the chemistry of the mixture. The formation and stability of the hydration products may be altered by a decrease in pH occurring due to an external environmental attack (e.g. CO_2 penetration) or from the decomposition of organic matter and biological activity producing the acids. Changes in pH and redox potential may lead to microstructural changes (shrinkage/expansion) arising from hydration product degradation or the formation of new precipitates, Thus, the mobility of contaminants may increase significantly (Fig. I.26, (ITRC, 2011)).

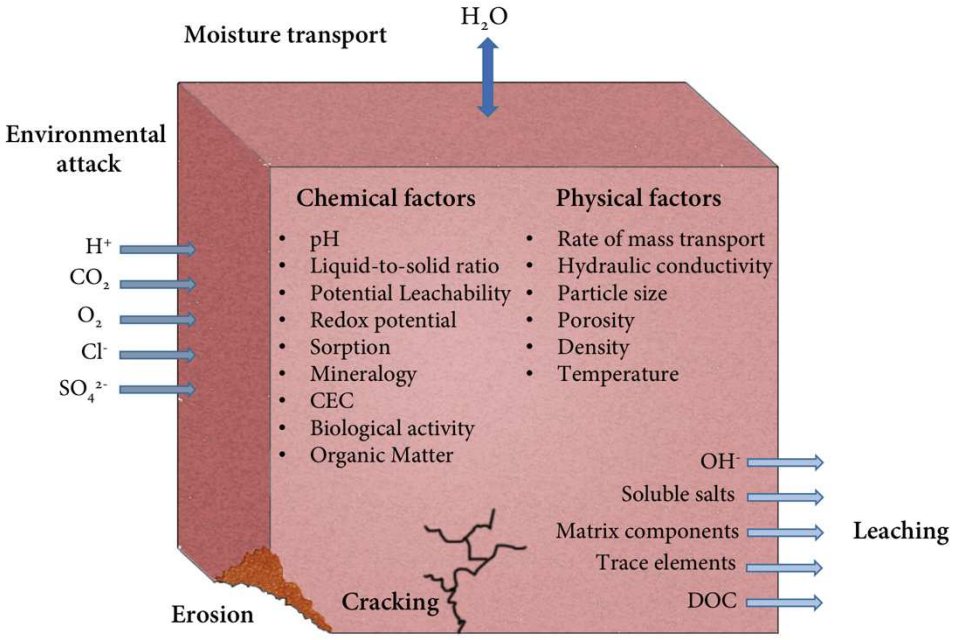

Fig. I.26 Potential risks of contaminants leachability

The microstructure of the treated material determines its hydraulic conductivity, which is a crucial physical parameter for the contaminant stability within the matrix. Finer and more disconnected pore structures may result in higher conductivity in comparison to larger pores, and thus the treated material and contaminants remain stable during contact with water.

External stresses such as mechanical stress or freeze/thaw cycles may also affect the

integrity of the hardened monolith due to cracking or erosion. Consequently, toxic elements may become more available for migration in the environment. However, there is a lack of studies investigating the durability of S/S treated sediments. Regarding all of these potential risks, degradation and aging processes should be accurately monitored in order to assess the performance and stability of the system.

I.7 Considered binding agent properties

(Kogbara, 2014) in his literature review sorted S/S binders according to their interaction and hydration with soils into primary and secondary stabilising agents. The first group comprises ordinary Portland cement (the most widely used S/S binder (Spence & Shi (2005)) and lime, materials that can be applied on their own in order to achieve some of the required parameters for remediation (e.g. mechanical strength, leachability). Secondary S/S agents require additional activation – these materials are PFA (pulverized fuel ash) and GGBS (ground granulated blast-furnace slag) (e.g. to produce pozzolanic reactions with cement or lime). Some other materials can also be used in solidification/stabilization processes – organophilic clays, bitumen, silica fume, natural bentonite clays, etc.

The cement industry is responsible for approximately 9.5% of total CO_2 emissions due to the global demand for cement increasing exponentially. It is known that cement production releases more than 900 kg of CO_2 for every one tonne of Portland cement produced (Naqi & Jang, 2019). The CO_2 emissions, as well as sulfur dioxides (SO_2) and nitrous oxides (NO_x) are responsible for the strengthening greenhouse effect and acid rains. Natural resource depletion also presents a big concern for the cement industry as one tonne of OPC requires nearly 1.5 tonnes of raw materials. Finally, the manufacturing process involves a high energy consumption – around 40% of CO_2 emissions are attributed to fuel combustion.

The use of alternative cements can significantly reduce energy consumption and carbon dioxide emissions. Granulated slag presents important advantages in terms of energy and raw materials reductions as well as leads to the utilisation of industrial by-products. For example, the replacement of 50% of OPC in a cement with GGBS may lead to a decrease of 0.5 tonnes of CO_2 emitted. The potential use of novel GGBS-based binders provides a beneficial solution over a wide range of applications, in particular in sediment Stabilization/Solidification processes, making it relevant for study.

I.7.1 Ordinary Portland cement (OPC)

Portland cement is one of the most widely used binding agents in Stabilization/Solidification processes. This binder is the major hydraulic binder used in civil engineering works all around the world and its production volume increased drastically over last 150 years and especially in the 21st century – from 1.5 billion

tonnes in 2000 to over 3 billion tonnes in 2012. This growth of Portland cement consumption is directly related to the fast economic progress of developing countries and subsequent infrastructure expansion (Naqi & Jang, 2019).

I.7.1.1 Composition of OPC

According to European standard NF EN 197-1, cement is a hydraulic binder which produces a hardened material after mixing with water resulting from a hydration reaction creating bonds. Portland cement is produced from very abundant raw materials – clay and limestone – through complex pyroprocessing in a rotary kilns (heating to about 1450°C, Fig. I.27). These raw materials are transformed into clinker containing four main minerals (Aïtcin, 2016):

- C_3S for $3CaO{\cdot}SiO_2$ (tricalcium silicate or alite)
- C_2S for $2CaO{\cdot}SiO_2$ (dicalcium silicate or belite)
- C_3A for $3CaO{\cdot}Al_2O_3$ (tricalcium aluminate)
- C_4AF for $4CaO{\cdot}Al_2O_3{\cdot}Fe_2O_3$ (tetracalcium ferroaluminate).

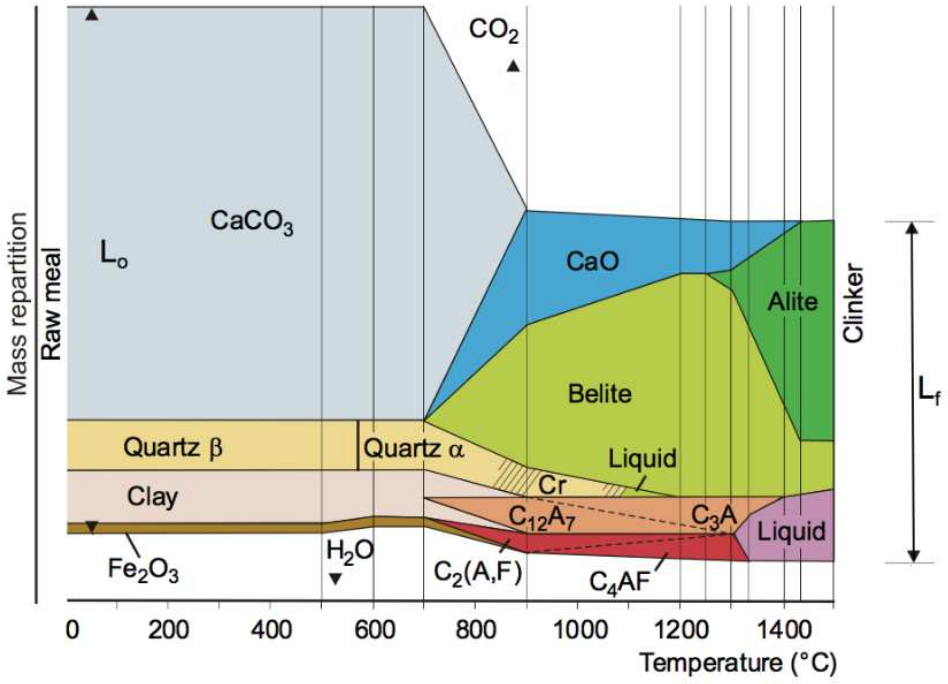

Fig.I.27 Transformation of raw components into clinker

The final material normally possesses a surface area (Blaine) of 300-350 m^2/kg. There exist some standards with regards to the main mineral components and additional chemicals in order to control the composition of the final material. The content of calcium silicates typically reaches 70-80%, with the dominant mineral being alite (C_3S, around 60%). Regarding the minor components of Portland cement clinker production, their content may vary as follows: C_3A and C_4AF (15-16% of the total mass of the

cement), 0.5-6% MgO, 0.5-3% of alkali Na_2SO_4 and K_2SO_4; 0.2-4% free lime (Hewlett & Liška, 2019).
Different cement clinkers are often compared in term of oxide contents (Table I.3) even if in a real system these oxides are part of different minerals. Briefly, the content of CaO may vary from 60 to 70%, the silica content is between 17-24%, however the Al_2O_3 and Fe_2O_3 content is more unstable and depends on the cement type.
The impurities content may influence the crystallinity of the minerals. For example, in some cases alkalis may become part of the crystalline lattice of minerals influencing the reactivity rate of the cement – cubic C_3A may become orthorhombic, which has lower solubility (Aïtcin, 2016).

Table I.3 Chemical composition of Portland cement

Oxide	Weight %
CaO	61–67
SiO_2	17–24
Al_2O_3	3–8
Fe_2O_3	1–6
MgO	0.1–4
$Na_2O + K_2O$	0.5–1.5
SO_3	1–3

In order to produce the final material 'Portland cement', the clinker should be ground with some amount of calcium sulfates, which can be in the form of gypsum, anhydrite, hemihydrate or synthetic calcium sulfate (Aïtcin, 2016). The reason why sulfates are added during the final stage of cement manufacturing, is to control the reactivity of C_3A which in the absence of calcium sulfate hydrates very rapidly by forming hydrogarnet, causing flash setting to occur at the beginning of hydration. Soluble calcium sulfates prevent this situation by instead leading to the rapid formation of ettringite ($Ca_6Al_2(SO_4)_3(OH)_{12}\cdot 26H_2O$). After a few hours, with the depletion of sulfates ettringite is transformed into monosulfoaluminate (Marchon & Flatt, 2016).

I.7.1.2 Hydration chemistry of OPC

When anhydrous cement compounds react with water, new compounds called 'hydrates' are formed resulting in physico-chemical modifications of the system impacting setting and hardening (Hewlett & Liška, 2019). Different factors may change the hydration kinetics of this system – the phase composition of cement minerals (the occurrence of foreign ions (impurities) within clinker phases), the fineness, the water-cement ratio, environmental conditions (e.g. temperature), chemical additives, etc. The hydration of the Portland cement was widely studied over recent decades – the dissolution-precipitation of the whole system as well as of individual components. The reactivity of the anhydrous phases follows the following order: $C_3A > C_3S > C_2S > C_4AF$ (Bone et al., 2004).
In general, the hydration of Portland cement presents a number of reactions between

clinker's minerals, calcium sulfates, and water. The hydration kinetics depend on the rate of dissolution of the different constituents, the rate of the nucleation of precipitated hydrates, and the diffusion of water and dissolved ions in the system (Odler, 1998).
The hydration reactions of Portland cement can be described as follows: in the first minutes the dissolution of anhydrous C_3S and C_2S occur producing exothermic reactions. Moreover, soluble aluminate minerals react with calcium sulfates to produce ettringite. A deceleration of the reactions is observed followed by an induction period. After the induction period, the acceleration period corresponds to the broad precipitation of C-S-H and portlandite from the intense dissolution of C_3S. Then the reactions slow down, however the exothermic reactions of sulfate depletion and ettringite precipitation after the complete dissolution of C_3A are observed (Marchon & Flatt, 2016). The period of low hydration rate occurs due to the densifying and hardening of the material (Fig. I.28).

1. *Hydration of C_3A*

Due to the highest reactivity of the C_3A phase, its role in early hydration is very important from the mechanical and rheological point of view. As was mentioned earlier, soluble calcium sulfates react with tricalcium aluminate to prevent rapid setting. As a result of this reaction, ettringite precipitates according to (9):

$$(CaO)_3.Al_2O_3 + 3(CaSO_4.2H_2O) + 26H_2O \rightarrow ((CaO)_3.Al_2O_3.(CaSO_4)_3.32H_2O + Al_2O_3.3H_2O \quad (9)$$

After sulfate depletion, ettringite reacts with the remaining C_3A and monosulfoaluminate is formed (10):

$$2(CaO)_3.Al_2O_3 + (CaO)_3.Al_2O_3.(CaSO_4)_3.32H_2O + 4H_2O \rightarrow 3(CaO)_3.Al_2O_3.CaSO_4.12H_2O \quad (10)$$

2. *Hydration of C_3S*

Tricalcium silicate is the most essential Portland cement component, controlling its Strength development. C_3S ($3CaO{\cdot}SiO_2$) is known to exist in numerous polymorphs (triclinic, monoclinic, trigonal). The calcium silicate chain presents often as an impure material in Portland cement containing different ions which can substitute for silicon (e.g. AlO_4^{5-} or PO_4^{3-} for SiO_4^{4-}) or oxygen (Walkley & Provis, 2019). This structure allows fast dissolution after the interaction with water to produce calcium silicate hydrate gel (C-S-H) and Portlandite ($Ca(OH)_2$), (11). C-S-H is an amorphous phase with a CaO/SiO_2 molar ratio between 1.2 and 2.1.

$$2(CaO)_3.SiO_2 + 6H_2O \longrightarrow 3CaO.2SiO_2.3H_2O + 3Ca(OH)_2 \quad (11)$$

The hydration of alite can be described by periods or hydration stages: the highly exothermic peak due to C_3S dissolution is marked at point 0; stage 1 presents a slowdown in dissolution, stage 2 is the induction period; stage 3 is the acceleration period, stage 4 a deceleration period, and stage 5 a slow ongoing hydration reaction (Fig. I.29, (Marchon & Flatt, 2016)). Many theories exist to explain the induction period of C_3S hydration. One of the most widely accepted hypotheses is the formation of metastable C-S-H hydrates on C_3S surfaces, preventing further dissolution. The end of the induction period is explained by the transformation of these membranes of metastable hydrates into a more permeable hydrates allowing for the migration of water ions, Ca^{2+} and silicon ions or by the membrane's rupture due to osmotic pressure. However, despite available techniques there have been no observations confirming the 'gel model' (Scrivener et al., 2015). Some authors describe the induction period as a latent time until the nucleation and polymerization of silicates meaning that C-S-H nuclei are formed from the first beginning of hydration and continue to precipitate even during the induction period - reaching some critical size just before the acceleration stage (Marchon & Flatt, 2016).

The acceleration period represents a massive precipitation and growth of C-S-H and portlandite corresponding to the main peak of heat release (Fig. I.29). During the acceleration stage the dissolution rate of C_3S achieves its maximum, therefore the highest amount of Ca^{2+} can be detected in the solution between the two stages. Precipitated C-S-H is poorly crystalline; its atomic structure can be compared to tobermorite/jennite. C-S-H can be described as sheets of calcium and oxygen enclosed in tetrahedral silica chains and separated by water layers (Marchon & Flatt, 2016).

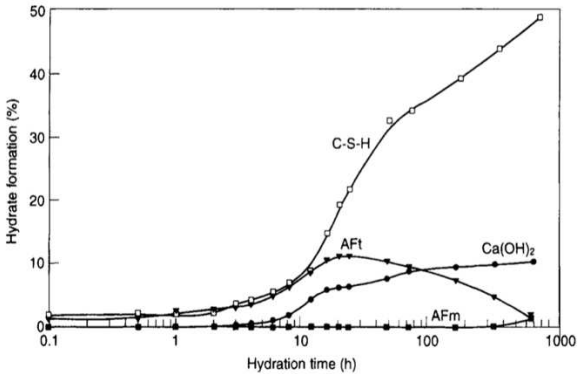

Fig. I.28 Hydration kinetic – formation of hydrates

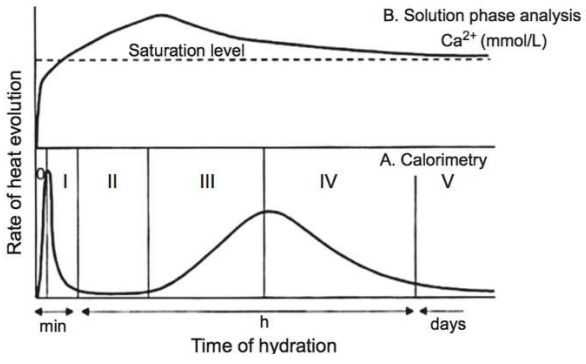

Fig. I.29 Stages of alite hydration

One of the explanations for the deceleration period can be the end of the nucleation of C-S-H on the new needles and further precipitation in the interface between anhydrous products and these new needles (Bazzoni, 2014). The low heat release of the last hydration stage coincides with low diffusion of ions because of the hydrates creating a dense microstructure.

I.7.2 Ground granulated blast-furnace slag (GGBS)

I.7.2.1 What is GGBS?

Blast furnace slag is a by-product of iron production in a blast furnace and it is composed mainly of silicates and aluminosilicates of calcium. Iron ore is heated to 1400-1600°C together with limestone or dolomite (as fluxing agents) and with coke in order to reduce iron oxides (Fig. I.30). After melting these materials, two products are generated – molten iron and slag. The slag is lighter, and it rises to the surface of the molten iron.

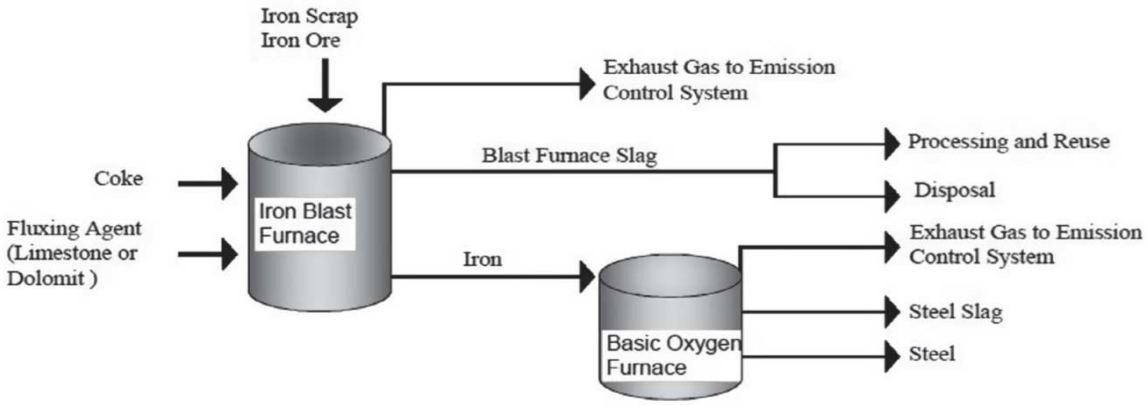

Fig. I.30 Production of slag

When the rapid cooling is applied through high-pressure water jets to the molten slag, a glassy Ca-Al-Mg silicate is formed. Granular particles of slag no larger than 5 mm in diameter, and almost fully amorphous, are formed as a result of the rapid cooling procedure. In order to obtain good cementitious properties, the granulated blast furnace slag must be dehydrated, dried and finely ground. The final product is GGBS cement (ground granulated blast-furnace slag) and it is a binder with latent hydraulic properties. In order to accelerate the hydraulic reaction of GGBS, a source of basic pH is required. Activators can be sourced from Ordinary Portland cement or alkalis (hydroxide, silicate, and carbonate) (Özbay et al., 2016; Siddique, 2008).

I.7.2.2 Chemical composition, mineralogy of GGBS

GGBS can present a mixture of small amount (5-10%) of low crystallinity phases within the melilite group resembling gehlenite ($2CaO{\cdot}Al_2O_3{\cdot}SiO_2$) and akermanite ($2CaO{\cdot}MgO{\cdot}2SiO_2$) as well as depolymerized calcium silicate glass. GGBS also contains some amount of sulfur, binding around 1 mole of Ca per mole of S (Duxson & Provis, 2008). The chemical composition of GGBS can vary depending on the ore used for the iron production, as well as on the specifics of the manufacturing processes. A typical chemical composition of blast furnace slag in term of oxides is

given in the table below (Table I.4).

Table I.4 Chemical composition of GGBS, (Glasser, 1997)

Oxide	Weight %
CaO	36–44
SiO_2	29–38
Al_2O_3	10–18
Fe_2O_3	0.2–2.0 [a]
MgO	4–12
Na_2O+K_2O	1–2
SO_3	1–2.5 [b]

[a] Iron is present as Fe(II) and Fe(III).
[b] Sulfur overwhelmingly present as S^{2-}.

The glass structure depends on the production conditions, such as temperature and cooling rate, which determine the degree of depolymerisation of the aluminosilicate framework and therefore its reactivity (Walkley & Provis, 2019). The formed glass can be described as a depolymerised silicate structure with Ca^{2+} and Mg^{2+} charge balanced Al as network modification cations. The degree of depolymerisation can be expressed with help of the basicity index and CaO/SiO_2 (C/S) ratio with calcium cations increasing the depolymerisation of the aluminosilicate system and consequently its hydraulic activity (Özbay et al.).
In order to explore the glass structure of GGBS, NMR studies of ^{29}Si and ^{27}Al were carried out. It was found that Si is present principally as a dimeric tetrahedral species and Al is present in tetrahedral coordination. (Shimoda et al., 2008) observed a depolymerised chain structure of SiO_4 tetrahedra branched with AlO_4 tetrahedra separated by Ca and Mg providing framework disorder to the system.

I.7.2.3 Hydration of GGBS-based binders

The ternary diagrams of Portland cement and alternative or supplementary cementitious materials (SCM) are presented in Fig. I.31. These SCM are mostly silico-aluminate materials with low calcium content compared to ordinary Portland cement, thus it can be seen that GGBS contains more silica, alumina, and magnesia and less CaO. Furthermore, the molecular structure of the OPC phases presents ionic bonding compared to the GGBS glass structure with covalent bonding. This means that the dissolution of Portland cement is easier and faster through hydrolysis than the dissolution of GGBS which requires breaking covalent bonds (Si-O). That is why concrete structures made with OPC usually set faster than concrete made with slag cement. At the same time, the addition of high amounts of GGBS to Portland cement results in a strength increase over longer periods, reduced permeability, good freeze-thaw resistance, and high sulfate resistance.

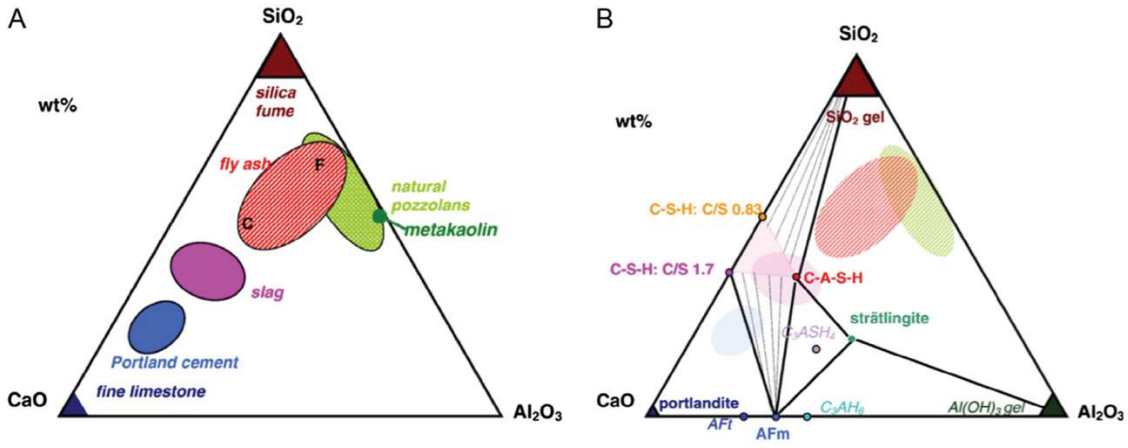

Fig. I.31 (A) CaO–Al2O3–SiO2 ternary diagram of cementitious materials, (B) hydrate phases in the CaO–Al2O3–SiO2 system

The potential phases development is shown in Fig. I.31, B in a CaO–SiO2–Al_2O_3 system. C-S-H is the main hydration product of GGBS-based binders and its chemical structure and C/S ratio varies according to the type of activation. Besides using slag as a Portland cement additive, GGBS can be used as an independent binder by increasing its reactivity with alkali activators. GGBS activation can be classified according to the type of substances applied as an activator (M as alkaline):

- pH-based activation (MOH where M stands for Na, K, Ca, or Mg): these activators provide a pH source for the rapid precipitation of hydrates. However, in some cases, this type of activation promotes inappropriate strength development due to bad rheology and uneven hydrate distribution. Caustic alkalis are considered as health hazardous and expensive.
- Alkali-silicates ($M_2O{\cdot}nSiO_2$): this activation gives a good strength development, better than OPC based binders. At the same time the activator is considered as health hazardous because of its high pH and it is also cost prohibitive. This type of GGBS-based binder is established to be effective for acid resistance.
- Carbonate salts (M_2CO_3): Carbonate activation provides a low pH rise and develops seeds for hydration. It is interesting from practical point of view as it is not expensive and safe to handle. However, some challenges should be solved such as a long induction period and low temperature sensitivity.
- Sulfate activation (M_2SO_4, $CaSO_4.nH_2O$) provides seeds (ettringite, gypsum) necessary for hydration and is environmentally friendly. This activation needs an additional pH source to enhance the dissolution of GGBS.
- Portland cement can also be used as a GGBS activator. In this case granulated slag is activated by hydroxyl attack. Portland cement serves as a source of pH, particularly by establishing an equilibrium of precipitation-dissolution of calcium hydroxides (Van Rompaey, 2006). As a result of the GGBS activation by OPC, a pozzolanic reaction is produced by the precipitation of calcium hydroxides with silicates/aluminosilicates. Consequently, the Portlandite formation is

decreased. The acceleration hydration stage of GGBS/OPC system is produced mainly between 10 hours and 3 days when lime from the clinker grains reacts with GGBS glass. After this period, some amount of portlandite can be produced and its formation plays a role in further GGBS activation over time, even after more than 90 days.

I.7.3 C-S-H structure

As was mentioned before, calcium silicate hydrate (C-S-H) is the main hydration product of Portland cement as well as of GGBS-rich binders. Its structure varies depending on binder composition, but generally it presents a silicate Q^2 Si chains of various length with Q^1 Si sites at chain termination points containing in the interlayer space cationic species and surrounded by calcium oxide sheets (Walkley & Provis, 2019). The 'dreierketten' silicate structure (Fig. I.32) is characteristic for C-S-H gel – the chain of dimeric silicates tetrahedra linked by a bridging silicate. It was established that the calcium to silicon ratio (Ca/Si) varies between 0.8 and 2 for cementitious materials. This value is lower in the case of GGBS-based binders making its C-S-H structure close to natural tobermorite (Kovačević et al., 2015). Moreover, in the case of the GGBS C-S-H structure, an important Al substitution may occur in bridging tetrahedral sites in the silicates chains (substitution of Si^{4+} by Al^{3+}). This substitution results in a significant modification of C-S-H's chemical structure compared to the plain OPC binder, resulting in the formation of C-A-S-H. Therefore, the charge deficit occurs from Al-Si substitution which should be counterbalanced by other cations. This charge deficit makes the activated slag calcium silicate structure a potential stabilizer for heavy metal cations due to their possible incorporation into C-A-S-H. It seems also that high GGBS content binders produce C-S-H with a different morphology compared to Portland cement binders –needle-like C-S-H is developed presenting a denser structure compared to the fibrous C-S-H of the OPC binder. It can be thus supposed that this type of morphology is responsible for the improved durability properties in the GGBS-based system.

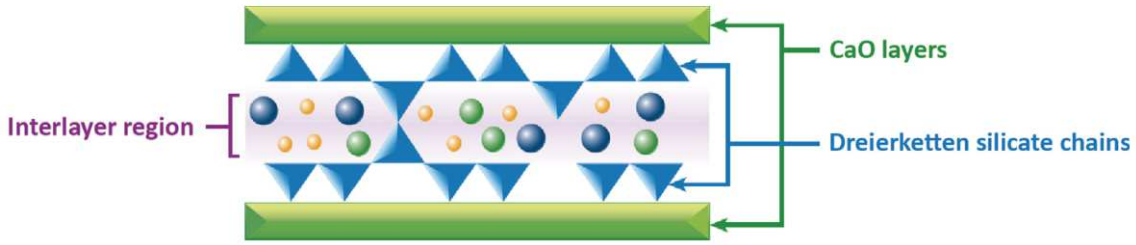

Fig. I.32 Schematic representation of the structural features of calcium-silicate hydrate (C-S-H) gels. Tetrahedral Si sites and CaO layers are shown by blue triangles and green rectangles, respectively. Circles denote various interlayer species (water or cations)

I.7.4 OPC and GGBS-based binders in S/S practice

In the Solidification/Stabilization practice of hazardous waste treatment, different types of cementitious materials were tested in terms of mechanical and leaching performances in order to achieve and maintain the necessary physical properties of the formed monolith and stabilize contaminants in the new matrix. Hydraulic binders may transform contaminated dredged material into a new material suitable for engineering applications, road construction, or base material which remains a cost-effective and efficient solution for remediation (Saeed et al., 2012). The S/S treatment for remediation of contaminated sites was reported to be the best technology for 57 Resource Conservation and Recovery Act (RCRA) listed hazardous wastes based on a report by the USEPA (2004). However, the choice of a suitable binder should be carefully evaluated before treatment due to the different mechanisms occurring between binders and organic and inorganic constituents of contaminated sediments impacting immobilization or retarding the hardening of a new system. The degree of effectiveness of different binders may vary considerably. One of the main controlling factors is the increase in pH in the presence of a hydraulic binder and further precipitation of metal ions as hydroxides at the optimum pH level, which differs according to specific metal. According to (Du et al., 2010) increasing the pH higher than 12-13 may significantly reduce the effectiveness of S/S.

I.7.4.1 OPC as a S/S agent

Ordinary Portland cement is the most widely used binder in S/S due to its low cost and high availability. Most S/S studies analyse the OPC-treated waste material after 28 days of storage. The general tendency shows an increase in compressive strength with increasing binder dosage (Bone et al., 2004; Kogbara, 2014). Studies considering the long-term behaviour of OPC-treated waste material show the plateau for uniaxial compressive strength (UCS) after the strength increase for a specific period. At the same time, (Al-Tabbaa & Boes, 2002) reported lower UCS after five years of curing. Many studies were conducted in order to investigate the impact of heavy metals on strength development as well as the impact of organic contaminants and organic matter. (Al-Sanad Hasan A. & Ismael Nabil F., 1997) reported lower UCS values for mixtures with hydrocarbon pollutants. (Tremblay, 2002) showed how different organic substances affect the properties of OPC-treated samples. The addition of 0.1% of sucrose retards cement hardening as was observed by (Taylor, 1997). (Saeed et al., 2012) in their review reported the formation of weakened OPC paste and a retardation effect in the presence of high concentrations of lead, zinc, and copper (Alford et al., 1981). (Du et al., 2010) in his review reported the retardation effect of HM on the hydration of cementitious materials during S/S treatment (Lee, 2005, Asavapisit, 2000). According to (Kogbara, 2014) the optimum OPC dosage for soils treatment is 20%, but 10% can also be sufficient in some cases. He also concluded that sandy and gravelly

soils develop higher UCS than clayey soils. In the same paper, some mechanisms of the impact of HM on the UCS development were investigated: Zn, Cr and Cd promote increased ettringite formation with posterior cracking; Pb retards hydration by forming precipitates on the C_3A and C_3S grains.
Regarding the leaching requirements, 15-20% of the OPC binder may significantly reduce the mobility of heavy metals. However, in some cases the leachability of some heavy metals increased in treated OPC material, making the OPC treatment not suitable for stabilization. This is especially concerning for Pb (Sanchez et al., 2002) and Cu (Voglar & Lestan, 2010). It seems that solubility was significantly affected by the high pH. There are very few studies assessing the long term behaviour of S/S treated material. (Antemir et al., 2010) reported the results for field trials of soils treated with 20% of sulfate-resisting PC after four years and showed that contaminant leaching remained low.
One of the important conclusions made by (Hale et al., 2012) about the limiting factors in OPC or lime treated contaminated soils is the release of organic matter in solution and therefore of the heavy metals associated with DOM due to the high pH development.

I.7.4.2 GGBS as a S/S agent

Despite the use of slag-based binders in S/S practice for contaminated soils, ground improvement, and other hazardous waste treatment, very few studies can be found investigating the application of GGBS for the stabilization/solidification of sediments and the main mechanisms responsible for effective stabilization and strength development.
From the review of (Kogbara, 2014) about the S/S of contaminated soils, the UCS of treated soil depends on the level replacement of OPC by GGBS. It seems that the higher replacement level gives lower strength, however the total amount of binder plays an important role (Allan & Kukacka, 1995). At the same time, there is a lack of UCS data measured after a long storage period, exceeding 28 days. An OPC replacement between 50 and 60 % was reported to be the optimum to achieve the best strength performance (Zhang et al., 2018), (Allan & Kukacka, 1995). (Zhang et al., 2018) demonstrated higher strength values for a 1:1 GGBS:OPC ratio after 28 days.
Regarding the leaching test performance, the OPC-GGBS binder was shown to be more effective in the stabilization of Pb than OPC alone (Akhter et al., 1990). An improved leaching performance was demonstrated by (Allan & Kukacka, 1995) through increasing the GGBS content in OPC-GGBS blends as well as the reduction of Cr(VI) to Cr(III) in chromium contaminated soils. The improved immobilization of Al, Cr, Mn, Ni, Cu, and Pb was observed by (Zhang et al., 2018) with increasing GGBS content, however the Zn, Cd, and As were better stabilized with only OPC. (Deja, 2002) studied the effect of alkali-activated slag pastes on the stabilization of different types of heavy metals. It was shown that Zn^{2+}, Pb^{2+}, Cd^{2+}, and Cr^{6+} can be immobilized in GGBS-

based binders activated with NaOH, Na_2CO_3, or with sodium silicate activation very effectively. (Qian et al., 2003) showed that Hg^{2+} was well stabilized in the alkali-activated slag cement. (Wang et al., 2019) demonstrated better efficiency of GGBS-based binders in comparison to the OPC samples for the immobilization of As as one of the big concerns of marine sediment remediation.

In order to reduce cement usage, different studies were conducted for cement replacement by GGBS. For example, (Wang et al., 2018) reported better leaching performance of OPC/GGBS blends compared to pure Portland cement systems by reducing the pH and therefore improving metal stabilization.

(Limbachiya et al., 2016) demonstrated the beneficial use of GGBS as partial replacement of OPC in paving blocks in terms of increased density, a decrease in permeability, and improved strength performance compared to the control OPC-only blocks.

GGBS was shown to be effective for the stabilization of soft marine clay using a combination of lime and GGBS. The compressive strength was higher for the lime/GGBS mixture than for the OPC-only condition. Lower porosity was also observed (Yi, Gu, et al., 2015). Soft marine clay can also be solidified using a combination of two types of slag as shown by (Yi, Li, et al., 2015) – GGBS and carbide slag (CS), which has a high $Ca(OH)_2$ content. This mixture provided a strength lower than an OPC-based formulation at 7 and 28 days, but higher strength at 90 days of storage. The binder demonstrating optimum performance was GGBS/CS activated by Na_2SO_4. This mixture exceeded the OPC strength at all ages. Reactive magnesia can be even more effective in the activation of GGBS for the stabilization of soft marine clays. (Yi et al., 2014) demonstrated a good resistance to the sulfate attack of MgO-activated slag compared to Portland cement stabilised clay, and better strength development.

One of the benefits of using GGBS is the improved sulfate and chloride resistance, especially for slag activated with lime (Wild et al., 1998). (Mahedi et al., 2018) demonstrated increased strength with curing time using high GGBS content in slag-cement samples for the stabilization of different expansive soils collected in Texas. This strength improvement is attributed to a decrease in the Ca/Si ratio and a decrease in swelling potential. Moreover, it was mentioned that high OPC content does not necessary provide a suitable strength development and may lead to the degradation of mechanical properties over time. The improved strength of sulfate-bearing clay soils was reported by (Wild et al., 1998) when lime was combined with GGBS. (Cheng et al., 2016) demonstrated an effective stabilization of chloride saline soil using alkali-activated GGBS. The 28-day strength was higher than the strength of Portland cement activation.

The effect of a binder prepared with 70% GGBS and 30% pozzolanic cement mixed with organophilic bentonite on the stabilization of chloro-organic contaminants was shown to be quite effective despite changes in the microstructure, such as increased porosity (Cioffi et al., 2001). (Bone et al., 2004) provide some reasons of enhanced performances for S/S treatment via GGBS-based binders based on previous studies:

a GGBS-based binder increases the binding of contaminants in its matrix due to its dense microstructure; one of the main factors is GGBS's E_h (redox potential) which produces a reducing environment compared to the oxidising OPC environment.

Bibliography

Aïtcin, P.-C. (2016). Portland cement. In *Science and Technology of Concrete Admixtures* (p. 27-51). Elsevier. https://doi.org/10.1016/B978-0-08-100693-1.00003-5

Akhter, H., Butler, L. G., Branz, S., Cartledge, F. K., & Tittlebaum, M. E. (1990). Immobilization of As, Cd, Cr and PB-containing soils by using cement or pozzolanic fixing agents. *Journal of Hazardous Materials*, *24*(2), 145-155. https://doi.org/10.1016/0304-3894(90)87006-4

Alamgir, Md. (2016). The Effects of Soil Properties to the Extent of Soil Contamination with Metals. In H. Hasegawa, I. Md. M. Rahman, & M. A. Rahman (Éds.), *Environmental Remediation Technologies for Metal-Contaminated Soils* (p. 1-19). Springer Japan. https://doi.org/10.1007/978-4-431-55759-3_1

Alford, N. Mcn., Rahman, A. A., & Salih, N. (1981). The effect of lead nitrate on the physical properties of cement pastes. *Cement and Concrete Research*, *11*(2), 235-245. https://doi.org/10.1016/0008-8846(81)90065-X

Allan, M. L., & Kukacka, L. E. (1995). Blast furnace slag-modified grouts for in situ stabilization of chromium-contaminated soil. *Waste Management*, *15*(3), 193-202. https://doi.org/10.1016/0956-053X(95)00017-T

Al-Sanad Hasan A., & Ismael Nabil F. (1997). Aging Effects on Oil-Contaminated Kuwaiti Sand. *Journal of Geotechnical and Geoenvironmental Engineering*, *123*(3), 290-293. https://doi.org/10.1061/(ASCE)1090-0241(1997)123:3(290)

Al-Tabbaa, A., & Boes, N. (2002). Pilot in situ auger mixing treatment of a contaminated site. Part 4. Performance at five years. *Proceedings of the Institution of Civil Engineers - Geotechnical Engineering*, *155*, 187-202. https://doi.org/10.1680/geng.2002.155.3.187

Alzieu, C. (1999). *Dragages et environnement marin*. 225.

Antemir, A., Hills, C. D., Carey, P. J., Magnié, M.-C., & Polettini, A. (2010). Investigation of 4-year-old stabilised/solidified and accelerated carbonated contaminated soil. *Journal of Hazardous Materials*, *181*(1-3), 543-555. https://doi.org/10.1016/j.jhazmat.2010.05.048

Apitz, S. E. (2010). Waste or resource? Classifying and scoring dredged material management strategies in terms of the waste hierarchy. Journal of Soils and Sediments, 10(8), 1657-1668. https://doi.org/10.1007/s11368-010-0300-9

Arsenic. Consulté 15 juin 2020, à l'adresse https://www.who.int/news-room/fact-sheets/detail/arsenic

Asavapisit S, Boonjam M, Polprasert C (2000). Effects of lead and chromium hydroxides on cement-based solidified waste properties

Barcelona Convention—Marine—Environment—European Commission. (s. d.). Consulté 15 juin 2020, à l'adresse https://ec.europa.eu/environment/marine/international-cooperation/regional-sea-conventions/barcelona-convention/index_en.htm

Bazzoni, A. (2014). Study of early hydration mechanisms of cement by means of electron microscopy. https://doi.org/10.5075/epfl-thesis-6296

Billon, G. (2001). Géochimie des métaux et du soufre dans les sédiments des estuaires de la Seine et de l'Authie [Lille 1]. In *Http://www.theses.fr*. http://www.theses.fr/2001LIL10064

Bone B. D., Barnard L H., Boardman D. I., Carey P. J., Hills C. D., Jones H. M., MacLeod C. L., Tyrer M., (2004) Review of scientific literature on the use of stabilisation/solidification for the treatment of contaminated soil, solid waste and sludges

Botta et al., 2015 Understanding your soil test: step by step

Burnol A., Duro L., Grive M. (2006). *INERIS-DRC-06-66246DESP-R01a*. 138.

Cao, H., Tsai, F. T.-C., & Rusch, K. A. (2010). Salinity and soluble organic matter on virus sorption in sand and soil columns. Ground Water, 48(1), 42-52. https://doi.org/10.1111/j.1745-6584.2009.00645.x

Cazalet, M. L. (2012). *Caractérisation physico-chimique d'un sédiment marin traité aux liants hydrauliques : Évaluation de la mobilité potentielle des polluants inorganiques*. 267.

Cheng, Y., Yu, H., Zhu, B., & Wei, D. (2016). Laboratory investigation of the strength development of alkali-activated slag-stabilized chloride saline soil. *Journal of Zhejiang University-SCIENCE A*, *17*(5), 389-398. https://doi.org/10.1631/jzus.A1500185

Chrysochoou, M., Theologou, E., Bompoti, N., Dermatas, D., & Panagiotakis, I. (2016). Occurrence, Origin and Transformation Processes of Geogenic Chromium in Soils and Sediments. *Current Pollution Reports*, *2*(4), 224-235. https://doi.org/10.1007/s40726-016-0044-2

Cioffi, R., Maffucci, L., Santoro, L., & Glasser, F. P. (2001). Stabilization of chloro-organics using organophilic bentonite in a cement-blast furnace slag matrix. *Waste Management*, *21*(7), 651-660. https://doi.org/10.1016/S0956-053X(00)00116-1

Convention on the Prevention of Marine Pollution by Dumping of Wastes and Other Matter. Consulté 15 juin 2020, à l'adresse http://www.imo.org/en/OurWork/Environment/LCLP/Pages/default.aspx

Couvidat, J. (2016). Gestion d'un sédiment de dragage marin contaminé : Caractérisation de la réactivité biogéochimique, valorisation en mortier et évaluation environnementale. 248.

Dede P., S. E. (2018). Dredges' management : Comparison of regulatory frameworks, legal gaps and recommendations. *Global NEST Journal*, *20*(1), 88-95. https://doi.org/10.30955/gnj.002358

Deja, J. (2002). Immobilization of Cr6+, Cd2+, Zn2+ and Pb2+ in alkali-activated slag binders. *Cement and Concrete Research*, *32*(12), 1971-1979. https://doi.org/10.1016/S0008-8846(02)00904-3

Directive 2008/98/EC on waste (Waste Framework Directive)—Environment—European Commission. (s. d.). Consulté 15 juin 2020, à l'adresse https://ec.europa.eu/environment/waste/framework/

Du, Y.-J., Liu, S.-Y., Liu, Z.-B., Chen, L., Zhang, F., & Jin, F. (2010). An Overview of Stabilization/Solidification Technique for Heavy Metals Contaminated Soils. In Y. Chen, L. Zhan, & X. Tang (Éds.), *Advances in Environmental Geotechnics* (p. 760-766). Springer Berlin Heidelberg. https://doi.org/10.1007/978-3-642-04460-1_93

Duxson, P., & Provis, J. L. (2008). Designing Precursors for Geopolymer Cements. *Journal of the American Ceramic Society*, *91*(12), 3864-3869. https://doi.org/10.1111/j.1551-2916.2008.02787.x

Eggleton, J., & Thomas, K. V. (2004). A review of factors affecting the release and bioavailability of contaminants during sediment disturbance events. *Environment International*, *30*(7), 973-980. https://doi.org/10.1016/j.envint.2004.03.001

Emerson, S., & Hedges, J. (2008). *Chemical oceanography and the marine carbon cycle*. Cambridge University Press.

European List of Waste, Commission Decision 2000/532/EC, Commission Decision of 3 May 2000 replacing Decision 94/3/EC establishing a list of hazardous wastes

Fairbrother, A., Wenstel, R., Sappington, K., & Wood, W. (2007). Framework for Metals Risk Assessment. *Ecotoxicology and Environmental Safety*, *68*(2), 145-227. https://doi.org/10.1016/j.ecoenv.2007.03.015

Gamsonré, C. (2014). *Gestion terrestre des sédiments de dragage et processus biophysicochimiques impliqués*. 382.

Glasser, F. P. (1997). Fundamental aspects of cement solidification and stabilisation. *Journal of Hazardous Materials*, *52*(2-3), 151-170. https://doi.org/10.1016/S0304-3894(96)01805-5

Guo, B., Liu, B., Yang, J., & Zhang, S. (2017). The mechanisms of heavy metal immobilization by cementitious material treatments and thermal treatments : A review. *Journal of Environmental Management*, *193*, 410-422. https://doi.org/10.1016/j.jenvman.2017.02.026

Hale, B., Evans, L., & Lambert, R. (2012). Effects of cement or lime on Cd, Co, Cu, Ni, Pb, Sb and Zn mobility in field-contaminated and aged soils. *Journal of Hazardous Materials*, *199-200*, 119-127. https://doi.org/10.1016/j.jhazmat.2011.10.065

Harrington J., Smith D., Guidance on the Beneficial Use of Dredge Material in Ireland, October 2013

Haydee, K. M., & Dalma, K. E. (2017). Concerning Organometallic Compounds in Environment : Occurrence, Fate, and Impact. In M. M. Rahman & A. M. Asiri (Éds.), *Recent Progress in Organometallic Chemistry*. InTech. https://doi.org/10.5772/67755

Hayet, A., Deram, A., & Bohain, D. (2017). *Contexte et cadre réglementaire de la gestion des sédiments de dragage. Premier chapitre de l'étude. Impacts écologiques de sédiments pollués extraits et déposés en milieux terrestres*. 136.

Hewlett, P. C., & Liška, M. (2019). *Lea's chemistry of cement and concrete*.

ITRC. (2011). *Development of Performance Specifications for Solidification/Stabilization*. 162.

Kabata-Pendias, A., & Pendias, H. (2001). *Trace elements in soils and plants* (3rd ed). CRC Press.

Keener, H. M. (1998). Contaminated Sediments in Ports and Waterways : Cleanup Strategies and Technologies: Committee on Contaminated Marine Sediments, National Research Council, National Academy Press, 2101 Constitution Ave., N.W., Washington, DC 20413. 1997. 295 p. ISBN 0-309-05493-1. *Journal of Environmental Quality*, *27*(2), 467-467. https://doi.org/10.2134/jeq1998.00472425002700020032x

Khalid, S., Shahid, M., Niazi, N. K., Murtaza, B., Bibi, I., & Dumat, C. (2017). A comparison of technologies for remediation of heavy metal contaminated soils. *Journal of Geochemical Exploration*, *182*, 247-268. https://doi.org/10.1016/j.gexplo.2016.11.021

Kodama, H., & Schnitzer, M. (1980). Effect of fulvic acid on the crystallization of aluminum hydroxides. *Geoderma*, *24*(3), 195-205. https://doi.org/10.1016/0016-7061(80)90023-3

Kogbara, R. B. (2014). A review of the mechanical and leaching performance of stabilized/solidified contaminated soils. *Environmental Reviews*, *22*(1), 66-86. https://doi.org/10.1139/er-2013-0004

Kovačević, G., Persson, B., Nicoleau, L., Nonat, A., & Veryazov, V. (2015). Atomistic modeling of crystal structure of Ca 1.67 SiH x. *Cement and Concrete Research*, *67*, 197-203. https://doi.org/10.1016/j.cemconres.2014.09.003

Kribi S. (2005). *Décomposition des matières organiques et stabilisation des métaux lourds dans les sédiments de dragage*. 224.

Kubier, A., Wilkin, R. T., & Pichler, T. (2019). Cadmium in soils and groundwater : A review. *Applied Geochemistry*, *108*, 104388. https://doi.org/10.1016/j.apgeochem.2019.104388

Lee D, Waite TD, Swarbrick G, Lee S, Comparison of solidification /stabilization effects of calcite between Australian and Korea (R. O.) cements, (2005).

Lesven. (2008). *Devenir des éléments traces métalliques au sein du sédiment, un compartiment clé de l'environnement aquatique*. 246.

Limbachiya, V., Ganjian, E., & Claisse, P. (2016). Strength, durability and leaching properties of concrete paving blocks incorporating GGBS and SF. *Construction and Building Materials*, *113*, 273-279. https://doi.org/10.1016/j.conbuildmat.2016.02.152

Mahedi, M., Cetin, B., & White, D. J. (2018). Performance Evaluation of Cement and Slag Stabilized Expansive Soils. *Transportation Research Record: Journal of the Transportation Research Board*, *2672*(52), 164-173. https://doi.org/10.1177/0361198118757439

Marchon, D., & Flatt, R. J. (2016). Mechanisms of cement hydration. In *Science and Technology of Concrete Admixtures* (p. 129-145). Elsevier. https://doi.org/10.1016/B978-0-08-100693-1.00008-4

Mayer T., Q, R., U, B., & W, S. (2008). Geochemistry and toxicity of sediment porewater in a salt-impacted urban stormwater detention pond. *Environmental Pollution (Barking, Essex : 1987)*, *156*(1), 143-151. https://doi.org/10.1016/j.envpol.2007.12.018

Mulligan, C. N., Yong, R. N., & Gibbs, B. F. (2001). An evaluation of technologies for the heavy metal remediation of dredged sediments. *Journal of Hazardous Materials*, *85*(1-2), 145-163. https://doi.org/10.1016/S0304-3894(01)00226-6

Naqi, A., & Jang, J. (2019). Recent Progress in Green Cement Technology Utilizing Low-Carbon Emission Fuels and Raw Materials : A Review. *Sustainability*, *11*(2), 537. https://doi.org/10.3390/su11020537

NF EN 12457-2—*December 2002*. (s. d.). Consulté 15 juin 2020, à l'adresse https://www.boutique.afnor.org/standard/nf-en-12457-2/characterization-of-waste-leaching-compliance-test-for-leaching-of-granular-waste-materials-and-sludges-part-2-one-stage-batch-t/article/663943/fa104282

NF EN 197-1 (April 2012), Cement - Part 1 : composition, specifications and conformity criteria for common cements – Cement

Odler, I. (1998). *Hydration, Setting and Hardening of Portland Cement*. 57, Lea's Chemistry of cement and concrete

Okoro, H. K., & Fatoki, O. S. (2012). A Review of Sequential Extraction Procedures for Heavy Metals Speciation in Soil and Sediments. *Journal of Environmental & Analytical Toxicology*, *01*(S1). https://doi.org/10.4172/scientificreports.181

OSPAR Commission | Protecting and conserving the North-East Atlantic and its resources. (s. d.). OSPAR Commission. Consulté 15 juin 2020, à l'adresse https://www.ospar.org/

Özbay, E., Erdemir, M., & Durmuş, H. İ. (2016). Utilization and efficiency of ground granulated blast furnace slag on concrete properties – A review. *Construction and Building Materials*, *105*, 423-434. https://doi.org/10.1016/j.conbuildmat.2015.12.153

Paria, S., & Yuet, P. K. (2006). Solidification–stabilization of organic and inorganic contaminants using portland cement : A literature review. *Environmental Reviews*, *14*(4), 217-255. https://doi.org/10.1139/a06-004

Peng, J., Song, Y., Yuan, P., Cui, X., & Qiu, G. (2009). The remediation of heavy metals contaminated sediment. *Journal of Hazardous Materials*, *161*(2-3), 633-640. https://doi.org/10.1016/j.jhazmat.2008.04.061

Piccolo. (1996). *Humic Substances in Terrestrial Ecosystems—1st Edition*. https://www.elsevier.com/books/humic-substances-in-terrestrial-ecosystems/piccolo/978-0-444-81516-3

Qian, G., Sun, D. D., & Tay, J. H. (2003). Immobilization of mercury and zinc in an alkali-activated slag matrix. *Journal of Hazardous Materials*, *101*(1), 65-77. https://doi.org/10.1016/S0304-3894(03)00143-2

Rinklebe, J., & Shaheen, S. M. (2017). Redox chemistry of nickel in soils and sediments : A review. *Chemosphere*, *179*, 265-278. https://doi.org/10.1016/j.chemosphere.2017.02.153

Robertson et al., 1999, Exchangeable Ions, pH, and Cation Exchange Capacity

Saeed, K. A., Kassim, K. A., & Eisazadeh, A. (2012). *Interferences of Cement Based-Solidification/Stabilization and Heavy Metals : A Review*. *17*, 11.

Sanchez, F., Gervais, C., Garrabrants, A. C., Barna, R., & Kosson, D. S. (2002). Leaching of inorganic contaminants from cement-based waste materials as a result of carbonation during intermittent wetting. *Waste Management*, *22*(2), 249-260. https://doi.org/10.1016/S0956-053X(01)00076-9

Sargent 2015, The development of alkali-activated mixtures for soil stabilisation, Handbook of Alkali-Activated Cements, Mortars and Concretes

Schulz, H. D., & Zabel, M. (2006). *Marine Geochemistry*. 582.

Scrivener, K. L., Juilland, P., & Monteiro, P. J. M. (2015). Advances in understanding hydration of Portland cement. *Cement and Concrete Research*, *78*, 38-56. https://doi.org/10.1016/j.cemconres.2015.05.025

Sharma, S., Tiwari, S., Hasan, A., Saxena, V., & Pandey, L. M. (2018). Recent advances in conventional and contemporary methods for remediation of heavy metal-contaminated soils. *3 Biotech*, *8*(4), 216. https://doi.org/10.1007/s13205-018-1237-8

Shimoda, K., Tobu, Y., Kanehashi, K., Nemoto, T., & Saito, K. (2008). Total understanding of the local structures of an amorphous slag : Perspective from multi-nuclear (29Si, 27Al, 17O, 25Mg, and 43Ca) solid-state NMR. *Journal of Non-Crystalline Solids*, *354*(10), 1036-1043. https://doi.org/10.1016/j.jnoncrysol.2007.08.010

Siddique, R. (2008). *Waste materials and by-products in concrete*. Springer.

Smedley. (2005). Arsenic in Natural Waters. In J. H. Lehr & J. Keeley (Éds.), *Water Encyclopedia* (p. mw13). John Wiley & Sons, Inc. https://doi.org/10.1002/047147844X.mw13

Snousy, M. G. (2017). An Overview on the Organic Contaminants. *SDRP Journal of Earth Sciences & Environmental Studies*, *1*(2). https://doi.org/10.25177/JESES.1.2.1

Sondi, I., Bišćan, J., & Pravdić, V. (1996). Electrokinetics of Pure Clay Minerals Revisited. *Journal of Colloid and Interface Science*, *178*(2), 514-522. https://doi.org/10.1006/jcis.1996.0146

Sparks, D. L. (2002). *Environmental Soil Chemistry*. 367.

Spence & Shi (2005) Stabilization and Solidification of Hazardous, Radioactive, and Mixed Wastes

Stevenson. (1982). *Humus Chemistry : Genesis, Composition, Reactions, 2nd Edition | Wiley*. Wiley.Com. https://www.wiley.com/en-us/Humus+Chemistry%3A+Genesis%2C+Composition%2C+Reactions%2C+2nd+Edition-p-9780471594741

SUBSED LIFE17 ENV/IT/000347, “Sustainable substrates for agriculture from dredged remediated marine sediments: from ports to pots", Review of legislation on dredged sediment management.

Tack, F. M., Callewaert, O. W. J. J., & Verloo, M. G. (1996). Metal solubility as a function of pH in a contaminated, dredged sediment affected by oxidation. *Environmental Pollution*, *91*(2), 199-208. https://doi.org/10.1016/0269-7491(95)00049-6

Taneez, M. (2016). *Stabilization of contaminated marine sediment by addition of bauxite residues : Evaluation of potential mobility of trace elements*. 205.

Taylor. (1997). *TAYLOR (1997)—Cement-Chemistry—2nd Edition*. Passei Direto. https://www.passeidireto.com/arquivo/18595148/taylor-1997-cement-chemistry-2nd-edition

Tessier. (1979). *Sequential extraction procedure for the speciation of particulate trace metals | Analytical Chemistry*. https://pubs.acs.org/doi/10.1021/ac50043a017

Tremblay. (2002). *Influence of the nature of organic compounds on fine soil stabilization with cement | Request PDF*. ResearchGate. http://dx.doi.org/10.1139/t02-002

Van Rompaey, G. (2006). *Etude de la réactivité des ciments riches en laitier, à basse température et à temps court, sans ajout chloruré*. http://hdl.handle.net/2013/

Voglar, G. E., & Lestan, D. (2010). Solidification/stabilisation of metals contaminated industrial soil from former Zn smelter in Celje, Slovenia, using cement as a hydraulic binder. *Journal of Hazardous Materials*, *178*(1-3), 926-933. https://doi.org/10.1016/j.jhazmat.2010.02.026

Walkley, B., & Provis, J. L. (2019). Solid-state nuclear magnetic resonance spectroscopy of cements. *Materials Today Advances*, *1*, 100007. https://doi.org/10.1016/j.mtadv.2019.100007

Wang, L., Chen, L., Tsang, D. C. W., Zhou, Y., Rinklebe, J., Song, H., Kwon, E. E., Baek, K., & Sik Ok, Y. (2019). Mechanistic insights into red mud, blast furnace slag, or metakaolin-assisted stabilization/solidification of arsenic-contaminated sediment. *Environment International*, *133*, 105247. https://doi.org/10.1016/j.envint.2019.105247

Wang, L., Yu, K., Li, J.-S., Tsang, D. C. W., Poon, C. S., Yoo, J.-C., Baek, K., Ding, S., Hou, D., & Dai, J.-G. (2018). Low-carbon and low-alkalinity stabilization/solidification of high-Pb contaminated soil. *Chemical Engineering Journal*, *351*, 418-427. https://doi.org/10.1016/j.cej.2018.06.118

Wild, S., Kinuthia, J. M., Jones, G. I., & Higgins, D. D. (1998). Effects of partial substitution of lime with ground granulated blast furnace slag (GGBS) on the strength properties of

lime-stabilised sulphate-bearing clay soils. *Engineering Geology*, *51*(1), 37-53. https://doi.org/10.1016/S0013-7952(98)00039-8

Yi, Y., Gu, L., & Liu, S. (2015). Microstructural and mechanical properties of marine soft clay stabilized by lime-activated ground granulated blastfurnace slag. *Applied Clay Science*, *103*, 71-76. https://doi.org/10.1016/j.clay.2014.11.005

Yi, Y., Li, C., & Liu, S. (2015). Alkali-Activated Ground-Granulated Blast Furnace Slag for Stabilization of Marine Soft Clay. *Journal of Materials in Civil Engineering*, *27*(4), 04014146. https://doi.org/10.1061/(ASCE)MT.1943-5533.0001100

Yi, Y., Liska, M., & Al-Tabbaa, A. (2014). Properties of Two Model Soils Stabilized with Different Blends and Contents of GGBS, MgO, Lime, and PC. *Journal of Materials in Civil Engineering*, *26*, 267-274. https://doi.org/10.1061/(ASCE)MT.1943-5533.0000806

Yousuf, M., Mollah, A., Vempati, R. K., Lin, T.-C., & Cocke, D. L. (1995). The interfacial chemistry of solidification/stabilization of metals in cement and pozzolanic material systems. *Waste Management*, *15*(2), 137-148. https://doi.org/10.1016/0956-053X(95)00013-P

Zhang, W., McCabe, B. A., & Morrison, L. (2018). Stabilisation of a dredged marine sediment : Geotechnical and contaminant leaching properties. 7.

Chapter II: Materials and Methods

II.1 Introduction

The experimental part of this study explores the mechanisms of the Solidification/ Stabilization treatment of contaminated sediments using GGBS-based binders. The purpose of this investigation is to explore the interaction between the sediment matrix and hydraulic binders in order to formulate a final mix design with an appropriate amount of GGBS, and to choose a type of activation for durable land disposal.
The first part of this chapter seeks to examine the physicochemical characteristics of sediment from the Dublin port, being the main case sediment in this study, and compare it to sediment from the Gothenburg port. The port authorities of these two locations consider the S/S method as one of the most propitious remediation techniques for the treatment of dredged material. The important indicators of the geochemical nature of the sediments considered in this study were pH, trace elements content and sequential extraction or fractionation of trace elements, total organic carbon, cation exchange capacity, mineralogy, as well as some physical characteristics such as density, porosity, and granulometry. Characterisation of the sediment is important to understand the effectiveness of the stabilizing agents. It was therefore examined at different levels – from the achievement of a required strength to the immobilization of trace elements through the formation of hydrates and developed microstructure.
To enable assessment on an elementary level of the considered treated materials, the sophisticated tools of NMR Spectroscopy and X-ray absorption near edge structure (XANES) were used. These techniques allow for a better understanding of the stabilization mechanisms when hydraulic binders are applied as stabilizing agents and helped in the investigation of the impact of some heavy metals on the early hydration of the binders.
In order to gain insights into the impact of clays and organic matter as important components of the sediment on the hydration of the mixtures, some investigations were conducted, and they are described in this chapter.

II.2 Raw materials

II.2.1 Sediment

II.2.1.1 Origin of the considered sediments

The considered sediment comes from the Dublin port. The Solidification/Stabilization method was considered as the main remediation strategy within the Alexandra Basin in Dublin (Fig.II.1). The dredging was performed at three different points by a special device for collecting sediment called a Van Veen grab (Fig. II.2).

Different types of works were scheduled for the area. The construction after infilling the

Graving Dock N2 is a special concern for this study resulting in a minimum compressive strength requirement after sediment treatment of at least 2 MPa.

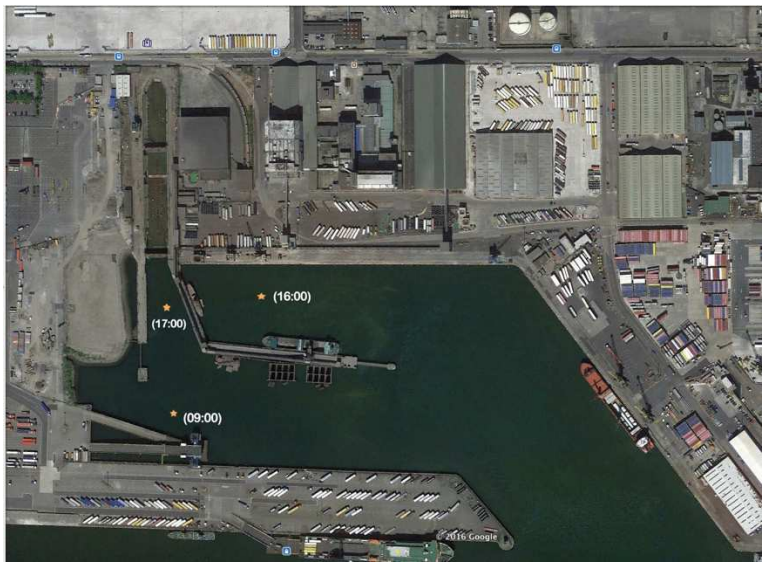

Fig. II.1 Alexandra Basin, Dublin port

Fig. II.2 Van Veen grab dredging device

After the dredging procedure the Dublin sediment (D0) was placed in special tubes and sent for laboratory testing. The samples were stored at 0°±2°C and protected from light during the entire experimental study.

Most research in the field of S/S treatment have focused only on one type of sediment when comparing different binders. However, a major problem with this kind of application is to find a product to be effective for all types of sediments from the mechanical point of view, as well as a good stabilizer for organic and inorganic contaminants. For that reason, it was necessary to use a sediment from another location in order to have physico-chemical properties different from the main case study. In view of that, a second sediment was received from the Gothenburg port, designated as G0 (Fig. II.3). This contaminated sediment will be reused as construction material during the Gothenburg port expansion (Berman & correspondent, n.d.).

Fig. II.3 Gothenburg project field trials, PEAB's Prosol mixing

The received Gothenburg samples (G0) were stored at the same conditions - at 0°±2°C

and with light protection. The Gothenburg sediment was mainly compared to the Dublin sediment in terms of compressive strength evolution.

II.2.1.2 Physical analysis of the sediments

II.2.1.2.1 Particle size distribution

There are different systems for soil classification to facilitate the determination of a soil's composition and texture in view of different applications such as construction, agriculture, etc.
It is rare when a soil contains one particle size range as its texture is typically composed of clays, sands, and silts (Table II.1). Hence it is useful to know, in terms of civil engineering purposes, the full particle size distribution range (Gee & Bauder, 1986).

Table II.1 Particle size analysis according to different classifications schemes (Gee & Bauder, 1986)

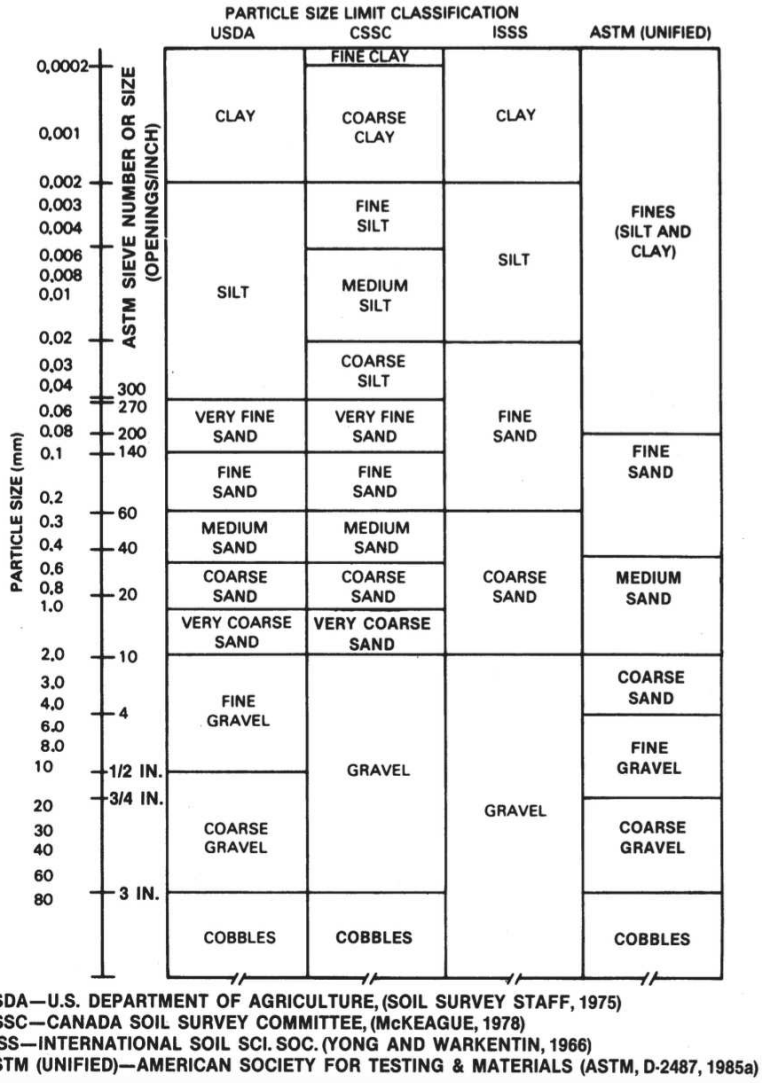

Sediments present a complex system as sinks for the storage of different types of contaminants, depending also on the particle size distribution. Fine-grained sediment shows a particular risk for heavy metals accumulation and thus environmental pollution. This sorption process of contaminants on a sediment's biofilm was described by (Flemming, 1995).

The technique of laser diffraction using a CILAS 1090 particle-size-analyzer was selected to specify the particle size distribution of the Gothenburg and Dublin sediments. This method consists of a phenomenon whereby the difference in particle size is determined by the scattering of light intensity. The laser diffraction technique assumes a spherical form for all particles (Pye & Blott, 2004), which is why some micas can be overestimated by this method (Hayton et al., 2001). The Mie theory describing the interaction of light and small particles was used as an optical model for the analysis with a coefficient of absorption of 1.6 + 0.1*i.

First of all, the sediments were sieved to remove large aggregates (≥2mm), then dried at 40°C, crushed and dispersed with 3%wt of hexametaphosphate solution (HMP) in order to put the samples in a deflocculated state.

Both sediments are mostly fine silty clayey sediments (Fig. II.4). 100% of particles in the Dublin sediment had a diameter below 80μm and had a d_{50} between 12 and 13 μm and $d_{90} \approx 40$ μm. The corresponding values for the Gothenburg sediment are $d_{50} \approx 20$ μm and $d_{90} \approx 72$ μm. The Gothenburg sediment also contains some larger particles which correspond to the fine sand (≈0,1mm). The Dublin sediment can be texturally classed into the finer category probably containing more clay and carbonates particles, whereas the Gothenburg sediment texturally presents as a sandy clayey sediment.

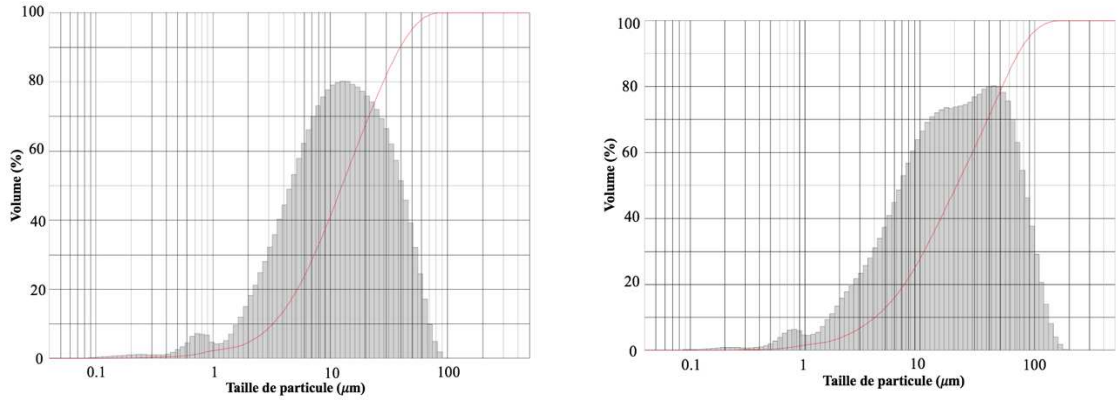

Fig. II.4 Particle size analysis by laser granulometer of the Dublin (D0) (left) and Gothenburg (G0) (right) sediments

II.2.1.2.2 Density

The bulk density of the considered sediments not only describes the physical properties of the materials but also defines the amount of binder needed for the S/S process. (Jepsen et al., 1997) demonstrated an increase of the bulk density of the sediment with depth due to the compaction phenomenon. It is related to the water

content which can be variable from one location to another.
This study used the pycnometer method for the determination of density according to NF EN ISO 17892-3. First, the samples were dried and passed through a 4mm sieve. After introducing the dry sediment sample into the pycnometer, the weight of the pycnometer plus the sample (m_s) was measured. Then it was filled with water (m_w) ensuring there is no air inside and the total mass was registered (m'). Thus the volume of the added water (V_w) can be determined by (12):

$$V_w = \frac{(m' - m_w)}{\rho_w} \qquad (12)$$

The volume of the solid and its density are calculated by (13, 14):

$$V_S = V_{pycnometer} - V_w \qquad (13)$$

$$\rho_s = \frac{m_s}{V_s} \qquad (14)$$

The measured bulk density (ρ_s) reveals the difference in physical properties of the two sediments. The Gothenburg sediment has a greater bulk density than the Dublin sediment (Table II.2). It is correlated with the water content and the organic matter content in both sediments and will be discussed further.

Table II.2 Bulk density of the Dublin (D0) and Gothenburg (G0) sediments

Samples	Bulk density (kg/m^3)
D0	1400±70
G0	1600±50

II.2.1.3 Mineralogy

II.2.1.3.1 XRD analysis

X-Ray diffraction is a semi-quantitative analytical technique providing information regarding the crystalline structure and mineralogy of poli- or monomineralic samples. The most important law giving the relation by which diffraction beam occurs is the Bragg law, (15):

$$\lambda = 2d_{hkl} sin\theta, \qquad (15)$$

λ - wavelength of X-rays;
d – interplanar spacing, the distance between parallel planes of atoms in the family (hkl); geometric function of the size and shape of the unit cell;
θ - X-ray angle.

In other words, this equation calculates the angle where reinforcing interference from X-rays scattered by parallel planes of atoms will produce a diffraction peak.

The apparatus used in this study is a D2 PHASER from BRUKER with the anode made of cobalt as a metal target (λ=1.79Å) with a step size of 0.02° and 1.2 s counting time per step. Before analysis, the samples were dried at 40°C. First, the fraction < 2 mm of both sediments were analysed. Samples D0 and G0 were ground thoroughly with a mortar and pestle. A small amount of ground material was placed in a special sample holder and X-rayed between 5° and 60° over a diffraction angle (2θ) (Fig. II.5).
The crystallographic analysis of D0 and G0 presents the variation in mineral structure of the samples. The sediment which originated from the Dublin port is a mostly clayey sediment with illite identified as a major clay mineral. It contains an important carbonate fraction (identified as calcite) unlike the Gothenburg sediment. The Gothenburg sediment is predominately a siliceous sediment; the peaks of quartz, albite, and microcline were detected.

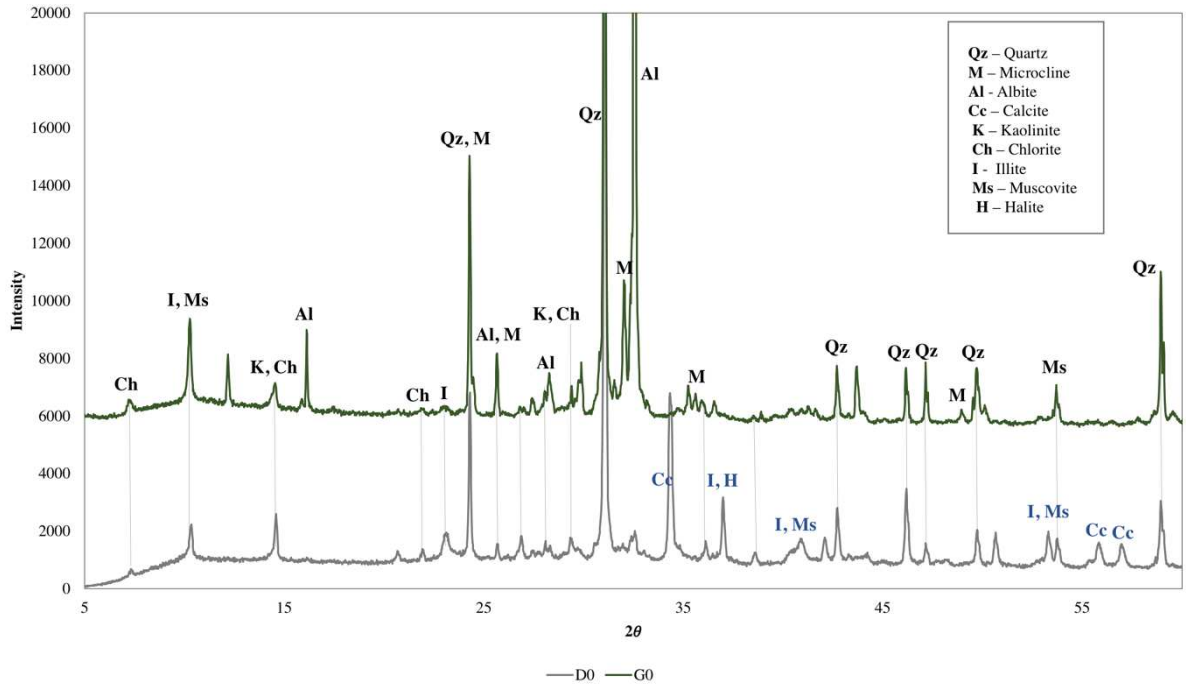

Fig. II.5 X-Ray Diffraction analysis of the Dublin (D0) and Gothenburg (D0) sediments

In order to more precisely identify the fine clayey fraction of the Dublin and Gothenburg sediments (<2μm), the samples were characterized in the Laboratory of Oceanology and Geosciences (CNRS). The main clay fractions are reported in Table II.3.
According to the report from the laboratory, the Dublin sediment (D0) is composed mainly of illite (59%) associated with chlorite (25%) and kaolinite (14%). Smectite is present in trace amounts <2%.
The Gothenburg sediment (G0) contains 52% of illite associated with 22% of non-swelling and non-heat resistant vermiculitic interstratified minerals. Chlorite and

kaolinite represent 18% and 13% respectively of the overall clay assemblage.

Table II.3 X-Ray Diffraction analysis of the clayey fraction of D0 and G0

Sample	Smectite	Interstratified Clays		Illite	Kaolinite	Chlorite	Accessory minerals
		Non-swelling	Swelling				
D0	<2%	3%	-	59%	14%	25%	Quartz
G0	-	22%	-	52%	13%	18%	Quartz, plagioclase feldspars (albite-anorthite)

II.2.1.3.2 TGA (Thermogravimetric analysis), DTA (Differential thermal analysis)

The thermal analysis presents a method which identifies the changes in properties of a material provoked by temperature alterations (Brown, 2001). The temperature changes in a material can be described as phase transitions (new arrangement of elements), melting (relaxing of solid system to a liquid state), thermal decomposition, or sublimation (Brown, 2001). The quantification of variations of samples is made using a thermobalance.

The technique of differential thermal analysis (DTA) is one of the most common procedures in thermal analysis. The difference between the reference material and the sample is measured ($T\Delta$) when both are under the same heating program. As a result, curves with exothermic (released energy; for ex. oxidation) and endothermic peaks (absorbed energy) are obtained which are in relation to thermal changes in the samples.

The apparatus used in this study was Sytsys 16/18 TGA-DSC/TMA Instrument. The heating rate was set at 10°C.min^{-1} with temperature rising to 1200°C under argon atmosphere.

Before introducing the sample in a special sample holder of 100μL volume, the sediments were dried at 40°C for 24h until all free water was removed. The samples were finely ground just before being placed in the TGA apparatus. To ensure the same procedural conditions, the mass of the samples was precisely measured to minimize the difference between the two samples, ~ 60μg of each sample was placed in a sample holder.

The data obtained from the TGA DTA analysis is shown in Fig. II.6. The exo- and endothermic peaks which correspond to sediment changes during heating have been analyzed on the basis of previous investigations on the mineral phases of the soils and sediments (Findoráková et al., 2015; Frost, 1996; Hasan & Masoud, 2014) as well as on the organic phase (Pallasser et al., 2013).

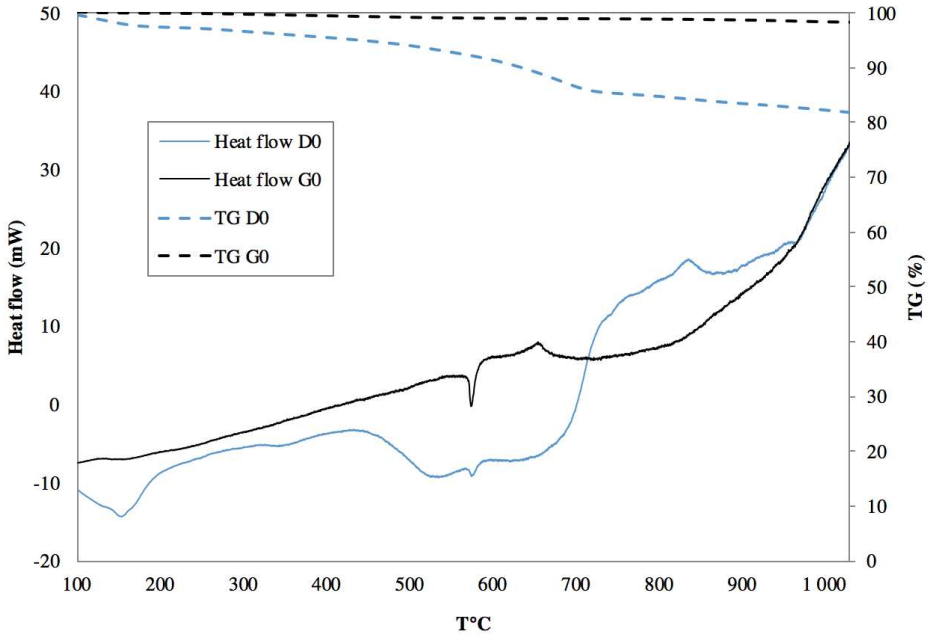

Fig. II.6 TGA DTA analysis of the Dublin (D0) and Gothenburg (D0) sediments

What stands out in the graph is the difference in mass loss – for the Dublin port sediment the loss goes up to almost 20% of the mass compared to ≈ 2% for the Gothenburg sediment. The first endothermic peak from 40°C till 260°C corresponds to the dehydration of the sediments and the effect is stronger for the Dublin sediment. It can arise from the larger amounts of organic matter and clay in D0, known to be good water holders. The X-Ray diffraction analysis demonstrated that the Dublin sediment is mostly clayey sediment whereas the Gothenburg sediment contains a large amount of different siliceous minerals. As a result, the endothermic peak at 573°C corresponds to quartz transformation and is bigger for G0. The endothermic reactions occurring in the region from 230°C to 430°C correspond to OM release. This area of endothermic reactions is more pronounced for D0. According to (Pallasser et al., 2013) the area of 430°C-590°C is attributed to the dehydroxylation of clay minerals. The data from the mineralogical analysis of the D0 sediment sample indicated a significant content of carbonate minerals. The TGA DTA analysis of the Dublin sediment highlighted the carbonates phase decomposition in the region between 700°C-840°C.

II.2.1.4 Chemical properties of the sediments

II.2.1.4.1 pH measurements

The liquid part of the sediment is a phase where chemical reactions take place. The release of contaminants from the solid phase into the pore water is a pH dependent process as was discussed in the Chapter I. According to (Helali et al., 2009) the pH is one of the main variables controlling the mobility, bioavailability, and toxicity of trace elements. The pH is mainly controlled by the buffer capacity of the sediment as well

as by the biological activity within the sediment. For example, the pH may rise if the reduction of sulfates to sulfides occurs, and on the contrary the pH decreases during the denitrification process. The sediment solid phase has non-permanent charge on the surface that can be changed with pH changes, when protonation or the dissociation of functional groups takes place, for example with the introduction of a hydraulic binder. These changes may considerably impact the adsorption process of metallic species.
pH profiles for the solid part of the sediments were determined from three different locations (denominated as A, B, C) for each sediment according to NF ISO 10390. This standard consists of placing of the fine fraction of a sediment (<2 mm), dried at 40°C, in a glass flask to the 5 ml volume. Then the flask is filled with demineralized water counting 5-times the sample's volume. The suspension is agitated till pH stabilization, avoiding any air penetration. The values of pH measurements are summarised in Table II.4.

Table II.4 pH of the Dublin (D0) and Gothenburg (G0) sediments

Sample	pH (A)	pH (B)	pH (C)
D0	7.3	7.6	7.6
G0	7.5	7.5	7.6

Both sediments have similar pH profiles for the solid part. These values are typical for marine sediments (Emerson & Hedges, 2008; Schulz & Zabel, 2006). In addition, the interstitial water pH was measured following the centrifugation of the raw samples. The obtained pore water is a result of compaction of the solid sediment fraction. Table II.5 below shows the values of the pH of the interstitial water for the Dublin and Gothenburg sediments. As can be seen the obtained values present slightly more alkaline pH profiles compared to Table II.4.

Table II.5 pH of the pore water of the Dublin (D0) and Gothenburg (G0) sediments

Sample	pH
D0	8.0
G0	8.1

II.2.1.4.2 Total Organic Carbon (TOC) analysis

Organic matter is one of the key parameters required in order to characterise a sediment's nature. It is also an important biodynamic marker used to evaluate the state of an aquatic ecosystem (Dong et al., 2017), (Schaanning, 1994). Organic matter is a complex dynamic component of the carbon cycle (Emerson & Hedges, 2008; Strong et al., 2012). Further, organic matter is important due to its ability to form complexes with metal ions and to interact with clays and organic contaminants. The structure of fulvic and humic acids, which are main components of sediment organic matter, is highly dependent on the pH and ionic strength of the environment (Klučáková, 2018).

During the Solidification/Stabilization process some reactions may occur between a highly alkaline hydraulic binder and OM, such as the complexation or dissolution of OM.

In this study the organic matter content was quantified using Total organic carbon analysis. The reliability of this method derives from the fact that the carbon is a major OM element : ~45% c. by mass for carbohydrates, ~85% c. by mass for lipids (Emerson & Hedges, 2008).

The samples D0 and G0 were analysed according to NF 10693, NF 10694, and NF 14235. First, the samples were oven dried to constant weight, homogenized, and sieved in order to obtain the fraction <250μm (NF ISO 23470).

Second, hydrochloric acid with concentration [HCl] = 4 mol/l was added to a small amount of solid (D0, G0) to remove carbonates from the samples according to NF 10693. The inorganic carbon value (IC) was obtained as an elimination product of the following chemical reactions (Me - Metal ion) (16), (17):

$$MeCO_3 + 2H^+ \rightarrow Me^{2+} + H_2CO_3 \qquad (16)$$

$$H_2CO_3 \rightarrow H_2O + CO_2 \uparrow \qquad (17)$$

Subsequently the samples were dried at 60°C-70°C for 4 hours and subjected to the heat till 900°C in a gas stream in order to oxidize the carbon to carbon dioxide. The amount of formed carbon dioxide was measured via a katharometer (thermal conductivity detector) after chromatographic separation. Thereby the total carbon (TC) value is obtained and so the total organic carbon value can be calculated as follows (18):

$$TOC = TC - IC \qquad (18)$$

The organic matter content is calculated by multiplying the TOC value by the conversion factor (f=1.72). The obtained values are summarised in Table II.6.

Table II.6 TOC analysis results of the Dublin (D0) and Gothenburg (D0) sediments

Sample	Organic carbon (g/kg)	($CaCO_3$) Total (g/kg)	Organic matter (g/kg)
D0	33.5	161	60
G0	12.9	<1	22.3

The results indicate higher TOC and OM content for the Dublin sediment as well as a significant carbonates content – 16%wt of the Dublin sediment against the absence of a carbonates fraction for the Gothenburg sediment. The results are in accordance with the XRD analysis. A number of studies have investigated the correlation between the particle size distribution and the amount of organic matter in sediments – the finer the sediment is, the higher the amount of organic matter (Pelletier et al., 2011; Strong et al., 2012). The granulometric measurements demonstrated that the Dublin sediment

contains finer particles that the Gothenburg sediment.

II.2.1.4.3 Cation Exchange Capacity (CEC) measurement

Clays and organic matter give a negative charge to sediment particles. This implies that its capacity to adsorb and release cations into the solution is governed by electrostatic forces (Sposito, 2008), (Sidi et al., 2015; Toth & Ott, 1970). The Cation Exchange Capacities (CEC) value is used to evaluate the amount of exchangeable cations held by the sediment. It is a value of a net negative charge on the sediment particles originating from isomorphous substitution at the boundaries (Terzaghi, 1996). Thereby, this sediment parameter is interesting to measure from the point of view of the stabilization/solidification process. For example, a higher CEC can demand a higher amount of the binder to maintain a high pH in a system.
The CEC test for the study was conducted according to NF ISO 23470. The determination of exchangeable cations (Al, Ca, Fe, K, Mg Mn, Na) was performed using a hexamminecobalt (III) chloride solution as extractant. The sediments samples D0 and G0 were prepared according to ISO 11464 and the fraction <250μm was used for the extraction. The hexamminecobalt ions were exchanged with cations in sediments by agitating for 60 min. The difference between the initial amount of hexamminecobalt and the rest in the solution after the reaction gives a CEC value. The ICP-AES spectroscopic method was used to measure the quantity of exchangeable cations.

Table II.7 CEC results of the Dublin (D0) and Gothenburg (D0) sediments

Sample	CEC (cmol/kg)
D0	19
G0	4.2

As can be seen from Table II.7 above, D0 and G0 have a big difference in measured CEC values. This gap can be explained by the mineralogical XRD analysis (Fig. II.5) with regard to the more siliceous nature of the Gothenburg sediment and the more clayey Dublin sediment. In addition, the organic matter content is higher for the Dublin sediment (Table II.6), thereby the CEC value is higher for D0.

II.2.1.5 Operational fractionation of inorganic pollutants

II.2.1.5.1 Total Attack of the Dublin sediment and the main binding agents

The total dissolution of Dublin port sediments, also called *Total attack*, determines the total concentration of heavy metals and major chemical species in said sediments. It should be mentioned that the term “heavy metals” seems not to be appropriate to describe potential pollution/toxicity of a metal (M. Hodson, 2004), but it is used in the

current study due to its common use in the environmental literature.
The Dublin sediments, which originated from three different locations and depths within the Alexandra basin, were analysed [D0 (A), D0 (B), D0 (C)]. Pure anhydrous hydraulic binders, *i.e.* Ordinary Portland Cement (OPC) and GGBS, were also analysed.
The total attack consists of a digestion procedure of all sediment components, with help of strong acids, in order to extract even the most stable heavy metals from the crystal lattices of the minerals (de Groot et al., 1982).
After the cement manufacturing process, trace elements may be found in the final cement product (Cipurkovic et al., 2014; Gineys et al., 2011). The main sources of hazardous pollutants in cement are raw materials as well as fuels and waste combustion in the clinkering process (limestone, clay, cement kiln dust, raw mill, pet coke, scrap tires) (Arfala et al., 2018). Consequently, the incorporation of some heavy metals in clinker's anhydrous phases can be expected. (Gineys et al. (2011) in their literature review reported the presence of Cu and Ni mostly in the ferrite phase, followed by alite. Zinc can be found in silicates as well as in ferrite phases. Ground granulated blast furnace slag may also contain some amount of heavy metals depending on the original ore composition.

II.2.1.5.1.1 Total attack procedure

In order to perform the total attack, the following protocol was applied (Fig. II.7):

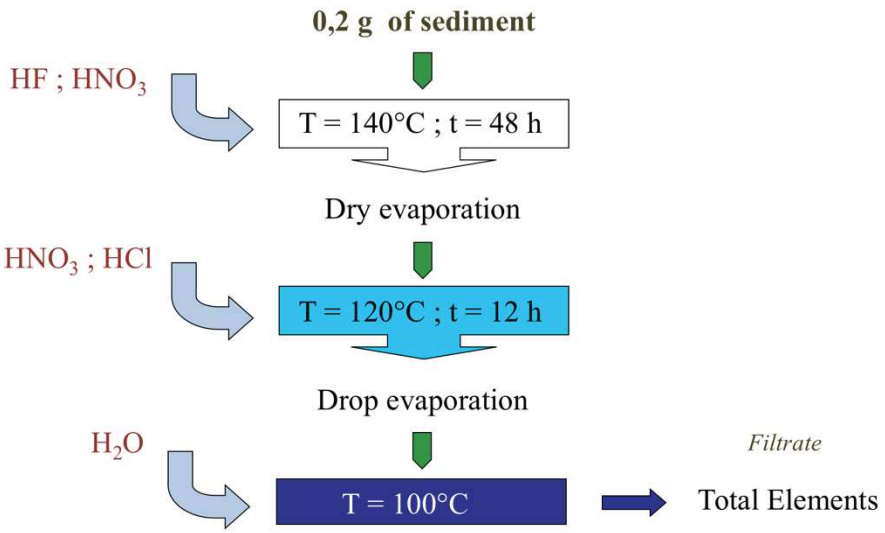

Fig. II.7 Total attack procedure

- 200 mg of particles was introduced into a polytetrafluoroethylene (PTFE) reactor.
- The first step was to add 10 mL of hydrofluoric acid (HF, 23 M Suprapur, Merck Millipore) and 5 mL of HNO_3 [HNO_3, 14M Normapur, VWR, further distillated in the laboratory at low temperature (~ 70°C) to remove trace metal impurities] and to heat

the mixture to get a temperature of 140°C for 48 h. The solution was then evaporated completely.

- The second step consisted of the addition of 6 mL of hydrochloric acid (HCl, 12M, Normapur, VWR, further distillated as for HNO_3) and 3 mL of nitric acid. The mixture was heated at 120°C for 24 h.
- The acids were finally completely evaporated to get a volume of about 0.5 mL and 10 mL of MilliQ water were added. The solution was kept at room temperature before analysis by ICP-AES or ICP-MS according to the concentration ranges.

For quality assurance, a certified reference sediment (MESS-3 provided by NRC-CNRC) was also analysed and the recovery range was from 81 to 101% with an average of 93%.

II.2.1.5.1.2 Results of the total attack of the Dublin sediment

Table II.8 provides the results of the total attack analysis of the raw Dublin sediment as well as extracted metals content for the OPC and GGBS powders.

Table II.8 Total attack results of the considered binders and the Dublin sediment (D0) from 3 different locations within the Dublin port. Concentrations are given in mg/kg. The relative standard deviations values performed on a triplicate are: 1% for Al, Ca, Cu, Mg, Ni, Sr, Ti and Zn; 3% for Co and Cr; 5% for Pb and 10% for Cd.

	D0 (A)	D0 (B)	D0 (C)	OPC	GGBS
Al	53500	54400	58400	22300	50600
Ca	76600	75600	67400	442000	327000
Fe	31900	31900	37300	21600	2000
Mg	11100	11400	11300	6300	34000
Ti	3960	3910	3860	1090	3780
Mn	560	555	552	196	1010
Co	13	13	15	6.6	4.4
Cr	70	67.8	74.8	36	12
Cu	62	63	104	230	0.49
Cd	3.7	3.6	14	0.77	0.16
Ni	35	33	43	34	1.1
Pb	252	257	872	35	0.11
Sr	260	258	232	910	332
Zn	1340	1410	4350	274	1.3

Major elements of the main sediment minerals such as Al, Ca, Fe, Mg and Ti were measured after rigorous application of the digestion procedure. The major element profiles of D0 (A) and D0 (B) are similar, however D0 (C) shows an increase in Al and Fe and a lower amount of calcium ions. For all samples, the content of the primary elements is in the following order: Ca>Al>Fe>Mg>Ti.

Regarding trace elements content of the Dublin sediment, closer inspection of the table

shows that the D0 (C) sample is the most contaminated by far. It can be seen that the amount of zinc is almost three times greater for D0 (C) than for D0 (A) and D0 (B) samples. D0 (C) also contains a large amount of Cd, Cu, and Pb compared to the two others locations in the harbour. No significant differences were noticed for Co, Cr, Ni and Sr concentrations in the three different points. The average values of the metallic abundance are in the order: Zn>Mn>Pb>Sr>Cu>Cr>Ni>Co>Cd.
With regard to the major elements of the Portland cement and GGBS, the prevalence of Ca and Fe ions can be observed for the OPC binder. On the other hand, the amount of Al and Mg is around twice as great in the case of GGBS. Portland cement presents a considerable content of trace elements compared to the ground granulated slag. Copper, strontium, and zinc metals have the values of 230mg/kg, 910 mg/kg and 274 mg/kg respectively with Cu and Sr exceeding the values of D0.

II.2.1.5.1.3 Enrichment factor

The Enrichment factor (EF) is one of the indicators used to assess heavy metal pollution and its intensity. The method of EF calculation uses the normalization of one metal concentration to the concentration of a reference element (Abrahim & Parker, 2007; Barbieri, 2016). The reference element is considered to be extremely stable in the sediment and is present at a relatively high concentration. Fe, Sr, or Al are often chosen as the reference element due to their mostly natural occurrence. In this study aluminium was used as a major constituent of clay minerals.
The Enrichment factor (EF) was calculated according to the following equation (19):

$$EF = \frac{([\,element\,]\,sample\,/\,[\,Al\,]\,sample\,)}{([\,element\,]\,reference\,/\,[\,Al\,]\,reference\,)}, \quad (19)$$

Where ‘reference’ are the values from the suitable background material. In this study the baseline reference material was adopted from (Sterckeman, 2006) with the reference values reported in Table II.9.

Table II.9 Reference values, (Sterckeman (2006))

	Al	Cd	Co	Cr	Cu	Ni	Pb	Zn
ref. values (mg/kg)	50300	0.12	11.1	65	13.6	27.8	18.6	55

According to the values obtained, the EF is used to define a pollution scale as proposed, for instance, by the French Water Agency (see Table II.10) in order to qualitatively rank the degree of environmental contamination.

Table II.10 Sediment quality according to EF

Value	Sediment quality
EF ≤ 1	Deficiency enrichment
1 < EF < 3	Minimal enrichment
3 < EF < 9	Moderate enrichment
EF ≥ 9	Very high enrichment

The results for the three sediments are displayed in Figure II.8. It can be noticed that samples D0 (A), D0 (B) and D0 (C) are highly contaminated by Cd, Pb, and Zn. The moderate enrichment factor is related to copper. Co, Cr, and Ni present a minimal contamination level. Finally, as already mentioned above, sample D0 (C) comes from the most polluted location. Note further that this kind of contamination is very conventional in a harbour because Cd, Cu, Pb, and Zn are four metals widely used for industrial purposes.

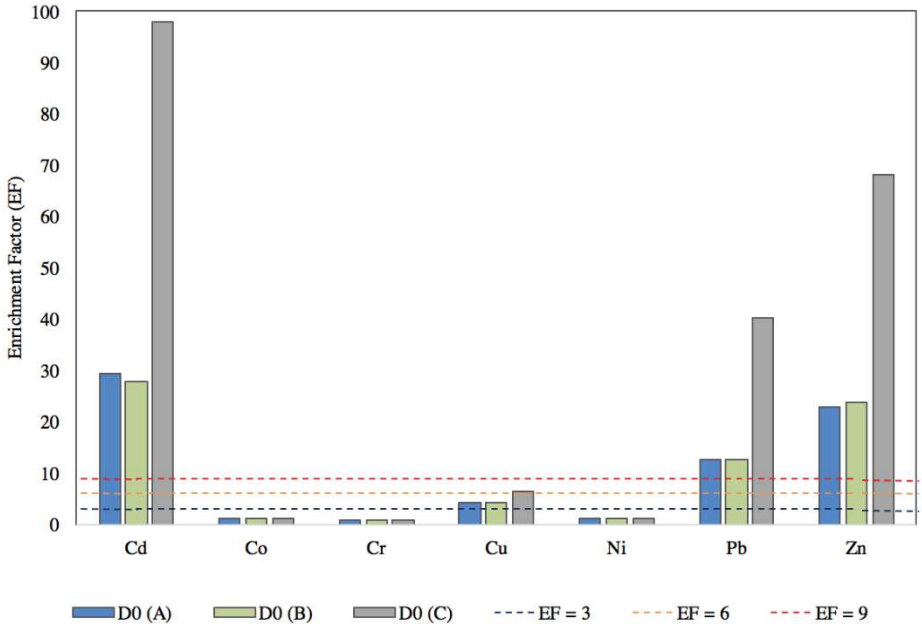

Fig. II.8 Enrichment factor of the Dublin sediment [D0 (A), D0 (B) and D0 (C)]

II.2.1.5.2 Sequential extraction of HM from the Dublin sediment

The sequential extraction method is a widely used technique for soils/sediments characterisation (Mufleh et al., 2010; Nowrouzi et al., 2014; Pagnanelli et al., 2004). The method provides a repartition of metallic elements in different sediment fractions. This fractionation technique helps to evaluate the potential risks of toxic elements according to their repartition in the sediment matrix and predicts the release of metals under different environmental conditions (Okoro & Fatoki, 2012).

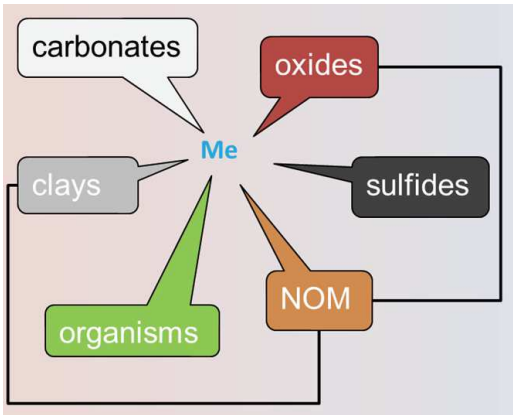

Fig. II.9 Repartition of heavy metals in different sediments' fractions. Abbreviation: NOM: Natural Organic Matter

Numerous complex extraction techniques have been proposed for the investigation of the major and trace elements repartition between the different sediment phases. The goal of these techniques is to provide information regarding the lability (that might be, to a certain extent, compared to the concept of bio-availability) of the pollutants by dissolving the sample successively with reagents of increasing aggressivity (Ahnstrom & Parker, 1999). These reagents are adapted in order to attack main sediment fractions such as clays, organic matter, carbonates, iron and manganese hydroxides, and enable the operator to keep track of the leaching rate of heavy metals for each fraction (Fig. II.9).

The first well known sequential extraction method was proposed by Tessier (1979) for cationic elements. Other methods have been developed using, for instance, different levels of acidity combined with EDTA (Maes et al., 2003). In Europe, the BCR (Community Bureau of Reference) has developed a normative procedure with a sediment reference material (CRM 701), based on the Tessier method (see Table II.11).

Table II.11 Summary of sequential extractions of heavy metals by the Tessier and BCR schemes (Vodyanitskii, 2006)

Stage no.	Tessier scheme	Stage no.	BCR scheme
1	8 ml 1 M MgCl, pH 7, shaking for 1 h (extraction of exchangeable metals)	–	–
2	8 ml 1 M acetic acid/Na acetate, pH 5, shaking for 5 h (extraction of metals bound with carbonates)	1	20 ml 0.11 M acetic acid, pH 3, shaking for 16 h (equivalent to stages 1 and 2 of the Tessier scheme)
3	20 ml 0.04 M hydrochloric hydroxylamine in 25% acetic acid, pH 2, 96°C, shaking for 6 h (reducing stage to extract metals adsorbed by Fe and Mn oxides)	2	20 ml 0.1 M hydrochloric hydroxylamine, pH 2, shaking for 16 h (reducing stage to extract metals adsorbed on Fe and Mn oxides)
4	27% hydrogen peroxide, 3.2 M ammonium acetate in 20% nitric acid (oxidizing stage to extract metals bound with organic matter, etc.)	3	27% hydrogen peroxide, 1 M ammonium acetate, pH 2 (oxidizing stage to extract heavy metals bound with organic matter)
5	Aqua regia (residual stage)	4	Aqua regia (residual stage)

II.2.1.5.2.1 Sequential extraction fractions proposed by Tessier protocol

Five main fractions are considered through the sequential extraction method proposed initially by Tessier (1979).

- *Exchangeable fraction*

The metals that are bound by the weak electrostatic interactions and that can be easily adsorbed or desorbed according to ion-exchange process are situated in this fraction. They are easily available to be released from the sediment matrix. For this purpose, some procedures use neutral salts (nitrate, chloride, or acetate salts) in order to replace the metals adsorbed on the negatively charged solid. This fraction usually represents a small proportion of leached heavy metals, except Mn, K, and Ca.

- *Carbonate fraction*

In order to extract metals bound on the carbonate phase, the sediment has to be acidified. This phase is sensitive to pH changes and 1M sodium acetate solution adjusted to pH=5 can be used in order to solubilize the carbonate phase (mainly composed of calcite). Note that some trace metals weakly associated to the organic matter and to AVS (Acid Volatile sulphides) are also likely to be leached out during the solubilisation of this fraction.

- *Reducible fraction*

Iron and manganese oxides are of the main concern of the reducible fraction of sediments. These oxides are able to accumulate trace metals due to adsorption/coprecipitation/surface complexation/penetration. These oxides are thermodynamically unstable under reducing conditions. Consequently, reagents generally used for this part of the extraction process are hydroxylamine hydrochloride in a nitric acid medium or oxalic acid/ammonium oxalate buffer (NH_4Ox/HOx) at pH 3.

- *Oxidisable fraction*

Several trace metals can be found in the organic matter fraction as specific complexes formed of trace elements with OM, or by bioaccumulation in living organisms. The degradation of organic matter in oxidizing conditions releases metals related to this phase. The organic matter has a special affinity to divalent ions in comparison to monovalent ions: Hg>Cu>Pb>Zn>Ni>Co (Filgueiras et al., 2002). The oxidants used for this phase extraction are hydrogen peroxide in an acid medium, NaOCl at pH=9.5, $Na_4P_2O_7$ at pH=9.5, or $K_4P_2O_7$. During this extraction step, trace metals associated with pyritic compounds are also leached out.

- *Residual fraction*

Several other minerals remain after the fourth extraction procedure such as refractory

oxides (*e.g.* rutile) or clays. An aqua regia solution, eventually combined with HF, allows for the extraction of the remaining metals in the sediments. As these metals are strongly bound to this refractory material, they are generally considered as inert and not bioavailable.

II.2.1.5.2.2 Procedure of sequential extraction applied in the study

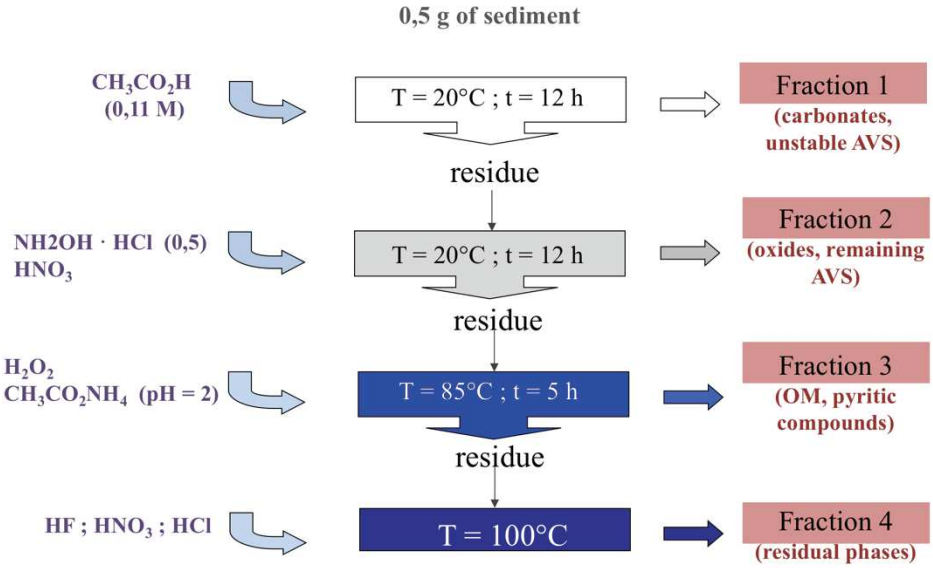

Fig. II.10 Sequential extraction procedure

In this work, the four step procedure proposed by the European Commission and validated with a certified sediment (BCR-CRM 701) has been applied (Fig. II.10). This procedure is dedicated to divalent and trivalent trace metals and certified for Cd, Cr, Cu, Ni, Pb, and Zn. In this work, it was decided to extend this to some other elements including Ca, Co, Fe, Mg, Mn, Sr, and Ti. The protocol that has been applied is precisely described in Rauret et al. (2001). Briefly:

- *Fraction 1 (F1):* The first step permitted the extraction of metals weakly adsorbed to the particles, associated with carbonate phases, and trapped in most acid volatile sulphides (AVS). 0.5 g of dry material was placed in 20 mL of acetic acid (0.11 mol/L) solution at pH=4 for 12 hours at room temperature. For the sediments previously treated with the cement, the concentration of acetic acid was increased to 1 mol L^{-1} to keep the pH value at 4 (optimisation procedure not detailed here).

- *Fraction 2 (F2):* The second step released the remaining metals associated with acid volatile sulphides, the metals associated with iron and manganese oxides, and some metals associated with organic matter into solution. 20 mL of a mixture of HNO_3 (0.05 mol L^{-1}) and a reducing reagent (hydroxylamine

hydrochloride, 0.5 mol L^{-1}) was used for a duration of 12 hours at room temperature.

- *Fraction 3 (F3):* Metals associated with pyritic compounds and refractory organic matter were extracted during the third step by heating the particles (85°C) in the presence of 2 × 5mL of hydrogen peroxide at a concentration of 9.8 mol/L and pH=2-3 for a duration of 5 hours. After reducing the volume to around 3 mL, 25 mL of ammonium acetate (1 M), adjusted to pH = 2 with HNO_3, was added to the particles to stabilize the extracted metals.

- *Fraction 4 (F4):* Finally, the last step consists of a mixture of acids as described in the section § II.2.1.5.1.1 (Total attack procedure). This allows for the recovery of the remaining metals associated with refractory materials like clays or titanium oxides.

Note that after each extraction step, the solution was centrifuged for 20 min at 3000 rpm and the supernatant was filtered at 0.45 *µ*m for trace metal analysis. The remaining particles were rinsed two times with Milli-Q water before the next step.

Finally, as this procedure is challenging, a certified reference sediment (BCR-CRM 701) was also used for quality control. For Cd, Cr, Cu, Ni, Pb, and Zn, 17 results of recovery ranged between 90 and 110%, 5 ranged between 110 and 150% and 2 ranged between 65 and 70%.

II.2.1.5.2.3 Sequential Extraction results for the major elements

The chemical fractionation of the Dublin sediment is quite similar for the three considered locations D0 (A), D0 (B) and D0 (C) (Fig. II.11, II.12, II.13).
The majority of aluminium is included in the residual fraction of the Dublin sediment (95% on average, Fraction 4). Al is mostly present in primary or secondary aluminosilicate compounds which reflects its detrital origin from natural sources (Nasr et al., 2018) (Khan et al., 2013). Almost no Al was present in the carbonate fraction (Fraction 1). In the present study, Al bound to Fe-Mn oxides (Fraction 2) or to organic matter (Nasr et al., 2018) is also negligible. In general, these results indicate that there is no risk for Al availability in the aquatic environment. In the same way, Ti as a lithogenic element is completely associated with Fraction 4 and is geochemically stable, hosted by refractory minerals (Boës et al., 2011).

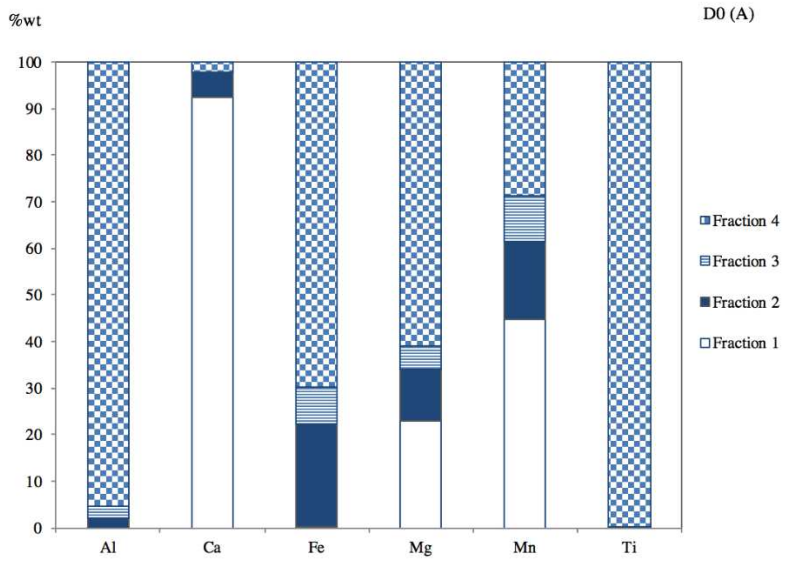

Fig. II.11 Sequential Extraction of D0 (A)

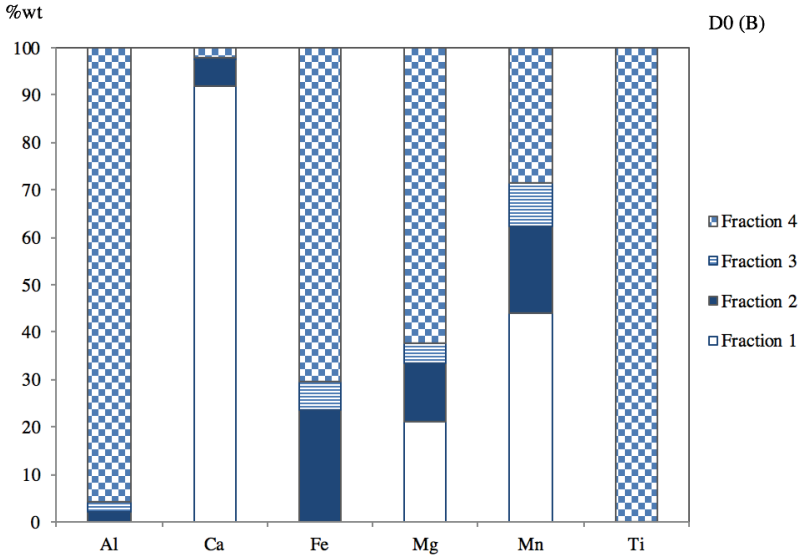

Fig. II.12 Sequential Extraction of D0 (B)

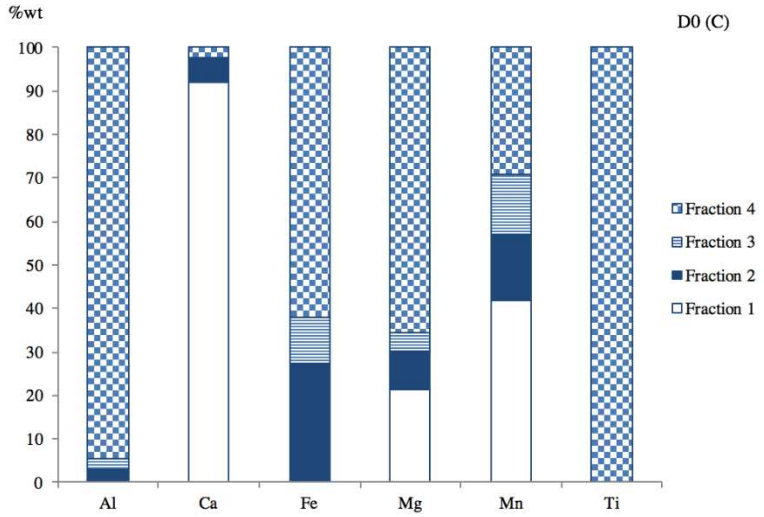

Fig. II.13 Sequential Extraction of D0 (C)

Regarding the calcium repartition among the sediment components, it showed a marked presence in the carbonate fraction with an average percentage of 92%. This significant presence of calcium in the carbonate and exchangeable fractions reflects its important mobility rate. It is generally known that Ca^{2+} ions are combined with inorganic carbon ($CaCO_3$) and to a lesser extent to phosphorous in aquatic environments (He et al., 2015). Some amount of calcium is also present in the second fraction (5-6%) due to the presence of a small fraction of more refractory Ca minerals such as dolomite.

Iron and manganese demonstrate a different geochemical pattern within the Dublin sediments. The majority of Fe (67% on average) is associated with aluminosilicate phases. This is in accordance with the XRD analysis of D0 that showed an important amount of chlorite present in the Dublin sediment. Fraction 2 contains a mixture of Fe and Mn oxyhydroxides. This fraction is more significant in the case of Fe (24% on average). It can be also attributed to the former presence of FeS (ferrous sulfides) that have been re-oxidized during the drying process (Hamilton-Taylor & Price, 1983). The large percentage of Mn is attributed to the Mn carbonate-bearing phase (~44%) and some of the Mn is located in detrital silicate minerals (~29%).

The magnesium speciation in the Dublin sediment is characterized by a high concentration in the residual fraction (~63%) and carbonate fraction (~22%). According to (Berg et al., 2019), magnesium is incorporated into the crystal structure of authigenic carbonates and aluminosilicates in sediment.

Finally, the results of the SE of the trace elements from the Dublin sediment and the sediment treated with Portland cement and GGBS-based formulations are presented in Chapter V.

II.2.2 Binders and other materials

a) GGBS and OPC

The Ordinary Portland cement was supplied by Cap Vracs Cement Group which is located in Fos-sur-Mer, France, and complied with the requirements of BS EN 197-1. The ground granulated blast furnace slag was provided by the ECOCEM factory also situated in Fos-sur-Mer. The GGBS was manufactured according to NF EN 15167-1 with a Blaine fineness of 4500 cm²/g. The chemical composition of both hydraulic binders is presented in Table II.12.

Table II.12. Chemical composition of OPC and GGBS (XRF technique)

wt%	CaO	SiO_2	Al_2O3	Fe_2O3	TiO_2	MgO	Na_2O	K_2O	SO_3	LOI
GGBS	43.9	37.6	10.26	0.33	0.81	6.93	0.22	0.26	0.03	-
OPC	64.06	20.01	3.96	3.08	0.17	1.25	0.15	0.74	5.2	1.26

b) Chemical additives

For the manufacture of the supersulfated formulation, an anhydrous calcium sulfate ($CaSO_4$) with a purity of 99% from Alfa Aesar was used. The other additives used as GGBS activators were provided by Sigma Aldrich (Na_2CO_3, $MgSO_4$, and MgO).
Dispersants used in this study were sodium hexametaphosphate (HMP) $(NaPO_3)_n$ and a phosphonate agent provided by Italmatch Chemicals group denoted as B dispersant.

II.3 Sediment-Binder Systems

II.3.1 Samples' preparation

II.3.1.1 Samples for the main case Dublin port sediment

In order to follow the evolution of the solidification process of sediments treated with hydraulic binders, the samples were prepared according to the procedure for the fabrication of standard mortars (NF 196-1). However, this procedure was slightly modified to take into account the use of raw sediment as a major element of the samples.
The sediment was first sieved to remove large aggregates (larger than 4 mm). Before being mixed with the binder, the sediment sample was allowed to settle over 24h and the bleeding water was removed. The samples were prepared with sediments having water content of approximately 45%±1.5%wt. All specimens were manufactured based on the dry binder/wet sediment ratio of 150kg/m^3 (~10,7%wt of sediment) with an estimated sediment bulk density of 1400kg/m^3.

The sediment-binder samples were manufactured as follows:

- The binder powder was first dispersed in tap water at a water-binder ratio of 0.45 to form a paste.
- The fresh paste was then gradually introduced into the sediment and mixed for 5 minutes using a mortar mixer at low speed (rotation at 140 ± 5 min^{-1}) until a homogeneous mixture was obtained. The mixing bowl was scraped after two minutes to remove unmixed components stuck to the bottom of the mixing bowl.
- Prismatic molds (40x40x160 mm) were half-filled and compacted using 60 jolts with a jolting apparatus. The same procedure was repeated after complete filling of the molds.
- The molds were wrapped with two layers of polyethylene film to prevent evaporation and maintained at constant temperature of 24°C±1°C.
- The samples were demolded as soon as a sufficient strength (hardness) was reached (Fig.II.14) and then stored in same curing conditions prior to testing (24°C±1°C and relative humidity 91%±1.5%).

Fig. II.14 Samples after demolding

II.3.1.2 Samples for the study of the impact of the nature of sediments

The Gothenburg sediment was used to help verify whether the selected binders demonstrate the same effectiveness when the S/S process is applied to sediments with different physicochemical characteristics, especially when Portland cement is replaced by a high percentage of GGBS (85%).
Both sediments were prepared for mixing in the same way as was described previously (II.3.1.1), but this time the amount of binder was doubled (to 300 kg/m^3) with the purpose of obtaining further in-depth information on the hydrates evolution by using the XRD method after the compressive strength test. All specimens were manufactured according to (NF 196-1).
For these specimens, two modes of storage were adopted prior to subsequent testing:

- T =24°C±1°C and RH= 91%±1.5%;
- T =24°C±1°C and RH= 100%.

II.3.2 Samples' characterization

II.3.2.1 Compressive Strength

The compressive strength of the binder-blended sediment samples was tested using an electromechanical press (Instron 3360, Fig.II.15) at a loading rate of 100 N/sec. The load was applied to the 40 mmx40 mm section of the horizontally placed samples. UCS strength testing was performed at curing times of 28 days, 3 months, and 6 months.

Fig.II.15 Instron 3360, Uniaxial Strength Testing

II.3.2.2 Shrinkage Test

To compare the shrinkage behaviour of two formulations – the first with only Portland cement and the second with high GGBS content - considered for the Dublin sediment S/S treatment, samples were prepared in the same way as for the compressive strength test (II.3.1.1). However, the amount of binder was doubled (to 300kg/m^3) to ensure good adhesion between the treated sediment and measurement pins. The binder-sediment mixtures were well homogenized to manufacture three specimens for each binder formulation and placed in special molds with 6 plugs in heads for the pins. The molds were protected by a plastic film and stored until sufficient hardening in order to avoid the plastic shrinkage of a fresh mixture. After demolding, the drying and endogenous shrinkage were measured at long term. The samples were stored at 24°C±1°C, and RH=91%±1.5%.

To measure the length variations of the solidified sediments, a standard length comparator for expansion and shrinkage was used. This device consists of an aluminium base with adjustable feet and two stainless steel contact pins with an electronic counter with an accuracy of 0.001 mm. A calibration rod (160mm) was used each time before samples were introduced into the apparatus. Three measurements from three samples for each formulation were recorded at each time increment (till 90 days of storage). Then the change in shrinkage-expansion was calculated with respect

to the initial sample length.

II.3.2.3 Leaching Test

The batch leaching test was carried out in order to assess the capacity of the considered binders to stabilize heavy metals. In parallel, the monolithic leaching test was performed to evaluate the stability of organic contaminates, especially tributyltin TBT (the details of the procedure and the results are given in Annex A).

The leaching test of heavy metals from the raw Dublin sediment and the treated sediment was performed according to NF EN 12457-2. The Dublin sediment mixed with 150kg/m^3 of binder was investigated. After the mechanical tests, the sample fragments were dried at 40°C for 24h. According to the standards, the leaching tests should be performed with particles smaller than 2mm, but not too fine. The particles were thus sieved between 2 mm and 0.1 mm. The test consisted of dispersing 90±5g of solid particles in 900 ml of demineralized water (pH=5-7.5 and conductivity <0.5 mS/m) for 24 hours at 10 rpm (horizontal rotation) in a room at a controlled temperature of 24°C±1°C (Fig. II.16).

Fig. II.16 Leaching apparatus

The leachates were then centrifuged to separate the solids, and filtered through vacuum filtration with filter paper with a pore size of 0.45µm to remove solid impurities. The leachates were stored in a refrigerator at 0°C before being sent to a chemistry laboratory for analysis using the ICP-MS technique.

II.3.2.4 XRD analysis

The same procedure as described in section § II.2.1.3.1 was applied to the sediments treated with hydraulic binders using a D2 PHASER apparatus from BRUKER.

II.3.2.5 Zeta Potential

The zeta potential (ζ potential) is an important electrokinetic measurement in mineral-water interfaces. When ionized solid particles become surrounded by dipolar water molecules, an electric potential occurs at the interface between these phases as a result of ionization of the surface, the adsorption of ions, or dissolution (Hunter, 1981). The ζ potential evaluates a theoretical function of electrostatic interactions between particles and is important from the point of view of dispersion-flocculation phenomena and hydrate formation in the current study. The charge of the solid particles impacts the arrangement of the surrounding ions in the liquid state – they attract the oppositely charged ions and repulse ions with equal charge (Salopek et al., 1992). The interface charge is governed by electrostatic interactions/thermic agitation and can be conceptualized as an electrical double layer.

There are several theories concerning this electrical double layer. The simplest model is the Helmholtz theory (Fig. II.17). It consists of the formation of a dense layer of oppositely charged ions on the charged surface of the particle. The second model developed by Gouy & Chapman takes into account the thermic and disordered agitation of ions but neglects the ions that are situated very close to the charged surface. Finally, the Stern model combines these two theories: it describes a dense ionic layer of counter charges (*Stern layer*) followed by a diffused layer of ions of equal charge as the surface.

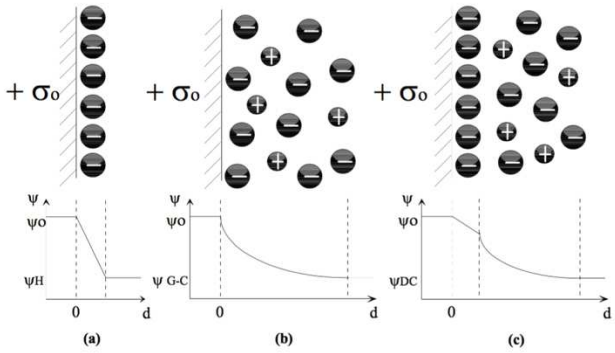

Fig. II.17 Schematic models of electric double layer

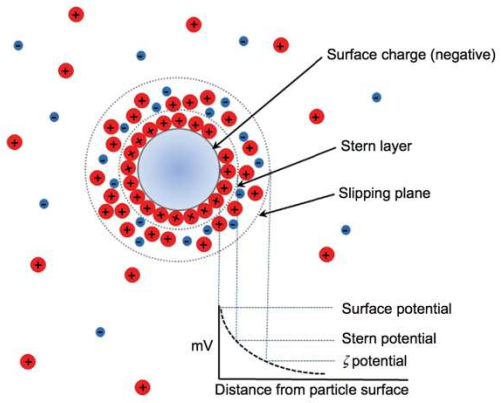

Fig. II.18 Zeta Potential according to (Pate, 2016)

Under external electric field solicitation, the particle moves with both the Stern and diffused layers. The layer between the Stern layer and diffused layer is called the 'slipping plane', which divides the immovable and diffuse parts. The zeta potential value is an average value at the level of the slipping plane situated between the Stern layer and the diffused layer: ψ (external value of diffused layer) < ζ < ψ(Stern layer) (Fig. II.18).

Mechanisms of zeta potential variations involve interparticle forces. Strong attractive forces produce a suspension with an unstable agglomerated state while a dispersed state occurs between particles through repulsive forces. The DLVO theory (Derjaguin,

Landau, Verwey and Overbeek theory) outlines the model when van der Waals forces are combined with electrostatic forces. This model describes the case when the electrostatic double layer forces and the van der Waals forces are independent; they can be overlapped or added for two particles. The ionic strength and pH of a solution are the factors that can significantly affect the ζ potential value by adjusting various forces in the system. The ionic strength has an influence on the slipping plane position, whereas an increase in pH will bring the zeta potential value to zero. This means that the overall net charge is zero (called the 'Isoelectric point') and flocculation may occur. In the binder mixes, the surface charge changes through the dissolution of the anhydrous phases and adsorption of potential-determining ions such as Ca^{2+}.
The samples for the zeta potential measurements were prepared as follows:

- *ζ potential of the raw Dublin sediment:* the raw sediment was put in demineralized water with a water:(dry) sediment ratio of 10 by taking into account the water content of the sediment (~45%);
- *ζ potential of the Dublin sediment with binders:* first, dry binder was added to the sediment at 10% per raw sediment weight. The remaining sample preparation procedure is the same as for the raw Dublin sediment.

Zeta potential measurements were carried out using a Zetaprobe Analyser from Colloidal Dynamics, performing through the electroacoustic method. The values of zeta potential, conductivity, and pH were recorded every 2 minutes with constant stirring at 250 rpm.

II.3.2.6 Rheology

Rheology represents an investigation of the deformation and flow of a matter (Vicente, 2012). Concentrated suspensions such as fresh sediment-binder mixes exhibit complex rheological behaviour due to the physical and chemical properties of the suspended particles. (Tadros, 2010) highlights four main types of particle interactions that may impact the rheology of suspensions: hard-sphere interaction, ''soft" or electrostatic interaction, steric interaction, and net attractive interaction or van de Waals attractions. Generally, sediments contain an important amount of clay particles that are expected to interact under electrostatic forces and to repulse due to increased double layers (Cruz & Peng, 2016). In the case when the electric charge of the double layer is neutral, van de Waals attractions govern the rheological behaviour of mixtures producing the maximum yield stress. Suspensions often show the same type of rheological behaviours: shear-thinning (with increasing shear rate the viscosity decreases); shear-thickening (with increasing shear rate the viscosity increases); yield stress (when the shear rate is decreased towards zero, the shear stress converges toward a constant value); viscoelasticity; etc. (Ancey, 2005). Sediments with high clay and organic matter content demonstrate a non-Newtonian nature with a high viscosity and decrease in shear rate suggesting the appearance of yield stress. Such materials

demonstrate different colloidal behaviours (thixotropy, viscoelasticity, yield stress) depending on the clay minerals, the composition of solution, CEC, pH, etc. Rheological properties may greatly impact the short and long term evolution of treated sediments, for example the mechanical strength of mixtures.
The rheological measurements were evaluated in terms of stress versus shear rate on the raw sediment and on the sediment after the addition of the binding agents. Due to the complex nature of this type of material, only qualitative analysis was undertaken. Small deformations were considered because of the probable occurrence of slippage. The yield stress of a material such as sediment is linked to the radical increase of the slope of the curve of the shear rate as a function of the stress above a certain critical stress (Chaari et al., 2003). (Chaari et al., 2003) explains the origin of the yield stress of the paste-like sludge by the required hydrodynamic drag force to break the largest flocs in the system. The addition of highly alkaline binding agents may change the rheological behaviour through increased particle attraction or flocculation. The procedure used here consisted of applying increasing shear-stresses and measuring the resulting shear-rate. The yield stress of the material is determined by the value of the stress for which a non-zero shear rate is obtained.

Fig. II.19 Rheometer AR2000ex, TA Instruments

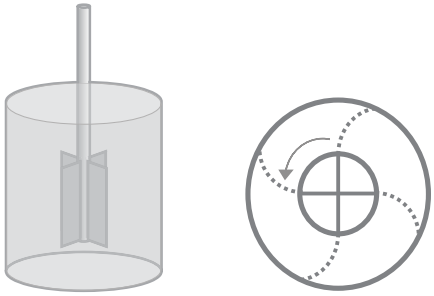

Fig. II.20 Vane geometry

The experiments were carried out with a stress-controlled rheometer AR2000ex from TA Instruments (Fig. II.19) adapted to study materials with fine particle sizes such as clay particles and binders. A constant temperature was maintained by a Peltier system at 20°C. The samples were sheared between two surfaces by rotating the central tool at a prescribed speed or torque. Vane geometry was used in this study (Fig. II.20) which allows minimal disturbance of the material and helps to avoid wall slip.

II.3.2.7 Tomography

X-ray microtomography was used in this study due to its ability to visualise the internal structure of a specimen in three dimensions in a non-destructive way, considering the relatively low mechanical properties of treated sediments. The method consists of two essential phases: acquisition of specimen projections and volume reconstruction.

During the acquisition phase, the sample is turned around the rotation axis at a specific angle while the sample is exposed to X-ray radiation. The 2D detector reconstructs the X-Ray absorption images. During this 360° rotation (Fig. II.22) a selected number of 2D radiographs is obtained (from 500 to 2000) and the volume reconstruction can be realised based on 2D projections(Hild, 2014).

Fig. II.21 Tomograph NSI (X50+)

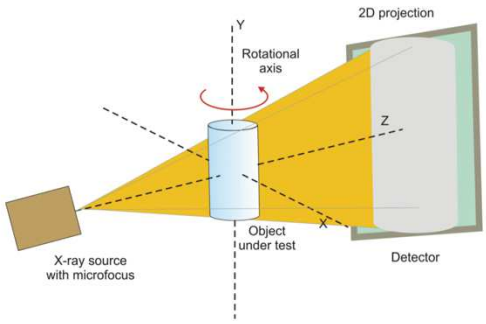

Fig. II.22 Principle of tomography technique (Hain et al., 2011)

Considering that specimens can be analysed without destructive pretreatment (physical cutting) and transformation, the samples of the Dublin sediment mixed with binders were placed in the special plastic molds (with ∅=6mm) after mixing and stored for 2.5 months at 24°C±1°C. The samples were placed in the Tomograph NSI (X50+) (Fig. II.21) directly in the molds and scanned in order to obtain a resolution of 7nm. Only comparative visual qualitative analysis of the samples was conducted in order to investigate the impact of different types of binders on the microstructure of the mixes.

II.3.2.8 SEM analysis

Scanning electron microscopy images are created when the apparatus' source of primary electrons provides enough energy to the sample's secondary electrons to be realised and collected from each point of the sample. The SEM chamber is maintained under vacuum conditions in order to prevent the interaction of electrons and gas molecules which can lower the image resolution. Furthermore, the primary electrons emitted by the SEM source are accelerated by heating or applying high energy (1-40keV). When the primary electrons reach the near surface area of a specimen, the interaction between sample's nuclei and electrons generates different signals – secondary electrons, backscattered electrons (BSE), photons, visible light (Fig. II.24). The SEM computer detector transforms these signals into images. The secondary electrons give the morphology of the sample while the backscattered electrons are responsible for the contrast of the created images (Akhtar et al., 2018).

Fig. II.23 SEM apparatus Hitachi S-3400N

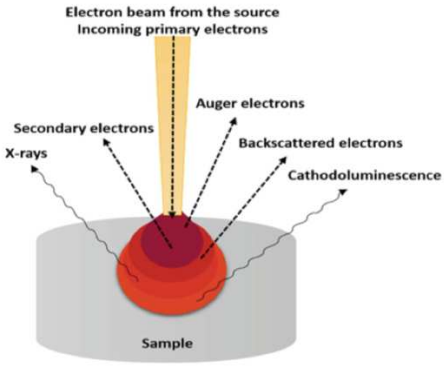

Fig. II.24 The interaction of electron beam with specimen

The apparatus used in this study was a Hitachi S-3400N (Fig. II.23). The samples for the microstructural investigation were prepared without polishing. The remaining parts of the 3 months aged specimens after the compression test were analysed. The samples were subjected to degassing and then coated with carbon as a conductive material to prevent charging of the surface, considering that samples of sediment-binder mixes are poor electrical conductors.

II.3.2.9 Solid State Nuclear magnetic resonance

One of the most powerful technique for assessing dynamics and structure of material at molecular level is Nuclear magnetic resonance (NMR). NMR signals are dependent on changes in the local environment of nuclei especially nature and numbers of the neighbours in the first coordination sphere inducing changes in molecular symmetry, bond lengths and angles. It appears as a complementary technique for mineralogical analysis of solids when amorphous phases cannot be detected by XRD analysis in the case of disordered crystalline material.

Only isotopes having non-zero nuclear spin are considered as NMR active. The basis of solid NMR spectroscopy is an interaction between nuclear spins (**I**) and an external magnetic field (B_0) (Fig. II.26), (Mehring, 1983).

The spectrometer apparatus (Fig. II.25, (Roberts, 1959)) includes a magnet, radio-frequency transmitter and oscillator and appropriate detector. Thereby the sample is placed in the magnetic field and undergone the radio-frequency field from oscillator, as a result the nuclei of atoms come into resonance in particular conditions (frequency and magnetic field strength) and produce an electromagnetic response. This response is then converted in NMR spectrum which is a fingerprint like of molecules (Roberts, 1959).

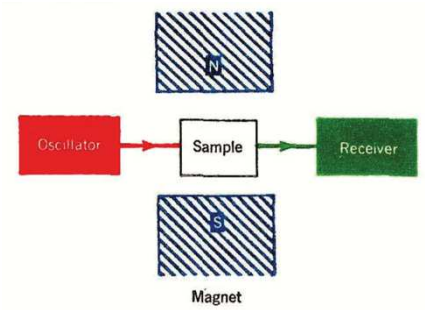

Fig. II. 25 Schematic view of NMR spectrometer

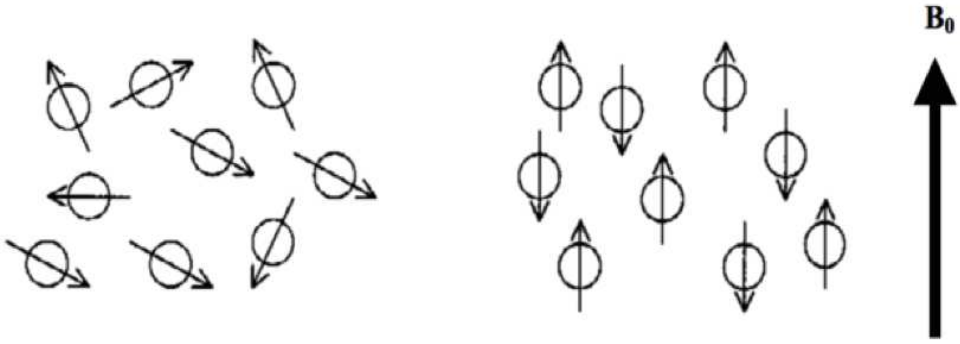

Fig. II.26 The effect of the magnetic field on the orientation of the spin magnetic moments

Depending on the state of the samples the NMR technique can be divided into two categories – solution and solid state NMR. The first one gives a high-resolution spectrum due to its low viscosity state producing rapid molecular tumbling (Chen, 2014). The solid state NMR does not have this fast molecular motion, so it conducts to broad powder patterns results. In order to cancel the interaction inducing this broadening, the magic-angle spinning method (MAS) is used (Andrew et al., 1958). This implies a fast spinning of the sample at a rotation angle of 54,74°. The spinning speed accessible range actually from few kHz to 110 kHz.

In the solid state NMR nuclei of interest, especially for hydraulic binders in both anhydrous and hydrated states, are ^{1}H, ^{13}C, ^{17}O, ^{19}F, ^{23}Na, ^{25}Mg, ^{27}Al, ^{29}Si, ^{31}P, ^{33}S, ^{35}Cl, ^{39}K, ^{43}Ca.

The study uses SS NMR method to evaluate chemical environment of ^{13}C to assess the Dublin sediment's organic matter changes in the presence of hydraulic binders.

Solid state ^{13}C cross polarization magic angle spinning nuclear magnetic resonance (CP MAS NMR) (Hartmann & Hahn, 1962) was performed in the UMR Metis of Sorbonne University Pierre and Marie Curie on a Bruker AVANCE 500 at 125 MHz for ^{13}C using 4 mm diameter zircon rotors. Cross polarization allows the magnetization transfer from ^{1}H to ^{13}C, leading to an increase in the signal/noise ratio. Magic angle spinning at 14 kHz was used to reduce chemical shift anisotropy and to average dipolar interactions, hence decreasing the linewidths. The contact time between ^{13}C and ^{1}H in the CP MAS sequence was set to 1 ms and the repetition time to 1 s.

II.3.2.10 Pyrolysis GC/MS

Analytical pyrolysis coupled with gas chromatography/mass spectrometry (GC/MS) provides structural information on a sediment's organic matter. The benefit of this approach in this study is that this analysis can help to understand changes in OM structure caused by the addition of a hydraulic binder, e.g. the degradation rate of OM. Sediment organic matter is a complex heterogeneous system in terms of its origin, degree of decomposition, etc. Therefore, different components of OM have to be fractioned to facilitate its characterisation (Mehrabanian, 2013).

The thermal pyrolysis technique decomposes the organic macromolecules into smaller organic components by cleaving the organic matter chemical bonds during heating in an oxygen free column. These smaller molecules are then separated in gas chromatography column and identified by mass spectroscopy. The identification of these molecules leads to the reconstruction of the initial chemical structure (Derenne & Quénéa, 2015).

After mixing, the samples were stored for 7 days before being subjected to water removal by a lyophilizing process in order to stop the hydration process and all types of reactions in the mixtures.

Samples were pyrolysed at a Curie temperature of 650 °C for 9.9 s using a pyrolysis unit (Pilodist), The pyrolysis unit is flushed with helium, which is also the carrier gas, and is mounted directly on the injector of a Agilent 7890B gas chromatograph (GC) coupled with a Agilent 5977B mass spectrometer (MS). The GC oven program includes a first step at 50 °C for 10 min prior to heating to 320 °C at 2 °C/min. After 10 min at 50 °C, the GC oven temperature gradually increased from 50 to 320 °C at 2 °C min^{-1}, to end by a 30 min stabilization at 320°C. The injector temperature was 280 °C in spitless mode. The ion source of the mass spectrometer was at 220 °C, which was scanned from 29 to 800 amu.

II.3.2.11 XAS (X-ray Absorption Spectroscopy)

In order to assess the distribution and speciation of metals in the complex heterogeneous system, such as a Dublin sediment before and after treatment with hydraulic binders, the XAS technique was applied.

XAS (X-ray Absorption Spectroscopy) is an element-specific and highly sensitive technique using Synchrotron as a powerful X-Ray source. Synchrotron accelerates electrons by magnets and undulators located perpendicularly to the electron beam providing strong magnetic fields, therefore the high electron energy is transformed into light (or other electromagnetic radiation) (Gaur et al., 2013). XAS consists of exiting a given atomic element to promote core electrons to continuum (photoelectric effect) and to measure the absorption coefficient as a function of the energy of the incident X-ray beam.

When X-Rays of intensity I_0 pass through a sample of thickness t (Fig. II.27), the

transmitted intensity can be described according to Beer's law, (20) (Schnohr & Ridgway, 2015a):

$$I_t(t) = I_0 e^{-\mu(E)t} \qquad (20)$$

where E – photon energy,
μ(E) - energy-dependent X-ray absorption coefficient.

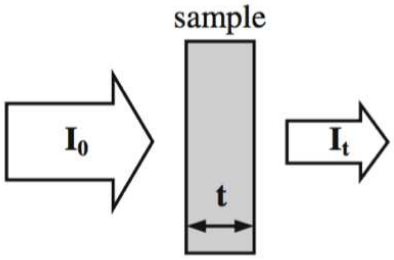

Fig. II.27 (left) Schematic of an X-Ray absorption measurement in transmission mode

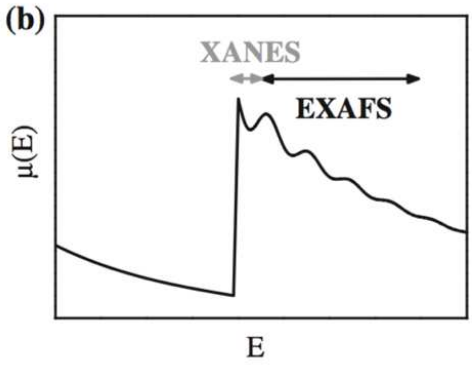

Fig. II.28 absorption coefficient μ(E) versus photon energy E including the fine structure above the edge divided into the XANES and EXAFS regions (Schnohr & Ridgway, 2015b)

XAS gives full information about the environment of the target atom including its oxidation state, coordination number/geometry/distortion, nature and spatial organization of the surrounding atoms at short distances, etc. The XAS signal can be divided into two parts: the region within about 50eV beyond the edge is called XANES (X-ray Absorption Near-Edge Structure). Because this region is characterized by the transition of photoelectrons to an unoccupied bound state, XANES provides an information about chemical bonding (oxidation state, coordination) of the atom. The region at high energy beyond 50 eV from the edge is called the EXAFS (Extended X-ray Absorption Fine Structure) Fig. II.28. This region depends on the atomic environment and thus it will provide information about local structure surrounding the absorber (coordination number, interatomic distances, etc.).
K-edge XAS characterization was performed at the Synchrotron SOLEIL (FRANCE) (Fig. II.29) at the beamline SAMBA. In the present study the speciation of Zn and Cu was investigated. Sediment-binder samples aged for three months were considered. The samples were collected from specimen remains after mechanical testing. The aggregates were ground using an agate mortar, and the obtained powder was dried in an oven at 40°C for 24h. Samples were finally prepared as pastilles of 1 mm thickness and 5 mm diameter for XAS measurements.

Fig. II.29 Synchrotron Soleil, France

II.4 Simplified models

II.4.1 Clay-Binder system

In order to study the impact of the clay fraction of sediments on the evolution of mechanical strength, the experiments described in this section were carried out on samples of pure commercial clay mixed with OPC and GGBS-based binders.

II.4.1.1 Materials

The same hydraulic binders as for the sediment treatment were used - OPC and GGBS (see § II.2.2).

The commercial clay was purchased from Argile de Velay, France (V0). The chemical analysis of the clay sample is presented in Table II.13.

Table II.13 Chemical composition of the Velay Clay (V0)

wt%	SiO_2	Al_2O_3	Fe_2O_3	MnO	CaO	K_2O	TiO_2	MgO	Na_2O	P_2O_5
Clay (V0)	42.6	25.5	8.5	11	8.2	7.1	0.8	3.5	3.05	0.25

The choice of this type of clay was made in relation to the main clay minerals of the Dublin and Gothenburg sediments which are mostly illitic clays. As can be seen in Fig. II.30 representing the XRD analysis of the clay V0, the sample contains mainly illite as well as some associated minerals such as kaolinite, montmorillonite, and calcite.

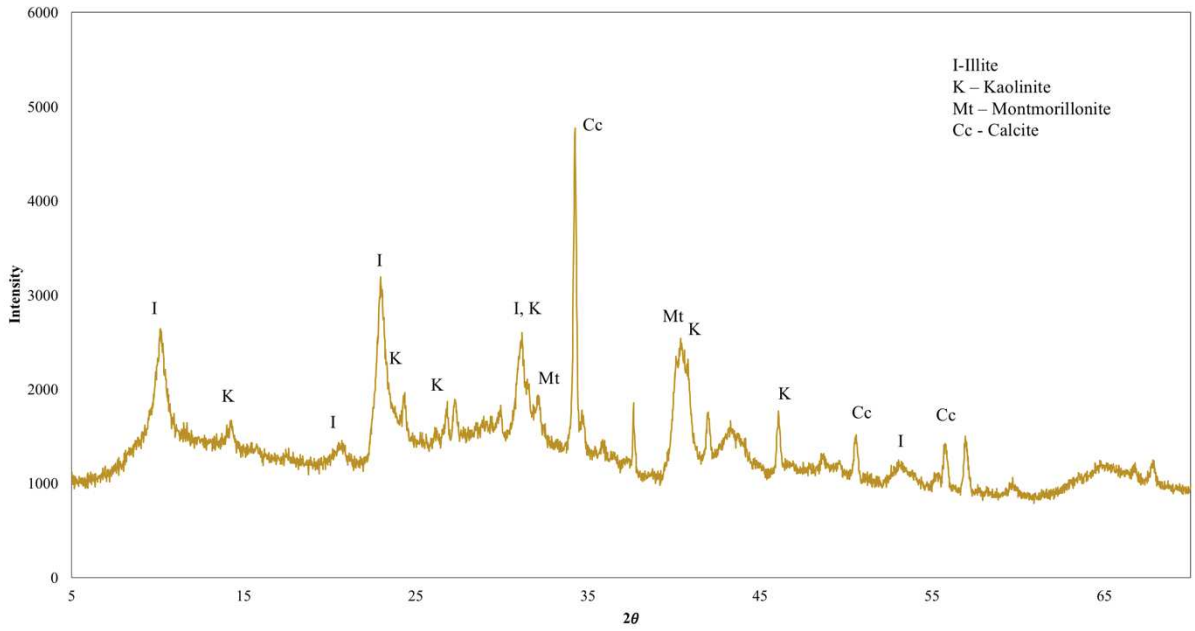

Fig. II.30 X-Ray diffraction analysis of the clay sample (V0)

II.4.1.2 Samples' preparation

In order to evaluate the impact of the clay as one of the important components of the sediments on the hydration kinetics of the binders considered for S/S treatment in this study, the samples were prepared as follows:

- First, the clay from Velay was mixed with tap water at a 0.55 clay:water ratio to ensure a good rheology of the mixture;
- The amount of the dry binder was set at 20% by weight of the wet clay mix. The hydraulic binder pastes were prepared with w:b=0.4 and then introduced in the wet clay mixture under a constant mixing speed for a total time of 5 min. The rest of the procedure was carried out according to (NF 196-1).

Two modes of storage were adopted:

- T=24°C±1°C and RH= 91%±1.5%;
- T =24°C±1°C and RH= 100%.

II.4.1.3 Samples' characterization

II.4.1.3.1 Compressive strength

UCS strength testing was performed after curing times of 28 days, 2 months, and 3 months according to the procedure described in section II.3.2.1.

II.4.1.3.2 XRD analysis

The mixtures of clay and hydraulic binders were X-rayed with the D2 PHASER apparatus from BRUKER in order to follow the formation of crystalline hydration products. The measurements were performed from 5° to 60° (2θ). More details are given in section II.2.1.3.1.

II.4.1.3.3 ^{27}Al MAS NMR investigation

The development of amorphous hydration products was assessed with the help of high resolution ^{27}Al Nuclear Magnetic Resonance. The experiment was conducted in the CEMHTI laboratory on the hydrated clay samples aged for six months. The details of the procedure are given in § II.4.2.3.2.

II.4.1.3.4 SEM analysis

The fracture surface of samples aged for three months were analysed after the compressive strength test. The procedure was the same as described in II.3.2.8.

II.4.1.3.5 Zeta Potential

Zeta potential measurements were performed on the mixtures of the pure clay introduced in the diluted interstitial solution of the hydraulic binders in order to examine the impact of the ions from both binders on the charge of the clay surface.
The interstitial solution of the OPC and GGBS-based binders was extracted after mixing with demineralized water with water:binder=4 for 10 min with magnetic stirring, then the obtained solutions were centrifuged and filtered.
Regarding sample preparation, the measurements of zeta potential were carried out with a particle concentration of 10g/100ml for 80min with constant rotation.

II.4.1.3.6 Rheology

Increasing shear-stress at increments of 5 Pa were applied to the samples and a creep response in term of shear rate was measured. The yield stress of the material was determined by the value of the stress for which a non-zero shear rate is obtained.
First, the interstitial binder solution was extracted with a water / binder ratio of 2. The rheological measurements were carried out on the samples of the clay mixed with the hydraulic binder's interstitial solution or demineralized water with clay:water=0.65 for 1 min. Section II.3.2.6 provides the details on the apparatus and geometry used in this study.

II.4.2 Heavy metals - binders' system for the investigation of early hydration

The approach of the separate interaction of heavy metals and hydraulic binders was adopted to gain a more detailed understanding of the impact of trace elements on the early hydration of the treated sediment samples.

II.4.2.1 Materials

The same hydraulic binders as for the sediment treatment were used - OPC and GGBS (see § II.2.2).

Heavy metals were added into the binders in the form of hydrated nitrate salts. They were procured from Sigma Aldrich: cadmium nitrate tetrahydrate ($Cd(NO_3)_2.4H_2O$), nickel nitrate hexahydrate ($Ni(NO_3)_2.6H_2O$), copper nitrate trihydrate ($Cu(NO_3)_2.3H_2O$), and zinc nitrate hexahydrate ($Zn(NO_3)_2.6H_2O$).

II.4.2.2 Samples' preparation

Three types of binders – 100%OPC (OPC), 85%GGBS/15%OPC (GGBS85) & Super-sulfated (85%GGBS/14%Ca_2SO_4/1%OPC) (SSC) - were mixed with heavy metals in the form of hydrated nitrate salts due to their high solubility. First, these salts were dissolved in demineralized water and then the solution was used as the mixing water with w:b=0.4. The dry binders were put in contact with water or the HM solution and mixed for 1 min before being introduced into the calorimeter cells. The remaining paste was put in small plastic molds and protected with parafilm to prevent carbonation. The samples for the XRD and NMR analysis were oven dried for 24 hours and hydration was stopped using isopropanol. The samples were analysed via XRD after 24 h and 7 days of storage. The mix-designs are presented in Table II.14.

Table II.14 Mix design of the system 'Hydraulic binders-Heavy metals'

Samples	**$Zn(NO_3)_2$ (%wt binder)**	**$Cu(NO_3)_2$ (%wt binder)**	**$Cd(NO_3)_2$ (%wt binder)**	**$Ni(NO_3)_2$ (%wt binder)**
100%OPC **(OPC)**	0%; 0.1%; 0.5%; 2%			
85%GGBS/15%OPC **(GGBS85)**				
85%GGBS/14%Ca_2SO_4/1%OPC **(SSC)**				

II.4.2.3 Samples' characterization

II.4.2.3.1 XRD analysis

The D2 PHASER apparatus from BRUKER was used for the analysis of the crystalline

phases of the hydraulic binders with and without the addition of heavy metals. The samples were X-rayed from 5° to 60° (2θ). More details are given in § II.2.1.3.1.

II.4.2.3.2 ^{27}Al and ^{29}Si MAS NMR investigation

The local environment of aluminium and silicon in the binders' systems was probed by solid state NMR in the CEMHTI laboratory in Orleans, France. In order to recognize the spectra only from hydrated phases, ^{1}H-^{29}Si and ^{1}H-^{27}Al Cross Polarization Magic Angle Spinning (CP-MAS) (Hartmann & Hahn, 1962) were performed for hydroxylated sites of Al and Si close to ^{1}H atom.
Aluminium spectra were recorded at room temperature on a Bruker AVANCE III 850MHz spectrometer (20T magnetic field). The instrument is equipped with high speed MAS probe heads with spinning speed of 30kHz in 2.5mm aluminum-free zirconia rotors. The applied resonance frequencies were 221.6 MHz for ^{27}Al and 850 MHz for ^{1}H. The MAS spectra were acquired after applying a 0.5μs short pulse (flip angle π/18) to ensure quantitative reliability of the intensities observed for the ^{27}Al central transition. Between 20000 and 30000 scans were accumulated with a 1s recycling delay.
CP-MAS spectra were acquired using a 500*μ*s contact time, around 5000 scans were added using a 1s recycling delay. The chemical shifts were referred to 1M aqueous solution of $Al(NO_3)_3$.
Silicon spectra were acquired on a Bruker AVANCE III 400 MHz (9,4 T magnetic field) spectrometer with Larmor frequency of 79.4 MHz for ^{29}Si and 400 MHz for 1H . The MAS spinning rate was fixed at 8kHz using a 7mm probehead. The MAS spectra were acquired after applying a 5μs pulse (flip angle π/4). Around 5000 scans were accumulated with a 10s recycling delay. CP-MAS spectra were acquired using a 5ms contact time, around 50000 scans were added using a 1s recycling delay. Tetramethyl silane (TMS) was used as reference compound for ^{29}Si. All the spectra were simulated using the DMFit software.

II.4.2.3.3 Isothermal calorimetry analysis

Isothermal conduction calorimetry is a largely used technique in the cement industry to evaluate the rate of hydration kinetics of different binders. When the binders are mixed with water and some chemical admixtures, exothermic reactions occur and output heat. The calorimetry test determines the heat release during the early age hydration until 7 days of storage. For example, for the pure OPC binder there are several hydration stages – dissolution of highly soluble constituents; dormant period; main peak of initial accelerating phase (C_3S); small peak of sulphate depletion and remaining aluminate hydration; decreasing rate of hydration (Frølich et al., 2016).

Fig. II.31 TAM Air Isothermal calorimeter

The Tam Air isothermal calorimeter (Fig. II.31) contains 8 coupled cells in the manner when one cell contains the sample and another one reference cell contains a blank sample which in this case is composed of 5g of sand and water. The output measurement is the difference between these two cells containing hydrated and reference samples.
Before starting the procedure according to NF EN 196-11, the apparatus must be at stable temperature and the baseline must correspond to threshold values of heat variation.
For each sample 50 g of dry binder was mixed with water for 60 s and 5 g of paste was placed immediately in the calorimeter cell. The measurements were performed for 72 hours.
The cumulative heat release of hydration was calculated without taking into account the first hour of measurements to avoid including the imbalance of the system due to the cell being opened (and thus destabilized) during sample placement.

II.4.2.3.4 Zeta Potential measurements

The electrokinetic properties of the OPC-based binder (OPC) and GGBS-based binder (GGBS85) in the presence of heavy metals salts Cu, Zn, Ni and Cd were measured in order to gain a more detailed understanding of the interaction mechanisms of trace elements and the surface of binders during primary hydration reactions.
For this purpose, the dry binders were introduced in a heavy metal solution with concentration of 50 g/L. The solution was prepared with nitrate salts at 0.5% by weight of binder.

II.4.3 Investigation of Ni and Cd in OPC and GGBS-based binders

In order to obtain a further in-depth understanding of the interaction between cadmium and nickel and the cementitious matrix, XAS and leaching tests were performed on the hydraulic binder systems containing different amounts of GGBS.

II.4.3.1 Materials

The same hydraulic binders as for the sediment treatment were used - OPC and GGBS (see § II.2.2).

Cadmium and nickel were added into the binders in the form of chloride salts. Anhydrous cadmium chloride ($CdCl_2$) and nickel chloride ($NiCl_2$) were purchased from Alfa Aesar.

II.4.3.2 Samples' preparation

The samples were prepared with water/binder ratios equal to 0.51. The heavy metals solution was used as a mixing water as well with metal salts dissolved in demineralized water at 0.5%wt of $CdCl_2$ or $NiCl_2$. After the samples were poured into plexiglass molds closed with polyethylene lids. They were stored at 23°± 1°C for 28 days. Just before analysis, the samples were ground and dried at 40°C.

Table II.15 Mix design of the considered samples

	0.5%wt $CdCl_2$	**0.5%wt $NiCl_2$**
100%OPC	0.5%CdOPC	0.5%NiOPC
50%GGBS/50%OPC	0.5%CdGGBS50	0.5%NiGGBS50
85%GGBS/14%Ca_2SO_4/1%OPC	0.5%CdSSC	0.5%NiSSC

II.4.3.3 Samples' characterization

II.4.3.3.1 Leaching test

The leaching tests were performed according to the same standards described in section II.3.2.3. For each formulation, three samples were prepared and analyzed using the ICP-MS technique. Only heavy metal leaching was investigated. Results are expressed as average values.

II.4.3.3.2 X-ray Absorption Fine Structure (XAFS) of Ni and Cd in binders

XAFS experiments were conducted at the Argonne national laboratory in Chicago at the 5-BMD beamline. Only the X-ray absorption measurements have been studied.
XAFS data analysis was performed using the ATHENA/ARTEMIS software. The software does automatically perform background reduction and normalization of the spectra. The X-ray absorption near edge structure (XANES) gives information on the local coordination environment and the element's oxidation state. This technique allows for the determination of the speciation of cadmium and nickel in samples. The radial structure function was obtained by Fourier transformation the k^3-weighted $\chi(k)$ function between 3.0 $\tilde{A}^{-1}$ and 10 $\tilde{A}^{-1}$. Then an identification analysis was carried out

to obtain information about the phases formed during sample hydration. Thus, a linear combination fit (21) is made from comparing pure phases χ function to samples between 1 and 8 $\tilde{A}^{-1}$. Above 8 $\tilde{A}^{-1}$ the signal was too noisy to be interpreted. The criterion used to determine the best combination is the minimum of the R-factor.

$$\chi_{mixture} = \sum_{i=1}^{n} f_i \chi_i \qquad (21)$$

All materials were crushed as fine as possible with a grinder. Then they were placed on an adhesive tape in order to be put in place.

Bibliography

Abrahim, G. M. S., & Parker, R. J. (2007). Assessment of heavy metal enrichment factors and the degree of contamination in marine sediments from Tamaki Estuary, Auckland, New Zealand. Environmental Monitoring and Assessment, 136(1–3), 227–238. https://doi.org/10.1007/s10661-007-9678-2

Ahnstrom, Z. S., & Parker, D. R. (1999). Development and Assessment of a Sequential Extraction Procedure for the Fractionation of Soil Cadmium. Soil Science Society of America Journal, 63(6), 1650–1658. https://doi.org/10.2136/sssaj1999.6361650x

Akhtar, K., Khan, S. A., Khan, S. B., & Asiri, A. M. (2018). Scanning Electron Microscopy: Principle and Applications in Nanomaterials Characterization. In S. K.

Sharma (Ed.), Handbook of Materials Characterization (pp. 113–145). Springer International Publishing. https://doi.org/10.1007/978-3-319-92955-2_4

Andrew, E. R., Bradbury, A., & Eades, R. G. (1958). Nuclear Magnetic Resonance Spectra from a Crystal rotated at High Speed. Nature, 182(4650), 1659–1659. https://doi.org/10.1038/1821659a0

Ancey C., Introduction to Fluid Rheology, 2005

Arfala, Y., Douch, J., Assabbane, A., Kaaouachi, K., Tian, H., & Hamdani, M. (2018). Assessment of heavy metals released into the air from the cement kilns co-burning waste: Case of Oujda cement manufacturing (Northeast Morocco). Sustainable Environment Research, 28(6), 363–373. https://doi.org/10.1016/j.serj.2018.07.005

ASTM C1308 – 08 (2017) Standard Test Method for Accelerated Leach Test for Diffusive Releases from Solidified Waste and a Computer Program to Model Diffusive, Fractional Leaching from Cylindrical Waste Forms

Barbieri, M. (2016). The Importance of Enrichment Factor (EF) and Geoaccumulation Index (Igeo) to Evaluate the Soil Contamination. Journal of Geology & Geophysics, 5(1). https://doi.org/10.4172/2381-8719.1000237

Berg, R. D., Solomon, E. A., & Teng, F.-Z. (2019). The role of marine sediment diagenesis in the modern oceanic magnesium cycle. Nature Communications, 10(1), 4371. https://doi.org/10.1038/s41467-019-12322-2

Berman, S., & correspondent. (n.d.). Port expansion project in Gothenburg – IHS Markit Dredging and Port Construction. Retrieved 16 June 2020, from https://dredgingandports.com/features/2019/port-expansion-project-in-gothenburg/

Boës, X., Rydberg, J., Martinez-Cortizas, A., Bindler, R., & Renberg, I. (2011). Evaluation of conservative lithogenic elements (Ti, Zr, Al, and Rb) to study anthropogenic element enrichments in lake sediments. Journal of Paleolimnology, 46(1), 75–87. https://doi.org/10.1007/s10933-011-9515-z

Brown, M. E. (2001). Introduction to Thermal Analysis: Techniques and Applications (2nd ed.). Springer Netherlands. https://doi.org/10.1007/0-306-48404-8

Chaari, F., Racineux, G., Poitou, A., & Chaouche, M. (2003). Rheological behavior of sewage sludge and strain-induced dewatering. Rheologica Acta, 42(3), 273–279. https://doi.org/10.1007/s00397-002-0276-5

Chen, F. (2014). Basic Principles and Applications of Solid-State NMR in Catalysis. Journal of Thermodynamics & Catalysis, 05(02). https://doi.org/10.4172/2157-7544.1000e127

Cipurkovic, A., Trumic, I., & Hod, Z. (2014). Distribution of heavy metals in Portland cement production process. 9.

Cruz, N., & Peng, Y. (2016). Rheology measurements for flotation slurries with high clay contents – A critical review. Minerals Engineering, 98, 137–150. https://doi.org/10.1016/j.mineng.2016.08.011

de Groot, A. J., Zschuppel, K. H., & Salomons, W. (1982). Standardization of methods of analysis for heavy metals in sediments. Hydrobiologia, 91(1), 689–695. https://doi.org/10.1007/BF00940158

Derenne, S., & Quénéa, K. (2015). Analytical pyrolysis as a tool to probe soil organic matter. Journal of Analytical and Applied Pyrolysis, 111, 108–120. https://doi.org/10.1016/j.jaap.2014.12.001

Dong, S., Li, Z., Chen, Q., & Wei, Z. (2017). Total organic carbon and its environmental significance for the surface sediments in groundwater recharged lakes from the Badain Jaran Desert, northwest China. Journal of Limnology, 77(1). https://doi.org/10.4081/jlimnol.2017.1667

Emerson, S., & Hedges, J. (2008). Chemical oceanography and the marine carbon cycle. Cambridge University Press.

Filgueiras, A. V., Lavilla, I., & Bendicho, C. (2002). Chemical sequential extraction for metal partitioning in environmental solid samples. Journal of Environmental Monitoring, 4(6), 823–857. https://doi.org/10.1039/b207574c

Findoráková, L., Šestinová, O., Hančuľák, J., Fedorová, E., & Špaldon, T. (2015). Thermal and Spectral Characterization of Bottom Sediment from the Water Reservoir Ružín No.1 in Eastern Slovakia. Procedia Earth and Planetary Science, 15, 839–843. https://doi.org/10.1016/j.proeps.2015.08.134

Flemming. (1995). Sorption sites in biofilms. Water Science and Technology, 32(8). https://doi.org/10.1016/0273-1223(96)00004-2

Frølich, L., Wadsö, L., & Sandberg, P. (2016). Using isothermal calorimetry to predict one day mortar strengths. Cement and Concrete Research, 88, 108–113. https://doi.org/10.1016/j.cemconres.2016.06.009

Frost, R. L. (1996). The Dehydroxylation of the Kaolinite Clay Minerals using Infrared Emission Spectroscopy. Clays and Clay Minerals, 44(5), 635–651. https://doi.org/10.1346/CCMN.1996.0440506

Gaur, A., Shrivastava, B. D., & Nigam, H. L. (2013). X-Ray Absorption Fine Structure (XAFS) Spectroscopy – A Review. 48.

Gee & Bauder, Particle-size Analysis, 1986

Gineys, N., Aouad, G., Sorrentino, F., & Damidot, D. (2011). Incorporation of trace elements in Portland cement clinker: Thresholds limits for Cu, Ni, Sn or Zn. Cement and Concrete Research, 41(11), 1177–1184. https://doi.org/10.1016/j.cemconres.2011.07.006

Hain, M., Nosko, M., & Siman, F. (2011). X-Ray Microtomography and Its Use for Non-destructive Characterisation of Materials. 4.

Hamilton-Taylor, J., & Price, N. B. (1983). The geochemistry of iron and manganese in the waters and sediments of Bolstadfjord, S.W. Norway. Estuarine, Coastal and Shelf Science, 17(1), 1–19. https://doi.org/10.1016/0272-7714(83)90041-0

Hartmann, S. R., & Hahn, E. L. (1962). Nuclear Double Resonance in the Rotating Frame. Physical Review, 128(5), 2042–2053. https://doi.org/10.1103/PhysRev.128.2042

Hasan, H. M. I., & Masoud, M. S. (2014). Thermal analysis (TGA), diffraction thermal analysis, infrared and XRD analysis for sediment samples of toubrouk city (Lybia), Thermal Analysis, 12.

Hayton, S., Nelson, C. S., Ricketts, B. D., Cooke, S., & Wedd, M. W. (2001). Effect of Mica on Particle-Size Analyses Using the Laser Diffraction Technique. Journal of Sedimentary Research, 71(3), 507–509. https://doi.org/10.1306/2DC4095B-0E47-11D7-8643000102C1865D

He, J., Liu, G. L., Zhu, D. W., Cai, J. B., Zhou, W. B., & Guo, W. W. (2015). Sequential extraction of calcium in lake sediments for investigating the cycle of phosphorus in water environment. International Journal of Environmental Science and Technology, 12(3), 1123–1136. https://doi.org/10.1007/s13762-013-0490-y

Helali, M. A., Added, A., & Oueslati, W. (2009). Note Mécanismes de fixation des métaux lourds dans les sédiments. 19.

Hunter, R. J. (1981). The Calculation of Zeta Potential. In Zeta Potential in Colloid Science (pp. 59–124). Elsevier. https://doi.org/10.1016/B978-0-12-361961-7.50007-9

Jepsen, R., Roberts, J., & Lick, W. (1997). Effects of bulk density on sediment erosion rates. Water, Air, and Soil Pollution, 99(1), 21–31. https://doi.org/10.1007/BF02406841

Khan, S., Kazi, T. G., Arain, M. B., Kolachi, N. F., Baig, J. A., Afridi, H. I., & Shah, A. Q. (2013). Evaluation of Bioavailability and Partitioning of Aluminum in Sediment Samples of Different Ecosystems by Modified Sequential Extraction Methods. CLEAN - Soil, Air, Water, 41(8), 808–815. https://doi.org/10.1002/clen.201000197

Klučáková, M. (2018). Size and Charge Evaluation of Standard Humic and Fulvic Acids as Crucial Factors to Determine Their Environmental Behavior and Impact. Frontiers in Chemistry, 6, 235. https://doi.org/10.3389/fchem.2018.00235

Maes, A., Vanthuyne, M., Cauwenberg, P., & Engels, B. (2003). Metal partitioning in a sulfidic canal sediment: Metal solubility as a function of pH combined with EDTA extraction in anoxic conditions. Science of The Total Environment, 312(1), 181–193. https://doi.org/10.1016/S0048-9697(03)00191-8

Mehrabanian, M. (2013). Molecular geochemistry of soil organic matter by pyrolysis gas chromatography/mass spectrometry (GC/MS) technique: A review. Journal of Soil Science and Environmental Management, 4(2), 11–16. https://doi.org/10.5897/JSSEM12.033

Mehring, M. (1983). Principles of High Resolution NMR in Solids (2nd ed.). Springer-Verlag. https://doi.org/10.1007/978-3-642-68756-3

Mufleh, A. E., Béchet, B., & Ruban, V. (2010). Etude des phases porteuses des polluants métalliques dans des sédiments de bassins d'infiltration des eaux pluviales. 11. H. Molinaro, F. Hild, S. Roux, La tomographie en sciences et mécanique des matériaux : voyage aux centres des matériaux, 2014

Nasr, S. M., Okbah, M. A., El-Anany, W. I., & Soliman, N. F. (2018). Chemical Fractionation of Aluminium in the Sediments of El-Burullus Lagoon of Nile Delta, Egypt. Geochemistry International, 56(2), 182–188. https://doi.org/10.1134/S0016702918020064

NF EN ISO 17892-3 Geotechnical investigation and testing - Laboratory testing of soil - Part 3 : determination of particle density - Reconnaissance et essais géotechniques - Essais de laboratoire sur les sols - Partie 3 : Détermination de la masse volumique des particules solides

NF ISO 10390 May 2005, Soil quality - Détermination of pH - Qualité du sol

NF EN ISO 10693 June 2014 Soil quality - Determination of carbonate content - Volumetric method - Qualité du sol

NF ISO 10694 June 1995Soil quality. Determination of organic and total carbon after dry combustion (elementary analysis). - Qualité du sol

NF ISO 14235 September 1998 Soil quality. Determination of organic carbon by sulfochromic oxidation. - Qualité du sol

NF EN ISO 23470 October 2018 Soil quality - Determination of effective cation exchange capacity (CEC) and exchangeable cations using a hexamminecobalt trichloride solution

NF ISO 11464 December 2006, Soil quality - Pretreatment of samples for physico-chemical analysis

NF EN 196-1 September 2016, Methods of testing cement - Part 1 : determination of strength

NF EN 12457-2 December 2002, Characterization of waste - Leaching - Compliance test for leaching of granular waste materials and sludges - Part 2 : one stage batch test at a liquid to solid ratio of 10 l/kg for materials with particle size below 4 mm (without or with size reduction)

NF EN 196-11 December 2018, Methods of testing cement - Part 11 : heat of hydration - Isothermal Conduction Calorimetry method

Nowrouzi, M., Pourkhabbaz, A., & Rezaei, M. (2014). Sequential extraction analysis of metals in sediments from the Hara Biosphere Reserve of Southern Iran. Chemical Speciation & Bioavailability, 26(4), 273–277. https://doi.org/10.3184/095422914X14141630849689

Okoro, H. K., & Fatoki, O. S. (2012). A Review of Sequential Extraction Procedures for Heavy Metals Speciation in Soil and Sediments. Journal of Environmental & Analytical Toxicology, 01(S1). https://doi.org/10.4172/scientificreports.181

Pagnanelli, F., Moscardini, E., Giuliano, V., & Toro, L. (2004). Sequential extraction of heavy metals in river sediments of an abandoned pyrite mining area: Pollution detection and affinity series. Environmental Pollution, 132(2), 189–201. https://doi.org/10.1016/j.envpol.2004.05.002

Pallasser, R., Minasny, B., & McBratney, A. B. (2013). Soil carbon determination by thermogravimetrics. PeerJ, 1, e6. https://doi.org/10.7717/peerj.6

Pate, K. (2016). Chemical metrology methods for CMP quality. ResearchGate. http://dx.doi.org/10.1016/B978-0-08-100165-3.00012-7

Pelletier, M. C., Campbell, D. E., Ho, K. T., Burgess, R. M., Audette, C. T., & Detenbeck, N. E. (2011). Can sediment total organic carbon and grain size be used to diagnose organic enrichment in estuaries? Environmental Toxicology and Chemistry, 30(3), 538–547. https://doi.org/10.1002/etc.414

Pye, K., & Blott, S. J. (2004). Particle size analysis of sediments, soils and related particulate materials for forensic purposes using laser granulometry. Forensic Science International, 144(1), 19–27. https://doi.org/10.1016/j.forsciint.2004.02.028

Roberts, J. D. (1959). Nuclear Magnetic Resonance: Applications to Organic Chemistry. McGraw-Hill Book Company, Inc. https://resolver.caltech.edu/CaltechBOOK:1959.001

Rauret et al. (2001)

Salopek, B., Krasi, D., & Filipovi, S. (1992). Measurement and application of zeta-potential

Schaanning, M. (1994). Distribution of sediment properties in coastal areas adjacent to fish farms and environmental evaluation of five locations surveyed in Oktober 1993. In 29. Norsk institutt for vannforskning. https://niva.brage.unit.no/niva-xmlui/handle/11250/207854

Schnohr, C. S., & Ridgway, M. (Eds.). (2015a). X-Ray Absorption Spectroscopy of Semiconductors. Springer-Verlag. https://doi.org/10.1007/978-3-662-44362-0

Schnohr, C. S., & Ridgway, M. C. (2015b). Introduction to X-Ray Absorption Spectroscopy. In C. S. Schnohr & M. C. Ridgway (Eds.), X-Ray Absorption Spectroscopy of Semiconductors (Vol. 190, pp. 1–26). Springer Berlin Heidelberg. https://doi.org/10.1007/978-3-662-44362-0_1

Schulz, H. D., & Zabel, M. (2006). Marine Geochemistry. 582.

Sidi, N., Aris, A. Z., Talib, S. N., Johan, S., Yusoff, T. S. T. Md., & Ismail, M. Z. (2015). Influential Factors on the Cation Exchange Capacity in Sediment of Merambong Shoal, Johor. Procedia Environmental Sciences, 30, 186–189. https://doi.org/10.1016/j.proenv.2015.10.033

Sposito, G. (2008). The chemistry of soils (2nd ed). Oxford University Press.

Strong, D. J., Flecker, R., Valdes, P. J., Wilkinson, I. P., Rees, J. G., Zong, Y. Q., Lloyd, J. M., Garrett, E., & Pancost, R. D. (2012). Organic matter distribution in the modern sediments of the Pearl River Estuary. Organic Geochemistry, 49, 68–82. https://doi.org/10.1016/j.orggeochem.2012.04.011

Tadros. (2010). Rheology of Dispersions: Principles and Applications | Wiley. Wiley.Com. https://www.wiley.com/en-us/Rheology+of+Dispersions%3A+Principles+and+Applications-p-9783527320035

Terzaghi. (1996). Soil Mechanics in Engineering Practice, 3rd Edition | Wiley. Wiley.Com. https://www.wiley.com/en-us/Soil+Mechanics+in+Engineering+Practice%2C+3rd+Edition-p-9780471086581

Toth, S. J., & Ott, A. N. (1970). Characterization of bottom sediments: Cation exchange capacity and exchangeable cation status. Environmental Science & Technology, 4(11), 935–939. https://doi.org/10.1021/es60046a005

Vicente, J. D. (2012). Rheology. https://doi.org/10.5772/2065

Vodyanitskii, Yu. N. (2006). Methods of sequential extraction of heavy metals from soils: New approaches and the mineralogical control (a review). Eurasian Soil Science, 39(10), 1074–1083. https://doi.org/10.1134/S106422930610005X

Chapter III. Solidification of contaminated sediments using GGBS-based binders

III.1 Introduction

Solidification/stabilization technology is applied to soils and sediments in order to modify and improve their engineering properties. Ordinary Portland cement and lime are the most commonly used binding agents in S/S and ground improvement practices and they were demonstrated to be effective in enhancing the mechanical properties of treated materials through primary and secondary hydration reactions. After the addition of OPC, hydrated calcium silicates (C_2SH_x, $C_3S_2H_x$), calcium aluminates (C_3AH_x, C_4AH_x), and hydrated lime $Ca(OH)_2$ are formed as the products of the primary reactions. Pozzolanic reactions occur at a later stage between hydrated lime and clay particles serving as a source of soluble silica and alumina. These secondary reactions lead to the formation of C-S-H and calcium aluminate hydrates. (Bergado et al., 1996; Chew et al., 2004).

The current study investigates the use of GGBS as a sustainable alternative material for the improvement of the mechanical properties of complex systems such as sediments. In order to achieve the required compressive strength of the treated sediments (>2 MPa), the amount of slag and the type of activation were varied. The 100% Portland cement formulation was selected as a reference because of its wide use in current S/S practices. It is known that several factors may affect the short and long term engineering properties of the treated materials such as the type of sediment, the water and organic matter content, clay content, exchangeable cations, etc. Therefore, the effect of binding agents on the development of compressive strength of sediments with different mineralogy was examined.

One of the main objectives was to better understand the mechanisms governing the hydration process of binders when mixed with sediments. For this reason, the clay fraction similar to the clay mineralogy of the Dublin sediment has been studied separately and the results are presented in this chapter. Interactions between binders and organic matter in the Dublin sediments were also assessed.

Finally, the role of particle dispersion as one of the key parameters modifying the mechanical properties and the microstructure of soils has been studied. This parameter was evaluated through rheological measurements on the original sediment as well as separately on the clay system with exchangeable ions of the two types of binders.

XRD analysis, shrinkage measurements, microtomography, and zeta potential were used as tools to investigate the evolution of the mechanical properties and to develop a deeper understanding of the beneficial use of GGBS.

III.2 Main case - S/S treatment of the Dublin port sediment

III.2.1 Compressive strength evolution of the Dublin sediment mixed with binders at 150 kg/m^3

Due to the application requirements, the Dublin sediment was mixed with the binders at 150 kg/m^3 in order to achieve the necessary strength. Different GGBS-based formulations were tested to identify the optimal formulation which satisfies both treatment criteria: solidification of the matrix and stabilization of heavy metals in the final product (Table III.1). The GGBS-based formulations were designed in two different ways. First, samples with different percentages of OPC replacement by GGBS were prepared (D2 and D3). Second, different types of GGBS activation have been tested in order to obtain a material without Portland cement (D4 – D7). Numerous studies have demonstrated the effectiveness of the use of sulfatic activation, carbonate activation, as well as the addition of MgO for the rapid development of mechanical strength of GGBS-based formulations in order to produce a durable material for different applications. In this study, the quantity of activators was limited to 5% of the total binder due to cost limitations regarding the actual conditions of the project.

Table III.1 Mix design of the considered formulations for the Dublin sediment S/S treatment

	Composition
D1	100% OPC
D2	50%OPC+50%GGBS
D3	15%OPC+85%GGBS
D4	1%OPC+85%GGBS+14%Ca_2SO_4
D5	95%GGBS+5%Na_2CO_3
D6	95%GGBS+5%$MgSO_4$
D7	95%GGBS+5%MgO

The results of the compressive strength test are presented in Figure III.1.

At 28 days, when replacing 50% of the OPC with GGBS, the strength is unchanged (comparing D1 and D2). Increasing the replacement level to 85% (D3) leads to a significant decrease of the strength at 28 days. Surprisingly, the strength is high enough in all three cases for the formulations to be used as non-structural elements, even though the binder contents are relatively low.

At 3 and 6 months the strength of the samples with OPC-activated GGBS exceeds that of the OPC-based condition (D1). In addition, the strength of the GGBS-based materials increases between 28 days and 6 months while the strength of D1 decreases. It is well known that long term performances, including mechanical strength and durability, of GGBS-based materials are superior to those of Portland cement-based materials (Divsholi et al., 2014; Shi et al., 2011, 2012; Teng et al., 2013).

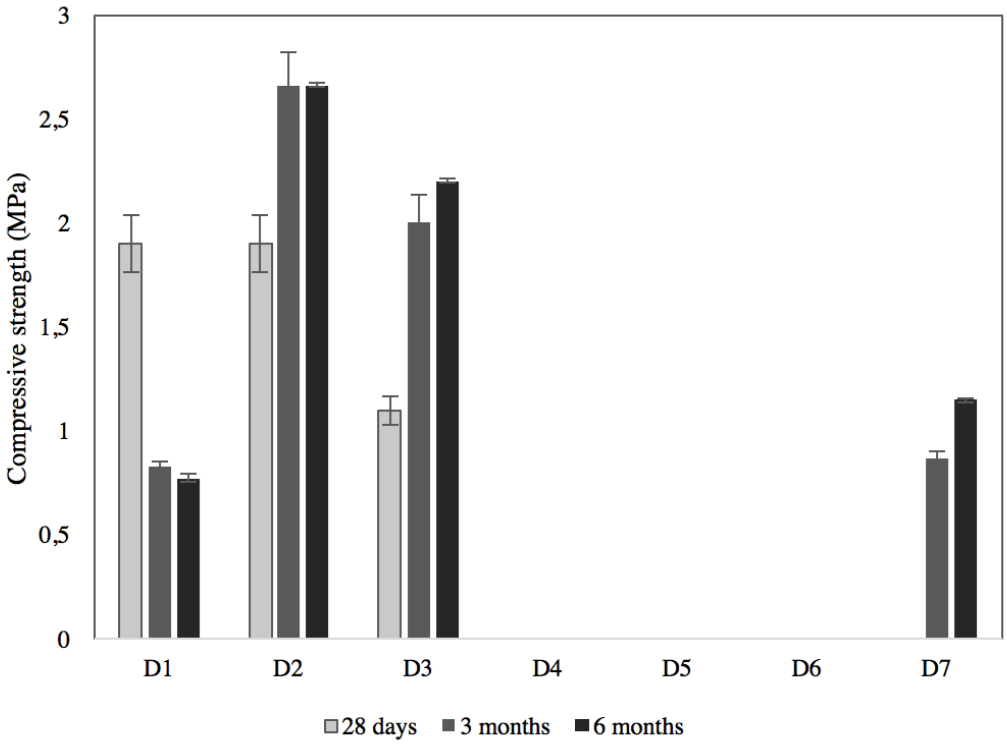

Fig. III.1 Compressive strength of the Dublin sediment mixed with different hydraulic binders at 150kg/m^3

The degradation of the strength of the OPC-based samples could be related to interactions with sediment constituents. For example, the organic matter fraction and clay fraction may potentially interfere with the hydration process of OPC (Chew et al., 2004; Gaucher & Blanc, 2006; Rekik et al., 2009; Tremblay, 2002). Carbonation may also affect the mechanical properties of the mixtures (Gervais et al., 2004) and different ions present in sediments may be considered as aggressive for the cement structures. In particular, the presence of sulfates and chlorides in the embedded marine sediment may have harmful effects for the solidified sediment's fabric (Borgne et al., 2008; kalıpcılar et al., 2016). Conversely, GGBS-based binders are characterized by high resistance to sulfate attack (Ortega et al., 2017).

The supersulfated formulations (D4 and D6) and carbonate activation (D5) did not provide a sufficient strength to be measured using the electromechanical press. The MgO activated samples (D7) achieved a strength of about 1MPa only after 3 and 6 months. At 28 days, these samples were not strong enough to be subjected to mechanical strength testing.

Based on the main Solidification/Stabilization criteria, the D3 formulation with high GGBS content was chosen as the main alternative binder to the D1 formulation and was studied using various tools in this chapter.

The following section provides pH measurements of the considered formulations as one of the main factors controlling the early strength development of the sediment after

the S/S treatment.

III.2.2 pH of the mixtures

The pH measurements are presented in Fig. III.2. The initial pH of the Dublin sediment D0 is ~8. The OPC introduction rapidly increases the pH of D1. This can be explained by highly soluble alkalines (K^+, Na^+, Ca^{2+}) being part of the chemical composition of Portland cement. The GGBS-OPC mixes D2 and D3 give a lower pH than that of D1 (12.5 and 11.8, respectively). The origin of the pH developed by D3 comes from the lower alkali content, as well as the lower portlandite content and its rapid consumption for the hydration process. In addition, the low C/S value of the C-S-H phase in GGBS-based binders is also responsible for pH buffering at lower values at long term (Richardson & Groves, 1992), (Codina, 2007).
Regarding leachates, the highest pH was achieved with D1 and D2 due to the higher alkali content. The leachate pH is slightly lower for D2. When binding agents were mixed with the Dublin sediment, the pH of the mixtures decreased due to the high water-cement ratio but also due to the presence of different pH buffers originating from the sediment: clays, sulfates, carbonates, etc. At long term (3 months) the pH value of the D1 leachates is around 12. This relatively high pH of the interporal solution of the OPC binder is maintained due to the presence of portlandite (Atkinson et al., 1989).
D3 had a pH of 11.8 once mixed with sediment. The pH of the D3 leachates at 1 and 3 months was 11.5 and 11.2, respectively. The reason for the lower pH of leachates over time of D3 can be attributed to the consumption of OH^- throughout the hydration process, especially the pozzolanic reactions.
Concerning D4 and D6, they present a dramatic decrease in pH after being mixed with the sediment compared to the other formulations. The pH values are under 10 and it is known that GGBS remains poorly dissolved in this pH range. Thus, this can explain the absence of strength of the samples because these binders did not hydrate even after 90 days of storage. Unlike D4 and D6, the pH of D5 was quite high after mixing with the sediment. However, as shown in Fig. III.2, a decrease in pH occurred over time. This may also be the reason for the lack of strength for this type of GGBS activation.
Finally, the leachate of D7 shows an increase in pH between 1 month and 3 months of storage. This pH evolution is in accordance with the appearance of strength measured only after 3 months of maturation of the samples (Fig. III.1).
The pH measurements suggest that it is extremely important to regulate the pH to the range where the hydration rate of the mixtures can provide the necessary mechanical properties. At the same time, pH values that are too high can be critical for the stabilization of heavy metals with regard to their amphoteric behaviour.

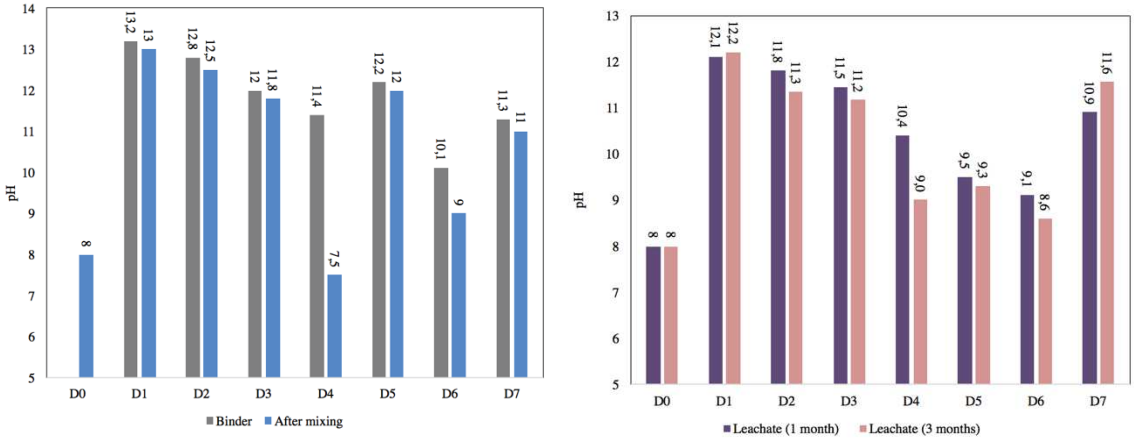

Fig. III.2 pH evolution of the binders-sediments mixtures: pH of the pure binder pastes and pH of the mixtures immediately after mixing with the binders (left); pH of the leachates (right)

III.2.3 Mineralogical analysis

XRD analysis was carried out to investigate the formation of hydration products in samples D1 and D3 mixed with a binder content of 150kg/m^3. Taking into account the low amount of binder and the amorphous nature of GGBS hydration products, XRD was finally not suitable in the case of the Dublin sediment treated with the D3 formulation. Therefore, only the analysis of the D1 mixture is presented here.
The results of the XRD measurements of D1 from 3 to 90 days are presented in Fig. III.3.

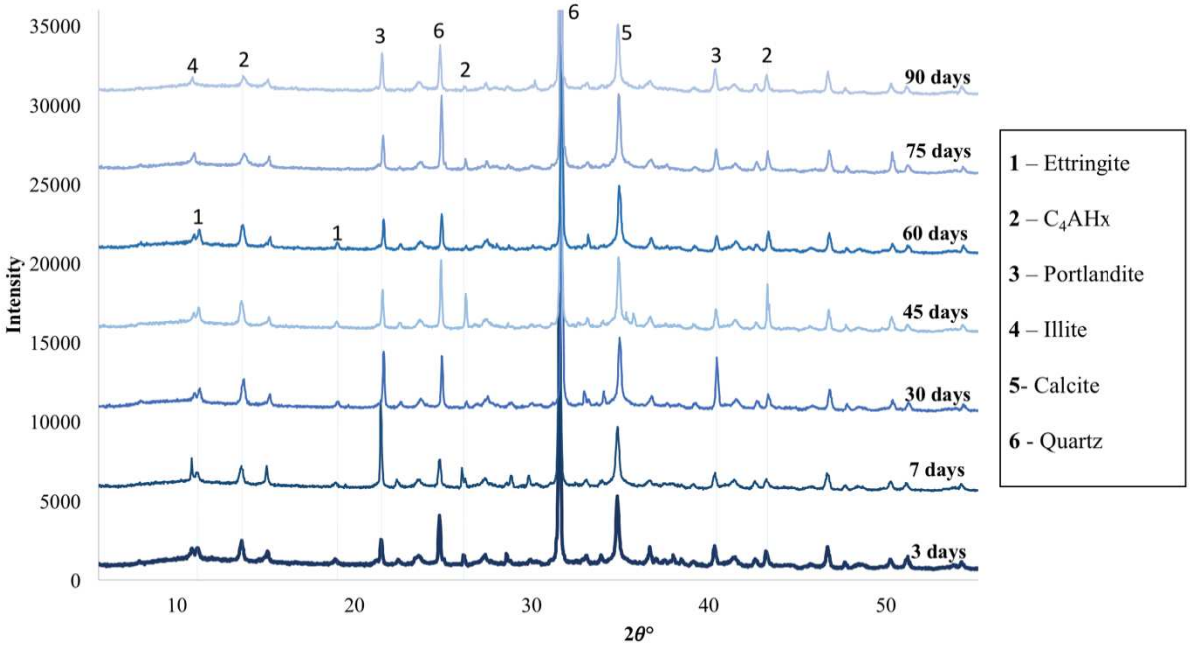

Fig.III.3 XRD analysis of D1

The hydration products identified in D1 that were precipitated after 90 days of storage are common phases for soils and sediments treated with Portland cement. The first stage of the hydration process of OPC-treated soils comprises the formation of hydrated calcium silicates (C_2SHx, C_3S_2Hx) and calcium aluminates in the form of C_3AHx and C_4AHx, as well as portlandite precipitation ($Ca(OH)_2$). At the second stage, slower pozzolanic reactions between calcium ions and silica and alumina from clay minerals occur depending on the nature of the soil. (Puppala, 2016; Wathiq Al-lJabban et al., 2017), (Dong, 2014).
As can be seen from the graph, the precipitated phases are not stable. The greatest amount of portlandite was formed between 7 and 30 days, but then its peaks decreased significantly. The ettringite phase completely disappeared after 45 days of storage. The C_4AHx phase reached its maximum at 45 days and then decreased. The reduction in the amount of these hydration products may be attributed to internal carbonation resulting from the eventual decomposition of organic matter at high pH (Mitchell, 1981). This can lead to microstructural changes and a degradation of strength. Another possible explanation may come from the reactions of the hydration phases of OPC with the clay fraction of the Dublin sediment. The XRD analysis of the 100% OPC formulation mixed with pure clay with similar mineralogy was carried out and is presented later in this chapter.
This characterization of the hydration of sediment-binder mixes was completed to corroborate the different hypotheses and for the further comparison of both formulations (D1 and D3). The shrinkage test was carried out as well as microstructural observation using microtomography and SEM analysis.

III.2.4 Shrinkage results

The results of the shrinkage test are presented in Fig. III.4. There are a number of differences in the evolution of the volumetric changes of the mixtures D1 and D3 during endogenous and drying shrinkage as well as variations in mass.
The evaporation of free water from large pores governs the early deformation of both formulations despite the storage conditions at RH=93%. Figure III.4 shows the rapid increase in deformation and mass loss for the D1 formulation after 60 days of storage. However, the D3 samples demonstrated a lower rate of deformation compared to D1, but higher loss of mass prior to 60 days. It is known that GGBS-based formulations develop a finer microstructure due to the essentially C-S-H formation that is characterized by a greater reticulation (Özbay et al., 2016).

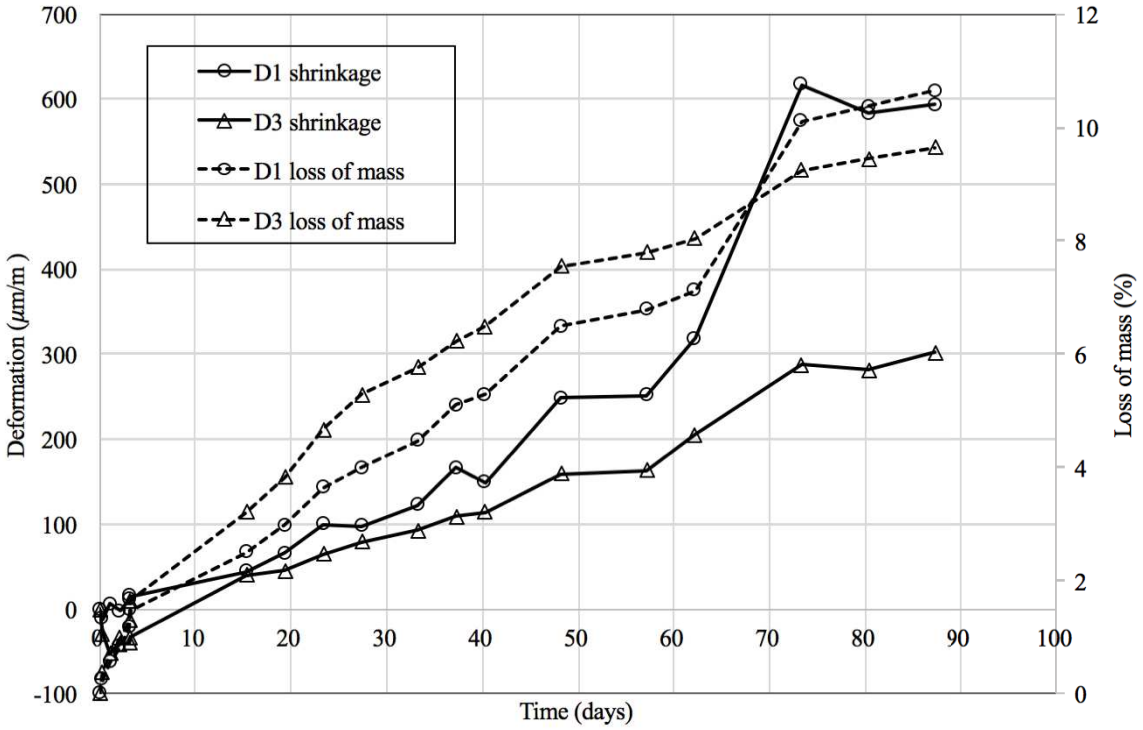

Fig. III.4 Shrinkage and loss of mass results of the D1 and D3 samples

A number of studies have investigated the shrinkage evolution when Portland cement has been partially replaced by GGBS. (Tazawa et al., 1989) shows that the use of slag in concrete and mortars increases the early age shrinkage (after 3 and 7 days). However, after 28 days the shrinkage was lower compared to the 100% OPC samples. (Yuan et al., 2015) concluded that GGBS-OPC mixtures have less free shrinkage that the samples containing only Portland cement. The study was conducted at equivalent paste volume and with the same w/c. However, there is a lack of consensus about the tendency of slag incorporation. For example, when (Brooks et al., 1992) replaced, from 30% to 70%, OPC by GGBS the same shrinkage as for the reference 100%OPC was found. (Hooton, 2004) reported almost the same tendency in his review. The results presented in Fig. III.4 are mostly in accordance with the first two references mentioned here – at long term GGBS improves the volumetric stability of the mixtures.

It is necessary to compare the results of the endogenous part of shrinkage test to the XRD results, at least for D1. The instability of some phases such as portlandite, ettringite, and CAH after 60 days of storage may lead to noticeable microstructural changes and thus to shrinkage and compressive strength degradation.

(Kalankamary P., 1968) in his study compared different types of clays treated with cement and concluded that kaolinite mixed with cement shrinks faster than montmorillonite clay mixed with cement. The general conclusion was that the type of clay is a primary function of volumetric changes. Therefore, one of the reasons for total shrinkage can be the reactions of the binders with clays due to the high pH. The potential carbonation phenomenon of the mixtures must also be taken into account.

III.2.5 Microstructure investigation

III.2.5.1 X-Ray microtomography

A qualitative approach to X-Ray microtomography was employed to visualise the microstructure of D1 and D3. The study of the microstructure and porosity of the considered materials is complex due to their low strength, and therefore the samples cannot be cut or subjected to high pressure.
The images of the samples after tomographical analysis at 75 days of storage are presented in Fig. III.5.

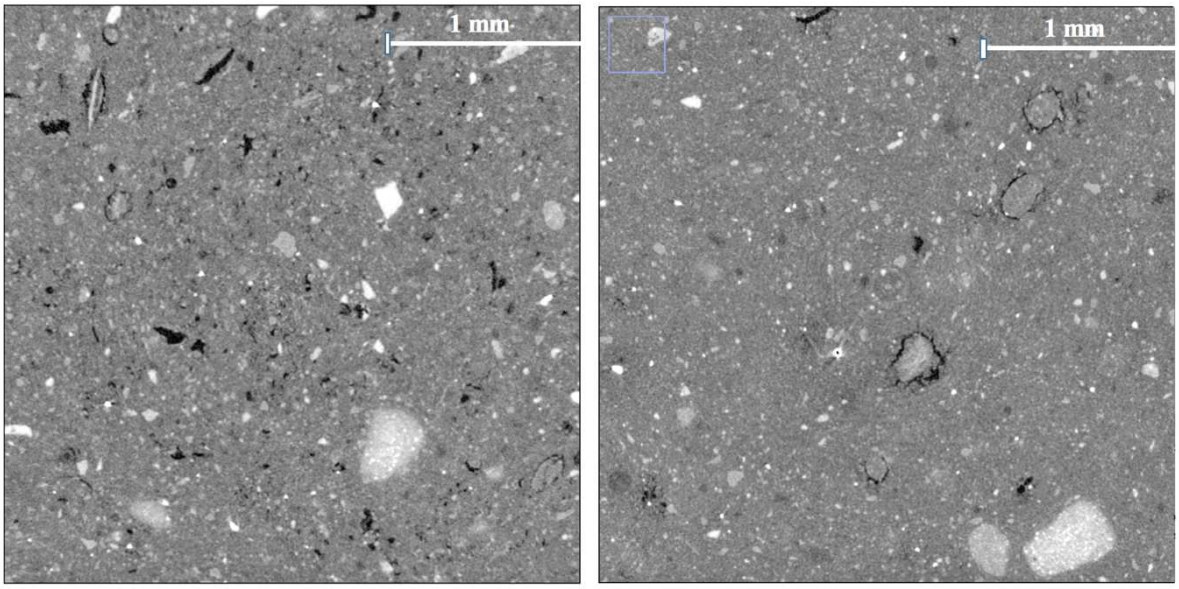

Fig. III.5 X-Ray microtomography of D1 (left) and D3 (right)

A significant difference between the two samples can be observed in term of porosity. D1 presents a very porous medium, containing many macro pores, compared to the denser structure of D3. The pore size that can be distinguished on the image of the D1 sample is in the range of 15-150 μm. The improvement in the microstructure could be due to secondary pozzolanic reactions which reduce the size and connectivity of the pores (Divsholi et al., 2014). GGBS can decrease the permeability of the mixtures – (Teng et al., 2013) highlighted the benefits of using ultrafine GGBS to reduce chloride migration.
A number of researchers have explored the role of GGBS when it is added partially to OPC in terms of improved durability through lower permeability and greater density in mortar (Condren & Pavía, 2007) . In the study of (Güneyisi & Gesoğlu, 2008), the optimal amount of GGBS for improved density and durability properties was 80% for wet cured samples.
Regarding S/S treatment, there are not many studies available exploring the role of GGBS/OPC mixes. As an example, (Jin et al., 2016) concluded in his study on soil

stabilization that GGBS activated by MgO demonstrated increased strength and durability by decreasing the permeability of mixtures due to the denser microstructure of the slag-based samples.

III.2.5.2 SEM observations

Considering the relatively low strength of the samples, the SEM images were obtained without polishing. The remaining parts of the samples stored for 3 months after the compressive strength test were collected and subjected to the degassing process and carbon deposition. On the global images (yellow area), both samples present a fracture surface with a rough texture and cracks (Fig. III.6).
The microstructure of the samples has a notable difference in the SEM images. In contrast to D1, D3 is more compact and dense, perhaps due to the more abundant gel-like C-S-H formation. D1 shows a considerable amount of pores in the range of ~10μm-40μm compared to D3. Portlandite crystals can also be distinguished in the D1 images. It should be mentioned that the D1 mixture presents an important agglomeration of particles resulting in a more open structure compared to the D3 sample containing GGBS. Sediment components such as quartz and clays are also visible in the SEM images.

D1 (100% OPC) **D3 (85%GGBS/15%OPC)**

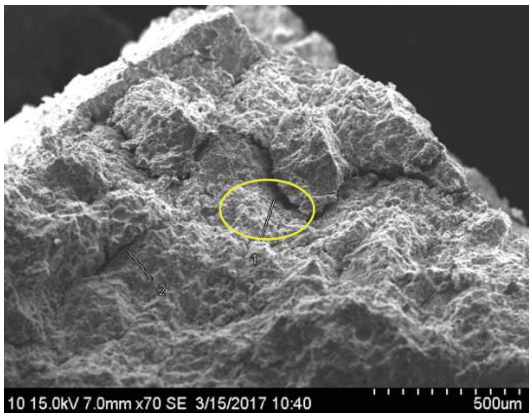

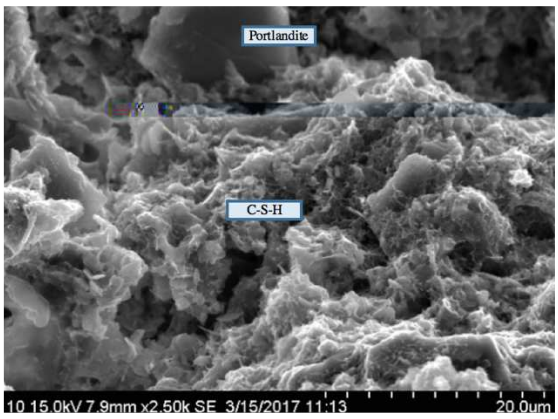

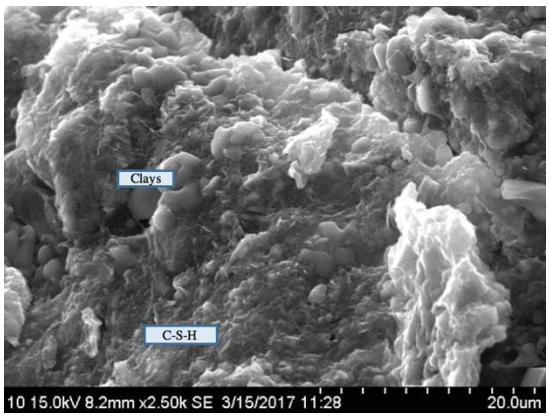

Fig. III.6 Comparative SEM analysis of the D1 and D3 samples

The microstructure investigation aimed to compare D1 and D3 in order to explain the differences in mechanical properties developed by the two formulations. Specifically, explanations for the degradation of strength of D1 and the role of GGBS in the compressive strength improvement of D3 were sought. The compressive strength differences are likely related to the denser hydrate repartition of D3 as can be seen in the SEM images and from microtomography analysis, in particular due to the C-S-H-like phase formation. D1 has developed an inhomogeneous porous structure which can have an impact on the solidification properties, as well as on the stabilization of contaminants that can be more easily leached. It can also be suggested that the significant increase in shrinkage for D1 may also result in carbonation of the hydrates. Under certain conditions (CO_2 content and humidity), carbonation can lead to a reduction in the volume of a solid and increased porosity (Thiery et al., 2004). Unfortunately, due to the high carbonate content in the Dublin sediment, it is not simple to evaluate changes in their quantity.

The zeta potential measurements provided in the next section allow for the determination of the impact of the OPC and GGBS-based binders on the surface charge of the Dublin sediment. The binders' addition can induce changes in the particle's arrangement within the sediment fabric compared to their original state and therefore have an impact on the engineering properties of the treated material.

III.2.6 Electrokinetic properties

Sediments can be described as complex colloidal systems. An electrokinetic experiment was carried out on the raw Dublin sediment and for the sediment mixed with the considered binders through zeta potential measurements in order to develop an understanding of the changes in surface charge of the sediment during the early hydration reactions. In addition to the zeta potential measurements, the apparatus recorded the pH and conductivity of the mixtures.

III.2.6.1 Results

The results of zeta potential, pH, and conductivity of the mixes D0, D1, and D3 are presented in Fig. III.7, Fig. III.8, and Fig. III.9.

The ζ potential of the untreated sediment (D0) is negative – it goes from -71.3 mV (the first measured value) and then it shows a steady evolution with a slight decrease in absolute value from -46.2 mV to -37.3 mV (Fig.III.7). The interesting aspect of this graph is that the GGBS-based mix (D3) shows almost the same electrokinetic potential evolution as the raw sample, only the first value defers – this time it is -52.1 mV. At the same time, the pH of D3 is much higher than the pH of the non-treated sediment:11.9 versus 8.3, respectively (Fig. III.8).

The evolution of ζ potential of the Dublin sediment in the presence of Portland cement presents a significant variation due to the rapid dissolution of ions from the anhydrous phases of the cement and their interaction with the sediment's constituents (e.g. adsorption) or by forming new precipitates in the solution. The lowest measured negative value was -71.5 mV and the highest positive value was +22.3 mV. It can be seen that in the presence of the OPC binder that the isoelectric point was obtained at the considered concentration. D1 produced a higher pH than D0 and D3, pH=12.3.

The conductivity values for all samples are presented in Fig. III.9. A gradual increase in conductivity can be observed for D1 and D3. However, D1 shows a greater slope with a more rapid dissolution of the cement grains compared to the GGBS-based formulation. This implies a higher amount of exchangeable ions available in the solution and therefore more considerable changes in the surface charge of the Dublin sediment at the early stage of hydration.

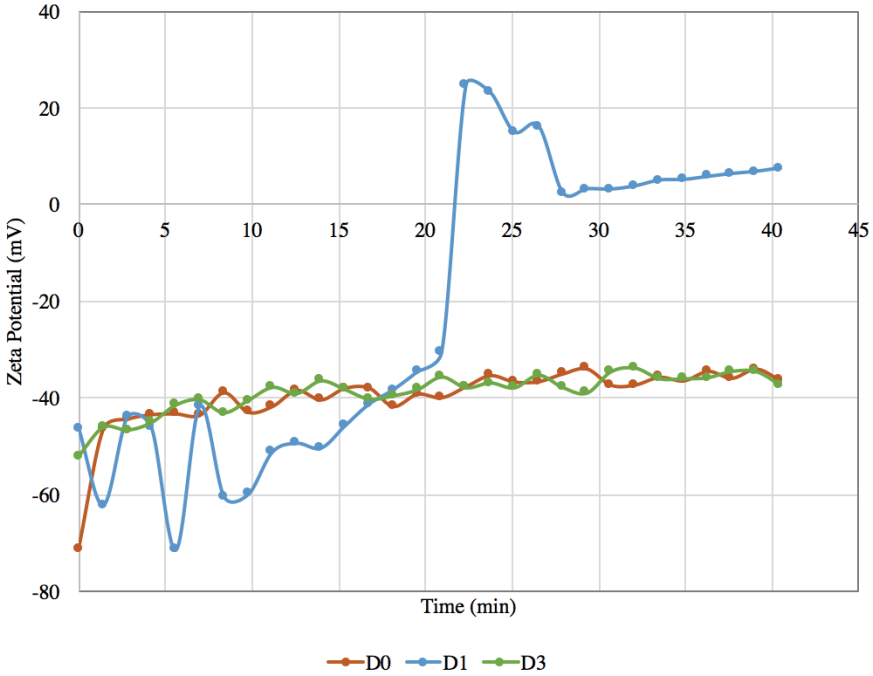

Fig. III.7 Zeta Potential of D0, D1, D3

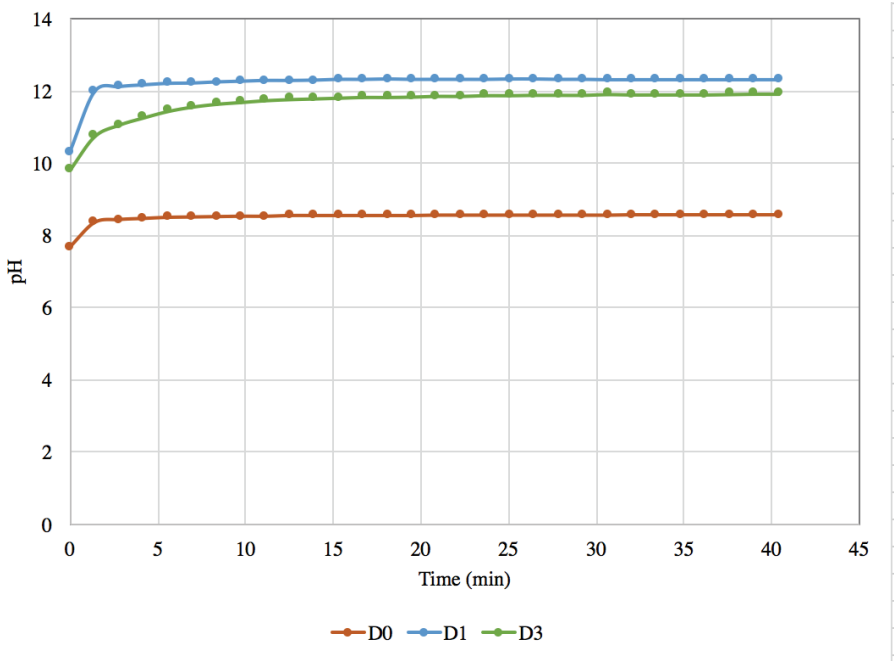

Fig. III.8 pH of D0, D1, D3

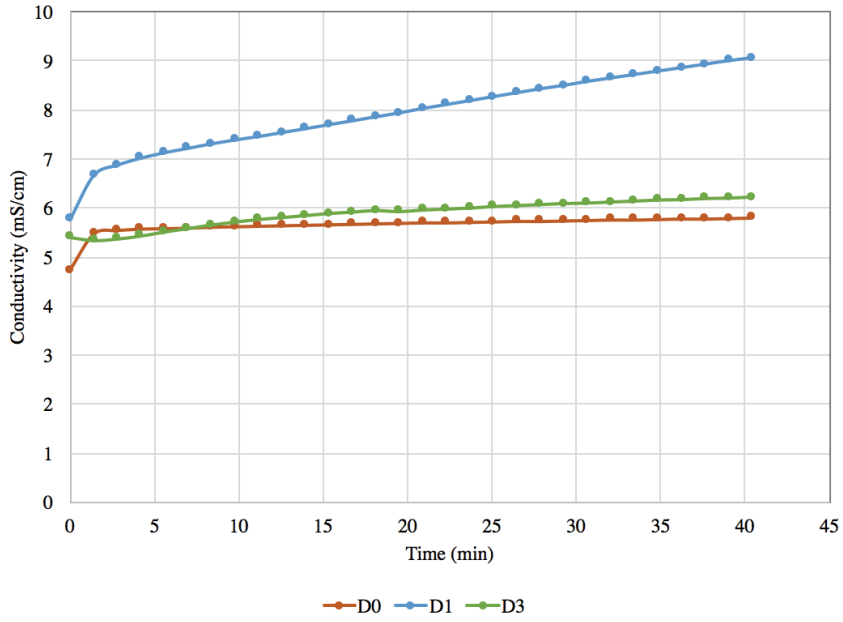

Fig. III.9 Conductivity of D0, D1, D3

III.2.6.2 Discussion

The zeta potential measurements of D1 and D3 indicate a different evolution of the sediment's surface charge in the presence of the OPC and GGBS-based formulations. The surface charge at the beginning of the hydration process can be responsible for the compressive strength evolution and will be discussed later in this chapter, in particular the flocculation/dispersion phenomenon.

Regarding the complexity of the sediment composition, it can be supposed that the main components likely to have an impact on the zeta potential of untreated sediments are clays and their CEC capacity (as well as the type of clay), organic matter, siliceous minerals, soluble ions present in the interstitial water of sediments, and also trace elements. Previous research has established that pure clay minerals present a high negative permanent charge (Sondi et al., 1996; Yukselen & Kaya, 2002). (Yukselen-Aksoy & Kaya, 2016) reported in his study that the higher the pH of a solution, a more negative ζ potential will be produced. This phenomenon arises from the dissociation of OH^- from the surface of clays due to the high pH, therefore more H^+ goes into solution and the ζ potential decreases. The same study explores the effect of different salts on changes in the zeta potential of clay minerals. Na^+ and Li^+ ions exhibit similar behaviour, the values of ζ potential remain negative and do not pass through the zero point charge. However, the introduction of a calcium salt into the clay suspension produces a much more positive charge on the surface of a clay due to the important replacing capacity of calcium compared to the other ions, and the precipitation of calcium hydroxides at alkaline pH (Yukselen-Aksoy & Kaya, 2016).
The pH-dependent behaviour of the Dublin sediment can be explained by the significant amount of illite and chlorite minerals, as well as by the organic matter content. (Sondi et al., 1996) investigated the electrokinetic behaviour of three types of clay minerals (illite, chlorite, and montmorillonite) as well as the influence of organic soil components, in particular FA (fulvic acid), on the development of the zeta potential of complex clay mixtures. The significant affinity for calcium ions and the charge reversal (from negative to positive) was obtained for the chlorite minerals producing the flocculation state. The capacity of organic substances to modify the electrokinetic response of a complex soil matrix has also been investigated by (Sondi et al., 1996). The surface of chlorite showed a noticeable increase in negative values in the presence of FA, at the same time illite and montmorillonite were less impacted.
The impact of calcium ions on the negatively charged FA suspension was also briefly discussed in the study of (Sondi et al., 1996) – the compensation of a negative surface charge by calcium cations can have a significant impact on changes in the charge of the suspensions. The strongly negative values of the zeta potential of an organic soil have also been reported by (Moayedi et al., 2011), however in the presence of Portland cement and $CaCl_2$ ions, the reverse positive charge was produced.

III.2.7 Conclusions

This section has attempted to provide a detailed understanding of the hydration of the treated Dublin sediment with OPC and GGBS-based binders. Some limitations have been encountered. The relatively low content of binding agent content as well as the very large number of potentially disturbing sediment constituents are the key parameters for a better understanding of the mechanisms of the hydration processes. The following section of this document compares the results of the compressive

strength and hydrate formation of two sediments with different natures and origins, treated with OPC and GGBS-based binders. This time the quantity of the binding agents was doubled. Moreover, the clay and organic matter fractions will be considered separately to obtain more data on the interaction of the binders with certain major components of the sediments through the study of simplified binder systems.

III.3 Study of the various factors impacting the evolution of compressive strength during S/S treatment

III.3.1 Impact of the nature of sediments

The origin of a sediment is one of the factors that can affect the solidification process. To investigate this parameter, the stabilisation of the Gothenburg sediment (G) by hydraulic binders was studied. The Gothenburg sediment has a significant siliceous fraction and a considerably lower amount of organic matter compared to the Dublin sediment (D), as well as no carbonate fraction. The characterization was conducted through compressive strength testing, pH measurements, and XRD.
The mix design for each sample prepared for this study is presented in Table III.2.

Table III.2 Mix design of the samples (D – Dublin sediment, G – Gothenburg sediment)

	Binder content in kg per m^3 of sediment	
Samples	**OPC**	**GGBS**
100%OPC (D-OPC, G-OPC)	300	-
85%GGBS/15%OPC (D-GGBS, G-GGBS)	45	255

The pH was measured after each compressive strength test. The samples were dried at 40°C, submerged in demineralized water counting 5-times the sample's volume and agitated.
For a better evaluation of the hydration product development via XRD, the amount of a binder was increased to 300 kg/m^3. The storage conditions were also changed. RH=100% was maintained in a special desiccator to prevent/limit CO_2 penetration.
It is possible to hypothesise that CO_2 can significantly impact the stability of precipitated hydrates. There are several reactions that can be produced in the presence of CO_2 that cause the degradation of mechanical properties of the mixtures. Briefly, due to the CO_2 penetration carbonic acid (H_2CO_3) is formed (see reactions 23, and 24) which is an instable molecule (Cazalet, 2012; Thiery et al., 2004):

$$H_2CO_3 \leftrightarrow HCO_3^- + H^+ \quad (23)$$
$$HCO_3^- \leftrightarrow CO_3^{2-} + H^+ \quad (24)$$

In alkaline media, CO_3^{2-} is a predominant ion. The carbonation of portlandite can be described through reactions 25 and 26:

$$Ca(OH)_2 \leftrightarrow Ca^{2+} + 2OH^- \quad (25)$$
$$Ca^{2+} + CO_3^{2-} \leftrightarrow CaCO_3 \quad (26)$$

It can be seen that the portlandite dissolution due to the pH drop (conversion of hydroxides to carbonate species, (Gervais et al., 2004)) will induce the formation of calcium carbonates. Once portlandite is depleted, carbonation of the C-S-H phase can occur by decalcification. The formation of $CaCO_3$ as well as the amorphous siliceous gel and water may take place according to reaction 27:

$$CaO_xSiO_{2y}H_2O_z + xH_2CO_3 \rightarrow xCaCO_3 + ySiO_2.tH_2O + (x - t + z)H_2O \quad (27)$$

III.3.1.1 Compressive strength results and pH measurements

Figure III.10 presents the results of the compressive strength of the Dublin (D0) and Gothenburg (G0) sediments mixed with 100%OPC (D-OPC and G-OPC) and 85%GGBS/15%OPC (D-GGBS and G-GGBS) at 300 kg/m^3 in order to investigate the impact of GGBS on the development of the mechanical strength of sediments with different mineralogies.

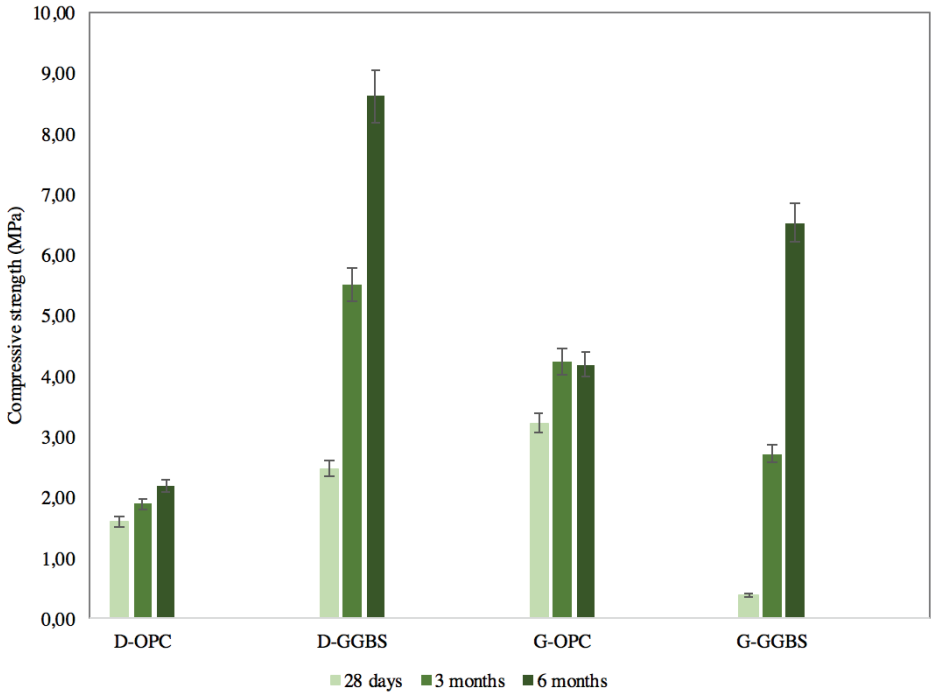

Fig. III.10 Compressive strength evolution of the OPC and GGBS-based formulations mixed with the Dublin and Gothenburg sediments at 300kg/m^3

GGBS significantly improved the compressive strength of both sediments at long term. The strength of D-GGBS is 3.5 times greater than that of D-OPC and G-GGBS is 1.5 times greater than G-OPC at 6 months of storage. Regarding D-OPC, in this case no degradation was observed compared to Fig. III.1. This evolution is probably due to the higher binder content and the different storage conditions. (Wathiq Al-lJabban et al., 2017) demonstrated that a small amount (1, 2, 4%wt) of the Portland cement binder tested on a clayey silt soil shows a decrease in mechanical properties after 28 days of storage or a stagnation of the strength development compared to the higher binder contents.

At the same time, the compressive strength was doubled when the same formulation was applied to the Gothenburg sediment. The G-OPC formulation showed an increase in compressive strength prior to 3 months of storage, but a slight decrease was then observed.

The strength values of the G-GGBS formulation were quite low after 28 days of storage compared to all of the other samples, however the results after 3 and 6 months were high and after 6 months the strength exceeded that of the Portland cement-based formulation (G-OPC).

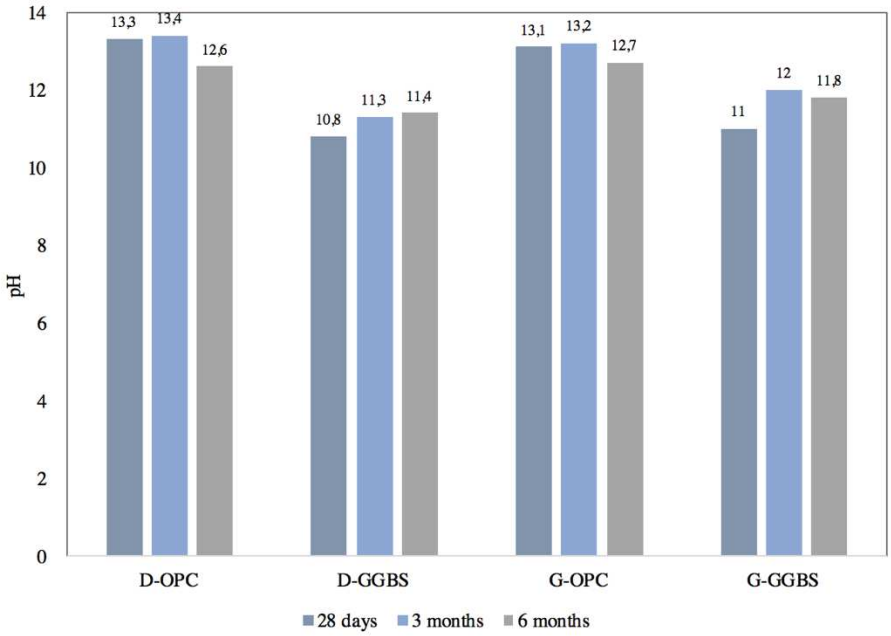

Fig. III.11 pH of the mixtures D-OPC, D-GGBS, G-OPC, G-GGBS

The pH measurements of the considered mixtures are presented in Fig. III.11. It can be seen that the pH of both 100% OPC formulations (D-OPC, G-OPC) were quite stable up to 3 months, but then it decreased, probably due to pozzolanic reactions with clays. A reduction in pH was observed and explained by (Wilkinson et al., 2010) as a consequence of the interaction between soils and cements over time. In some cases, an increase in mechanical strength occurs through pozzolanic reactions which are accompanied by the depletion of hydroxyl ions. The GGBS-based formulations (D-

GGBS, G-GGBS) develop a lower pH compared to 100% OPC.

III.3.1.2 XRD analysis of the Dublin and Gothenburg sediments mixed with the binders

Fig. III.12 and Fig. III.13 present the XRD analyses of the Dublin sediment mixed with the OPC and GGBS-based binders (D-PC and D-GGBS). The samples after 28 days, 3 and 6 months of storage were analysed and compared to the raw Dublin sediment (D0).

For D-OPC, a decrease in the intensity of the illite and kaolinite peaks can be observed. This can be attributed to the pozzolanic reaction of the cement with clays. However, this time the portlandite and ettringite phases, as well as C_4AH_x are relatively stable between 3 and 6 months in contrast to the samples with 150 kg/m^3 of OPC (see Fig. III.3). This can be related to the storage conditions and to the higher binder content. Regarding D-GGBS, no crystalline hydration phases can be observed except for the low intensity peak of the C_4AH_x phase at 28 days of storage, which thereafter disappears. The amount of clays (illite, kaolinite, and montmorillonite) is likely to decrease over time. This could mean that there is a place for the pozzolanic reaction to occur over time which takes place at pH≥105 (Eades and Grim) when silicates and aluminates become soluble (Fig. III.14). The other minerals of the Dublin sediment such as calcite and quartz do not seem to be affected.

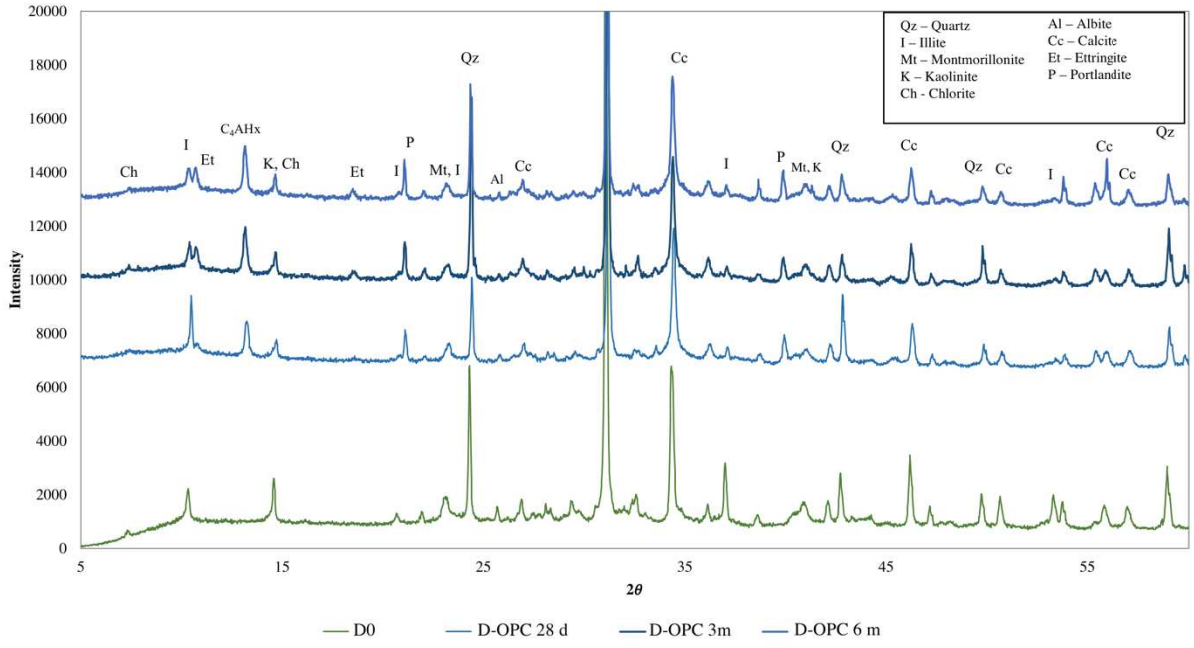

Fig. III.12 XRD analysis of D-OPC

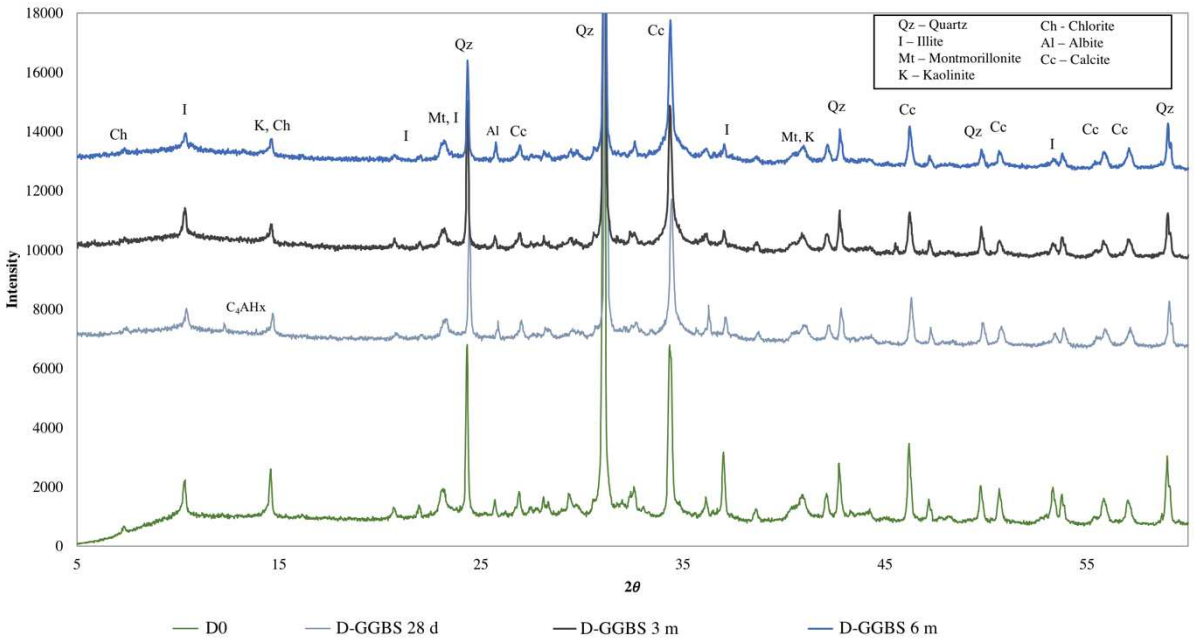

Fig. III.13 XRD analysis of D-GGBS

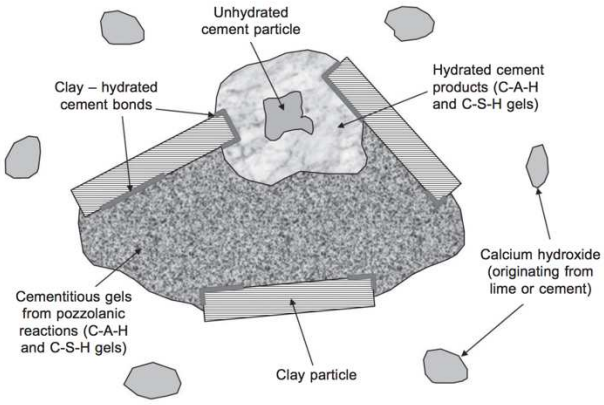

Fig.III.14 Schematic pozzolanic reaction (P. Sargent, 2015)

Figures III.15 and III.16 present the X-ray diffractograms of G-OPC and G-GGBS. As in the case of D-OPC and D-GGBS, G-OPC shows more crystalline hydration products formation compared to G-GGBS. The growth of the portlandite, ettringite and C_4AH_x phases can be observed over time. G-OPC shows stable phase development. For G-GGBS there are fewer peaks of hydration products, except for the formation of ettringite at long term, and of the unstable C_4AHx phase. It can be concluded that in the case of G-GGBS mostly amorphous phases were produced inducing a higher strength measured after 3 and 6 months compared to the G-OPC samples.

The same trend occurred for the clay fraction of the Gothenburg sediment as in the case of the Dublin sediment mixed with the hydraulic binders; a steady decline in the intensity over time for illite and montmorillonite. These results are in line with previous studies concerning cement-clay interactions. (Gaucher & Blanc, 2006) reviewed the literature on the impact of an aggressive alkaline cement medium on the stability of

clay minerals as a function of clay reactivity (illite, kaolinite, and montmorillonite) and non-clays (micas, calcite, carbonates, sulfates, cristobalites, etc.) under alkaline conditions. One of the possible scenarios is the dissolution of clay as well as the dissolution of accessory minerals and further pH buffering limiting the pH rise. Therefore, the precipitation of C-S-H and C-A-S-H can be expected.

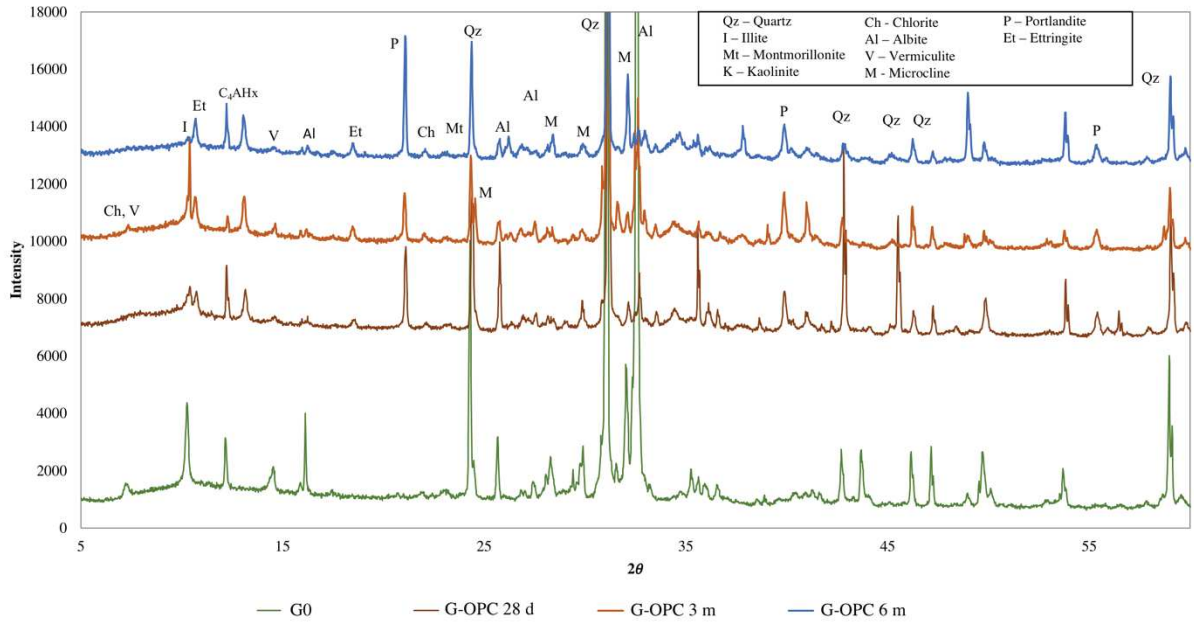

Fig. III.15 XRD analysis of G-OPC

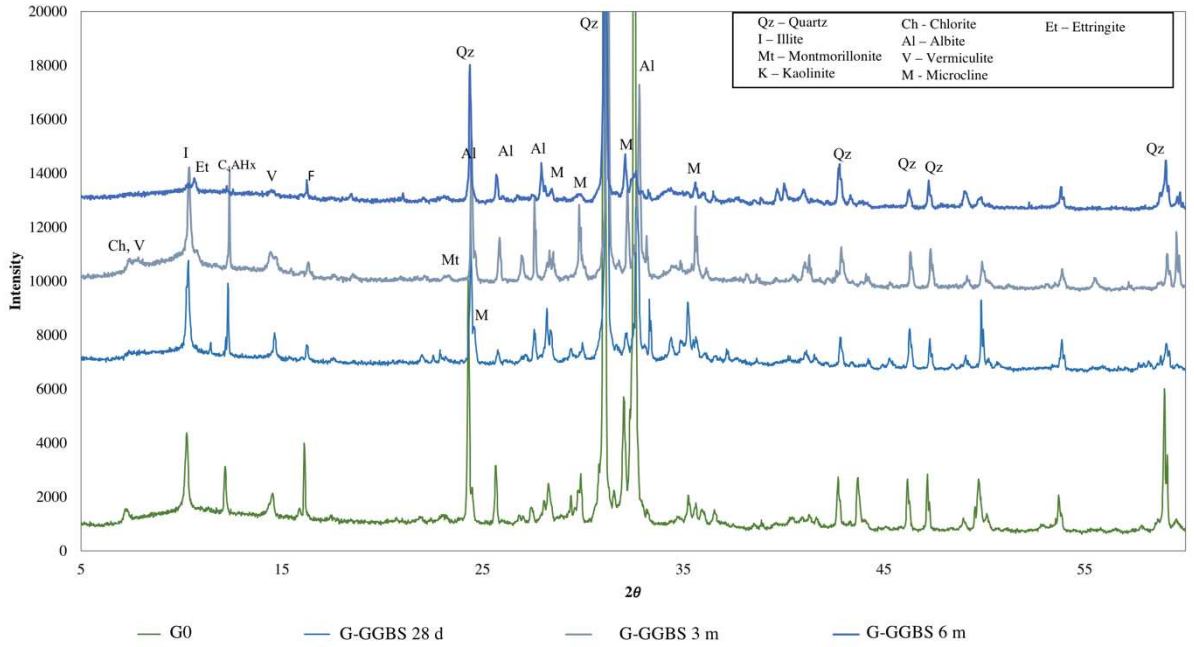

Fig. III.16 XRD analysis of G-GGBS

It should be noted that organic matter can prevent the dissolution of the clay fraction (Claret et al., 2002). It can thus be suggested that the Dublin sediment induces a lower

strength development in the case of the plain OPC binder due to the higher organic matter content. The OM covers the clay particles and forms a weak acid buffer due to the soluble organic matter fraction.

III.3.1.3 Conclusions

This part of the study was undertaken to demonstrate the importance of a sediment's nature on the short and long-term compressive strength after the introduction of a hydraulic binder. This finding has important implications for the development of a mix design for S/S treatment, meaning the physicochemical characteristics of the sediment must be taken into account. The results indicate that the GGBS-based binder can provide very performant mechanical characteristics at long term when it is activated in a correct way, for example with a sufficient amount of OPC to maintain a necessary pH. The OPC-based samples show sufficient strength development at 28 days, but further stagnation or degradation of compressive strength occurs at long term. The difference between two binders may arise from the differences in pH development over time; the pH of OPC (~13) is more aggressive for the sediment matrix compared to the GGBS-based formulation (~12). As mentioned by (Gaucher & Blanc, 2006), numerical modelling of the alkaline disturbance of clays has shown that clays will be affected 10 times more when the pH is one unit higher. Thus this disturbance of the sediment's minerals may induce the degradation or stagnation of compressive strength development.

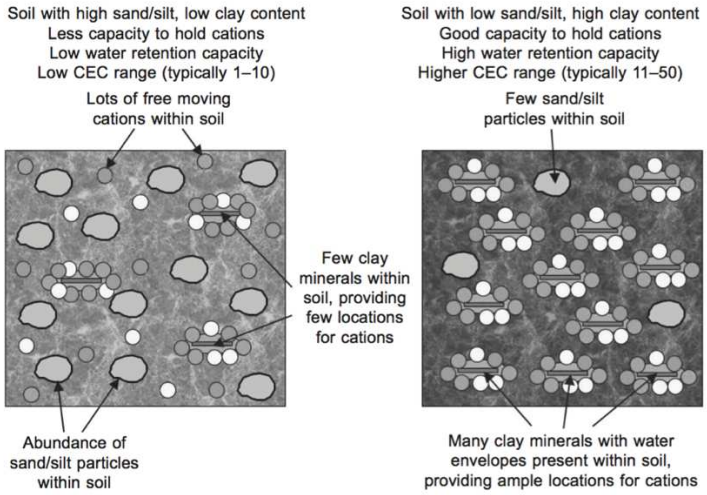

Fig. III.17. Variations of CEC according to the soil composition

The granulometry and cation exchange capacity (CEC) of the treated sediments also play an important role in the compressive strength development ((P. Sargent, 2015), Fig. III.17).

For example, as can be seen in Table III.3 (Topolnicki & Pandrea, 2012), the unconfined compressive strength of fine soils (high CEC) are lower than for sandy coarse grain soils (low CEC). These field strength values corroborate the results shown

here for the samples with the OPC treatment, but the opposite trend can be observed for the GGBS-based formulation mixed with the Dublin and Gothenburg sediment. One of the reasons for the strong performance of GGBS at 28 days with the Dublin sediment may come from the interaction with the sediment's constituents such as the clay fraction, organic matter, etc. It is known that soils with a high clay and organic matter content have a greater capacity to hold water (P. Sargent, 2015). Therefore, GGBS may have a constant and homogenous water storage to produce the hydration reactions at long term.

Table III.3 Typical field strength and permeability for ranges of cement factors and soil types, (Topolnicki & Pandrea, 2012)

Soil type	Cement factor α [kg/m³]	U.C.S. 28-days q_{uf} [MPa]	Permeability k [m/s]
Sludge	250 – 400	0.1 - 0.4	1×10-8
Peat, organic silts/clays	150 – 350	0.2 - 1.2	5×10-9
Soft clays	150 – 300	0.5 - 1.7	5×10-9
Medium/hard clays	120 – 300	0.7 - 2.5	5×10-9
Silts and silty sands	120 – 300	1.0 - 3.0	1×10-8
Fine-medium sands	120 – 300	1.5 - 5.0	5×10-8
Coarse sands and gravels	120 – 250	3.0 - 7.0	1×10-7

Several studies have evaluated the effectiveness of the use of GGBS from the point of view of mechanical performance as well as for the stabilization of contaminants. (Wilkinson et al., 2010) demonstrated a higher shear strength value achieved with GGBS activated by lime for soil solidification. (Paul Sargent et al., 2013) presents the combination of NaOH and Na_2SiO_3 as activators for GGBS for an artificial silty sand stabilization. At 28 days the strength was twice the strength of Portland cement. Further case studies are needed to determine the main parameters that can help in selecting a binder composition and quantity, depending on the sediment's nature.
In the section that follows, certain components of sediments will be investigated separately in terms of their role on the evolution of mechanical properties.

III.3.2 Impact of the sediment pore water

In order to assess the impact of the Dublin sediment pore water on the development of the mechanical strength of the binder-sediment mixtures, standard mortars were prepared according to EN 196-1 with the water/binder ratio fixed at 0.5. For this reason, demineralized water was replaced by the sediment pore water. The Dublin sediment was centrifuged and the obtained solution was filtered in order to prepare the samples. The amount of chlorides and sulfates was measured (Table III.4).

Table. III.4 Chlorides and sulfates content in the Dublin sediment interstitial water

Anion	Concentration (mg/L)
Cl^-	19300
SO_4^{2-}	399

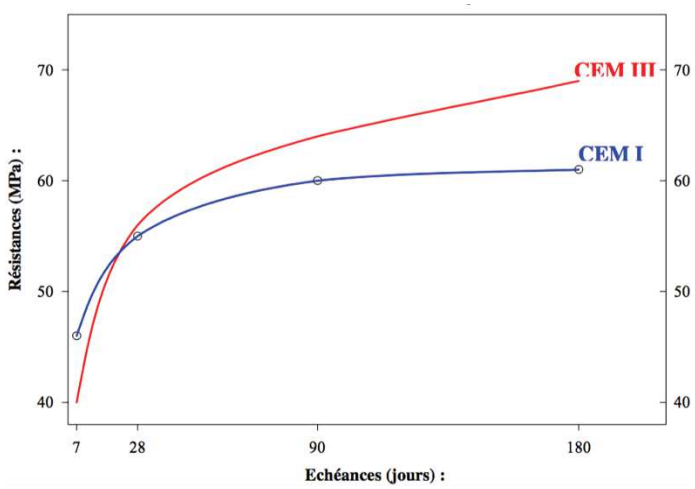

Fig. III. 18 Mechanical strength evolution of CEM I and CEM III (Van Rompaey, 2006)

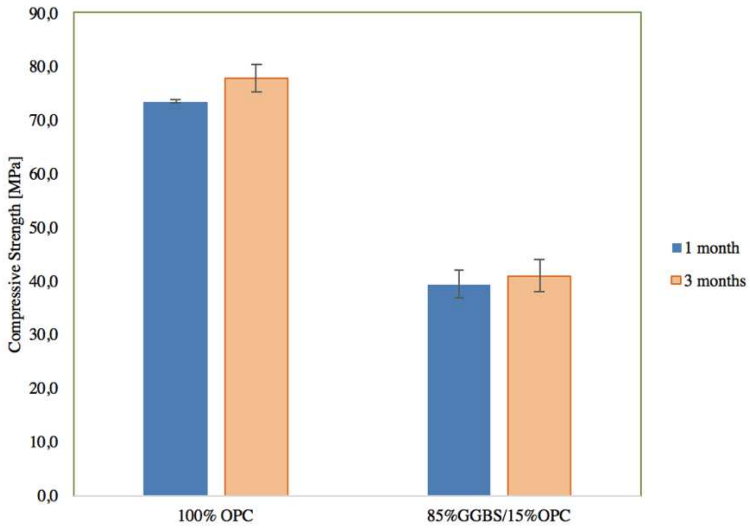

Fig. III.19 Standard mortars compressive strength with the Dublin sediment interstitial water as a mixture water

Figure III.19 compares the results obtained for the 100% OPC and 85% GGBS / 15% OPC formulations after 1 and 3 months of storage. The Portland cement formulation demonstrates a mechanical strength performance almost twice as great compared to the GGBS-based formulation. This evolution differs considerably from the evolution of the sediment treated with the same hydraulic binders. Such a performance of OPC compared to CEM I in Fig. III.18 can be explained by the presence of sediment ions which may be favourable for hydrate formation. For example, the presence of chlorides can significantly improve the mechanical properties of Portland cement (Table III.4) (Huang & Shen, 2011; Van Rompaey, 2006).

These results may indicate that the liquid phase of the Dublin sediment has no or little impact on the compressive strength development of D1 and D3. Therefore, in the following sections the other fractions of the sediment will be examined more carefully.

III.3.3 Impact of the clay fraction. Clay-Binder system's study

According to the compressive strength evolution of both the Dublin and Gothenburg solidified sediments, it can be inferred that the long term behaviour of the treated sediments can be highly improved by the proper activation of GGBS. The differences in the compressive strength evolution between 100% OPC and 85% GGBS / 15% OPC mixed with sediment can be explained by various mechanisms, one of which may be the impact of the clay fraction during the interaction with binders. Clay and cement media have highly contrasting chemistries that may lead to changes in mechanical properties during S/S treatment.
In order to obtain further in-depth information on the interaction of clays and the considered hydraulic binders, the green illitic clay from Saint Paulien ("Argile du Velay") was selected because of its similar mineralogical composition to the clay fraction of the considered sediments. It is denoted as V0. This clay consists mainly of natural illite clay (~80%) with some accessory minerals (montmorillonite, kaolinite, calcite, and quartz). V1 is designated for the OPC binder and V2 for the GGBS-based binder (85%GGBS/15%OPC). The sample preparation procedure was described previously (see §II.4.1.2). The results discussed in this section were obtained from samples stored at 90%RH and 100%RH to evaluate the influence of curing conditions.
The considered conditions are presented in Table III.5.

Table III.5 Samples considered for studying the impact of clay

Samples	RH curing conditions	OPC (%wt wet clay mixture)	GGBS (%wt wet clay mixture)
V0		-	-
V1_90RH	90%	20	-
V2_90RH		3	17
V1_100RH	100%	20	-
V2_100RH		3	17

III.3.3.1 Compressive strength and pH of the clay-binder systems

The compressive strength results for samples with binder contents of 20%wt by the wet clay mixture (or 31%wt by the dry clay) are presented in Figure III.20.
The general evolution of the compressive strength from 1 to 3 months is quite similar for each curing condition. However, V1_100RH presents a slight degradation at 3 months compared to the stable strength values of V1_90RH from 1 to 3 months. At the same time, the GGBS-based samples V2_100RH and V2_90RH show a progressive increase in strength over time. These results are similar to those of the sediments mixed with the considered binders at different percentage. The general trend that is

observed is the deterioration or stagnation of mechanical strength development for OPC-based treatment and the continuous increase in strength for the GGBS-based binders.

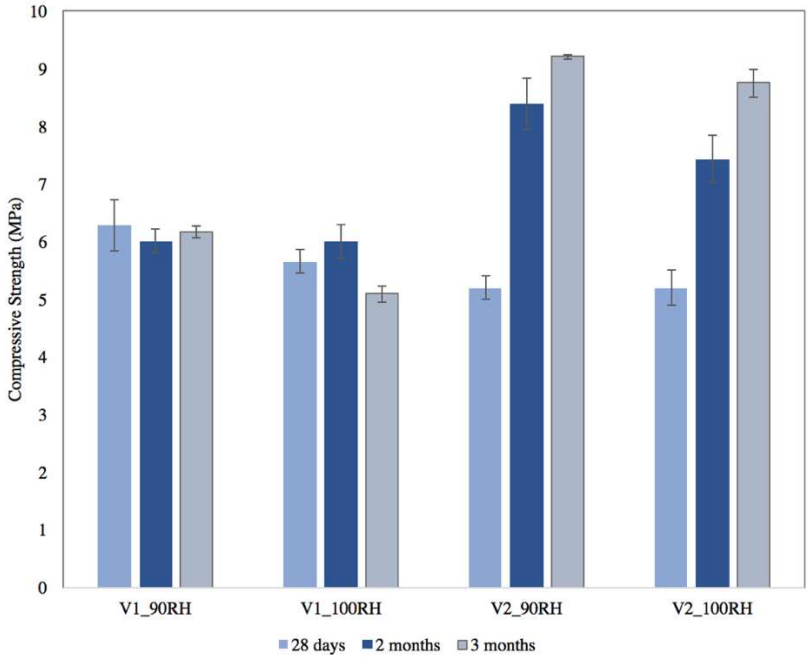

Fig. III.20 Results of the compressive strength of the samples V1 and V2 in two different curing conditions (90%RH and 100%RH)

Regarding the pH measurements presented in Fig. III.21, the pH differs for V1 according to the storage conditions.

At 100%RH, the pH increased from 11.9 at 1 month to 12.4 at 3 months. In contrast, V1_90RH showed a decrease in measured pH values. This evolution can be explained in different ways. As was discussed previously, both pozzolanic reactions and carbonation may lower the pH at long term. The samples stored at 100%RH could theoretically be more protected against carbonation due to saturation of porosity than those stored at 90%RH. The same tendency in pH evolution was observed for V2, but with lower average values than for V1: at 90%RH the pH decreased slightly, but at 100%RH the pH value continued to grow.

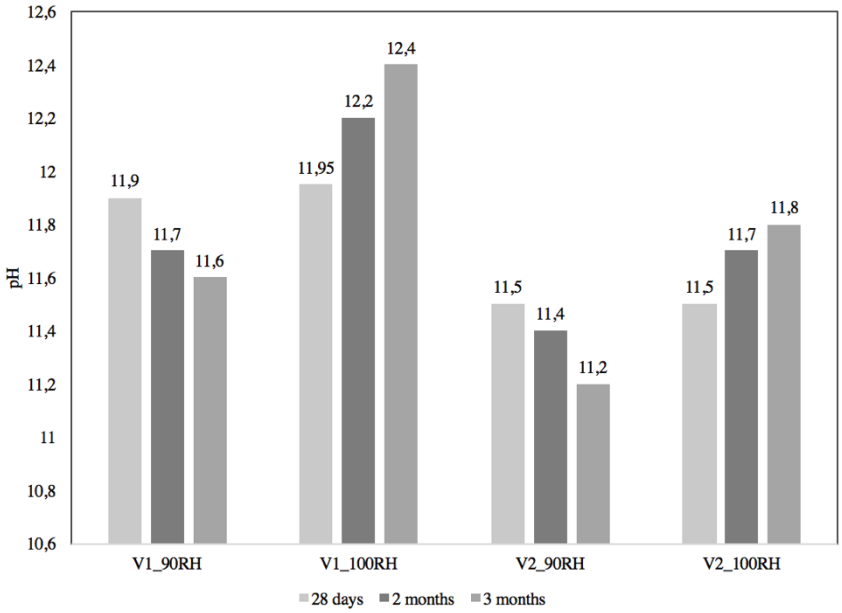

Fig. III.21 pH measurements of the samples V1 and V2 in two different curing conditions (90%RH and 100%RH)

III.3.3.2 XRD analysis of the clay-binder systems

In order to assess the evolution of the crystalline hydration products of both types of binders mixed with the clay, XRD was used.

The results of XRD analysis for V1 are presented in Fig. III.22. The main hydration products produced at both storage conditions were portlandite, ettringite and monocarboaluminate phases (AFm). Portlandite almost completely disappeared at 100%RH according to the results. A decrease in portlandite was previously observed for D1 at a binder content of 150 kg/m^3. At 90% relative humidity, the portlandite phase slightly decreased at 3 months of storage. As can be seen from the graph, monocarboaluminate is a quasi-stable phase for both types of storage. This phase is formed in the presence of carbonates in solution, which probably originate from a partially soluble carbonate fraction present in the clay sample. The intensity of the ettringite phase is higher at 100%RH that at 90%RH. The samples stored at 90%RH show a decrease in ettringite over time. It is known that ettringite is highly sensitive to the presence of carbonates. A sufficiently high carbonate content destabilizes sulfate rich AFm phases and promotes monocarboaluminate precipitation (Feng et al., 2016; Pajares et al., 2003).

At the same time, no visible modifications were observed for the V2 sample over 3 months of storage (Fig. III.23). There is a small stable peak at 20.9 ($2\theta°$) at both storage conditions, which can be attributed to the formation of a small amount of portlandite. It can be then supposed that the strength of the V2 samples originates mostly from the precipitation of amorphous phases.

The following section aims to assess the evolution of the aluminate phases using NMR.

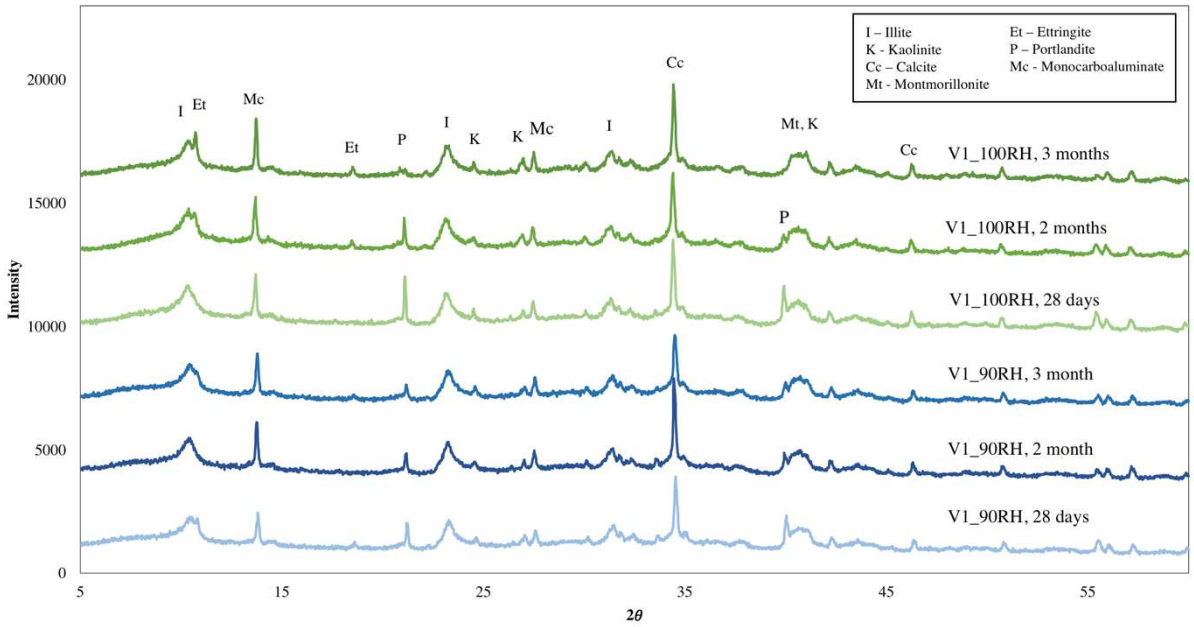

Fig. III.22 XRD analysis of the V1 samples

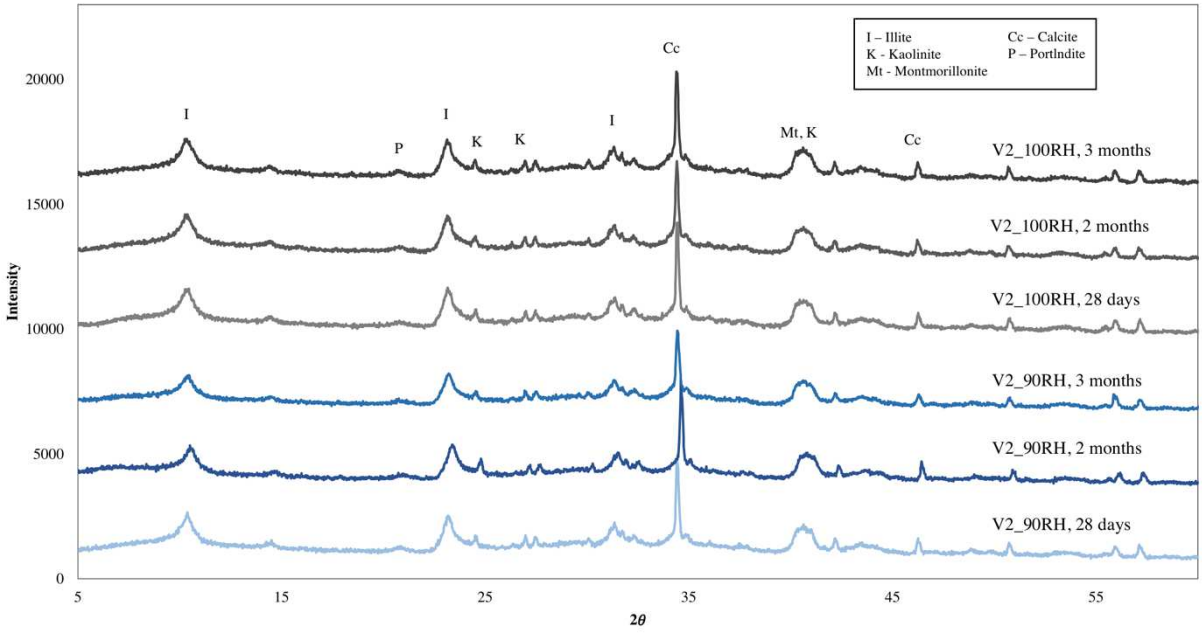

Fig. III.23 XRD analysis of the V2 samples

III.3.3.3 ^{27}Al NMR analyses of the clay-binder systems

As was mentioned previously, illitic clays have a dioctahedral 2:1 mineral structure of one octahedral sheet between two tetrahedral sheets (Fig. III.24) with the general formula $Si_8(Al,Mg,Fe)_{4\sim6}O_{20}(OH)_4.(K,H_2O)_2$. The interlayer space of this structure is filled by K^+ cations arising from the charge deficiency. The origin of this charge deficiency occurs from the Si^{4+} tetrahedral sheet replaced by Al^{3+}. Aluminium is therefore an important element in the naturally occurring aluminosilicates structure,

such as illite with some associated clay minerals in this case.

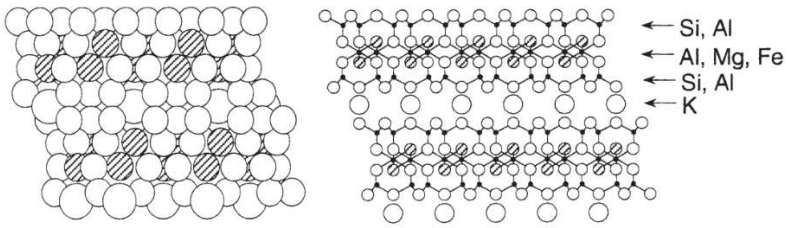

Fig. III.24 Schematic representation of Illitic clay (Sparks, 2002)

NMR is one of the most powerful tools in studying the structure of synthetic or natural aluminosilicate minerals. The ^{27}Al isotope has a spin I=5/2, therefore a nuclear quadrupole moment arises from a non-spherical distribution of nuclear electrical charge and can interact with electric field gradients at the nucleus. NMR is an effective tool to investigate the Al environment since the ^{27}Al isotope is 100% abundant and presents rather fast relaxation times enabling a short recycling delay to be used.
A High Resolution ^{27}Al Nuclear Magnetic Resonance approach was chosen to allow a deeper insight into the evolution of a clay fraction (V0) mixed with two types of binders – V1 and V2– with a special attention given to the development of the amorphous phases over a 6-month hydration period (Fig. III.25). The samples studied here were stored at 90% RH.

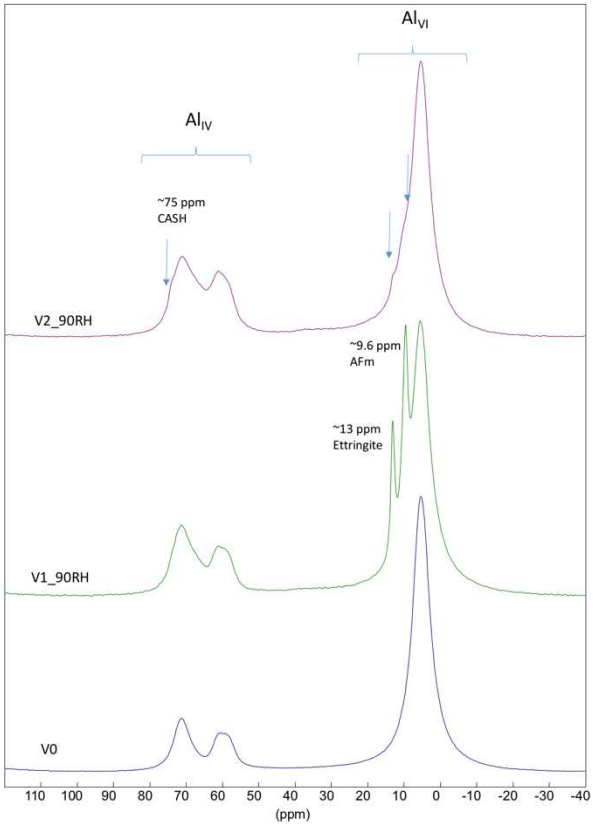

Fig. III.25 ^{27}Al NMR spectra of V0, V1, V2 after 6 months of storage

The V0 NMR spectrum exhibits both octahedral (0 to 20 ppm) and tetrahedral (50 to 80 ppm) Al environments. As detected via XRD analysis, V0 is composed mainly of illite, but also of other types of clay minerals such as montmorillonite and kaolinite. All of these phases are composed of an octahedral aluminium sheet, the main signal at 5 ppm is then the convolution of Al(VI) signal of each phase (Kinsey et al., 1985). In the same way, in almost all clay minerals aluminium can appear as a silicon substitute in a tetrahedral sheet. This is probably the reason why at least three signals are detected in Al(IV) range (at 71, 61, and 58 ppm), (Kinsey et al., 1985).
In the V1 NMR spectrum, the signal previously assigned to V0's mineral phases can be clearly distinguished. However, no signals possibly attributed to OPC can be detected. At the same time, the main component of Portland cement also contains aluminium. According to (Skibsted et al., 1993) the ^{27}Al MAS spectrum of OPC is composed of a signal with a center of gravity at 86 ppm attributed to Al incorporated in dicalcium silicate (C_2S) / tricalcium silicate (C_3S) and a second signal with a center of gravity at 81 ppm corresponding to Al in tricalcium aluminate (C_3A); tetracalcium aluminoferrite phase being negligible. These signals are not distinguishable in the spectra due to the low amount of OPC or due to its disappearance during the hydration process. Additionally, for clay signals two narrow octahedral signals are observed at 13 and 9.6 ppm. The first one is unambiguously attributed to aluminium in the ettringite phase (Aluminate ferrite trisulphate (AFt)) (Andersen et al., 2006). Ettringite precipitates from the dissolution of C_3A in the presence of sulfates and forms a columnar crystal structure with octahedrally coordinated AlO_6 (Walkley & Provis, 2019). The second signal could be coherent with aluminium of octahedral sheet in layered double hydroxides (LDH). Its assignment remains ambiguous: AFm (Aluminate ferrite monosulphate, or monocarbonate). Finally, in the Al(IV) range, the signal is slightly different from those of V0. In particular, the signal at 71 ppm is broader and dissymmetric. This seems to indicate the presence of other Al(IV) species.

On the V2 NMR spectrum, the spectral signature of clay materials, as well as slight contribution of ettringite and LDH are found. These last two are less intense than in the case of V1, consistent with the X-Ray analyses. As with V1, no signal corresponding to the aluminium of OPC can be detected. However, the signals observed in the Al(IV) range are slightly different. This is probably due to the overlapping of the clay signals with the broad peak corresponding to aluminium in GGBS. Indeed, the vitreous network of GGBS is mainly composed of SiO_4 and AlO_4 tetrahedra linked each other and charge balanced by calcium and magnesium. This type of aluminium species is known to induce a broad signal extending from 40 to 90 ppm (Neuville et al., 2008). Finally, a slight signal at around 75 ppm is also observed. This narrow signal corresponds to Al(IV) and could be attributed to aluminium incorporated in a C-A-S-H network (Colombet et al., 1998). Indeed, the incorporation of Al in the C-S-H gel structure is possible, that is to say, the formation of C-A-S-H gel depends on the

availability of Al^{3+} and its amount may increase with hydration time. Fig. III.25 reveals that there has been a slight increase in the intensity in the C-A-S-H region for the GGBS-based formulation compared to the OPC-based system. The formation of a higher amount of the aluminium-substituted C-S-H can be explained by the significant Al content within GGBS's aluminosilicate depolymerised structure. Regarding the much higher strength development of V2, the C-A-S-H phase may theoretically contribute to this strong mechanical performance.
Despite the efficiency of the ^{27}Al MAS NMR technique in studying the structure of the hydrated binders, some limitations occurred here regarding the complexity of the considered system. The high amount of the clay considerably impacted and overlapped the regions of Al in the precipitated hydrates due to illite's inner structure with Al in tetrahedral coordination.
The next part of this study uses TGA analysis to allow a deeper insight into the hydrate evolution of the OPC and GGBS treated clay samples.

III.3.3.4 TGA

Fig.III.26. presents the evolution of V1 and V2 over time. The samples were stored at 90% RH. The measurements performed for V0 show dehydration: loss of structure and absorbed water (< 180°C), dehydroxylation between (180 - 500°C), and rupture of bonds and collapse of the clay structure (600 - 850°C) (Flegar et al., 2019). The comparison of V1 and V2 reveals the development of the C-S-H phase in the presence of clay in the region of 200°C. The samples also demonstrate a difference in the region of carbonate polymorphs (calcite, aragonite, vaterite, etc.), with a different structure for the clay sample compared to that of the binders. The carbonates fraction was detected in the X-ray difractogram (Fig. II.30) of the raw clay sample. The peak at around 800°C corresponds to the formation of calcium carbonates within V1 and V2 due to the reactions of calcium bearing phases with CO_2. This peak is more important for V1.
V1 has a decrease in ettringite from 1 to 3 months with little modifications for other hydration products. This correlates with the XRD analysis (see Fig. III.22). V2 does not allow for the identification of ettringite because of its low proportion in the sample and the superposition with the peak attributed to the dehydration of clays. Finally, no significant evolution in hydration products can be observed except for a greater loss of mass with a time near to 600°C. Consequently, the formation of hydrates in the GGBS-based system cannot fully explain the mechanical evolution of V2.

Based on the above, the evolution of the mechanical properties can be linked to other factors, such as a lower pH of the GGBS-based formulations which presents a smaller disturbance for the clay-based systems as well as the distribution of the hydrates in a highly diluted matrix plays an important role.
Taking into account previously discussed findings regarding the development of the microstructure for the two formulations mixed with the Dublin sediment (D1 and D3),

the distribution of hydrates providing strength may be different for the two types of activation. In order to observe the microstructure of the clay-based systems, SEM analysis was performed and the images are analyzed in the next section.

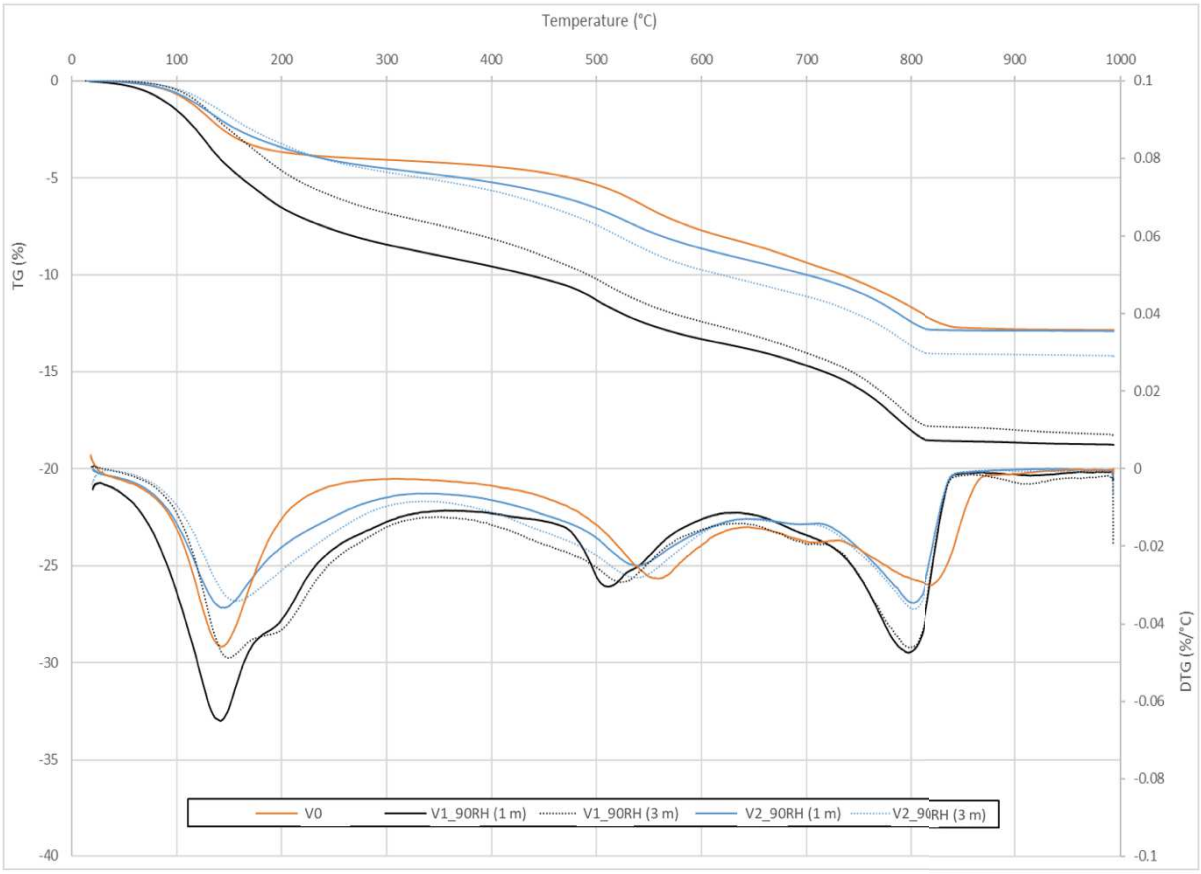

Fig. III.26. Thermogravimetric analysis of the OPC and GGBS based binders mixed with clays (V1 and V2) at 1 month and 3 months compared with the clay sample (V0)

III.3.3.5 SEM observations

Figure III.27 compares the SEM images of V1_90RH and V2_90RH. More specifically, the fracture surface after compressive strength testing at 3 months for the samples stored at 90%RH are shown. The effect of the replacement of cement by GGBS can be clearly seen. V1_90RH presents a highly friable heterogeneous surface (green area) with visible flocs compared to V2 which shows a higher microstructure density. Slag's unreacted angular particles with a sharp irregular morphology can be observed (yellow area). Some large pores and cracks can also be observed. The uniform matrix with high reticulation of C-S-H gel covering clay particles can be observed for both V1 and V2 by increasing the magnification. However, the degree of reticulation of C-S-H gel for the GGBS-based sample seems to be higher and the gel structure is finer, thus the enhancement in the compressive strength can be explained by the microstructure development in the GGBS-based mixture.

The origin of the differences observed in the SEM images can potentially result from the very early interaction of the binder solutions with the clay fabric when the flocculation/dispersion phenomenon may take place. The impact of the binder ions on the clay particles is assessed in the next section through zeta potential and rheological measurements.

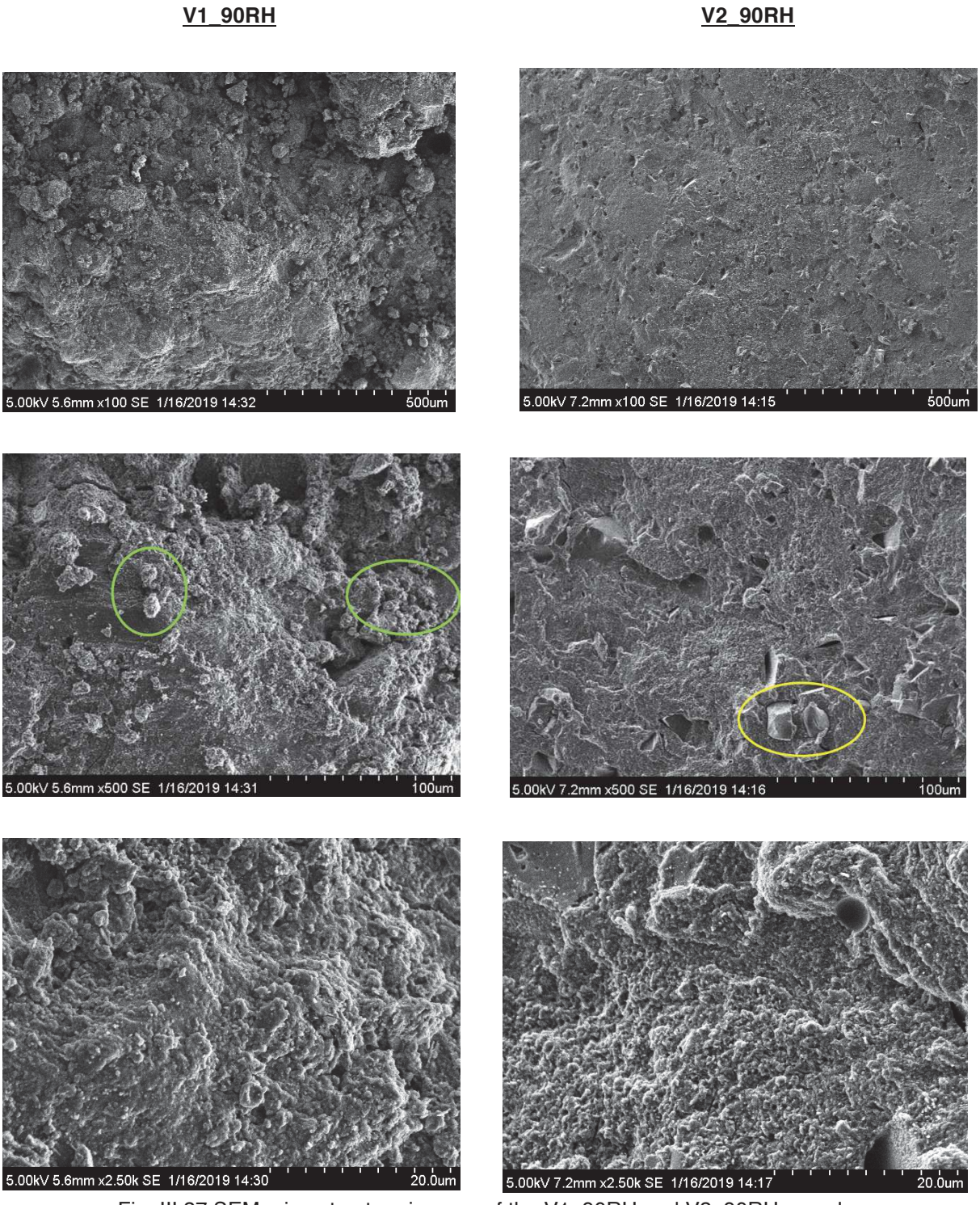

Fig. III.27 SEM microstructure images of the V1_90RH and V2_90RH samples

III.3.3.6 Impact of the binder's ions on the rheology and zeta potential of the clay

The results of the study of the impact of the clay fraction on the development of mechanical strength indicates the difference in behaviour for each formulation. According to the microstructure investigation, it can be supposed that changes in the physicochemical characteristics of clays occur after the clay comes into contact with binder solutions. The pH, ionic strength, and water content play an important role in the development of the mechanical properties and microstructure of the final material. (P. Sargent, 2015) suggests that there are several mechanisms which can cause a profound alteration in the physicochemical parameters of clays during treatment with binders: cation exchange, flocculation/agglomeration, formation of hydrates, secondary pozzolanic reactions, and eventually carbonation.

In this part of the study the role of two first reactions produced during the solidification of clays are investigated. These reactions occur quite rapidly at the beginning. Thus, it can be supposed that the composition of binding agents and the effect of the interstitial solution of the binders have a considerable impact on the development of the mechanical properties in the soils/sediments Solidification/Stabilization practice.

The schematic representation of cation exchange and further flocculation/agglomeration phenomena is presented in Fig. III.28. The majority of hydraulic binders contain calcium as the main exchangeable ion – it can replace the monovalent cations in a soil and cause potential flocculation (Dong, 2014). (Prusinski & Bhattacharja, 1999) showed a reduction of the double-layer thickness between negatively charged clay particles due to the higher charge density of di- or trivalent ions. Therefore, according to the cation order of replaceability, Ca^{2+} can easily replace Na^{+} and K^{+} due to its higher valence. As can be seen in the image, the interparticle forces created between clay particles influence their arrangement due to flocculation or dispersion. It can be supposed that the position of particles or the fabric of clay has a great impact on the engineering properties of stabilised clayey soils (Le et al., 2012), (J.K. Mitchell, 1981).

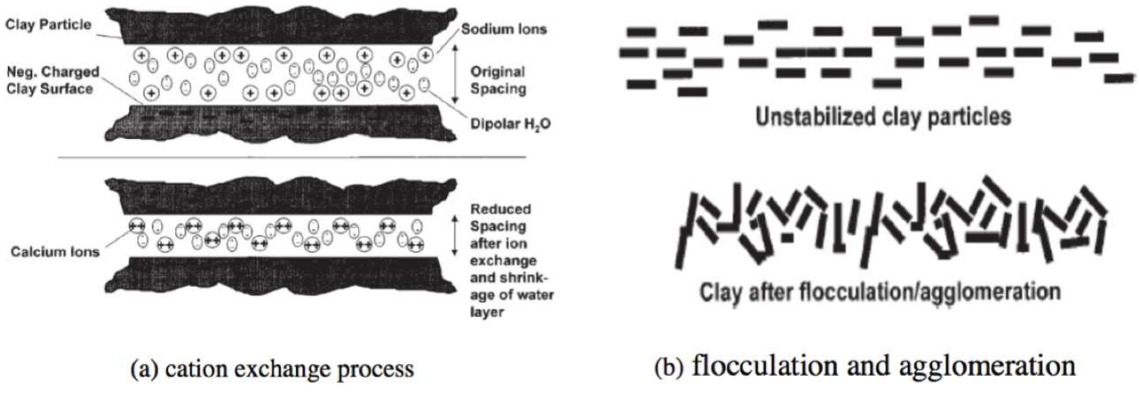

Fig. III.28 Cation exchange, flocculation and agglomeration processes (Prusinski & Bhattacharja, 1999)

In order to provide a detailed illustration of the role of the interstitial solutions of two types of binders considered earlier in this study for the solidification of the illitic clay, rheology and zeta potential measurements were chosen as relevant tools for this purpose.

To analyze the interstitial solution of the binders, dry mixtures were put into contact with demineralized water with a water to binder ratio of 2 for 10 min with magnetic stirring, then centrifuged and filtered before being sent for analysis in the laboratory using ICP-AES, except for the sulfate concentration which was determined using ion liquid chromatography. The chemical composition of the interstitial solutions of the two binders is presented in Table III.6. As can be seen, the concentration of Ca^{2+}, Na^{+}, K^{+}, and sulfates is greater in the Portland cement solution.

Table III.6. Chemical composition of the interstitial solutions of 100%OPC and 85%GGBS/15%OPC after 10 min of stirring

Chemical element (mg/L)	Formulations	
	100%OPC	**85%GGBS/15%OPC**
SO_4^{2-}	2900	1500
Ca	983	543
Na	373	56
Al	<0.02	<0.02
K	2415	263
Mg	<0.02	<0.02

The sample preparation procedure for obtaining the interstitial solution of two different formulations was reported in §II.4.1.3.5 and §II.4.1.3.6.

III.3.3.6.1 Zeta Potential results of the clay-binder systems

The values of the surface charge of the clay particles in demineralized water and in two types of interstitial solutions are presented in Fig. III.29. The clay particles in water (V0), at low ionic strength, show the most negative values of zeta potential: from -3.2mV to -2.6mV with pH reaching a stable value from 7 to 7.8 and conductivity around 0.5 mS/cm^2. The 100%OPC solution (V1) significantly changed zeta potential of the clay from negative to positive. The measurements were between 0.8 and 1.0 mV. The highest pH as well as conductivity were measured for V1 with pH=12.6-12.9 and conductivity 10.5-10.6 mS/cm^2 respectively (Fig. III.30, Fig. III.31). In contrast to V1, the zeta potential measurements for V2 show a similar behaviour to V0, but with greater variations in values over time, probably due to the reactions produced between the clay particles and the alkaline solution of 85%GGBS/15%OPC. Zeta potential slightly increased in comparison to V0 and varies from -2.6mV to -2.3mV; the pH of V2 decreases from 12 to 11 over time. A stable conductivity value around 3 mS/cm^2 was measured for V2.

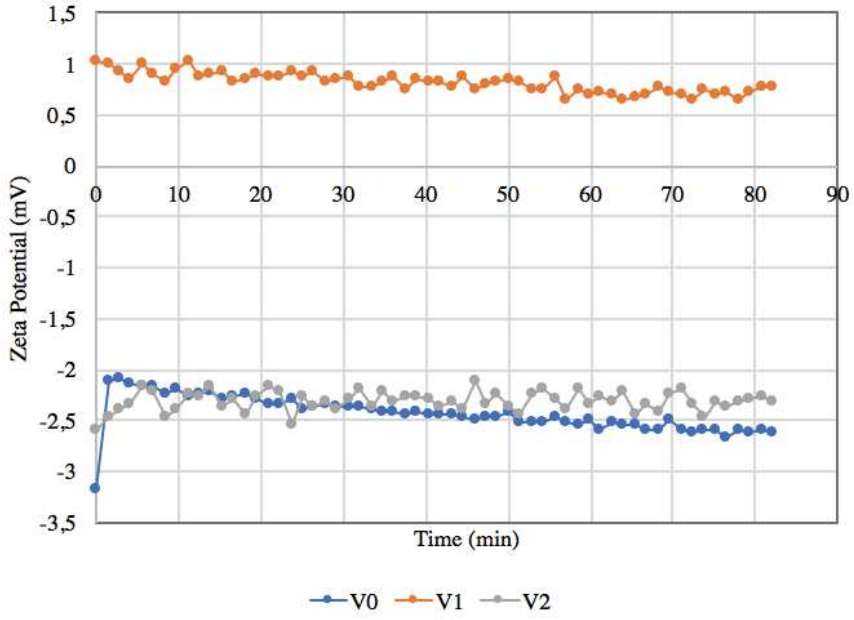

Fig. III.29 Zeta Potential measurements of V0, V1, V2

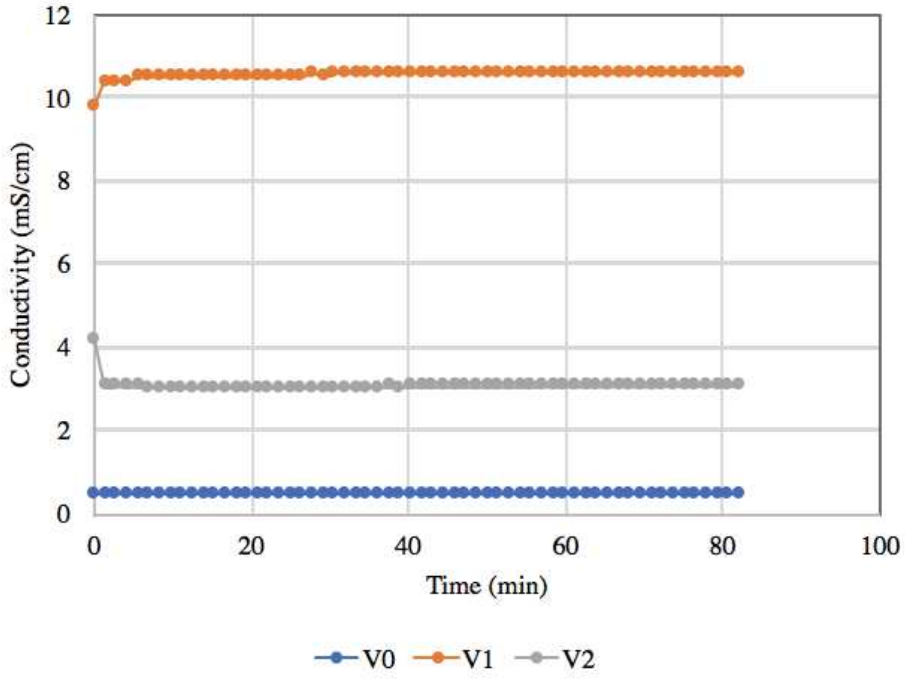

Fig. III.30 Conductivity measurements of V0, V1, V2

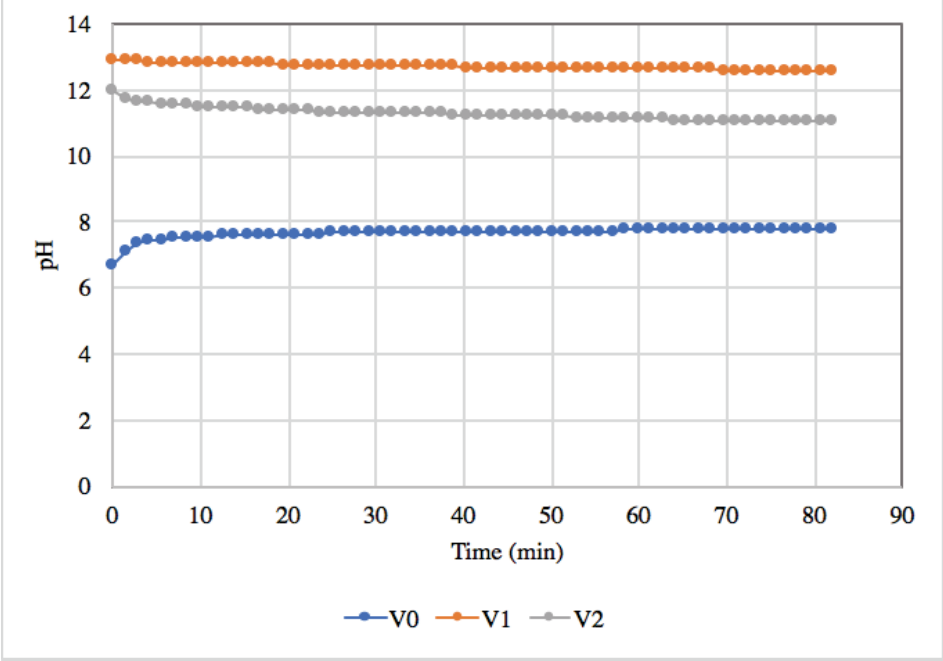

Fig. III.31 pH measurements of V0, V1, V2

According to (Yukselen & Kaya, 2002), the decrease in the pH of clays in an alkaline solution may result from chemical reactions of Si^{4+} and Al^{3+} in the octahedral and tetrahedral clay layers and water, by increasing the concentration of H^+ in solution (28), (29):

$$Si^{4+} + H_2O \Leftrightarrow Si(OH)_4 + 4H^+ \quad (28)$$

$$Al^{3+} + 3H_2O \Leftrightarrow Al(OH)_3 + 3H^+ \quad (29)$$

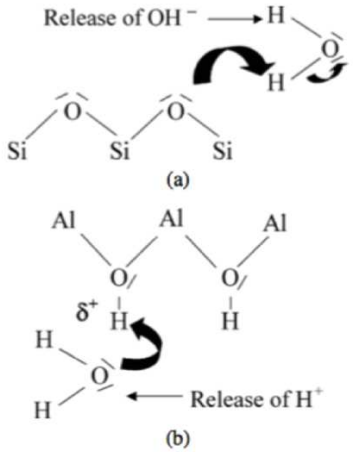

Fig. III.32 Schematic representation of possible reactions between (a) siliceous faces or (b) aluminous faces (from (Konan et al., 2007))

However, according to (Konan et al., 2007), illite only has a siliceous layer whose proton acceptors govern pH changes, which is why illitic clay has a weakly basic pH compared to the mainly acidic pH of other types of clays (Fig. III.32).

What can be clearly seen from the obtained results is the difference between V1 and

V2 in terms of surface charge. The amount of soluble calcium is higher for Portland cement (Table III.6) as is the initial pH (Fig.III.31). When OPC is replaced by GGBS the content of Ca^{2+} cations decreases, thus the electrokinetic behaviour of the clay will predominantly depend on this element, especially at the beginning of the interaction of the binders with the clay system.
Previous studies (Konan et al., 2007), (Avadiar et al., 2012) have suggested that when Ca(II) is going into solution its large hydration energy captures 6 water molecules in the hydrated state ($Ca(H_2O)_6^{2+}$). (Konan et al., 2007) reported that these hydrated calcium ions, when they interact with clay suspension, will adsorb on silica faces (Figure III.33) and on deprotonated alumina faces when the pH increases above 9.5. Therefore, zeta potential increases significantly, especially in the high pH range, and this is in line with observations made here.

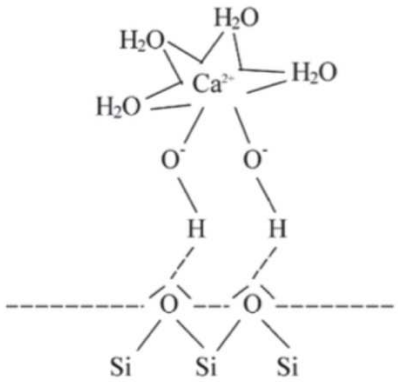

Fig. III.33 Schematic representation of possible interactions between silica faces and hydrated calcium ions

III.3.3.6.2 Rheological measurements of the clay-binder systems

Figures III.34 and III.35 present the rheological behaviour of the clay in two different solutions - the variation of yield stress was measured using a vane geometry at constant temperature (20°C). The yield stress is an important rheological parameter which can be described in general terms as a transition state of elastic solid-like behaviour at low stress to liquid (viscous) behaviour at high stresses (Liddel & Boger, 1996). In the case of clays this is an appropriate procedure for observing changes in terms of the flocculation rate.
The lowest value of the yield stress immediately after mixing (Fig. III.34) was obtained for V0. Both binders increased the yield strength, which means the flocculation effect was produced for the clay mixed with two types of binder solutions. However, V1 showed a much more significant effect on the creep behaviour of the clay – the yield stress of V1 is 100 Pa higher than that of V2. This behaviour can be explained by the interaction of 100%OPC ions with the illite clay system, more specifically the adsorption of Ca^{2+} onto illite particles causing flocculation, resulting in a high yield

stress due to the higher electrolyte concentration. The high amount of calcium ions introduced into the clay induces the flocculation and thickening of the system.
As can be seen in Fig. III.35, the yield stress increased for all samples 10 min after mixing. At the same time, the general tendency remains the same – the highest yield stress was achieved with 100%OPC interstitial solution (V1).

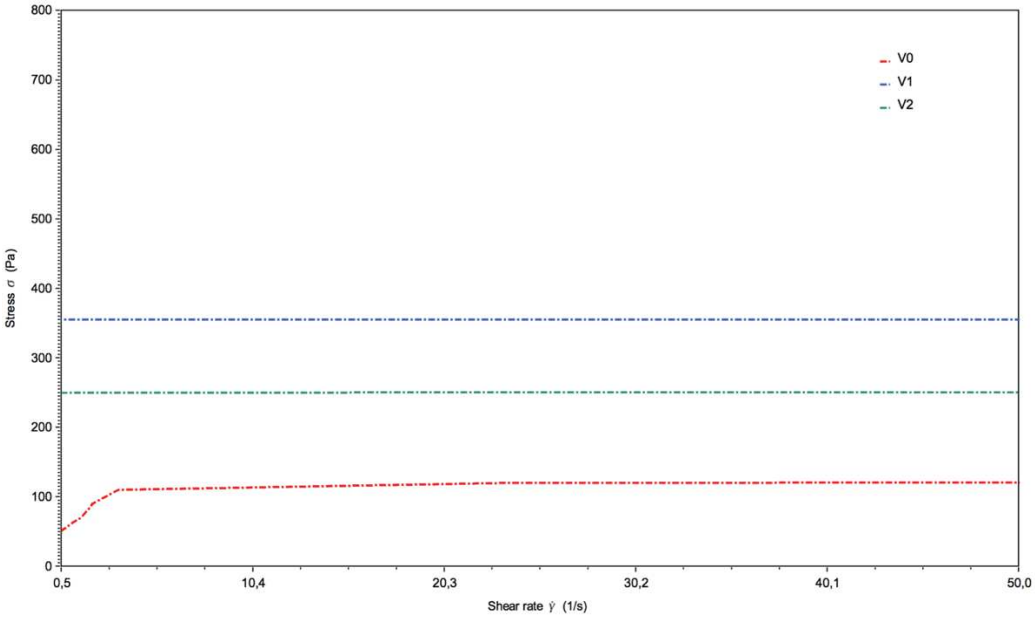

Fig. III.34 Rheological measurements of V0, V1, V2 (immediately after mixing)

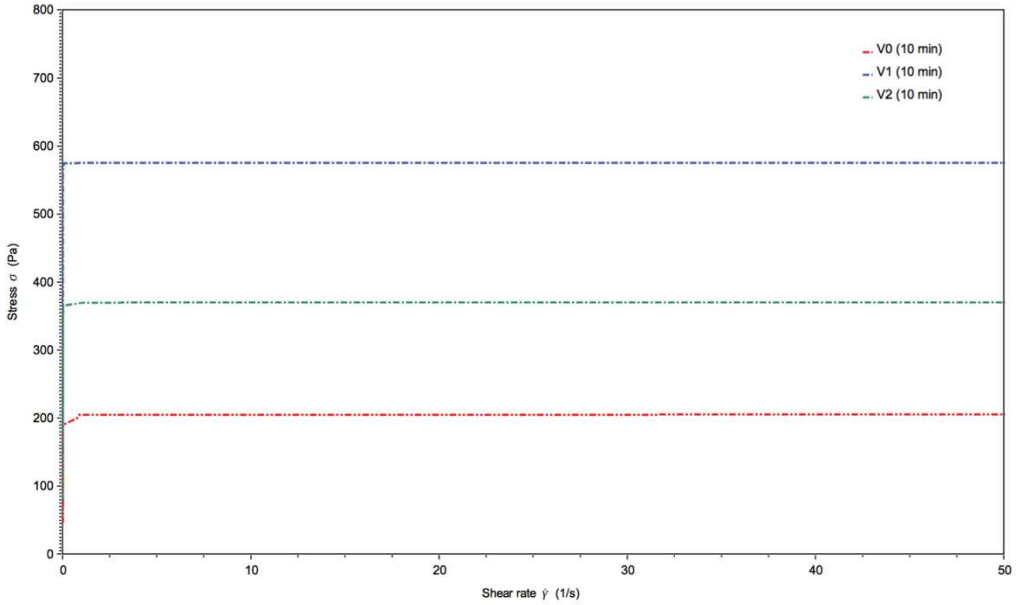

Fig. III.35 Rheological measurements of V0, V1, V2 (10 min after mixing)

III.3.3.7 Discussion

In this investigation, the objective was to determine the effect of the clay fraction of sediments on the development of mechanical properties of the OPC and GGBS-based mixtures. The results revealed the same tendency in the development of compressive strength as for sediments mixed with binders – the gradual increase in strength in the case of GGBS treatment and the degradation/stagnation of the mechanical properties in the case of Portland cement. Thus, it can be supposed that the clay fraction is responsible for the evolution of mechanical properties of solidified sediments.

The microstructure investigation together with the rheological and zeta potential measurements demonstrated the role of Ca^{2+} on the disturbance of the arrangement of clay particles, in particular concerning flocculation.

(Avadiar et al., 2012) showed the strong attractive interaction when Ca(II) was added into kaolin slurries. The yield stress increased significantly due to the strong interaction of calcium cations with negatively charged clay particles in a highly alkaline medium. (Lowke & Gehlen, 2017) studied the oxide minerals, in particular the changes in the zeta potential of ground quartz with various salt contents. This study established the high affinity of the surface of minerals for calcium ions (Ca^{2+}) compared to K^+ or Na^+ and therefore an important gradual increase in zeta potential with the increase in the molar concentration of $Ca(OH)_2$.

In this study the illite particles flocculated due to a high calcium content, especially in the OPC-based mixture. The formation of new clay fabric with face to edge contact resulting in a more open structure was observed. Some other studies in this area seem to be consistent with the findings presented here. The calcium-based reactions in soil-water systems are complex and were largely studied in previous research (Barzegar et al., 1994; Cruz & Peng, 2016; Dong, 2014; Gaucher & Blanc, 2006; Lemaire, 2012). (Chew et al., 2004) investigated the microstructure evolution of a mixture of soft Singapore marine clay and Portland cement. The development of the microstructure leads to large pore formation due to flocculation which was increased with increasing content of OPC.

This flocculated structure was also reported by (McCallister & Petry, 1992) for expansive clays treated with lime; the permeability was much greater for treated clays than for untreated clays. (Barzegar et al., 1994) investigated the effect of exchangeable cations on the compressive strength of different types of soils. It was found that the Na-based soils were highly dispersed compared to the flocculated calcium based soils, so the contact between clay particles was more important for Na-based soils resulting in a higher tensile strength. In the section that follows, the role of dispersing agents on the compressive strength of the Dublin sediment is evaluated.

III.3.4 Impact of dispersing agents. Dublin sediment – Binder system

Based on the results discussed in this chapter, it can be concluded that one of the key aspects of the solidification process is the phenomenon of flocculation/dispersion. The dispersed or aggregated (flocculated) state of a treated soil/sediment may have a considerable impact on the development of mechanical properties. Briefly, the improved rheology plays an important role in the development of fresh state properties through better homogeneity and hydrates repartition within the system. Therefore, the long term hydration can be also significantly improved.
With the introduction of a hydraulic binder such as Portland cement or lime, the amount of calcium ions increases which are known to suppress the double layer of negatively charged clay particles producing the flocculation effect. It is well established from a variety of studies the role of simple inorganic ions on the flocculation/dispersion of clay particles, for example in ceramic processing. It has been demonstrated that sodium ions may disperse clays particles because of their monovalent nature and greater hydrated radii in contrast to Ca^{2+}. The repulsion of clayey soils/sediments particles may occur due to the replacement of calcium ions by sodium ions.
In this section 100%OPC and 70%GGBS/30%OPC formulations were added into the Dublin sediment (D0) at 10%wt with and without dispersing agents (Table III.7).

Table III.7 Considered samples (OPC – Portland cement, GGBS - ground granulated blast-furnace slag, HMP – hexametaphosphate, B – phosphonate dispersing agent)

Sample	Composition (%wt of the raw Dublin sediment)
D-OPC	10%OPC
D-OPC-HMP	10%OPC+1%HMP
D-GGBS	3%OPC+7%GGBS
D-GGBS-B	3%OPC+7%GGBS+0,1%B
D-GGBS-HMP	3%OPC+7%GGBS+1%HMP

III.3.4.1 Effect on the rheological behaviour

Two types of dispersants have been tested in this study. The first one is sodium hexametaphosphate (HMP, $NaPO_3$) which is a widely used phosphate deflocculant. The action of hexametaphosphate consists of the sequestration of Ca^{2+} and introduction of Na^+ into the system (Rolfe B. N., 1960). The reactions involved in the hexametaphosphate ionization according to (Rolfe B. N., 1960) are shown below in reactions 30 and 31:

$$(NaPO_3)_N \Leftrightarrow 2Na^+ + (Na_{n-2}(PO_3)_n)^- \quad (30)$$

$$(Na_{n-2}(PO_3)_n)^- \Leftrightarrow 2Na^+ + (Na_{n-4}(PO_3)_n)^- \quad (31)$$

As a result of these two steps, ionized sodium ions are ready to interact with the soil

surfaces. At the same time the formation of complex salts ($CaNa_{n-2}(PO_3)_n$ or $2CaNa_{n-4}(PO_3)_n$) may take place. Consequently, less calcium is present to flocculate the soil system and the double layer thickness is increased as well as the interparticle repulsion due to Na cations having lower valence. This type of dispersant acts mainly on negatively charged clay particles. Another mechanism for increasing the dispersion of soil or sediment systems can be through the introduction of complex anions which change the remaining partially positive charge on the broken edges of the clay particles. (Rolfe B. N., 1960).

The effect of different dosages of HMP on the rheological behaviour of the Dublin sediment is presented in Fig. III.36. The yield stress was gradually decreased with the increase in the HMP content from 0.5% to 2% by the weight of the sediment, which means that the dispersing effect occurs.

However, the sediment is a very complex and heterogeneous fabric containing different components. It was noted that phosphonate organic salts dispersing agents (denoted as B) are effective enough to disperse the Dublin sediment, probably acting mainly on the carbonate fraction which is strongly present in this sediment. The phosphonate dispersing agents act mainly by adsorption on carbonate minerals as well as by producing the Ca^{2+} chelating effect and its sequestration (Nowack, 2003). The B dispersant agent considerably decreased the yield strength even at 0.1%wt of the sediment as shown in Fig. III.37.

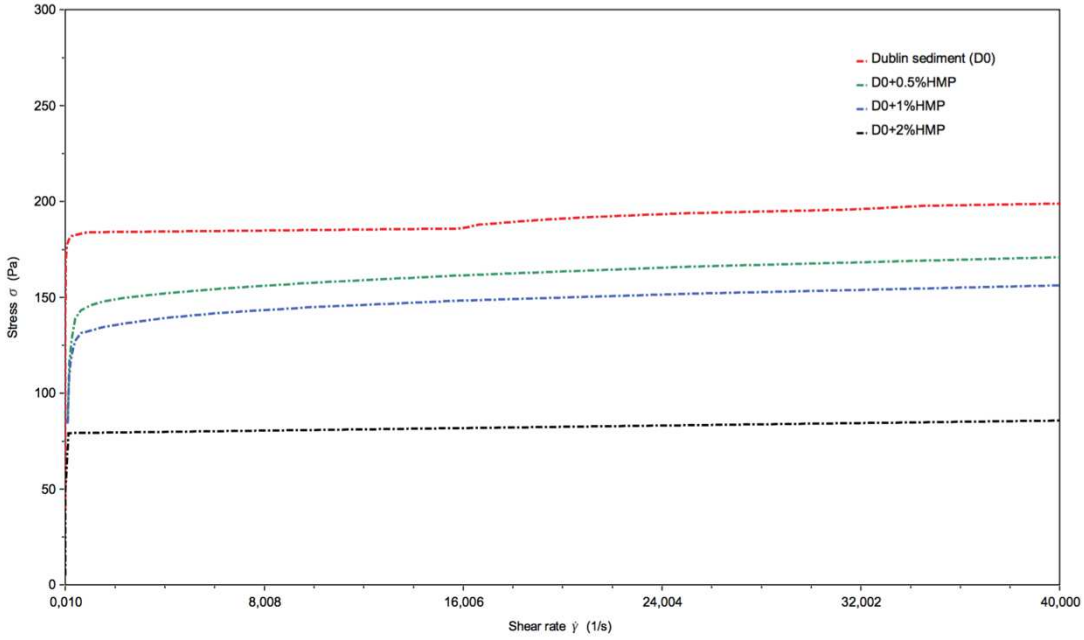

Fig. III. 36 Impact of HMP on the rheological behaviour of the Dublin sediment

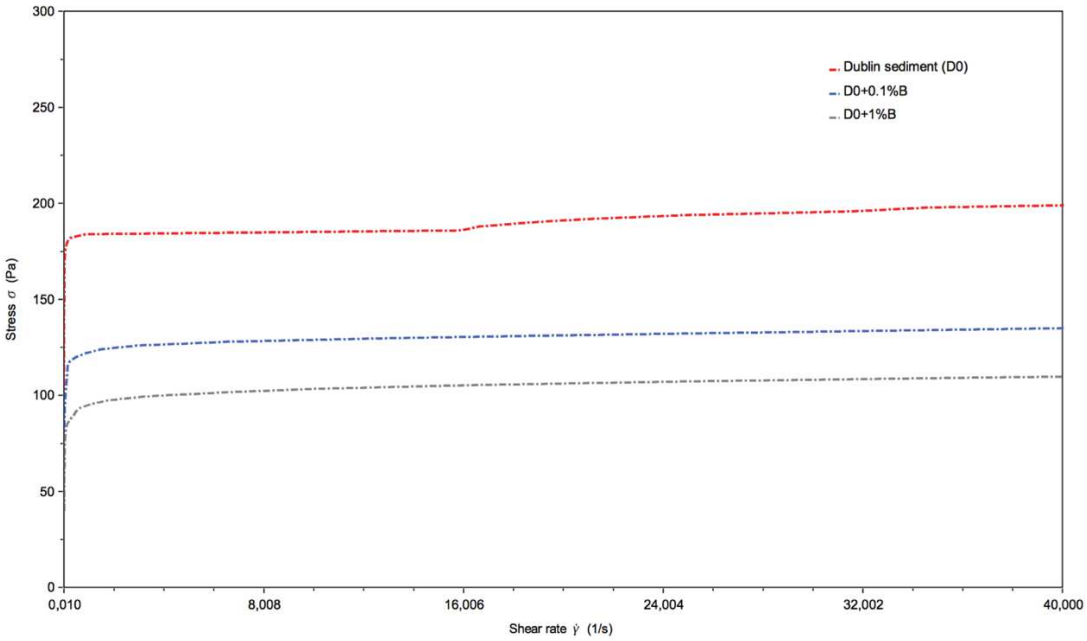

Fig. III.37 Impact of B-dispersant on the rheological behaviour of the Dublin sediment

III.3.4.2 Compressive strength results

The compressive strength results are presented in Fig. III.38. The effect of HMP on the development of compressive strength of the Dublin sediment treated with Portland cement was assessed after 14 days of storage. The measured compressive strength was more than doubled in the presence of the HMP dispersant for the D-OPC-HMP samples.

The D-GGBS-B samples containing a phosphonate-based organic dispersing agent demonstrated a retardation in hardening, so the compressive strength was measured after 28 days of storage instead. Despite this retardation effect, the strength of the GGBS-based treated samples with 0.1%B was almost twice the strength without the dispersing agent– 370 kPa for D-GGBS against 700 kPa for D-GGBS-B (Fig. III.39).

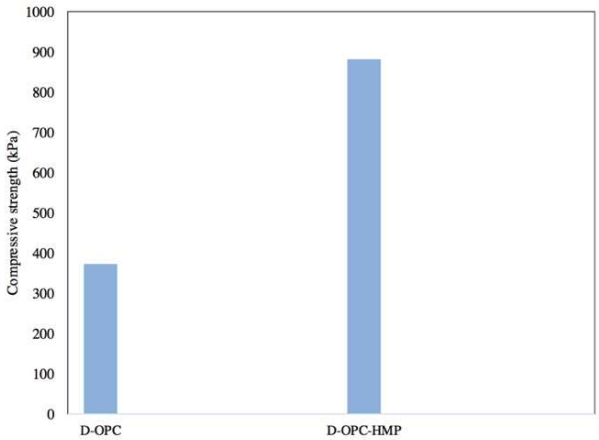

Fig. III.38 14-day compressive strength results of D-OPC, D-OPC-HMP

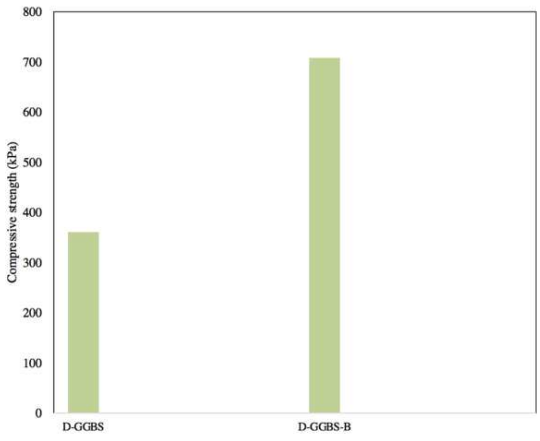

Fig. III.39 28-day compressive strength results of D-GGBS, D-GGBS-B

III.3.4.3 Zeta Potential measurements

The zeta potential results are shown in Fig. III.40 and Fig. III.41. The measurements were carried out on a solution of demineralized water with a particle concentration of 5% for 30 min. As can be seen in Fig. III.40, the raw Dublin sediment (D0) exhibits particles with negatively charged surfaces. The introduction of 1% of HMP slightly lowered the value of ζ potential. The most remarkable changes in zeta potential of the Dublin sediment was obtained with the Portland cement binder (D-OPC) – a significant fluctuation in electrokinetic potential was observed. The ζ potential twice reaches positive values crossing the zero-point charge. However, the presence of the dispersing agent considerably impacted the electrokinetic potential of the D-OPC-HMP mixture – the zeta potential remains negative across the measurement period with less fluctuation. The sequestration of calcium ions in the presence of 1%HMP lowered the ζ potential values.

In contrast to D-OPC, the values of the D-GGBS remains negative with some significant fluctuations compared to the D0 due to the dissolution of the binder (Fig. III.41). As was discussed previously, the GGBS contains fewer calcium ions, therefore the zeta potential remains more negative for the Dublin sediment mixed with the GGBS-based binder. The HMP effect can be clearly observed in the first 10 min of the measurements – the electrokinetic potential was lowered from -8 mV for D-GGBS to -13 mV for D-GGBS-HMP.

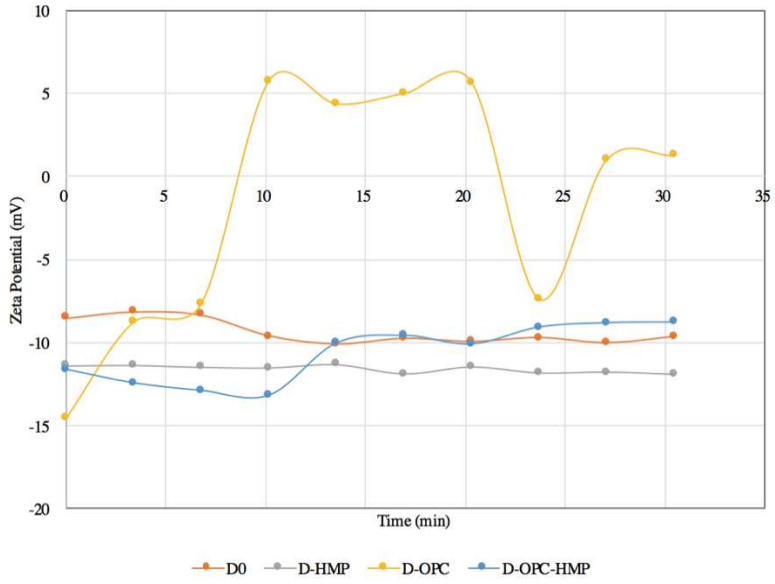

Fig. III.40 Zeta Potential measurements of D0, D-HMP, D-OPC, D-PC-HMP

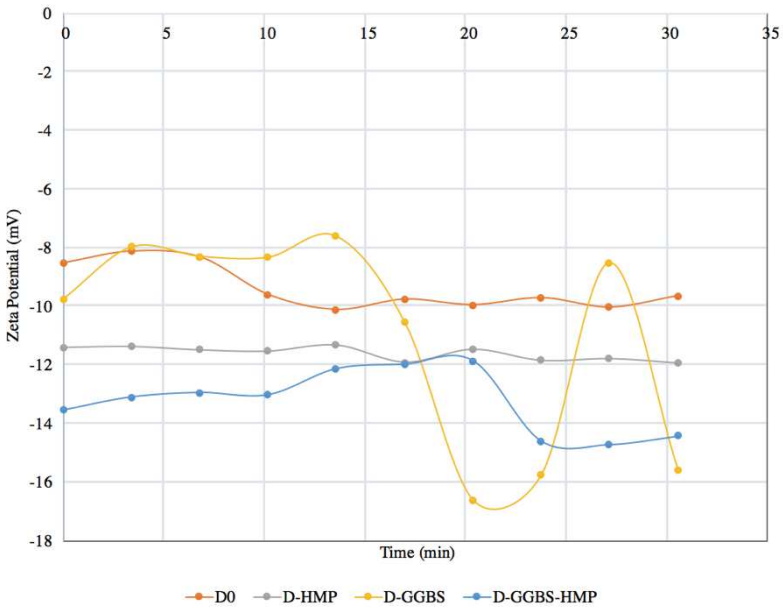

Fig. III.41 Zeta Potential measurements of D0, D-HMP, D-GGBS, D-GGBS-HMP

III.3.4.4 Discussion

The measured compressive strength obviously results from the dispersed state of the sediment fabric in the presence of dispersing agents. In the study of Moevus et al., (2016) the impact of the clay platelets arrangement on the mechanical strength of soils mixed with hydraulic binders was investigated. It was concluded that a more compact structure is formed due to the addition of dispersants resulting in a more parallel arrangement of clay platelets.

Barzegar et al., (1994) points out in his paper the difference in the microstructure development in Na- and Ca-soils. According to their observations, sodium ions in clay soils disperse the soil system and increase contact points between clay particles in the soil by increasing the tensile strength. In contrast to sodium ions, in calcium soils the microstructure presents a flocculated state with the development of a coarser granular configuration of the particles.

The results of this study indicate the potential improvement in the mechanical performance of treated sediments with the introduction of dispersing agents. The successful use of dispersants depends on the sediment's composition – the types of clays in the system, the organic matter content, etc. may complicate the action of dispersants. Nevertheless, the use of dispersants may potentially improve the processing of sediment treatment by improving the rheology, for example when pumping is necessary. Additional work is needed to study other types of sediment as well as other types of dispersants in order to provide economical and practical solutions for S/S treatment.

III.4 Interaction between the Dublin sediment's organic matter and binders

The organic fraction of the Dublin sediment cannot be neglected from the point of view of its interaction with hydraulic binders and its impact on the ability of binders to develop mechanical properties during the solidification process. Hydraulic binders may also disturb the mobility of heavy metals, considering that some of them are complexed by organic matter in the Dublin sediment.
The changes in environmental factors such as pH, ionic concentration, and the nature of counter ions may strongly disrupt the organic matter species (Klučáková, 2018). The pyrolysis technique coupled with gas chromatography followed by mass spectroscopy (Py-GC-MS) investigation was applied to the sediment just after mixing in order to carry out the reconstruction of the organic matter in the raw sample D0 and in the treated Dublin sediment D1 (OPC-based treatment) and D3 (GGBS-based treatment). The ^{13}C-NMR technique contributed to a complete characterization of OM.

III.4.1 Organic matter reconstruction before and after S/S treatment

Figure III.42 provides the pyrochromatograms of D0, D1, and D3. It shows the main building blocks of the organic matter of the sediment and provides information on their sources. Typical pyrolysis products of carbohydrates are identified (furaldehyde, furfural) as well as acetamide for aminosugars. Some nitrogen containing heterocycles reflect a proteinaceous origin (Fig. III.42 B and C). D0 also presents some sulfur components (Fig. III.42 D), which completely disappeared in D1 after 28 days, but not in D3.
The main observation from the pyrolysis analysis is the decrease in most of the organic compounds in the order D0<D3<D1, especially for those mentioned above (Fig. III.42 B, C and D). These results suggest that there is an important impact of hydraulic binders on the organic molecules, especially with Portland cement. Nitrogen compounds, aromatic and amino- sugars as well as proteins were significantly influenced by the addition of OPC. The peaks of the relative abundance were decreased noticeably for D1 compared to the raw sediment. It can be concluded that the decrease in the quantity of the molecular rate is in the same order as the pH development in both formulations. The OPC-based binder develops a pH of approximately 13 compared to the GGBS-based binder with pH≈11.8 just after mixing. It can be thus supposed that the highly alkaline pH medium induces the dissolution of some organic compounds.
Based on the characterization of the organic matter species, it is now interesting to follow the evolution of these components in D1 and D3 over time. Figure III.43 presents the global pyro-chromatograms of the sediment-binder systems at 1 month and 3 months. The graphs are presented in detail in Fig. III.44 and Fig. III.45. After 3 months there is no evolution in the proportion of nitrogen compounds for D1 and D3. However, the peak at 27 min corresponding to the phenolic compounds increases with time for

the two samples. Also, it can be noted that after 3 months, the sulfur components decreased in D3.

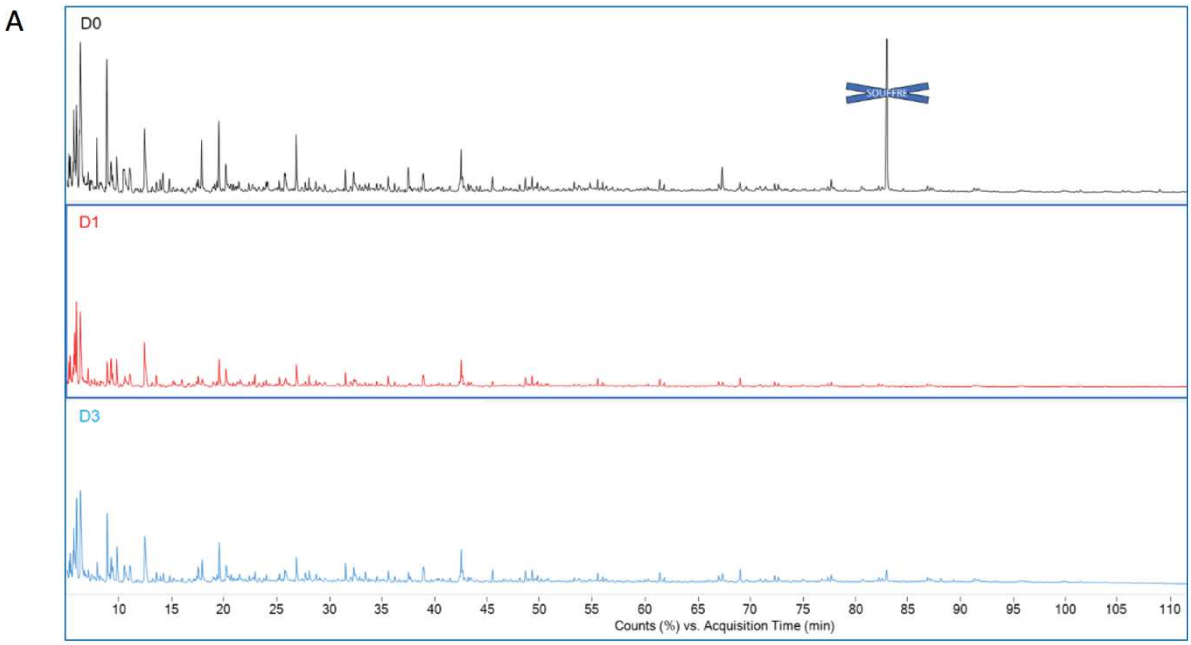

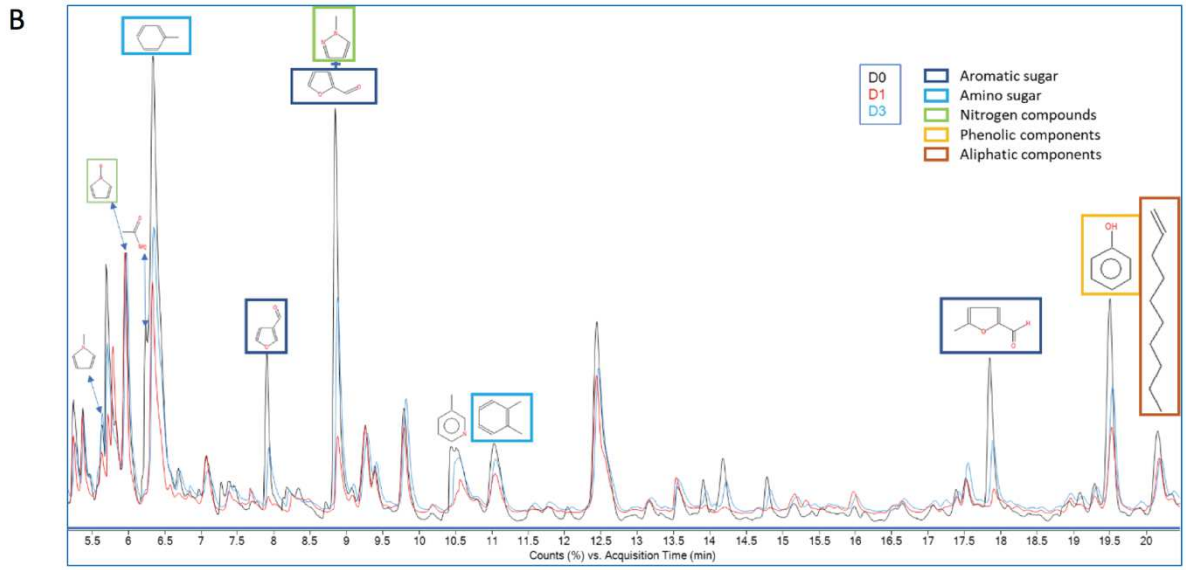

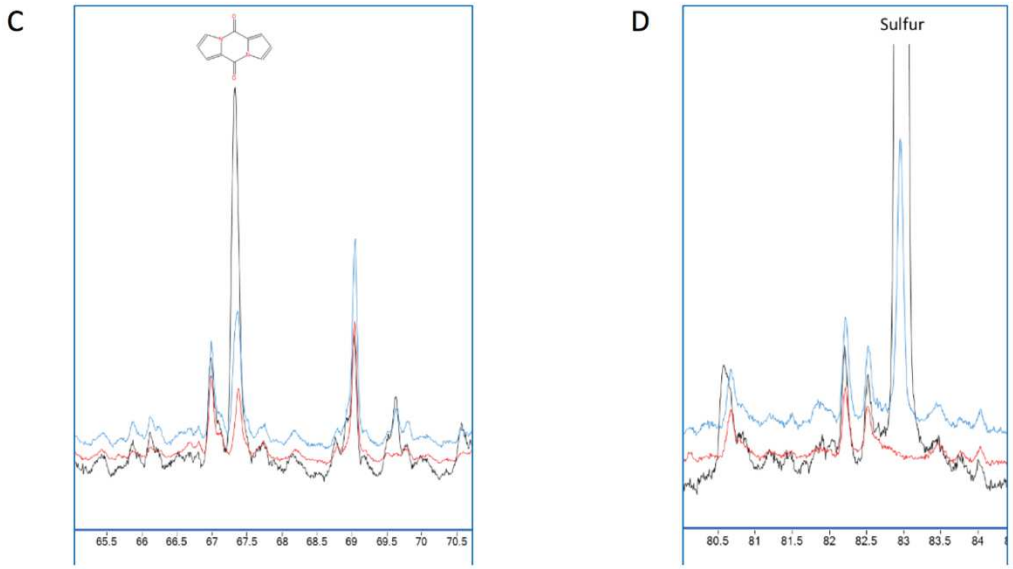

Fig. III.42 Pyrochromatograms of the sediment and 'sediment-binders' systems: (A) Global chromatograms, (B) Aromatic and amino sugars, (C) Proteins and (D) Sulfur

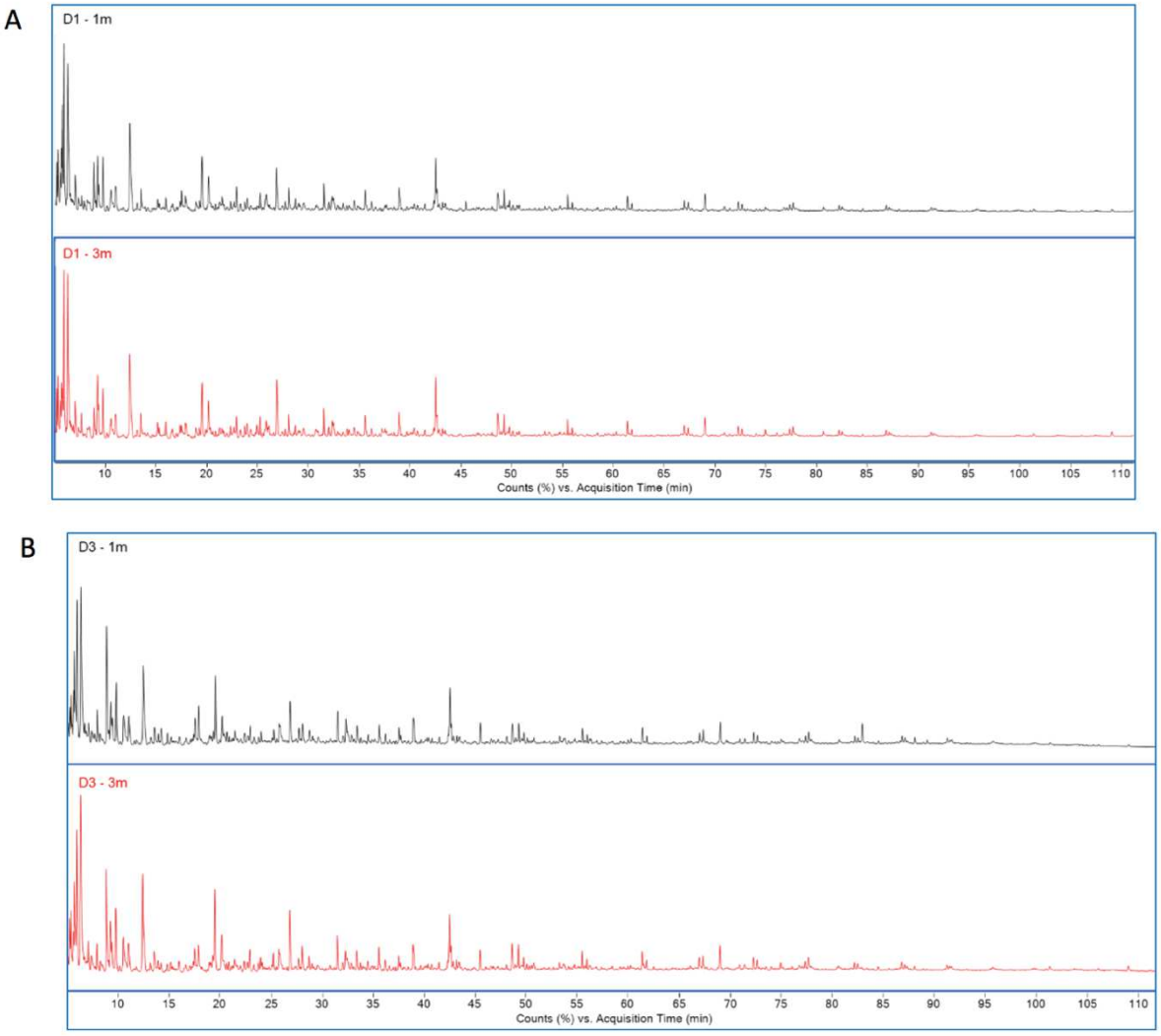

Fig. III.43 Global pyrochromatograms of the 'sediment-binders' system at 1 month and 3 months: (A) OPC binder D1, (B) OPC-GGBS binder D3

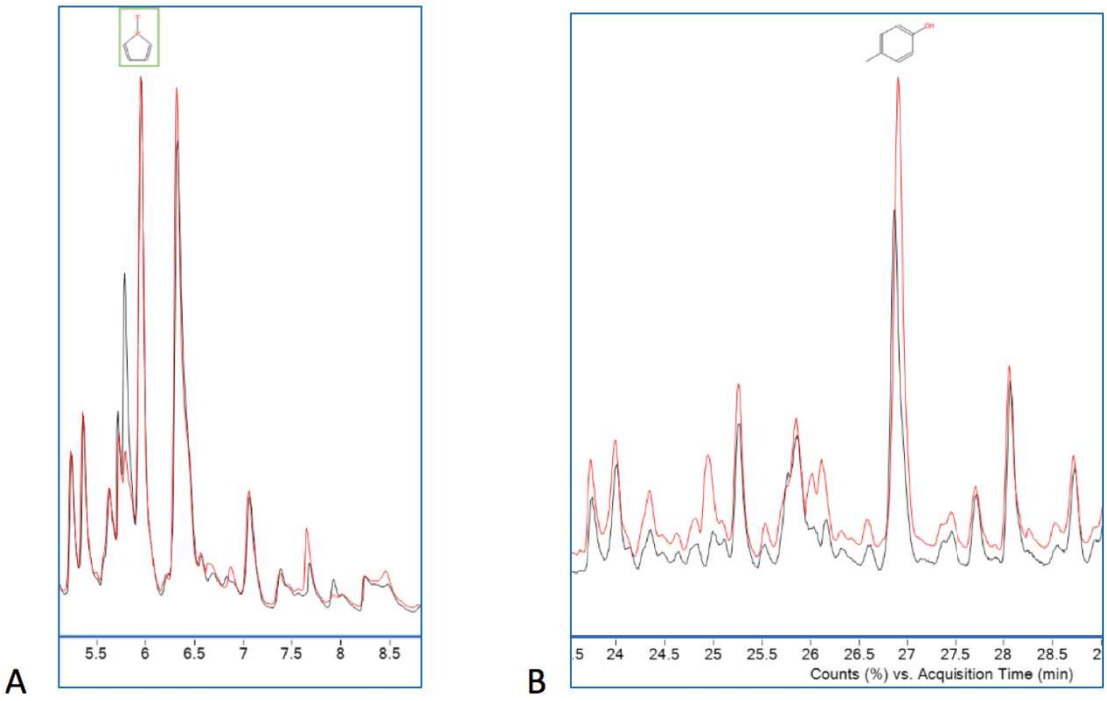

Fig. III.44 Evolution with time of the pyrochromatograms of sediment-OPC binder system D1 at 1 month (black) and 3 months (red): (A) Nitrogen compounds, (B) Phenolic compounds

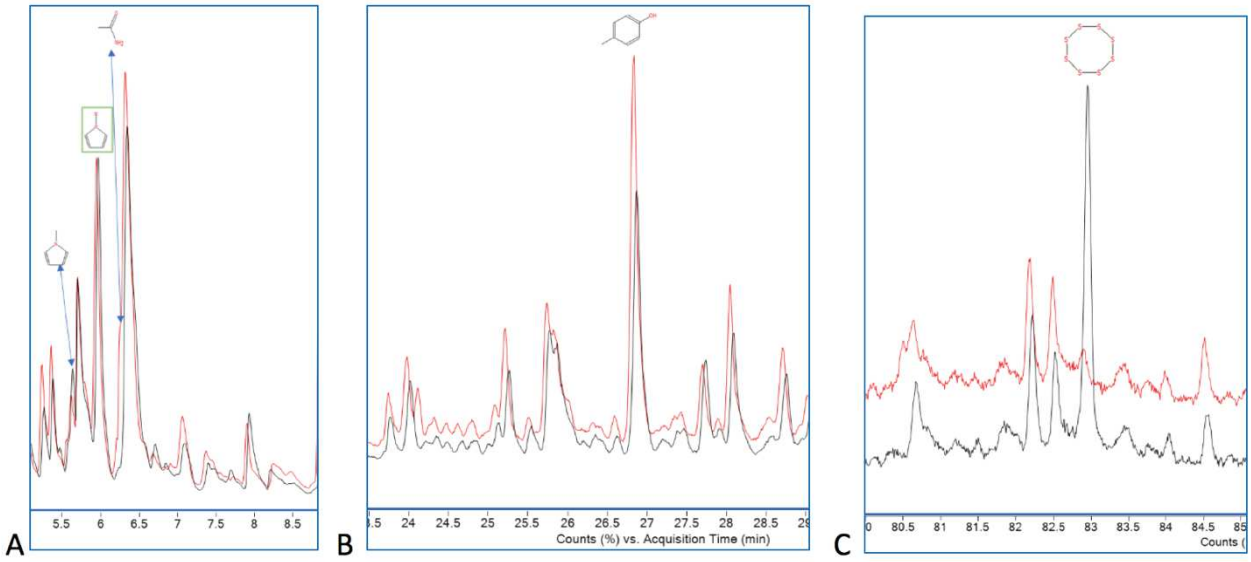

Fig. III.45 Evolution with time of the pyrochromatograms of sediment-OPC/GGBS binder systems D3 at 1 month (black) and 3 months (red): (A) Nitrogen compounds, (B) Phenolic compounds, (C) Sulfur compounds

III.4.2 ^{13}C – NMR investigation

The ^{13}C-NMR investigation adds supplementary information towards characterizing organic matter modifications in the sediment by hydraulic binder treatment. The ^{13}C NMR spectra of the sediment D0 and the samples D1 and D3 are presented in Fig.

III.46. The ^{13}C NMR spectra show the main organic functions in the samples. They exhibit a broad peak between 0 and 95 ppm that can be decomposed into several regions: 0-40 ppm aliphatic carbons, 40-60 ppm carbons in methoxyl groups and/or in amino acid side chains, 60-80 ppm carbon in C-O groups such as in carbohydrates. The peak located at 130 ppm is associated with aromatic carbons and at 160-180 ppm corresponds to carboxyl groups (including acids and amides functions).
When normalized to the aliphatic peak (considered as the most stable functional groups), a substantial decrease is observed in the peak at 70 ppm from D0 to D3 and D1, which reflects the alteration of the carbohydrates with the addition of the hydraulic binders. This evolution is in perfect agreement with the observations made with Py-GC-MS.

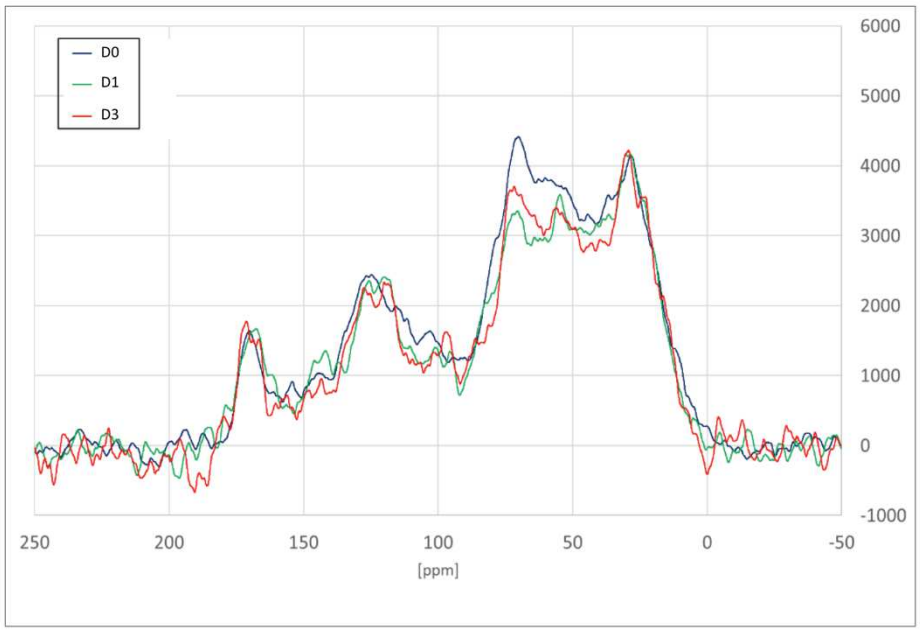

Fig. III.46 ^{13}C NMR spectra of the sediment and the 'sediment-binders' system

III.4.3 Discussion

Different factors affecting the solubility of organic matter have been investigated in previous studies (Baldock & Skjemstad, 2000; Chantigny et al., 2010; Curtin et al., 2016) such as environmental factors (salinity, pH, temperature, mineralogy of the soil) and proper OM characteristics (the size and chemical structure of OM compounds). (Curtin et al., 2016) investigated the effect of high pH on the solubility of organic matter and argued that the amount of DOM (dissolved organic matter) depends on the cation valence – the effect of $Ca(OH)_2$ in comparison to the monovalent cations effect KOH was demonstrated. The pH and electrolyte concentration were greater for KOH, therefore in the higher pH medium (high OH^- content) there was a greater release of organic (DOM) and inorganic anions. As soon as the organic matter solubilized it is decomposed quickly. Thus taking into account the lower concentration of Na^+ and K^+ in the GGBS interstitial solution, it can be concluded from the results shown here that

in the presence of the GGBS-based binder the sediment's organic matter is more stable than in the presence of the OPC-based binder.

Various studies have investigated the role of organic matter on the effectiveness of the S/S remediation technique. In the study of (Tremblay, 2002) different organic compounds were mixed with two types of soils and then treated with 10% of the OPC binder. She reported that the presence of organic compounds greatly delayed the hydration of mixtures compared to inorganic soil samples – the most important negative impact on undrained shear strength was produced with acetic acid, humic acid, tannic acid, and sucrose. Moreover, the lowest pH was produced with these compounds. Consequently, at low pH no hydration products were formed. Other tested compounds delayed hydration by coating the grains of cement. (Rekik et al., 2009) showed how different amounts of organic matter (from 2.5 to 7%) affects the geotechnical properties and the microstructure (higher flocculation-agglomeration rate) of the treated sediments. (Ma et al., 2016; Onitsuka et al., 2003) emphasized how the humic acid may affect the strength development of stabilized materials. In the study of (Ma et al., 2016) the hydrated lime reacts with black humic acid due to its special affinity to Ca^{2+} ions and forms insoluble calcium based humic acid. The last one may also cover the cement and clay particles and delay hydration. (Ma et al., 2016) have also discussed the role of fulvic acid which may affect the durability of cement treatment by the decomposition of the main hydration products such as C-S-H, C-A-H (calcium aluminate hydrates), etc. It is worth mentioning that GGBS activated by OPC has been reported as the best solution for highly organic peat soils, Table III.8 (EuroSoilStab, 2002).

Table III.8 Relative strength increase based on laboratory tests (UCS at 28 days) on Nordic soils (EuroSoilStab, 2002)

Binder	Silt	Clay	Organic Soils, e.g. Gyttja, Organic Clay	Peat
	Organic content (0 - 2%)	Organic content (0 - 2%)	Organic content (2 - 30%)	Organic content (50–100%)
Cement	xx	x	x	xx
Cement + gypsum	x	x	xx	xx
Cement + furnace slag	xx	xx	xx	xxx
Lime + cement	xx	xx	x	-
Lime + gypsum	xx	xx	xx	-
Lime + slag	x	x	x	-
Lime + gypsum + slag	xx	xx	xx	-
Lime + gypsum + cement	xx	xx	xx	-
Lime	-	xx	-	-

Note:
xxx very good binder in many cases
xx good in many cases
x good in some cases
- not suitable

To assess the delay in hydration of the binders caused by organic matter molecules, some model samples of binding agents and humic acids were examined through the calorimetry technique in the following section.

III.4.4 Effect of the organic matter on early age hydration of hydraulic binders

In order to investigate the impact of organic matter on the early hydration of the binders considered in this chapter, humic acids were introduced into the binders during the mixing process. Humic substances are considered to be the most abundant organic molecules with two main different fractions being fulvic and humic acids. Humic acid molecules are often larger (2000-5000 g/mol) than fulvic acid's (500-2000 g/mol) and mostly exist in colloidal form. The most important and common functional groups of both fractions are carboxylic acids, phenolic hydroxyl, carbonyl, and aliphatic hydroxyl groups.

Isothermal calorimetry analysis was chosen to illustrate the impact of humic acids on the hydration kinetics of both types of binders. Humic acid in the solid state was introduced in the binders at different dosages – at 0.1%, 0.5%, 1%, 5%, 10% (by weight of the binder). First, the dry solid humic acids were premixed with binder powders (OPC - 100%OPC and GGBS85 - 85%GGBS/15%OPC) in order to obtain homogeneous mixtures; then the final formulations were prepared with a water:binder ratio of 0.4.

III.4.4.1 Heat flow results

Figure III. 47 presents the evolution of the heat produced during the hydration reactions of the 100%OPC binder with and without humic acids (HA). As can be seen on the graph, the low content of humic molecules (0.1% and 0.5%) slightly lowered the main peak of hydration. A delay of hydration was produced at 1% of HA, but it can be considered as an insignificant effect. However, after the introduction of noticeably higher dosages of HA (5% and 10%), the reaction pathways were greatly disturbed. The main peak of hydration of OPC mixed with 5%wt HA appeared only after 63 hours of measurements, but the heat release was very low. The addition of 10%wt HA completely annihilated the hydration process.

The hydration evolution of the GGBS-based formulation in the presence of humic acids is presented in Fig. III.48. There is some correlation in the results between OPC and GGBS85 mixed with humic acids. The 0.1% and 0.5% dosages of HA slightly reduced the heat produced over the acceleration stage. At 1% the effect is more pronounced and the reaction kinetics are different. Almost the same negative impact of the higher dosages of humic acids can be observed in the figure. At the same time, the main hydration peak of GGBS85 with 5%HA occurs two times faster than in the case of the Portland cement with the same humic acid content. The most negative effect on hydration of GGBS85 was detected in the presence of 10%wt HA.

It is important to understand the mechanisms of the interaction of humic acids with ions from the dissolution of binders. (Zhao et al., 2019) in his study of the fouling behavior of humic acids investigates the interaction of calcium ions and HA. Figure III.49 summarizes mechanisms discussed in this paper: when calcium ions interact with humic acid molecules, there is an aggregation that can be produced due to charge

neutralization. The complexation occurs by reducing the negative charge of carboxilyc groups by Ca^{2+}, therefore a bridge between HA molecules can be produced. This strong interaction (complexation) between calcium ions and humic acids may cause the delay in hydration of the considered binders regarding the important role of Ca^{2+} as an essential element for hydrate precipitation.

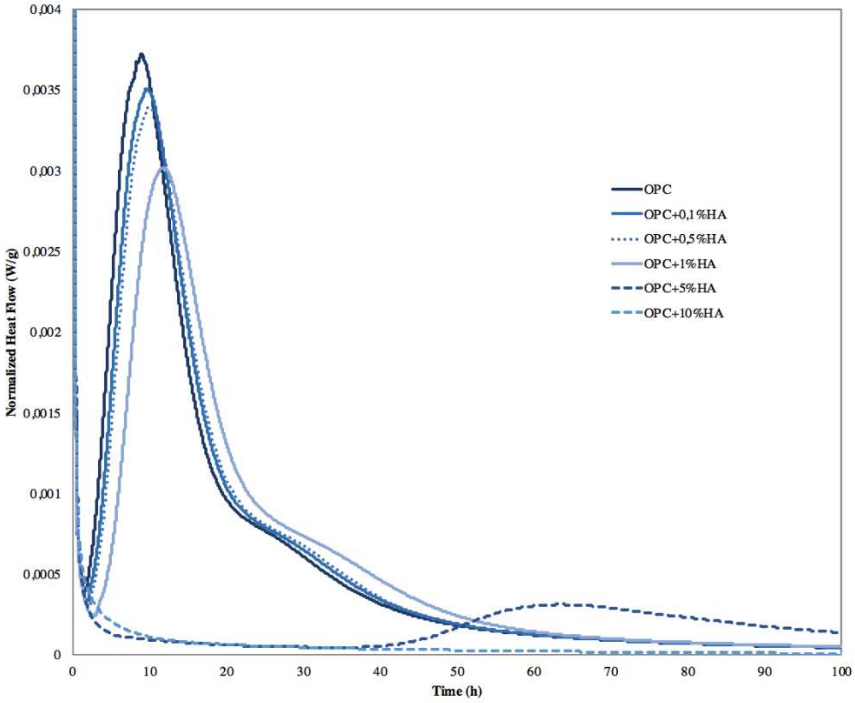

Fig. III.47 Calorimetry measurements of OPC/HA impact

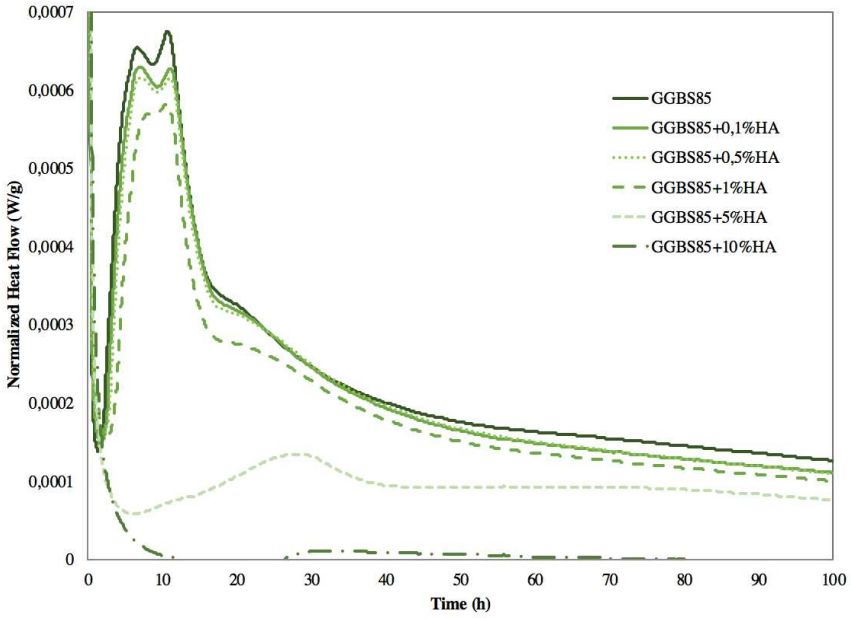

Fig. III.48 Calorimetry measurements of GGBS85/HA impact

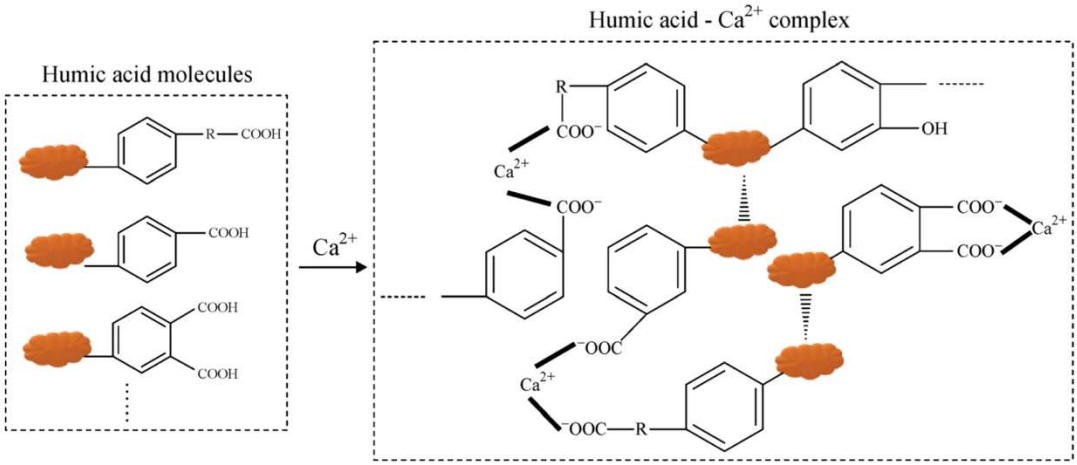

Fig. III.49 Proposed mechanism of the influence of Ca^{2+} on the structure of humic acid (Zhao et al., 2019)

III.5 Conclusions

This study was undertaken to design the most appropriate GGBS-based formulation in order to provide the necessary engineering properties for the dredged Dublin sediment. The range of different types of mix designs was subjected to compressive strength testing after between 28 days and 6 months of storage. The results indicate that GGBS activated by a small amount of OPC (D3) provided the optimal strength, especially at long term storage and exceeded that of the OPC-based samples. Moreover, the strength of the OPC treated sediment showed a degradation of mechanical performances from 3 to 6 months.

The purpose of the current study was to determine the mechanisms of the strength evolution of the Dublin sediment treated with two types of binding agents – OPC (D1) and GGBS-based (D3):

- First, a sediment with a different origin (Gothenburg port) and having a substantially different mineralogy and organic matter content was treated with the same binding agents and compared to the Dublin sediment in terms of compressive strength. The results confirmed the good long term performance of the GGBS-based formulation for both sediments with OPC samples showing stagnation/slight degradation of mechanical performance. The differences in CEC and particle size of the sediments seem to be responsible for the strength development. It was concluded that the interaction of hydraulic binders with the sediment constituents such as clays, organic matter, etc. play an important role in the solidification process.
- The impact of the clay fraction on the mechanical strength evolution was examined separately, as well as the action of exchangeable ions of the binder solutions on the surface charge and rheology of the raw clay sample. This study

showed that the evolution of mechanical strength of both types of mixtures is similar to the sediment's mechanical behavior. The rheological and zeta potential measurements revealed the role of calcium ions in the appearance of the flocculation phenomenon in the presence of the binders, especially of Portland cement having a greater amount of calcium in solution.

- It was then supposed that the dispersed state of the sediment fabric could contribute to the higher strength development. Two types of dispersing agents were applied to the Dublin sediment before treatment with OPC and GGBS-based binders. Indeed, the improvement of rheology through dispersion increased twice the compressive strength of the mixtures.
- Finally, the interaction of the binders with organic matter within the Dublin sediment was assessed through the pyrolysis technique coupled with gas chromatography followed by mass spectroscopy and ^{13}C NMR. The results of this research demonstrate a higher disturbance level of organic matter components with the Portland cement binder (D1) compared to the GGBS-based formulation (D3).

Taken together, these findings have significant implications for understanding of the main mechanisms governing sediment solidification:

- The pH is one of the most important parameters for strength development.
- Different sediments constituents (clays, organic matter) can affect the solidification process.
- It was shown that the strength of the treated material comes not only from the hydrates of the binders but also depends on their repartition within the sediment and on the impact of the binders on the microstructure development. The dispersed state of the sediment matrix shows the relationship between the rheological and microstructure improvements leading to a better strength development.

Bibliography

Andersen, M., Jakobsen, H., & Skibsted, J. (2006). A new Aluminium-Hydrate Species in Hydrated Portland Cements Characterized by 27Al and 29Si MAS NMR Spectroscopy. Cement and Concrete Research - CEM CONCR RES, 36, 3–17. https://doi.org/10.1016/j.cemconres.2005.04.010

Atkinson, A., Everitt, N. M., & Guppy, R. M. (1989). Time dependence of pH in a cementitious repository. Scientific Basis for Nuclear Waste Management XII. http://inis.iaea.org/Search/search.aspx?orig_q=RN:21037560

Avadiar, L., Leong, Y.-K., Fourie, A., & Nugraha, T. (2012). Rheological response to Ca(II) concentration - the source of kaolin slurry rheological variation

Baldock, J. A., & Skjemstad, J. O. (2000). Role of the soil matrix and minerals in protecting natural organic materials against biological attack. Organic Geochemistry, 31(7–8), 697–710. https://doi.org/10.1016/S0146-6380(00)00049-8

Barzegar, A., Murray, R., Churchman, J., & Rengasamy, P. (1994). The strength of remolded soils as affected by exchangeable cations and dispersible clay. Australian Journal of Soil Research - AUST J SOIL RES, 32. https://doi.org/10.1071/SR9940185

Bergado, D. T., Anderson, L. R., Miura, N., & Balasubramaniam, A. S. (1996). Soft Ground Improvement in Lowland and Other Environments. https://cedb.asce.org/CEDBsearch/record.jsp?dockey=0102545

Borgne, T., Cuisinier, O., Deneele, D., & Masrouri, F. (2008). Effects of potential deleterious chemical compounds on soil stabilisation. Advances in Transportation Geotechnics - Proceedings of the 1st International Conference on Transportation Geotechnics, 657–663. https://doi.org/10.1201/9780203885949.ch90

Brooks, J. J., Wainwright, P. J., & Boukendakji, M. (1992). Influence of Slag Type and Replacement Level on Strength Elasticity, Shrinkage and Creep of Concrete. Special Publication, 132, 1325–1342. https://doi.org/10.14359/1230

Cazalet, M. L. (2012). Caractérisation physico-chimique d'un sédiment marin traité aux liants hydrauliques: Évaluation de la mobilité potentielle des polluants inorganiques. 267.

Chantigny, M. H., Curtin, D., Beare, M. H., & Greenfield, L. G. (2010). Influence of Temperature on Water-Extractable Organic Matter and Ammonium Production in Mineral Soils. Soil Science Society of America Journal, 74(2), 517–524. https://doi.org/10.2136/sssaj2008.0347

Chew, S. H., Kamruzzaman, A. H. M., & Lee, F. H. (2004). Physicochemical and Engineering Behavior of Cement Treated Clays. Journal of Geotechnical and Geoenvironmental Engineering, 130(7), 696–706. https://doi.org/10.1061/(ASCE)1090-0241(2004)130:7(696)

Claret, F., Bauer, A., Schäfer, T., Griffault, L., & Lanson, B. (2002). Experimental investigation of the interaction of clays with high-pH solutions: A case study from the Callovo-Oxfordian formation, Meuse-Haute Marne underground laboratory (France). Clays and Clay Minerals, 50(5), 633–646. https://doi.org/10.1346/000986002320679369

Codina, M. (2007). Les bétons bas pH - Formulation, caractérisation et étude à long terme. 202.

Colombet, P., Grimmer, A.-R., Zanni, H., & Sozzani, P. (Eds.). (1998). Nuclear Magnetic Resonance Spectroscopy of Cement-Based Materials. Springer-Verlag. https://doi.org/10.1007/978-3-642-80432-8

Condren, E., & Pavía, S. (2007). A comparative study of the moisture transfer properties and durability of PC and GGBS mortars. 10.

Cruz, N., & Peng, Y. (2016). Rheology measurements for flotation slurries with high clay contents – A critical review. Minerals Engineering, 98, 137–150. https://doi.org/10.1016/j.mineng.2016.08.011

Curtin, D., Peterson, M. E., & Anderson, C. R. (2016). pH-dependence of organic matter solubility: Base type effects on dissolved organic C, N, P, and S in soils with contrasting mineralogy. Geoderma, 271, 161–172. https://doi.org/10.1016/j.geoderma.2016.02.009

Divsholi, B. S., Lim, T. Y. D., & Teng, S. (2014). Durability Properties and Microstructure of Ground Granulated Blast Furnace Slag Cement Concrete. International Journal of Concrete Structures and Materials, 8(2), 157–164. https://doi.org/10.1007/s40069-013-0063-y

Dong, J. (2014). Investigation of aggregates size effect on the stiffness of lime and/or cement treated soils: From laboratory to field conditions. 379.

Eades and Grim, A Quick Test to Determine Lime Requirements For Lime Stabilization

EuroSoilStab (2002) “Development of Design and Construction Methods to Stabilize Soft Organic Soils,” Design Guide Soft Soil Stabilization, Industrial & Materials Technologies Programme (Brite- EuRam III), European Commission, CT97-0351, Project No. BE 96-3177, pp. 15-60

Feng, P., Miao, C., & Bullard, J. W. (2016). Factors influencing the stability of AFm and AFt in the Ca–Al–S–O–H system at 25 °C. Journal of the American Ceramic Society. American Ceramic Society, 99(3), 1031–1041. https://doi.org/10.1111/jace.13971

Flegar, M., Serdar, M., Londono-Zuluaga, D., & Scrivener, K. (2019). Overview of clay as supplementary cementitious material. https://doi.org/10.5592/CO/PhDSym.2019.14

Gaucher, E. C., & Blanc, P. (2006). Cement/clay interactions – A review: Experiments, natural analogues, and modeling. Waste Management, 26(7), 776–788. https://doi.org/10.1016/j.wasman.2006.01.027

Gervais, C., Garrabrants, A. C., Sanchez, F., Barna, R., Moszkowicz, P., & Kosson, D. S. (2004). The effects of carbonation and drying during intermittent leaching on the release of inorganic constituents from a cement-based matrix. Cement and Concrete Research, 34(1), 119–131. https://doi.org/10.1016/S0008-8846(03)00248-5

Güneyisi, E., & Gesoğlu, M. (2008). A study on durability properties of high-performance concretes incorporating high replacement levels of slag. Materials and Structures, 41(3), 479–493. https://doi.org/10.1617/s11527-007-9260-y

Hooton, D. (2004). The Effect of Ground, Granulated Blast Furnace Slag (Slag Cement) on the Drying Shrinkage of Concrete-A Critical Review of the Literature. ResearchGate. https://www.researchgate.net/publication/228391396_The_Effect_of_Ground_Granulated_Blast_Furnace_Slag_Slag_Cement_on_the_Drying_Shrinkage_of_Concrete-A_Critical_Review_of_the_Literature

Huang, H., & Shen, X. (2011). Statistical study of cement additives with and without chloride on performance modification of Portland cement. Progress in Natural Science: Materials International, 21, 246–253. https://doi.org/10.1016/S1002-0071(12)60038-0

Jin, F., Wang, F., & Al-Tabbaa, A. (2016). Three-year performance of in-situ solidified/stabilised soil using novel MgO-bearing binders. Chemosphere, 144, 681–688. https://doi.org/10.1016/j.chemosphere.2015.09.046

Kalankamary P. (1968). Shrinkage Characteristics of Soil-Cement Mixtures. 17.

kalıpcılar, İ., Mardani, A., Sezer, A., S, G., & Altun, S. (2016). Assessment of the effect of sulfate attack on cement stabilized montmorillonite. Geomechanics and Engineering, 10. https://doi.org/10.12989/gae.2016.10.6.807

Kinsey, R. A., Kirkpatrick, R. J., Hower, J., Smith, K. A., & Oldfield, E. (1985). High resolution aluminum-27 and silicon-29 nuclear magnetic resonance spectroscopic study of layer silicates, including clay minerals. American Mineralogist, 70(5–6), 537–548.

Klučáková, M. (2018). Size and Charge Evaluation of Standard Humic and Fulvic Acids as Crucial Factors to Determine Their Environmental Behavior and Impact. Frontiers in Chemistry, 6, 235. https://doi.org/10.3389/fchem.2018.00235

Konan, K. L., Peyratout, C., Bonnet, J.-P., Smith, A., Jacquet, A., Magnoux, P., & Ayrault, P. (2007). Surface properties of kaolin and illite suspensions in concentrated calcium hydroxide medium. Journal of Colloid and Interface Science, 307(1), 101–108. https://doi.org/10.1016/j.jcis.2006.10.085

Le, T. M., Fatahi, B., & Khabbaz, H. (2012). Viscous Behaviour of Soft Clay and Inducing Factors. Geotechnical and Geological Engineering, 30(5), 1069–1083. https://doi.org/10.1007/s10706-012-9535-0

Lemaire, K. (2012). Evolution des caractéristiques physico-chimiques, microstructurales et hydromécaniques de limon traités aux liants lors d'une circulation d'eau. 263.

Liddel, P. V., & Boger, D. V. (1996). Yield stress measurements with the vane. Journal of Non-Newtonian Fluid Mechanics, 63(2–3), 235–261. https://doi.org/10.1016/0377-0257(95)01421-7

Lowke, D., & Gehlen, C. (2017). The zeta potential of cement and additions in cementitious suspensions with high solid fraction. Cement and Concrete Research, 95, 195–204. https://doi.org/10.1016/j.cemconres.2017.02.016

Ma, C., Chen, B., & Chen, L. (2016). Effect of organic matter on strength development of self-compacting earth-based construction stabilized with cement-based composites. Construction and Building Materials, 123, 414–423. https://doi.org/10.1016/j.conbuildmat.2016.07.018

McCallister, L. D., & Petry, T. M. (1992). Leach Tests on Lime-Treated Clays. Geotechnical Testing Journal, 15(2), 106–114. https://doi.org/10.1520/GTJ10232J

Moayedi, H., Asadi, A., Huat, B. B. K., & Kazemian, S. (2011). Zeta potential of Organic soil in Presence of Calcium Chloride, Cement and Polyvinyl Alcohol. Int. J. Electrochem. Sci., 6, 11.

J.K. Mitchell, Soil Improvement — State-of-the-Art Report, 1981

Moevus, M., Jorand, Y., Olagnon, C., Maximilien, S., Anger, R., Fontaine, L., & Arnaud, L. (2016). Earthen construction: An increase of the mechanical strength by optimizing the dispersion of the binder phase. Materials and Structures, 49(4), 1555–1568. https://doi.org/10.1617/s11527-015-0595-5

Neuville, D. R., Cormier, L., Montouillout, V., Florian, P., Millot, F., Rifflet, J.-C., & Massiot, D. (2008). Amorphous materials: Properties, structure, and durabilityStructure of Mg- and Mg/Ca aluminosilicate glasses: 27Al NMR and Raman spectroscopy investigations. American Mineralogist, 93(11–12), 1721–1731. https://doi.org/10.2138/am.2008.2867

Nowack, B. (2003). Environmental chemistry of phosphonates. Water Research, 37(11), 2533–2546. https://doi.org/10.1016/S0043-1354(03)00079-4

Onitsuka, K., Modmoltin, C., Kouno, M., & Negami, T. (2003). Effect of organic matter on lime and cement stabilized Ariake clays. Doboku Gakkai Ronbunshu, 729, 1–13. https://doi.org/10.2208/jscej.2003.729_1

Ortega, J. M., Esteban, M. D., Rodríguez, R. R., Pastor, J. L., Ibanco, F. J., Sánchez, I., & Climent, M. Á. (2017). Long-Term Behaviour of Fly Ash and Slag Cement Grouts for Micropiles Exposed to a Sulphate Aggressive Medium. Materials (Basel, Switzerland), 10(6). https://doi.org/10.3390/ma10060598

Özbay, E., Erdemir, M., & Durmuş, H. İ. (2016). Utilization and efficiency of ground granulated blast furnace slag on concrete properties – A review. Construction and Building Materials, 105, 423–434. https://doi.org/10.1016/j.conbuildmat.2015.12.153

Pajares, I., Martínez-Ramírez, S., & Blanco-Varela, M. T. (2003). Evolution of ettringite in presence of carbonate, and silicate ions. Cement and Concrete Composites, 25(8), 861–865. https://doi.org/10.1016/S0958-9465(03)00113-6

Prusinski, J. R., & Bhattacharja, S. (1999). Effectiveness of Portland Cement and Lime in Stabilizing Clay Soils. Transportation Research Record, 1652(1), 215–227. https://doi.org/10.3141/1652-28

Puppala, A. J. (2016). Advances in ground modification with chemical additives: From theory to practice. Transportation Geotechnics, 9, 123–138. https://doi.org/10.1016/j.trgeo.2016.08.004

Rekik, B., Boutouil, M., & Pantet, A. (2009). Geotechnical properties of cement treated sediment: Influence of the organic matter and cement contents. International Journal of Geotechnical Engineering, 3(2), 205–214. https://doi.org/10.3328/IJGE.2009.03.02.205-214

Richardson, I. G., & Groves, G. W. (1992). Microstructure and microanalysis of hardened cement pastes involving ground granulated blast-furnace slag. Journal of Materials Science, 27(22), 6204–6212. https://doi.org/10.1007/BF01133772

Rolfe B. N. (1960). Dispersion characteristics of montmorillonite, kaolinite, and illite clays in waters of varying quality, and their control with phosphate dispersants. https://pubs.er.usgs.gov/publication/pp334G

Sargent, P. (2015). The development of alkali-activated mixtures for soil stabilisation. In Handbook of Alkali-Activated Cements, Mortars and Concretes (pp. 555–604). Elsevier. https://doi.org/10.1533/9781782422884.4.555

Sargent, Paul, Hughes, P. N., Rouainia, M., & White, M. L. (2013). The use of alkali activated waste binders in enhancing the mechanical properties and durability of soft alluvial soils. Engineering Geology, 152(1), 96–108. https://doi.org/10.1016/j.enggeo.2012.10.013

Shi, X., Xie, N., Fortune, K., & Gong, J. (2012). Durability of steel reinforced concrete in chloride environments: An overview. Construction and Building Materials, 30, 125–138. https://doi.org/10.1016/j.conbuildmat.2011.12.038

Shi, X., Yang, Z., Liu, Y., & Cross, D. (2011). Strength and corrosion properties of Portland cement mortar and concrete with mineral admixtures. Construction and Building Materials, 25(8), 3245–3256. https://doi.org/10.1016/j.conbuildmat.2011.03.011

Skibsted, J., Henderson, E., & Jakobsen, H. J. (1993). Characterization of calcium aluminate phases in cements by aluminum-27 MAS NMR spectroscopy. Inorganic Chemistry, 32(6), 1013–1027. https://doi.org/10.1021/ic00058a043

Sondi, I., Bišćan, J., & Pravdić, V. (1996). Electrokinetics of Pure Clay Minerals Revisited. Journal of Colloid and Interface Science, 178(2), 514–522. https://doi.org/10.1006/jcis.1996.0146

Sparks, D. L. (2002). Environmental Soil Chemistry. 367.

Tazawa, E., Yonekura, A., & Tanaka, S. (1989). Drying Shrinkage and Creep of Concrete Containing Granulated Blast Furnace Slag. Special Publication, 114, 1325–1344. https://doi.org/10.14359/2604

Teng, S., Lim, T. Y. D., & Sabet Divsholi, B. (2013). Durability and mechanical properties of high strength concrete incorporating ultra fine Ground Granulated Blast-furnace Slag. Construction and Building Materials, 40, 875–881. https://doi.org/10.1016/j.conbuildmat.2012.11.052

Thiery, M., Dangla, P., Villain, G., Platret, G., Massieu, E., Druon, M., & Baroghel-Bouny, V. (2004). Modelisation de la carbonatation atmospherique des materiaux cimentaires. BULLETIN DES LABORATOIRES DES PONTS ET CHAUSSEES, 252–253. https://trid.trb.org/view/944335

Topolnicki, M., & Pandrea, P. (2012). Design of in-situ soil mixing. 8.

Tremblay. (2002). Influence of the nature of organic compounds on fine soil stabilization with cement | Request PDF. ResearchGate. http://dx.doi.org/10.1139/t02-002

Van Rompaey, G. (2006). Etude de la réactivité des ciments riches en laitier, à basse température et à temps court, sans ajout chloruré. http://hdl.handle.net/2013/

Walkley, B., & Provis, J. L. (2019). Solid-state nuclear magnetic resonance spectroscopy of cements. Materials Today Advances, 1, 100007. https://doi.org/10.1016/j.mtadv.2019.100007

Wathiq Al-lJabban, W., Knutsson, S., Al-Ansari, N., & Laue, J. (2017). Modification-Stabilization of Clayey Silt Soil Using Small Amounts of Cement. 21.

Wilkinson, A., Haque, A., & Kodikara, J. (2010). Stabilisation of clayey soils with industrial by-products: Part B. Proceedings of the Institution of Civil Engineers - Ground Improvement, 163(3), 165–172. https://doi.org/10.1680/grim.2010.163.3.165

Yuan, J., Lindquist, W., Darwin, D., & Browning, J. (2015). Effect of slag cement on drying shrinkage of concrete. ACI Materials Journal, 112(2). https://doi.org/10.14359/51687129

Yukselen, Y., & Kaya, A. (2002). Zeta Potential of Kaolinite in the Presence of Alkali, Alkaline Earth and Hydrolyzable Metal Ions. 14.

Yukselen-Aksoy, Y., & Kaya, A. (2016). The Zeta Potential of a Mixed Mineral Clay in the Presence of Cations. 1(1), 8.

Zhao, X., Wu, Y., Zhang, X., Tong, X., Yu, T., Wang, Y., Ikuno, N., Ishii, K., & Hu, H. (2019). Ozonation as an efficient pretreatment method to alleviate reverse osmosis membrane fouling caused by complexes of humic acid and calcium ion. Frontiers of Environmental Science & Engineering, 13(4), 55. https://doi.org/10.1007/s11783-019-1139-y

Chapter IV: Impact of heavy metals pollutants contained in dredged sediments on the hydration of hydraulic binders

IV.1 Introduction

The effectiveness of the Stabilization/Solidification process may be modified depending on the different constituents of a treated waste. During the treatment of sediments with cement, a delay or prevention of setting may occur, which can alter the properties of the final material. The type of heavy metals, their ionic radii, and their concentration may impact the hydration kinetics of binders and the growth and nucleation of hydrates in different ways (Mahedi et al., 2019).

Numerous studies have attempted to explain the mechanisms involved in the retardation/acceleration of cementitious systems (Chen et al., 2009; Fernández Olmo et al., 2001; Gineys et al., 2010; Lu et al., 2017). Some heavy metals are thought to cover cement grains like a protective membrane of amorphous hydroxide species, preventing the dissolution of binders. However, there is a lack of direct evidence of such mechanisms and the experimental data are rather controversial. (Scrivener et al., 2019; Weeks et al., 2008) doubt the validity of the protective membrane theory because such membranes have never been detected, even with help of advanced modern tools. Another possible retardation mechanism can potentially arise from the delayed nucleation of some important hydrates which usually occur during early hydration and cause the hardening of the treated material. This theory credits the induction period to the slow nucleation and growth of hydrates such as CH and C-S-H until the solution becomes supersaturated. In addition, some theories explain the induction and acceleration period only by C-S-H nucleation and growth which starts from the very beginning of hydration (Bazzoni, 2014). The recent theory of undersaturation of solution and dissolution of minerals is proposed in the literature. This theory explains the non-linear decrease in dissolution rate of minerals with the undersaturation decrease, meaning that the system goes towards equilibrium (Scrivener et al., 2019). With the decrease in the degree of undersaturation of the solution, the reaction rate decreases severely, which is related to the induction period observed through calorimetry analysis. With an increase in the degree of undersaturation at the end of dormant period, cement dissolution takes place (Bazzoni, 2014; P. Aïtcin and R. Flatt, 2016). After supersaturation with a sufficient concentration of calcium and silicates in solution, a massive nucleation of stable C-S-H occurs. However, further works need to be done in order to validate the theories and explain the first hydration steps of complex cement systems, especially concerning alternative cementitious materials and their use for waste treatment. The complexity arises from the variation of each type of binder, as well as from the coupling processes of dissolution-growth of hydrates. In a general sense, the extended induction period of the cement systems in the presence of foreign ions such as heavy metals may have two origins: ion-ion interaction or interactions taking place at the surface of a solid in solution (Nicoleau et al., 2014; Viallis-Terrisse et al., 2001).

There are relatively few studies on the mechanisms changing the hydration kinetics of GGBS-based binders in the presence of heavy metals (Garg & White, 2017; Hekal et

al., 2012; Yoon et al., 2020). The present study was designed to determine the effect of Zn, Cu, Ni, and Cd on the early hydration of OPC, super-sulfated cements, and OPC-activated GGBS-based binders in order to optimize the S/S process and enhance its efficiency in various applications. The compressive strength results of the sediment mixed with the binders showed that the super-sulfated formulation (D4) did not reach a sufficient strength to be measured after being mixed with the contaminated sediment, whereas the OPC-based samples were hard enough after only a few days of storage. The GGBS formulation activated with OPC (D3) did sufficiently hydrate after 2 weeks, however at long term storage the strength of the samples with GGBS exceeded those of the OPC-based mixes (Fig. III.1). These findings demonstrated wide variations in hydration kinetics for the different types of binding agents once mixed with contaminated sediments, which could potentially be the result of the interaction with trace elements. Thus, four types of metal cations (Zn, Cu, Ni, and Cd) in the form of nitrate salts were chosen according to their abundance in polluted soil/sediment matrices as well as for the difference in their ionic size. They were introduced separately to the binders. The XRD, calorimetry, and zeta potential methods were used as tools to evaluate the impact of zinc, copper, nickel, and cadmium on the hydration kinetics of the binders at early age. NMR spectroscopy provided a deeper insight into how the hydraulic binders interacted with the considered heavy metals after 28 days and 3 months.

IV.2 Early age hydration of the binders with HM

IV.2.1 Impact of zinc

Table IV.1 presents all the samples considered in this section:

Table IV.1 Samples prepared for the zinc impact investigation on the early hydration of the binders

	$Zn(NO_3)_2$		
	0.1%	**0.5%**	**2%**
100%OPC	0.1%ZnOPC	0.5%ZnOPC	2%ZnOPC
85%GGBS/15%OPC	0.1%ZnGGBS85	0.5%ZnGGBS85	2%ZnGGBS85
85%GGBS/14%Ca_2SO_4/1%OPC	0.1%ZnSSC	0.5%ZnSSC	2%ZnSSC

IV.2.1.1 100%OPC formulation

The OPC formulation mixed with different amounts of zinc nitrate exhibited changes in the hydration behaviour (Fig. IV.1). For the control mixture (without zinc nitrate), the main hydration peak (MHP), corresponding to the rapid growth of CH (portlandite) and C-S-H, occurs at 11.4 h with a peak heat flow of 3.87 mW/g. The addition of a small dosage of zinc nitrate (0.1%wt) leads to the acceleration of the hydration kinetics with the MHP occurring at 8.7 h and with slightly higher peak heat rate release. However, a delay in hydration can be observed for the higher dosages of zinc. The induction

period is longer with MHP appearing at 13.6 h and 19.4 h, with a larger peak heat flow rates of 4.8 mW/g and 6 mW/g at 0.5% and 2% $Zn(NO_3)_2$ respectively. The value of the total heat flow after 72 h of hydration progressively decreased with increasing zinc nitrate dosage.

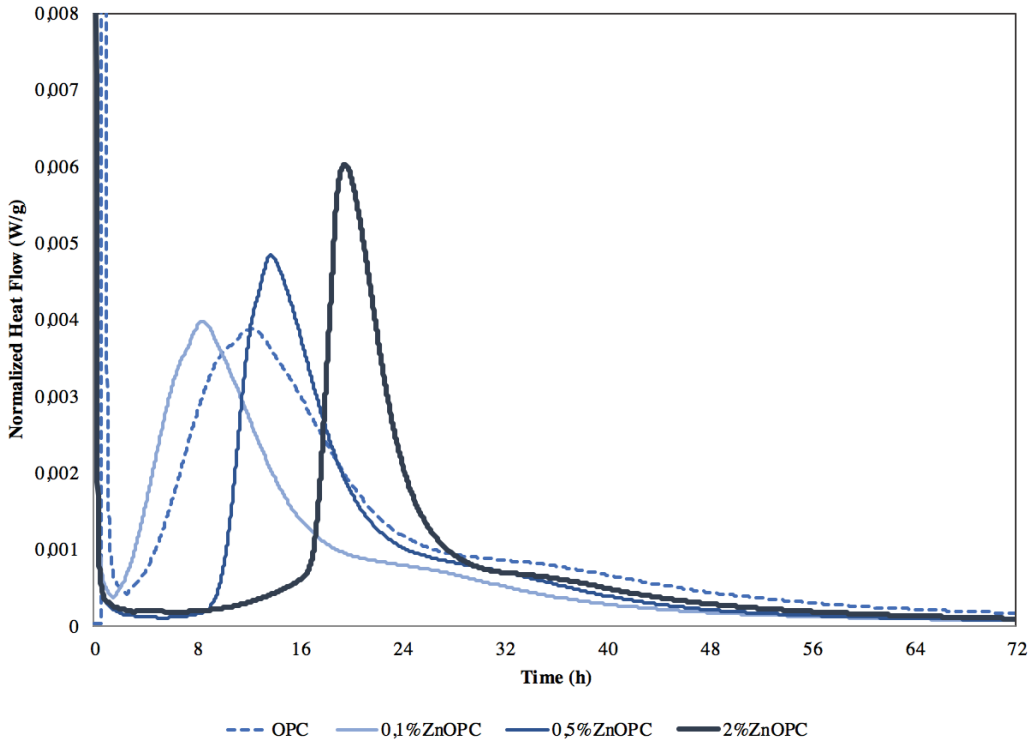

Fig. IV.1 Isothermal calorimetry of 100%OPC with addition of 0,1%$Zn(NO_3)_2$, 0,5%$Zn(NO_3)_2$, 2%$Zn(NO_3)_2$

The main OPC hydration products, with and without zinc addition, were identified via XRD after 24 h and 7 days of storage (Fig. IV.2, Fig. IV.2). The compounds containing zinc were not detected due to the low amount of this element within the sample.
Almost no difference in hydration product development can be observed between the control formulation and with the addition of 0.1% and 0.5% of $Zn(NO_3)_2$. At the same time for the 2% dosage of zinc nitrate, there is a higher amount of calcite and a lower amount of portlandite precipitation. The amount of calcite can indicate carbonation of the sample due to the effect of zinc during the deceleration and hardening period (8-24 h) previously reported by (Chen et al., 2007; Taylor, 1997). This phenomenon was also observed by (McWhinney & Cocke, 1993), and is explained through a lowering of the buffering capacity of calcium due to the presence of different metal cations. As can be seen in Fig. IV.3, no significant difference in hydrate development was observed at 7 days of storage between the control sample and 0.1%ZnOPC, 0.5%ZnOPC, and 2%ZnOPC.

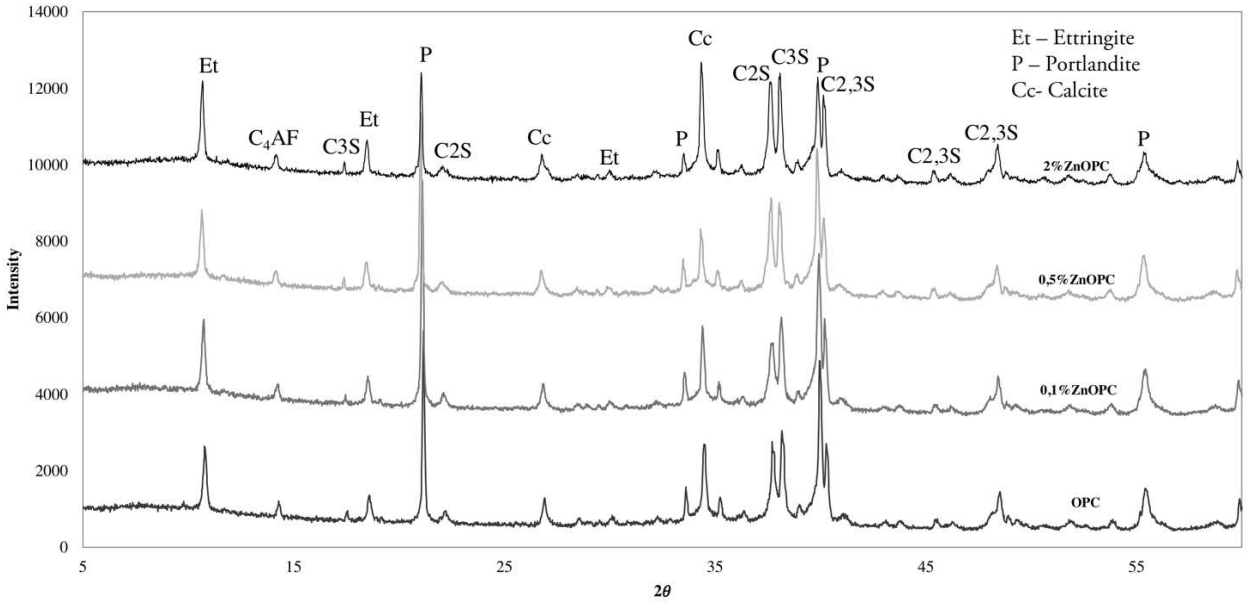

Fig. IV.2 XRD analysis of 100%OPC with addition of 0,1%$Zn(NO_3)_2$, 0,5%$Zn(NO_3)_2$, 2%$Zn(NO_3)_2$ after 24 hours of storage

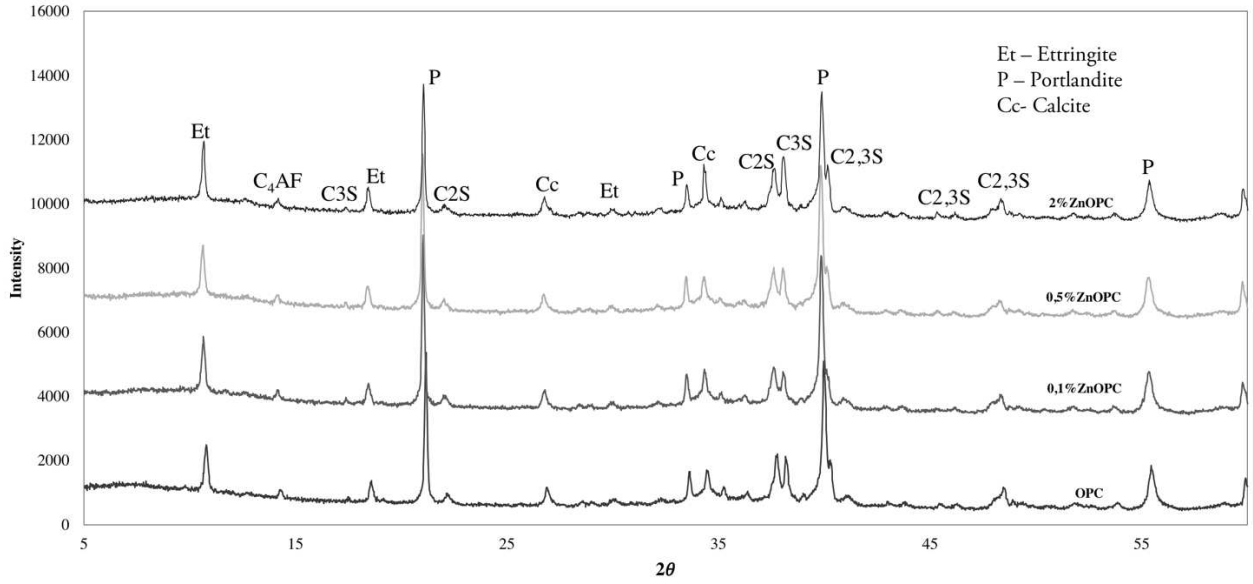

Fig.IV.3 XRD analysis of 100%OPC with addition of 0,1%$Zn(NO_3)_2$, 0,5%$Zn(NO_3)_2$, 2%$Zn(NO_3)_2$ after 7 days of storage

IV.2.1.2 85%GGBS/15%OPC formulation

Figure IV.4 presents the heat release profiles for the GGBS85 formulation with and without zinc nitrate. The main hydration peak of the control mixture (GGBS85) is attributed to the pozzolanic reaction of GGBS following Portland cement hydration acting as an activator of the system. It occurs at 13.5 h after mixing, releasing 0.71 mW/g of heat. The 0.1%wt of zinc nitrate exhibits an acceleration of the main hydration peak. Meanwhile, the higher zinc dosages significantly impacted early hydration. The 0.5%$Zn(NO_3)_2$ dosage has an significant retarding effect with the MHP occurring at 50.7 h, with a peak heat release two times lower than the control at 0.34 mW/g, and

with an acceleration period that starts and ends over a longer duration. Moreover, the introduction of 2% $Zn(NO_3)_2$ completely annihilated the early hydration process.

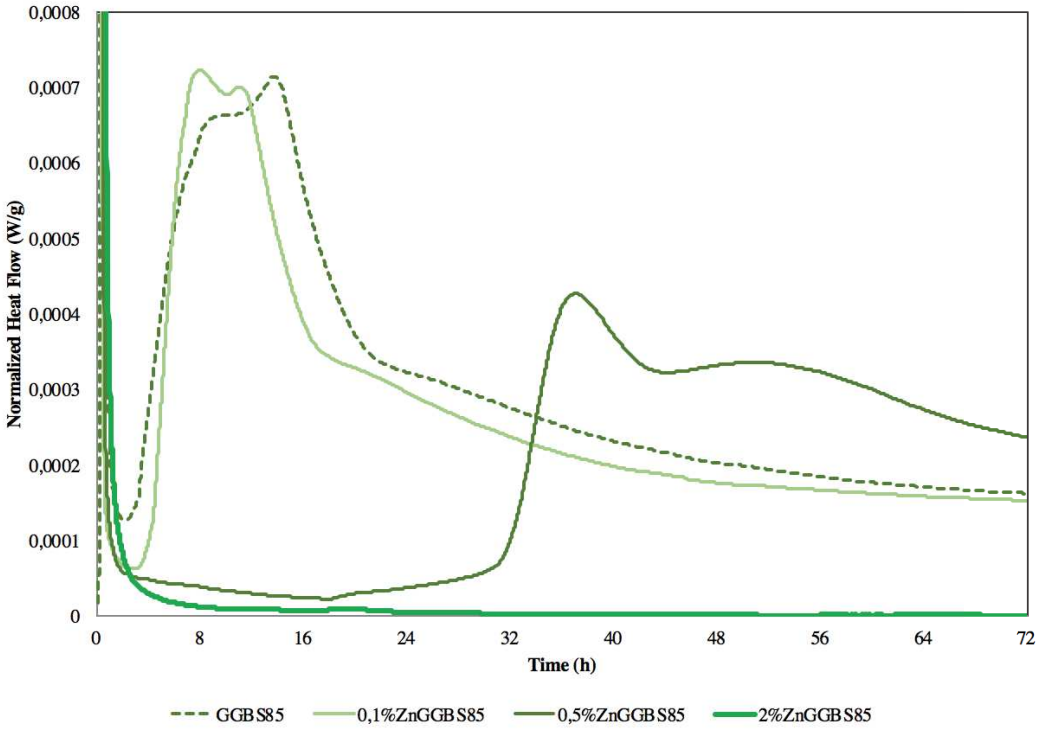

Fig. IV.4 Isothermal calorimetry of 85%GGBS/15%OPC with addition of 0,1%$Zn(NO_3)_2$, 0,5%$Zn(NO_3)_2$, 2%$Zn(NO_3)_2$

The XRD analysis after 24 hours of hydration shows the precipitation of ettringite and portlandite for the control condition (Fig. IV.5). With the introduction of 0.1%$Zn(NO_3)_2$ the intensity of these hydrates was two times lower. However, in the case of 0.5% and 2% zinc nitrate, only ettringite was formed. The absence of portlandite is in accordance with the presence of the anhydrous peaks of C_2S and C_3S compared to their significant disappearance via dissolution in the case of the reference formulation and 0.1%ZnGGBS85. It can be clearly seen that no portlandite is present even after 7 days of storage when 2% of $Zn(NO_3)_2$ was added (Fig. IV.6). The dissolution of alite and belite (C_3S, C_2S) was greatly inhibited by increasing the amount of zinc nitrate to 2%. The formation of C-S-H gel (broad peaks at 34°) can be detected on the XRD graph after 7 days of storage for GGBS85, 0.1%ZnGGBS85, and 0.5%ZnGGBS85, however for 2% of $Zn(NO_3)_2$ only calcite is present in this region.

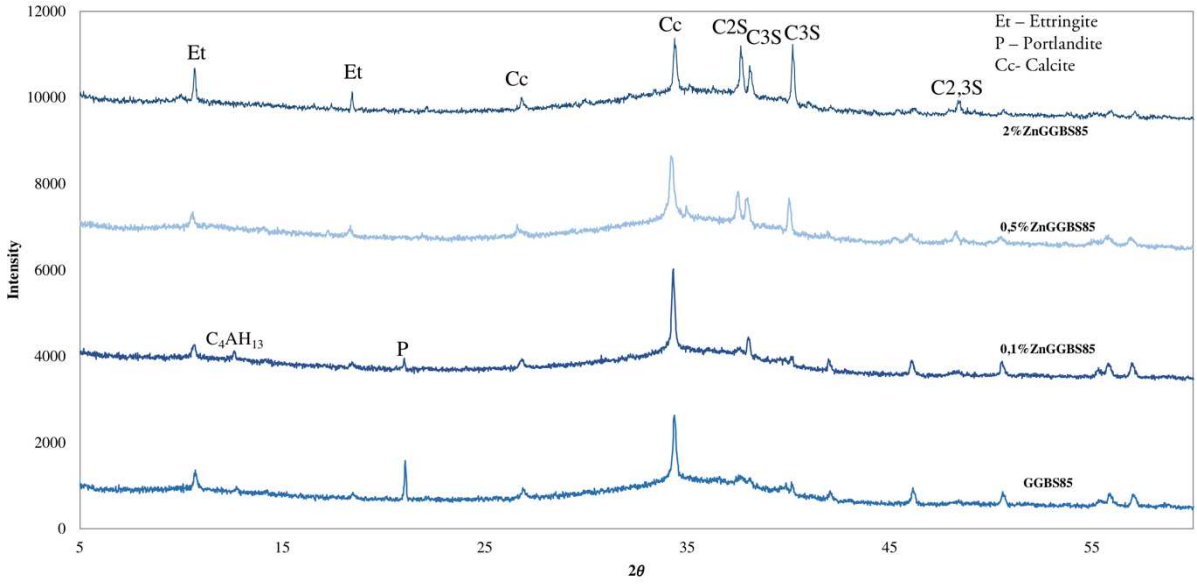

Fig. IV.5 XRD analysis of 85%GGBS/15%OPC with addition of 0,1%$Zn(NO_3)_2$, 0,5%$Zn(NO_3)_2$, 2%$Zn(NO_3)_2$ after 24 hours of storage

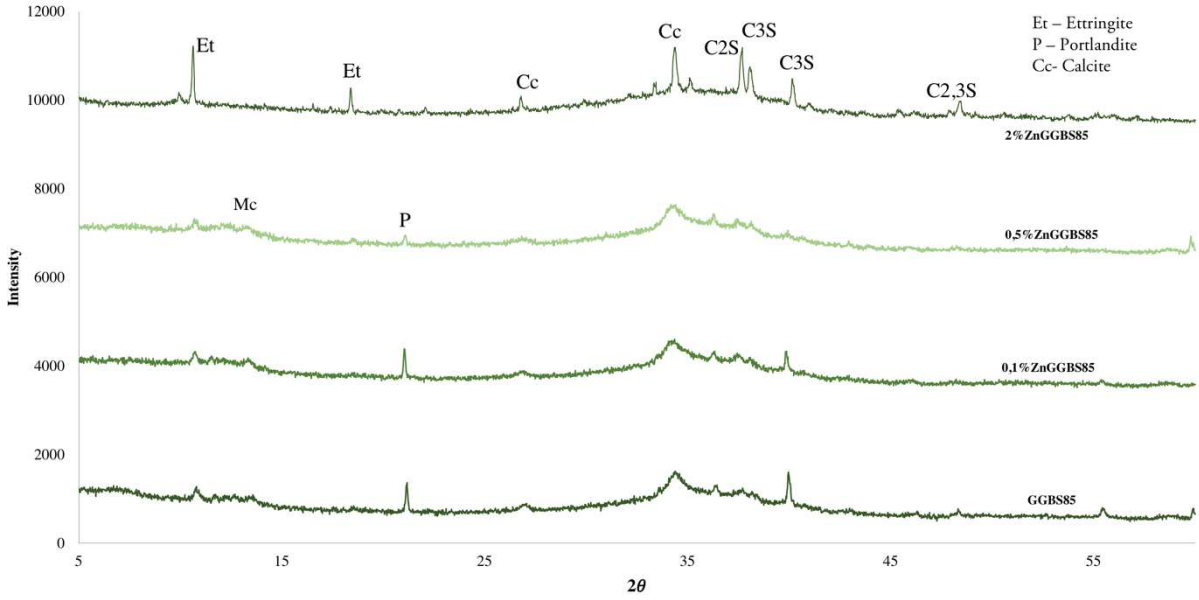

Fig. IV.6 XRD analysis of 85%GGBS/15%OPC with addition of 0,1%$Zn(NO_3)_2$, 0,5%$Zn(NO_3)_2$, 2%$Zn(NO_3)_2$ after 7 days of storage

IV.2.1.3 Supersulfated formulation

The supersulfated (SSC) formulation seems to be the most negatively impacted by the addition of zinc nitrate compared to OPC and GGBS85 (Fig. IV.7). The main hydration peak of the control sample of SSC was recorded after 14 h of hydration with a heat flow rate of 0.48 mW/g. In the presence of 0.1% $Zn(NO_3)_2$ the induction period was twice as long. The MHP was considerably delayed, occurring after 28.3 h but with a similar heat flow rate. At the higher zinc dosages of 0.5%wt and 2%wt, no hydration reactions were detected over entire period of the calorimetry measurements.

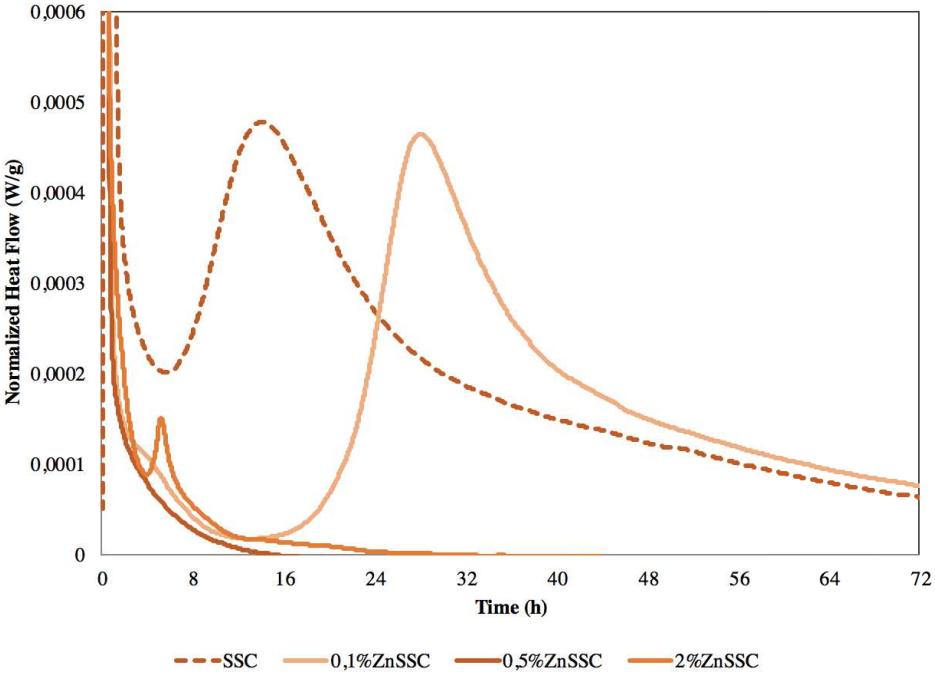

Fig. IV.7 Isothermal calorimetry of the Supersulfated formulation with addition of 0,1%$Zn(NO_3)_2$, 0,5%$Zn(NO_3)_2$, 2%$Zn(NO_3)_2$

According to the XRD results at 24 hours of storage, ettringite is the main hydration product of the control sample (Fig. IV.8). Ettringite was also detected for the lowest zinc nitrate dosage. At higher zinc amounts the only phase identified on the graphs is gypsum. The same evolution is observed after 7 days of storage but with a more pronounced ettringite intensity for SSC and 0.1%ZnSSC (Fig. IV.9). An AFm peak of very low intensity can be observed in the case of 0.5% and 2% zinc nitrate at both time frames.

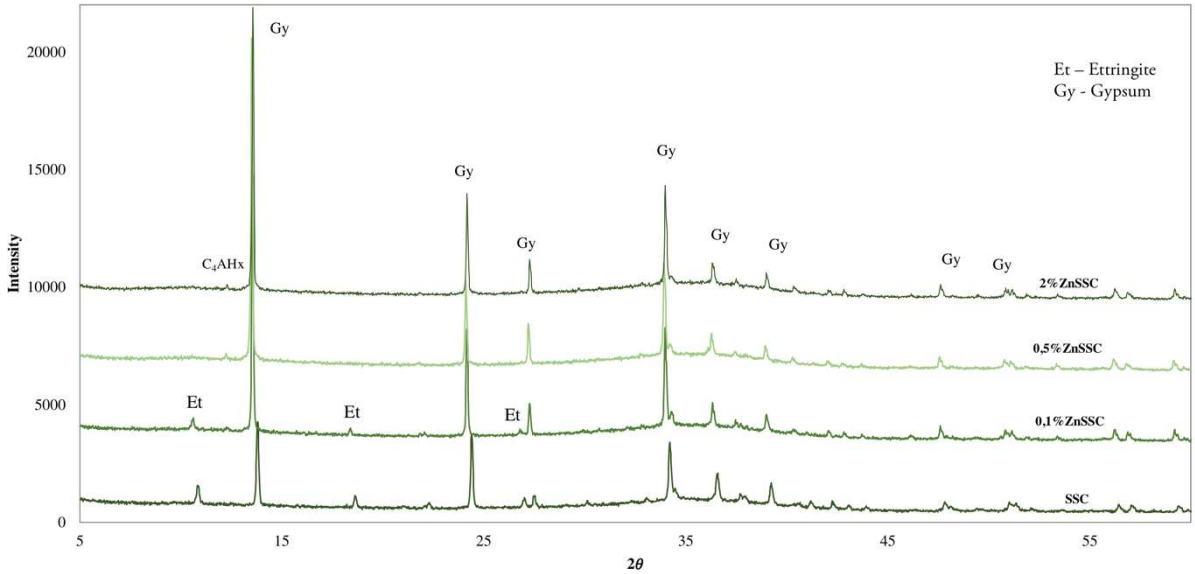

Fig. IV.8 XRD analysis of the Supersulfated formulation with addition of 0,1%$Zn(NO_3)_2$, 0,5%$Zn(NO_3)_2$, 2%$Zn(NO_3)_2$ after 7 days of storage

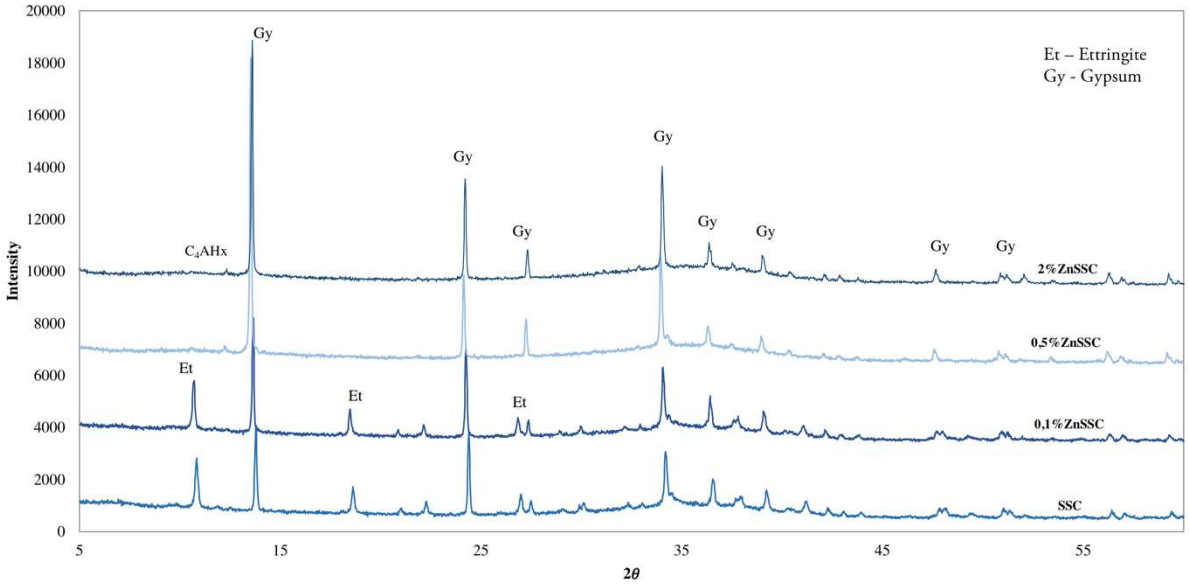

Fig. IV.9 XRD analysis of the Supersulfated formulation with addition of 0,1%$Zn(NO_3)_2$, 0,5%$Zn(NO_3)_2$, 2%$Zn(NO_3)_2$ after 7 days of storage

IV.2.1.4 Discussion

The results of the hydration heat evolution and XRD analysis indicate a retardation effect of zinc on the early hydration of the binders, except for 0.1%ZnOPC. The retardation of hydration in the presence of zinc was attributed, by many authors, to the coating of cement grains by the formation of the insoluble gel-like amorphous compound $CaZn_2(OH)_6.2H_2O$ which prevents surface dissolution. (Komarneni et al., 1988) studied the solubility products of some metal hydroxides and established that heavy metals precipitate more readily on the surface of silica than in bulk solution (Table IV.2).

Table IV.2 The solubility product of metal hydroxides

Metal ions	$\log K_{sp}$ (in solution)	$\log K_{sp}$ (on the surface of silica)
Ca^{2+}	−5.19	−6.67
Mg^{2+}	−11.15	−12.75
Cu^{2+}	−19.32	−20.91
Pb^{2+}	−15.1	−16.52
Zn^{2+}	−16.6	−18.17
Cr^{3+}	−29.8	−32.19
Al^{3+}	−33.5	−35.97
Fe^{3+}	−38.8	−41.2

However, (Weeks et al., 2008) in his study highlights that there is no direct evidence of the formation of amorphous metal hydroxide gel layers on the cement grains. This was proposed to explain the delay in cement hydration by the lack of calcium and hydroxide ions to saturate the solution in order to form $Ca(OH)_2$ and C-S-H gel due to the formation of calcium zincate ($CaZn_2(OH)_6.2H_2O$). (Chen et al., 2007) observed that

calcium zincate was stable when the pH was lower than 12, therefore portlandite did not precipitate in this pH range (Fig. IV.10). However, calcium zincate may dissolve at later ages of hydration (over 1 year) because the hydration of C_3S at long term will cause the pH to rise up to 12.5. This means that there is possibly an optimum pH for the stability and precipitation-dissolution of calcium zincate with an increase of the concentration of available hydroxides.

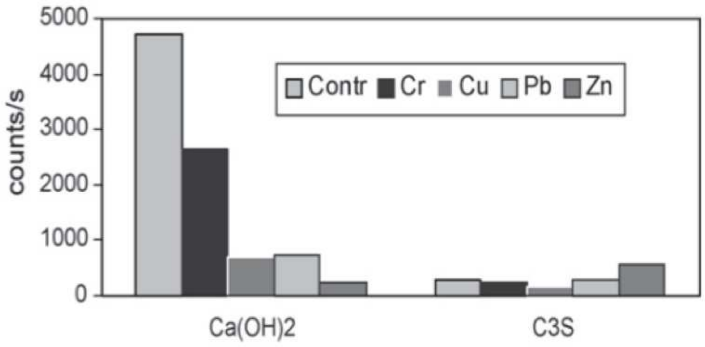

Fig.IV.10 XRD analysis of the C3S pastes with HM after 1 month of storage (Chen et al., 2007)

(Scrivener et al., 2019) confirms the inhibition of C-S-H nucleus formation within C_3S samples doped with zinc during early hydration. At the same time, what is interesting about the incorporation of zinc in Portland cement is a greater magnitude of the MHP for dosages of 0.5% and 2%. According to (Scrivener et al., 2019) this increase in MHP corresponds to the changes in C-S-H morphology, in particular to the formation of longer C-S-H needles. (Bazzoni et al., 2014) observed the enhanced outward growth of C-S-H at some dosages of zinc.

The evolution of the GGBS-based formulations seems to be attributed to the same mechanisms of the inhibition of hydration or even its absence. The formation of calcium zincate results in a lack of soluble calcium, from C_2S and C_3S, available for the formation of hydrates and for pozzolanic reactions to occur. In the case of GGBS85 this retardation effect is more pronounced than in the case of OPC because of the lower amount of available calcium. Therefore, the impact of the same content of zinc will more strongly retard the hydration of the GGBS-based samples as can be seen from the XRD and heat evolution results. The supersulfated formulation contains only 1% of OPC needed for the activation of the system. Therefore, the effect of the presence of zinc is more important compared to OPC and GGBS85, arising from the fast setting and the formation of gypsum.

Table IV. 3 Summary for the hydration heat rate results of OPC, GGBS85 and SSC mixed with $Zn(NO_3)_2$

			OPC	GGBS85	SSC
$Zn(NO_3)_2$	0%	MHP (h)	11.4	13.5	14
		Peak height (mW/g)	3.87	0.71	0.48
		Total Heat Flow, 72h (J/g)	274.8	76.7	50.9
	0.1%	MHP (h)	8.7	10.9	28.3
		Peak height (mW/g)	3.96	0.70	0.46
		Total Heat Flow, 72h (J/g)	205.6	68.5	39.4
	0.5%	MHP (h)	13.6	50.7	-
		Peak height (mW/g)	4.8	0.34	-
		Total Heat Flow, 72h (J/g)	201.7	50	2.3
	2%	MHP (h)	19.4	-	-
		Peak height (mW/g)	6	-	-
		Total Heat Flow, 72h (J/g)	192.9	2	4.2

IV.2.2 Impact of copper

Table IV.4 presents the samples prepared to investigate the impact of copper on the early hydration of the binders:

Table IV.4 Samples prepared for the copper impact investigation on the early hydration of the binders

	$Cu(NO_3)_2$		
	0.1%	**0.5%**	**2%**
100%OPC	0.1%CuOPC	0.5%CuOPC	2%CuOPC
85%GGBS/15%OPC	0.1%CuGGBS85	0.5%CuGGBS85	2%CuGGBS85
85%GGBS/14%Ca_2SO_4/1%OPC	0.1%CuSSC	0.5%CuSSC	2%CuSSC

IV.2.2.1 100%OPC formulation

The early hydration of Portland cement in the presence of 0.1% of $Cu(NO_3)_2$ does not seem to be affected by the presence of the Cu^{2+} ions, the acceleration part of the curve was shifted only slightly to the right and the MHP occurred one hour later. As can be seen in Fig. IV.11, the 0.5% dosage of $Cu(NO_3)_2$ slightly shortened the induction period with the MHP occurring at 9.3 h. Nevertheless, the mixture with 2% of the copper salt exhibits an important retardation effect – the main peak finally occurs after 37.9 h with a relatively poor MHP heat release of 2.44 mW/g and with the total heat flow considerably lower than that of the control sample.

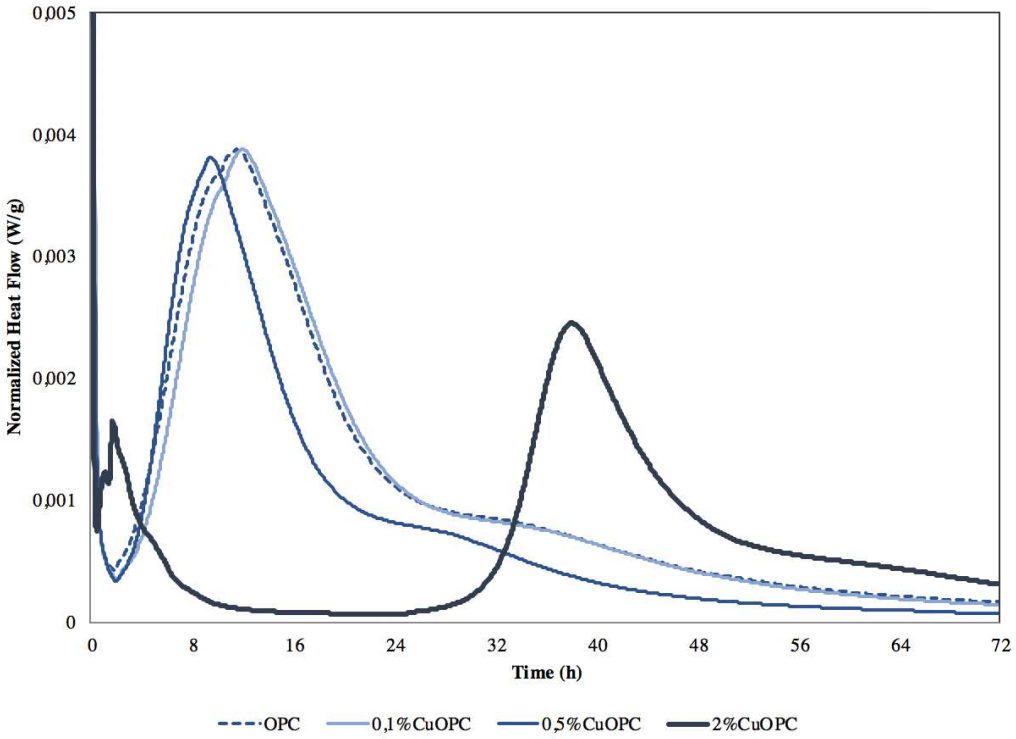

Fig. IV.11 Isothermal calorimetry of 100%OPC with addition of 0,1%$Cu(NO_3)_2$, 0,5%$Cu(NO_3)_2$, 2%$Cu(NO_3)_2$

The 0.1% and 0.5% dosages of copper nitrate did not modify the formation of the main hydration phases of the 100% OPC formulation after 24 hours (Fig. IV.12). The most remarkable effect of the copper nitrate solution was obtained at the 2%$Cu(NO_3)_2$ dosage. As can be seen on the graph, the anhydrous peaks of C_2S and C_3S seem to be unreacted. Portlandite was not formed and the ettringite peak is the only hydration product present in any significant amount for the 2%CuOPC mixture at 24 h. The intensity of the calcite peak is higher for 2%CuOPC compared to the other samples which can be related to accelerated carbonation. Almost no difference in hydration products was noticed after 7 days of storage for the control sample and for OPC doped with copper (Fig. IV.13).

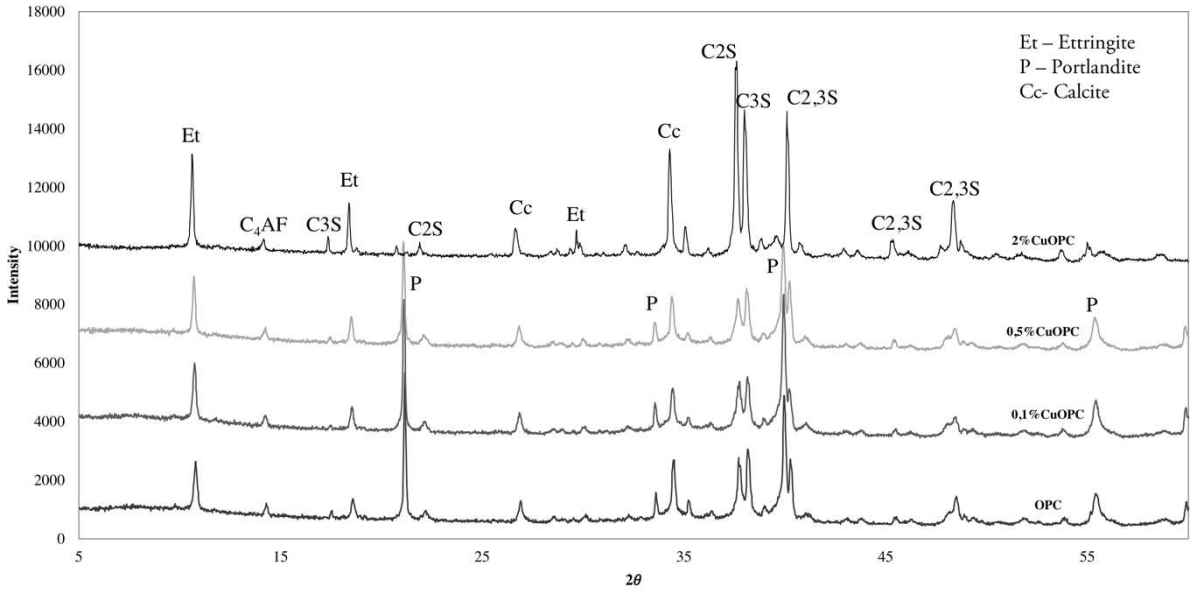

Fig. IV.12 XRD analysis of 100%OPC with addition of 0,1%$Cu(NO_3)_2$, 0,5%$Cu(NO_3)_2$, 2%$Cu(NO_3)_2$ after 24 hours of storage

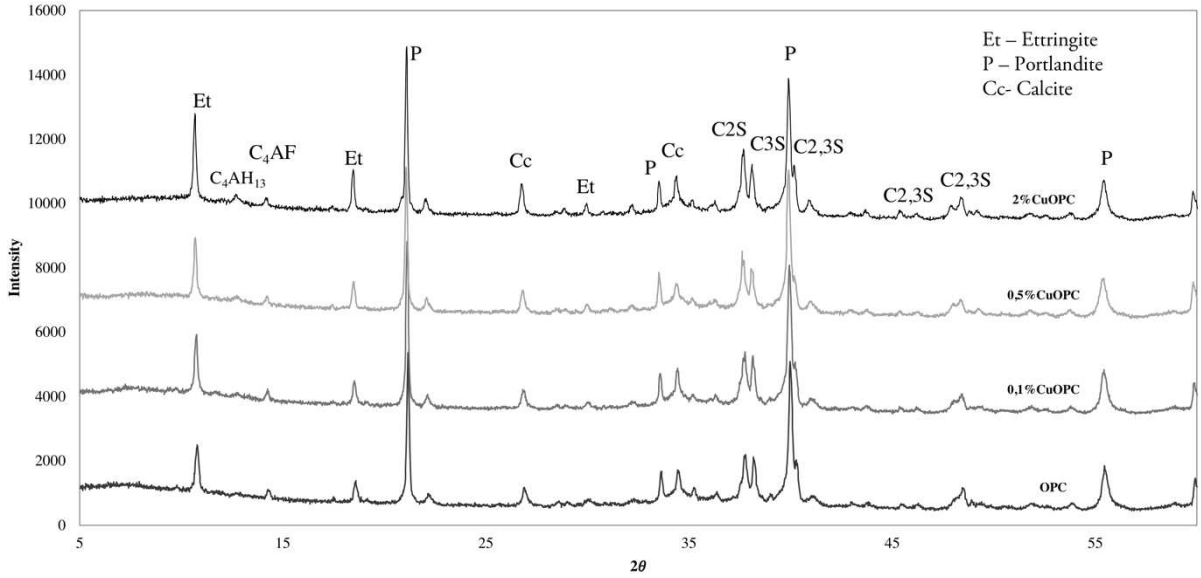

Fig. IV.13 XRD analysis of 100%OPC with addition of 0,1%$Cu(NO_3)_2$, 0,5%$Cu(NO_3)_2$, 2%$Cu(NO_3)_2$ after 7 days of storage

IV.2.2.2 85%GGBS/15%OPC formulation

The results obtained over 72 hours of calorimetry measurements for the 85%GGBS/15%OPC formulation mixed with different dosages of copper nitrate are set out below (Fig. IV.14). The induction period for 0.1%CuGGBS85 was extended with the main hydration peak of the acceleration-deceleration stages occurring at 15.4 h, almost without change to the hydration evolution compared to the control. However, the higher dosages of Cu^{2+} had a severe negative impact on the early hydration of GGBS85. A very low heat release was measured for 0.5%CuGGBS85 with a value of

0.08 mW/g of the MHP emerging after 25 hours. The 2% dosage of copper nitrate impacted the GGBS85 mixture in the same way as 2% of zinc nitrate; a complete annihilation of hydration was observed.

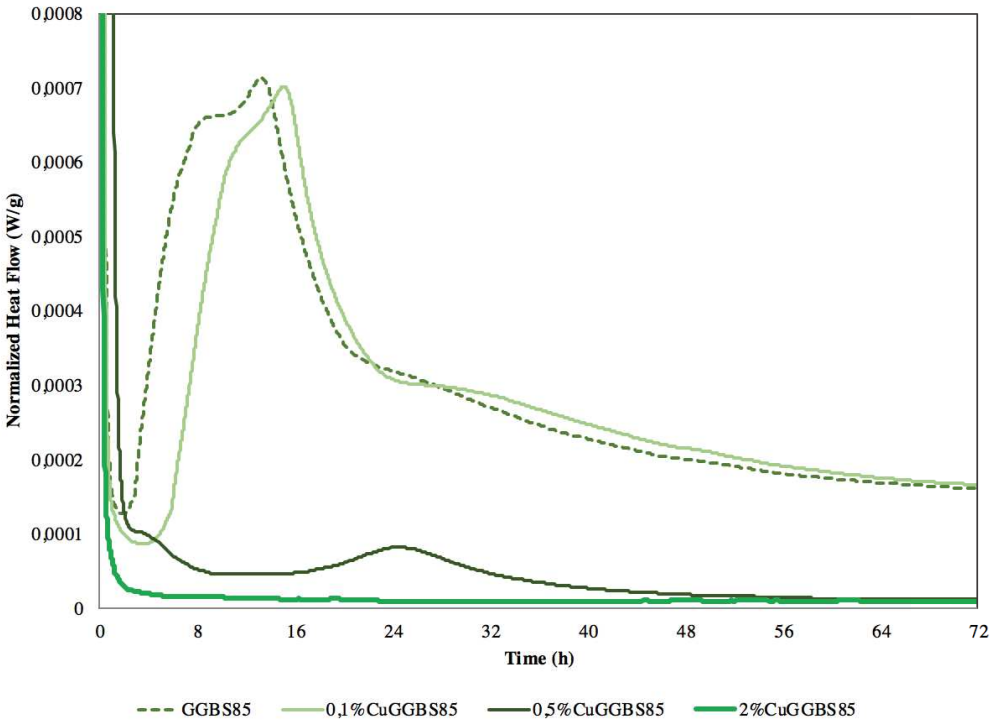

Fig. IV.14 Isothermal calorimetry of 85%GGBS/15%OPC with addition of 0,1%$Cu(NO_3)_2$, 0,5%$Cu(NO_3)_2$, 2%$Cu(NO_3)_2$

The impact of copper nitrate on the precipitation of hydrates of the GGBS85 formulation can be clearly seen in Fig. IV.15 and Fig. IV.16. At 24 hours and 7 days the peak of portlandite was identified only for the control sample and for 0.1%CuGGBS85. The dissolution of the anhydrous phases of C_2S and C_3S was inhibited by the introduction of 0.5% and 2% of copper salt. At the same time the ettringite phase is present at all dosages of copper nitrate. C-S-H formation can be distinguished after 7 days of storage only for the reference formulation and for 0.1%CuGGBS85 – the broader peak can be observed in the region of 34°Theta (Fig. IV.16). The AFm phase (C_4AH_{13}) was also detected for the 0.1%CuGGBS85 sample. Ettringite was precipitated for all samples and in both time frames.

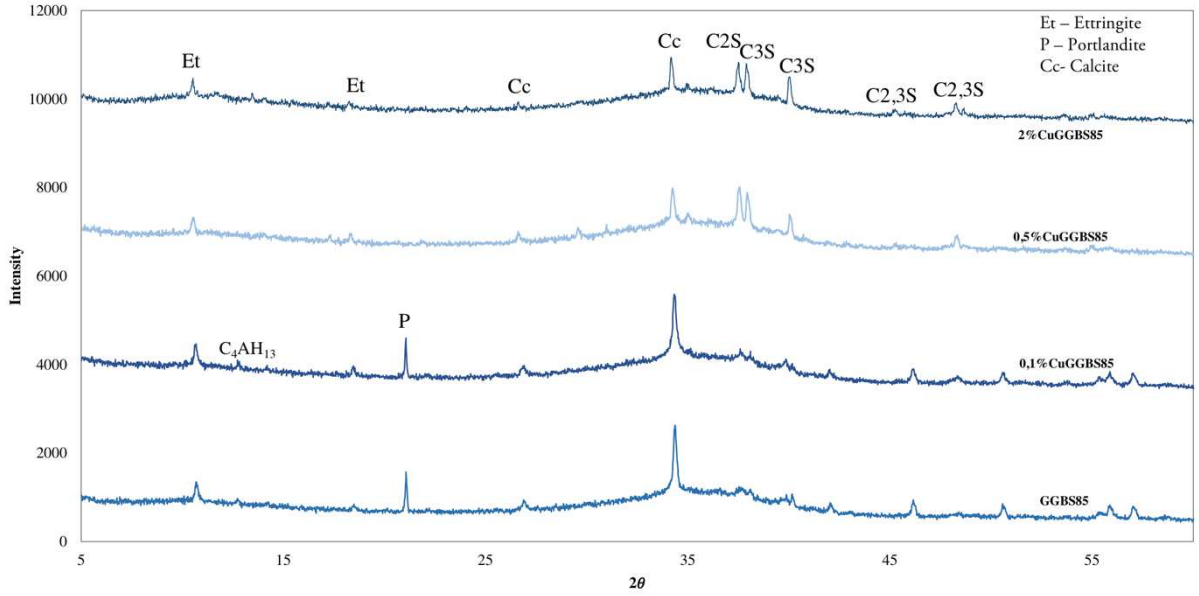

Fig. IV.15 XRD analysis of 85%GGBS/15%OPC with addition of 0,1%$Cu(NO_3)_2$, 0,5%$Cu(NO_3)_2$, 2%$Cu(NO_3)_2$ after 24 hours of storage

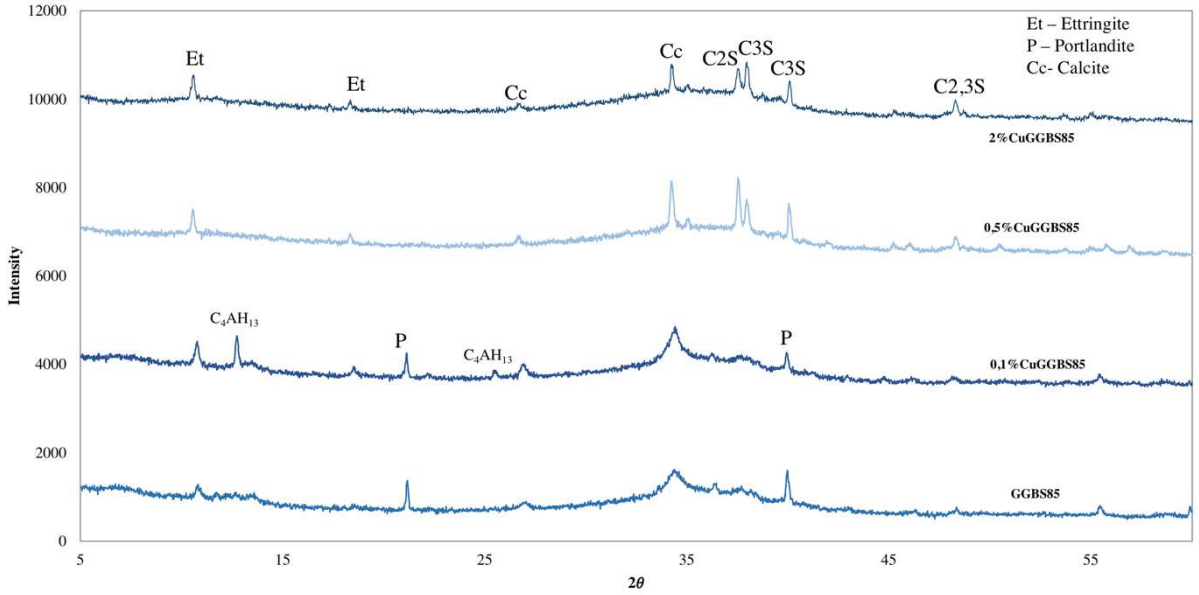

Fig. IV.16 XRD analysis of 85%GGBS/15%OPC with addition of 0,1%$Cu(NO_3)_2$, 0,5%$Cu(NO_3)_2$, 2%$Cu(NO_3)_2$ after 7 days of storage

IV.2.2.3 Supersulfated formulation

The impact of copper on the hydration of the supersulfated formulation is even more noticeable that in the case of zinc (Fig. IV.17). This time the MHP for 0.1%CuSSC occurred after 41.3 h, but the heat rate of the exothermic reactions corresponding to the MHP was not as strongly affected. The reactivity of the supersulfated binder was completely annihilated in the presence of the higher copper dosages.

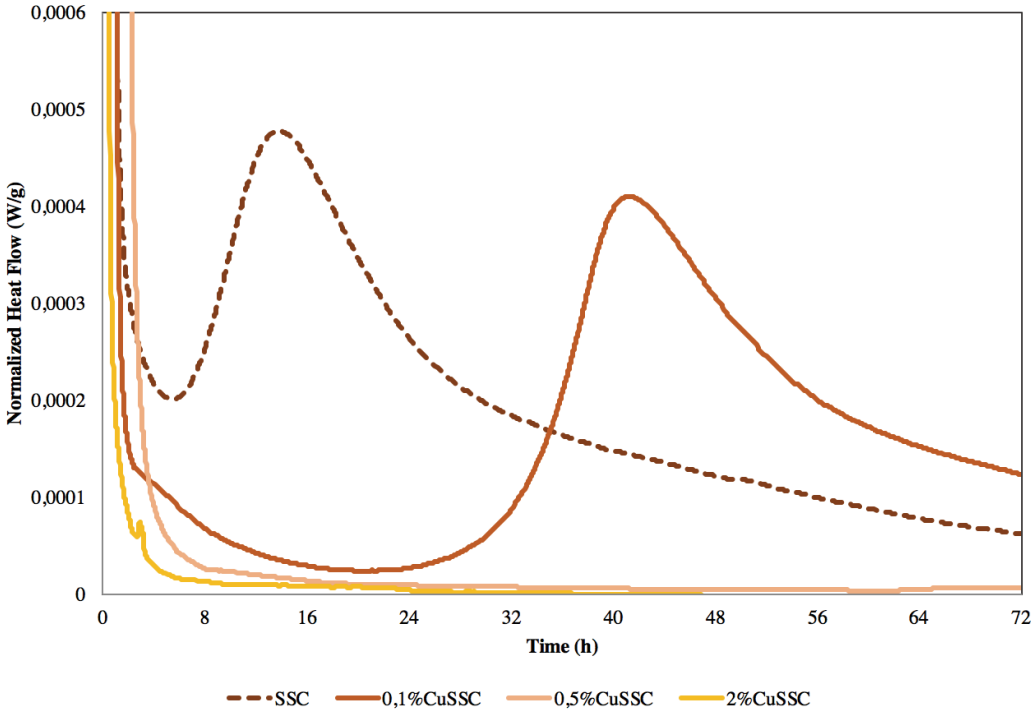

Fig. IV.17 Isothermal calorimetry of the Supersulfated formulation with addition of 0,1%$Cu(NO_3)_2$, 0,5%$Cu(NO_3)_2$, 2%$Cu(NO_3)_2$

After 24 hours of hydration only the reference sample shows the precipitation of ettringite. The copper nitrate at all dosages induced only gypsum formation after 24 h (Fig. IV.18). Further XRD analysis after 7 days exhibits almost the same amount of ettringite and gypsum precipitation for SSC and 0.1%CuSSC (Fig. IV.19). However, there is still only gypsum present for 0.5%$Cu(NO_3)_2$ and 2%$Cu(NO_3)_2$.

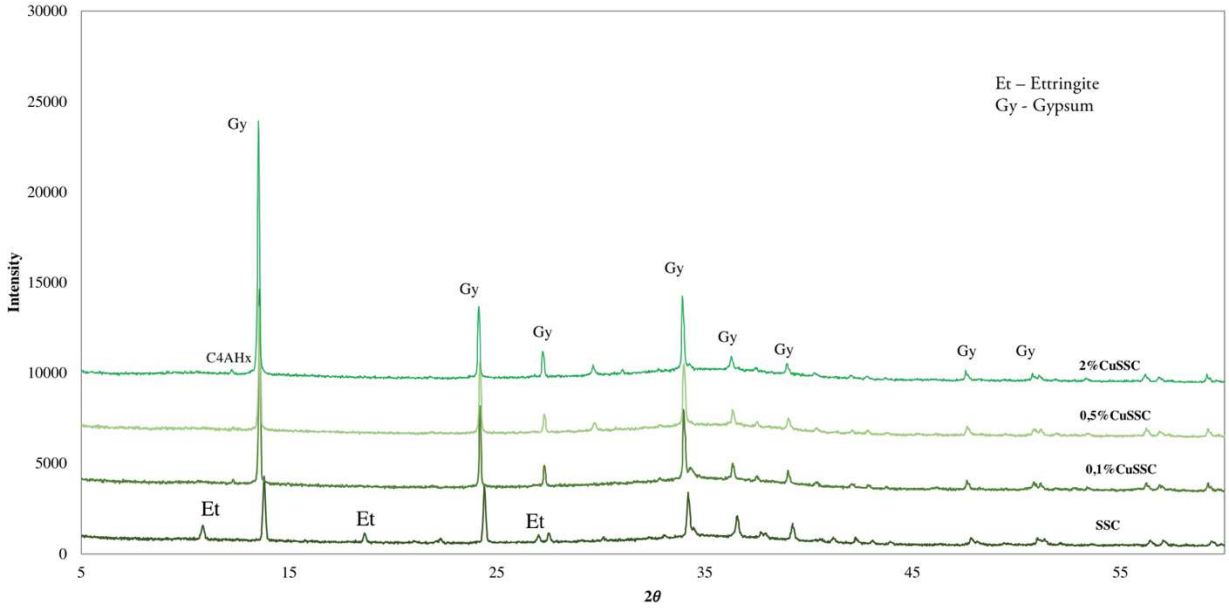

Fig. IV.18 XRD analysis of the Supersulfated formulation with addition of 0,1%$Cu(NO_3)_2$, 0,5%$Cu(NO_3)_2$, 2%$Cu(NO_3)_2$ after 24 hours of storage

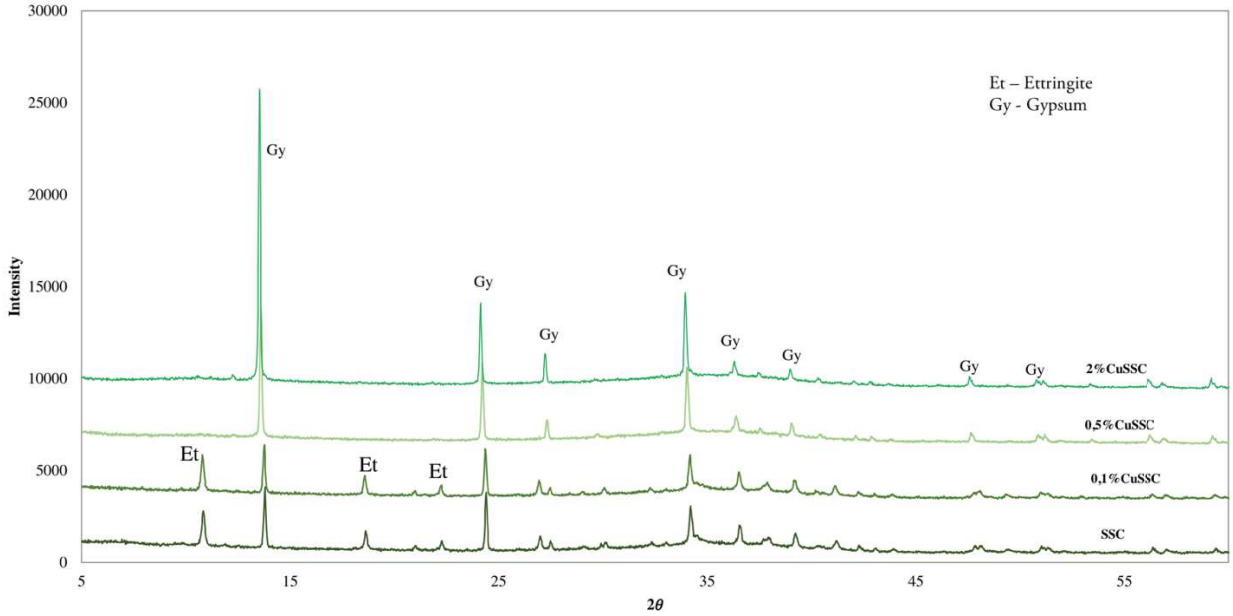

Fig. IV.19 XRD analysis of the Supersulfated formulation with addition of 0,1%$Cu(NO_3)_2$, 0,5%$Cu(NO_3)_2$, 2%$Cu(NO_3)_2$ after 7 days of storage

IV.2.2.4 Discussion

The addition of copper produced the most negative impact on the early hydration of the considered binders. In the case of 2%CuOPC, the Portland cement hydration was considerably impacted and no CH was detected after 24 hours. As in the case of zinc, copper greatly impacted the GGBS-based formulations by retarding the hardening of the samples at early age. The effect is more dramatic on the early hydration of the slag-based formulations than for the plain OPC samples due to the decrease in calcium required for the precipitation of portlandite and C-S-H nucleation. The annihilation of hydration of the supersulfated formulation can be explained by the same mechanism as for zinc – the dissolution of the anhydrous OPC and GGBS grains was slowed in presence of copper, or even completely annihilated.

The retardation effect of copper was discussed in previous studies. (Gineys et al., 2010) reported the considerable delay effect of copper on cement paste hydration, with the compressive strength at 2 days tending to be approximately non-existant. This retardation due to soluble copper salt at early age was attributed by the author to the low C_3S dissolution rate. Two possible models related to the retardation of hydration in the presence of heavy metals in cement pastes were discussed in this study. The first one explains the retardation effect by a coating of the surface of cement grains by heavy metal hydroxides and the second one discusses the conversion of metal hydroxide species to metal hydroxyls. Due to this reaction there is a consumption of calcium and hydroxide ions and a lowering of the pH. Consequently, the precipitation of $Ca(OH)_2$ and C-S-H are delayed and the dissolution of C_3S remains low. (Chen et al., 2007) in his study detected the formation of the crystalline phase $Ca_2(OH)_4.4Cu(OH)_2{\cdot}H_2O$. The highest rate of carbonation was reported in the

presence of copper as well.

Table IV.5 Summary for the hydration heat rate results of OPC, GGBS85 and SSC mixed with $Cu(NO_3)_2$

			OPC	GGBS85	SSC
$Cu(NO_3)_2$	0%	MHP (h)	11.4	13.5	14
		Peak height (mW/g)	3.87	0.71	0.48
		Total Heat Flow, 72h (J/g)	274.8	76.7	50.9
	0.1%	MHP (h)	12.4	15.4	41.3
		Peak height (mW/g)	3.85	0.7	0.41
		Total Heat Flow, 72h (J/g)	267	72.3	39.8
	0.5%	MHP (h)	9.3	25	-
		Peak height (mW/g)	3.79	0.08	-
		Total Heat Flow, 72h (J/g)	205.5	12	18,3
	2%	MHP (h)	37.9	-	-
		Peak height (mW/g)	2.44	-	-
		Total Heat Flow, 72h (J/g)	163.1	3.1	1.6

IV.2.3 Impact of nickel

The samples prepared for the investigation of the impact of nickel on the early hydration of the binders are summarized in Table IV.6:

Table IV.6 Samples prepared for the Nickel impact investigation on the early hydration of the binders

	$Ni(NO_3)_2$		
	0.1%	**0.5%**	**2%**
100%OPC	0.1%NiOPC	0.5%NiOPC	2%NiOPC
85%GGBS/15%OPC	0.1%NiGGBS85	0.5%NiGGBS85	2%NiGGBS85
85%GGBS/14%Ca_2SO_4/1%OPC	0.1%NiSSC	0.5%NiSSC	2%NiSSC

IV.2.3.1 100%OPC formulation

Figure IV.20 presents the isothermal calorimetry measurements for the Portland cement formulation mixed with $Ni(NO_3)_2$ at different percentages. The hydration reactions were accelerated in the presence of nickel ions and the induction period was considerably shortened, especially for the 2%NiOPC mixture. The 0.1%NiOPC and 0.5%NiOPC formulations show almost the same hydration behaviour with earlier occurrences of the MHP at 7-8 h, almost without changing the heat release rate of the MHP compared to the control mixture.

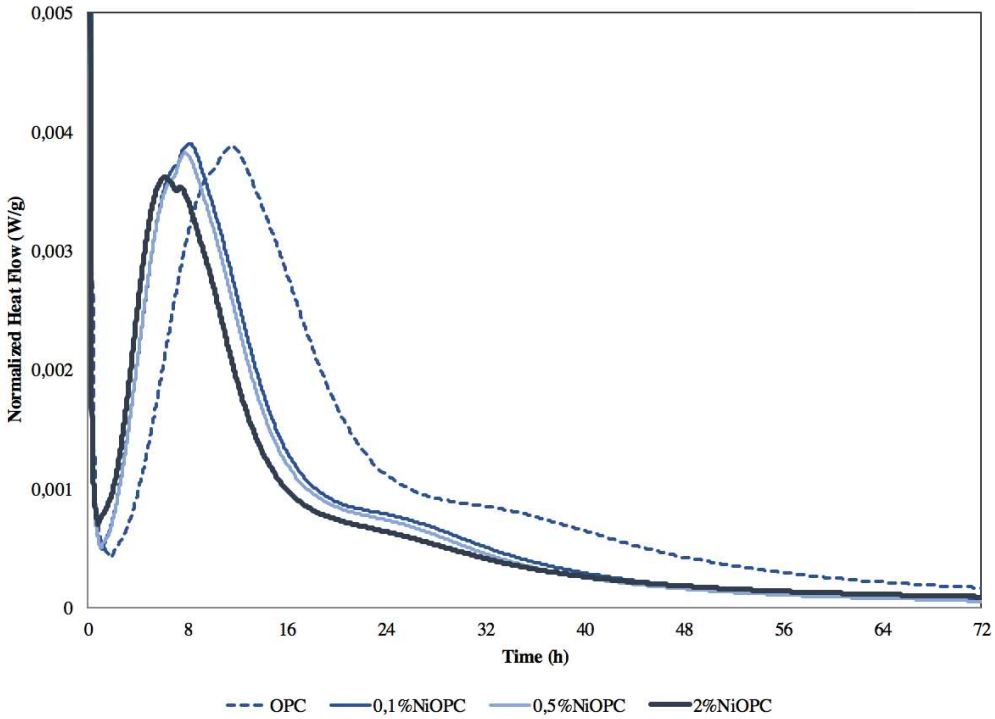

Fig. IV.20. Isothermal calorimetry of 100%OPC with addition of 0,1%$Ni(NO_3)_2$, 0,5%$Ni(NO_3)_2$, 2%$Ni(NO_3)_2$

Figure IV.21 compares the XRD results of the hydration products formed at 24 hours of storage for the OPC sample doped with different amounts of $Ni(NO_3)_2$. There was no significant difference for the control sample and the samples containing nickel, except for the higher dissolution rate of C_2S and C_3S with 0.5% $Ni(NO_3)_2$. The lowest amount of portlandite was precipitated in the case of 2%NiOPC, as well as the highest amount of calcite. At first glance it seems that ettringite is more abundant for 2% $Ni(NO_3)_2$. It can be supposed that nickel favoured the formation of ettringite, which explains the acceleration effect. After 7 days of storage there is almost no difference in the hydrate formation apart from the slightly higher dissolution rate of C_2S and C_3S for 0.5%NiOPC (Fig. IV.22).

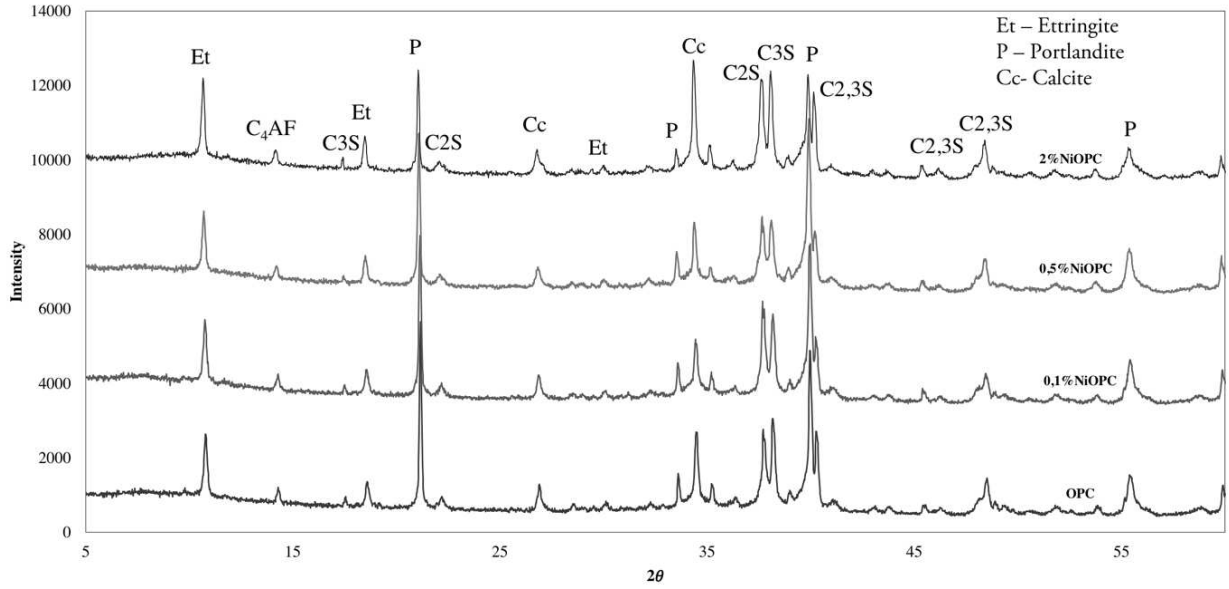

Fig. IV.21 XRD analysis of 100%OPC with addition of 0,1%$Ni(NO_3)_2$, 0,5%$Ni(NO_3)_2$, 2%$Ni(NO_3)_2$ after 24 hours of storage

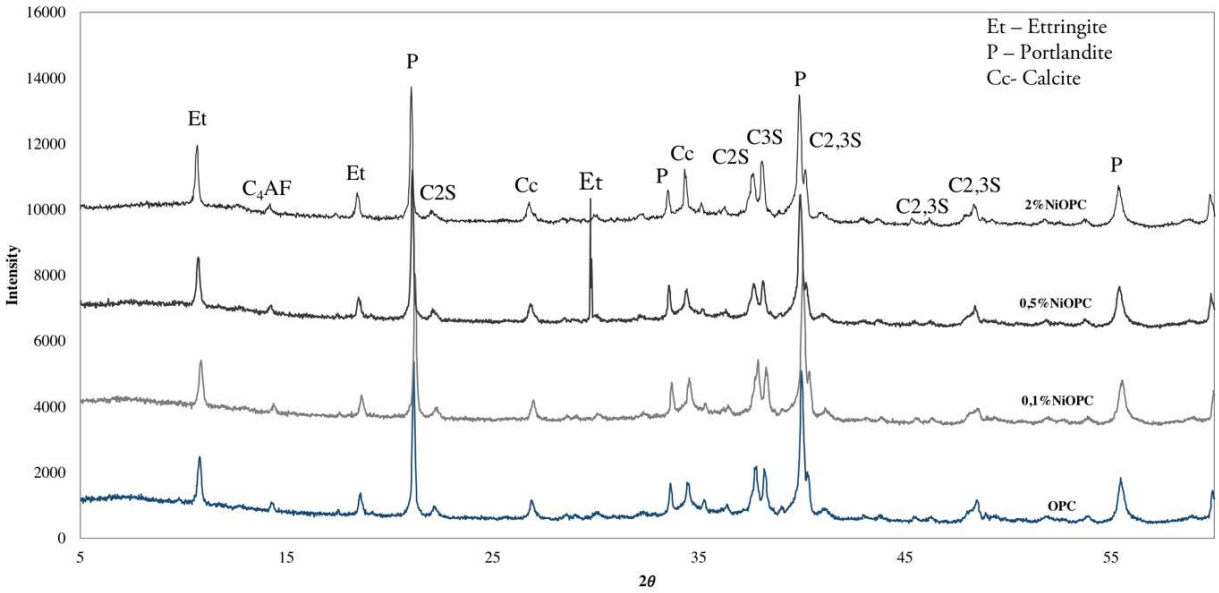

Fig. IV.22 XRD analysis of 100%OPC with addition of 0,1%$Ni(NO_3)_2$, 0,5%$Ni(NO_3)_2$, 2%$Ni(NO_3)_2$ after 7 days of storage

IV.2.3.2 85%GGBS/15%OPC formulation

With regard to GGBS85 mixed with nickel nitrate, the general trend demonstrates an acceleration of the hydration reactions for all considered dosages of Ni^{2+} (Fig. IV.23). The main hydration peak for GGBS85 in the presence of 0.1%$Ni(NO_3)_2$ emerges after 8.8 h of hydration. The 0.5% and 2% dosages of nickel salt also shifted the MHP forward, occurring at 8.2 h and 8.6 h respectively. The heat rate corresponding to the MHP of all mixtures has almost the same value as the reference formulation, however the cumulative heat produced over 72 h of measurements was slightly lower for

0.1%NiGGBS85 and 0.5%NiGGBS85, but higher for 2%NiGGBS85.

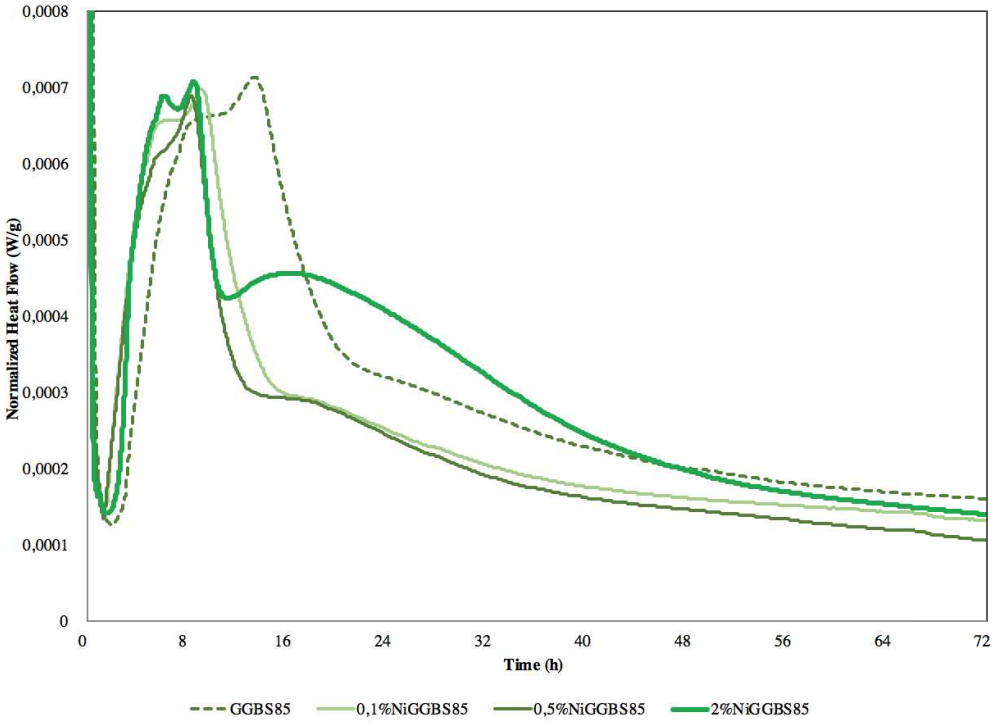

Fig. IV.23 Isothermal calorimetry of 85%GGBS/15%OPC with addition of 0,1%$Ni(NO_3)_2$, 0,5%$Ni(NO_3)_2$, 2%$Ni(NO_3)_2$

The evolution of the hydration products of GGBS85 and 0.1%NiGGBS85 is similar after 24 hours (Fig. IV.24). By increasing the amount of nickel salt to 0.5%$Ni(NO_3)_2$ there is much less precipitated portlandite at 24 hours. In the presence of 2% $Ni(NO_3)_2$ the dissolution of C_2S and C_3S was inhibited. Consequently, no portlandite can be detected after 24 h. However, the highest intensity of the ettringite peak was obtained for 2%NiGGBS85 as in the case of the OPC formulation. The samples with 0.1% and 0.5% nickel nitrate showed almost the same hydration product evolution as the reference sample; the portlandite, ettringite, and C-S-H phases can be distinguished after 7 days of storage (Fig. IV.25). Furthermore, the calcium aluminate phase C_4AH_{13} was precipitated with the addition of 0.1% $Ni(NO_3)_2$. In the presence of 2% nickel nitrate the inhibition of the hydration of GGBS85 was observed also after 7 days with the lowest dissolution rate of the anhydrous OPC phases C_2S and C_3S and with a more significant calcite intensity. At the same time the most abundant ettringite precipitation was detected for 2%NiGGBS85 after 7 days of hydration, compared to the other samples.

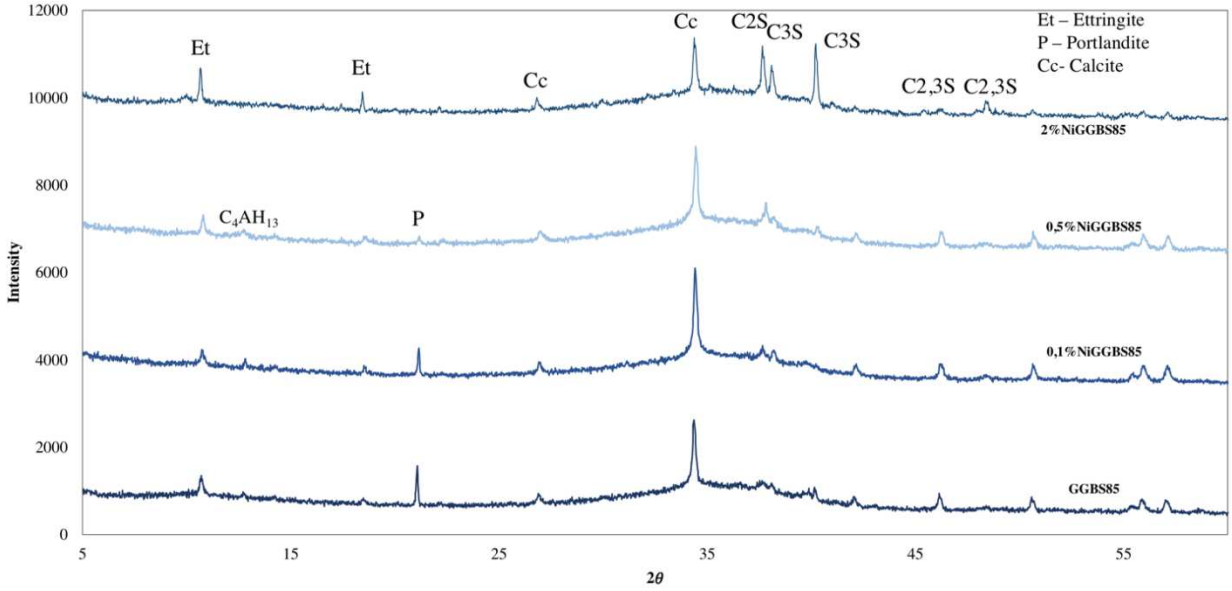

Fig. IV.24 XRD analysis of 85%GGBS/15%OPC with addition of 0,1%$Ni(NO_3)_2$, 0,5%$Ni(NO_3)_2$, 2%$Ni(NO_3)_2$ after 24 hours of storage

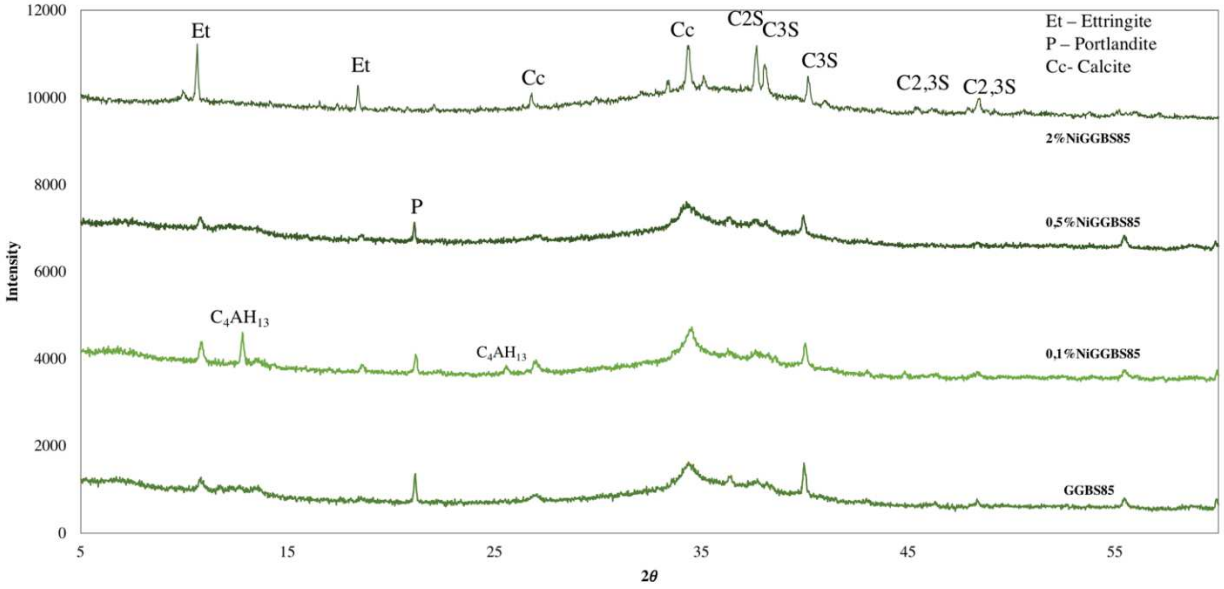

Fig. IV.25 XRD analysis of 85%GGBS/15%OPC with addition of 0,1%$Ni(NO_3)_2$, 0,5%$Ni(NO_3)_2$, 2%$Ni(NO_3)_2$ after 7 days of storage

IV.2.3.3 Supersulfated formulation

The addition of 0.1%$Ni(NO_3)_2$ to the supersulfated formulation shortened the induction period with the MHP occurring after 11.4 h, without impacting the heat release rate (Fig. IV.26). The 0.5%NiSSC formulation also demonstrated an acceleration of the main hydration reactions, however the measured heat rate of the MHP was two times lower than in the case of the control formulation. The addition of 2% $Ni(NO_3)_2$ produced an extension of the induction period, with the occurrence of the MHP occurring after 32.9 hours with a heat rate of 0.25 mW/g.

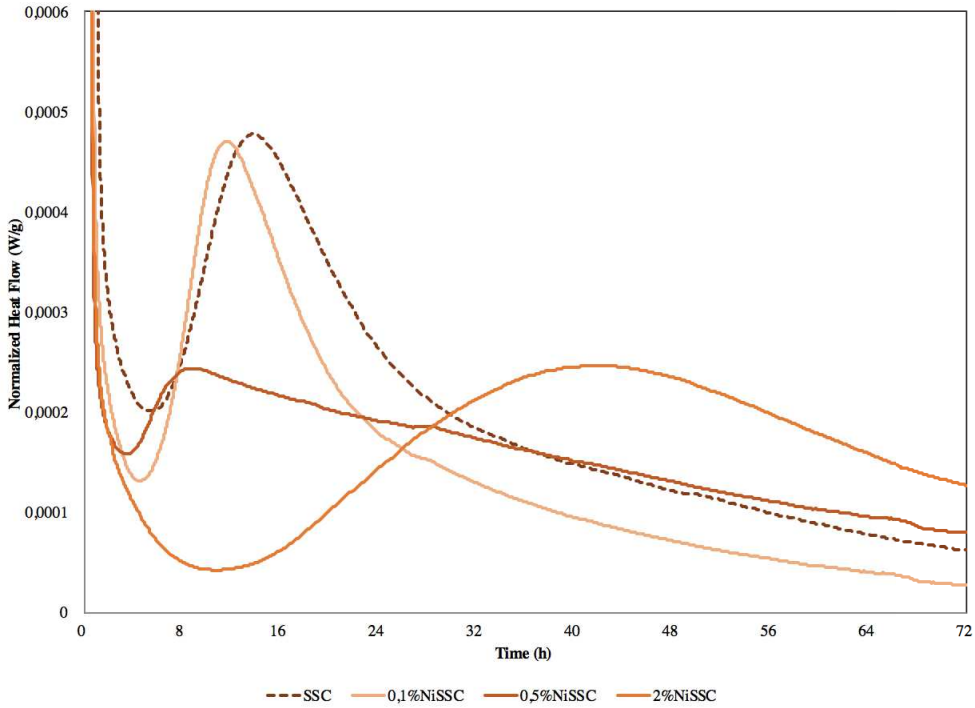

Fig. IV.26 Isothermal calorimetry of the Supersulfated formulation with addition of 0,1%$Ni(NO_3)_2$, 0,5%$Ni(NO_3)_2$, 2%$Ni(NO_3)_2$

Regarding the results of the XRD analysis of the supersulfated formulation doped with nickel, there is an almost even hydrate repartition in terms of phases and intensity for the control sample (SSC), 0.1%NiSSC, and 0.5%NiSSC after 24 hours and 7 days of storage (Fig. IV.27, Fig. IV.28). With addition of 2%$Ni(NO_3)_2$ the only detected phase was gypsum at both time frames.

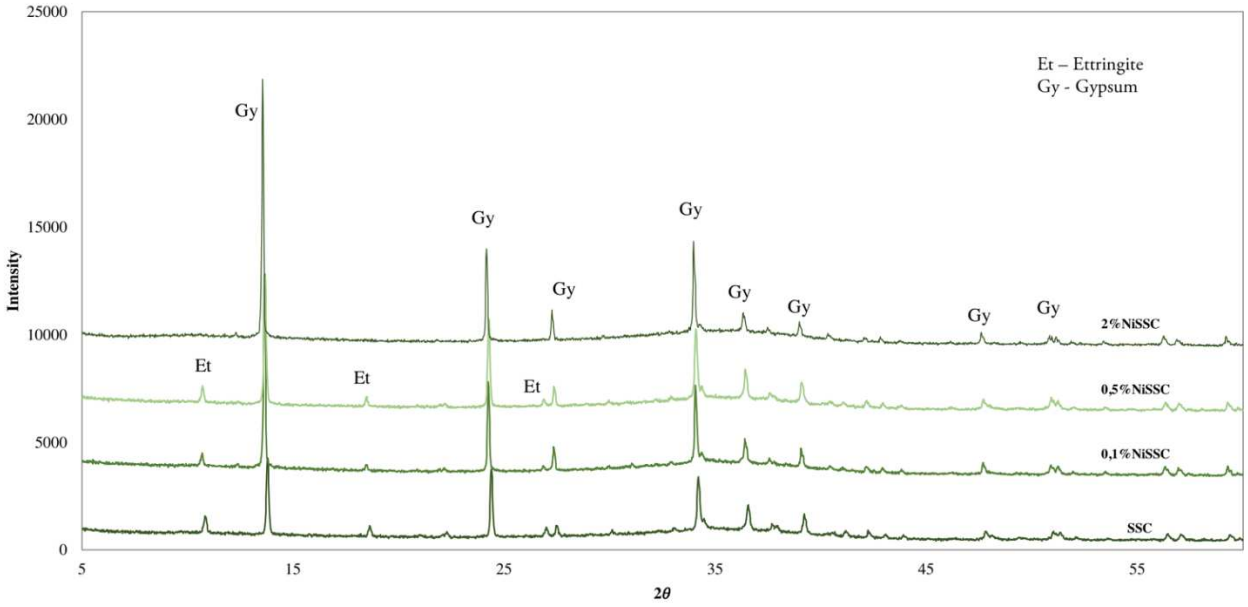

Fig. IV.27 XRD analysis of the Supersulfated formulation with addition of 0,1%$Ni(NO_3)_2$, 0,5%$Ni(NO_3)_2$, 2%$Ni(NO_3)_2$ after 24 hours of storage

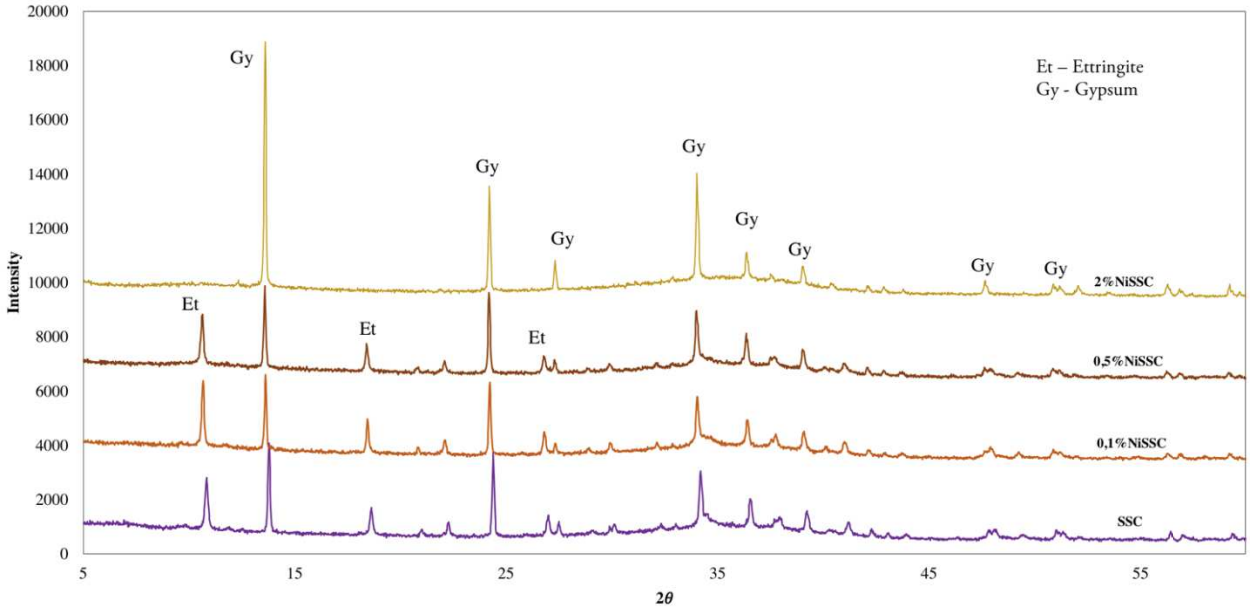

Fig. IV.28 XRD analysis of the Supersulfated formulation with addition of 0,1%$Ni(NO_3)_2$, 0,5%$Ni(NO_3)_2$, 2%$Ni(NO_3)_2$ after 7 days of storage

IV.2.3.4 Discussion

In contrast to the impact of copper and zinc, the addition of nickel nitrate produced mostly an accelerating effect on early hydration. Nickel, at some specific dosages, appears to promote the hydration of the cementitious materials by the rapid dissolution of aluminium bearing phases and rapid precipitation of the ettringite and minor Ni-Al layered double hydroxides (Ni-Al LDH) phases (Scheidegger et al., 2000; Vespa et al., 2006). (Vespa et al., 2006) performed an XAS study of cement mixed with different nickel salts. The predominance of Ni-Al LDH at first hours of hydration was demonstrated, and the competition for aluminium consumption between ettringite and LDH was observed. The EXAFS results of Ni presented later in this study confirm these findings (see Chapter V). According to the results of (Gineys et al., 2010), nickel did not affect the early compressive strength of the cement samples after 2 days of storage compared to the negative impact of zinc and copper.

An acceleration of the MHP was observed in almost all samples, as well as the formation of more abundant ettringite. According to (Achternbosch et al., 2003), nickel in the alkaline pH range of 9-11 precipitates as $Ni(OH)_2$ and remains quite stable. It can be supposed that the retardation of hydration of the GGBS-based formulations at 2%wt $Ni(NO_3)_2$ arises from the $Ni(OH)_2$ precipitation and therefore the consumption of OH^-.

Table IV.7 Summary for the hydration heat rate results of OPC, GGBS85 and SSC mixed with $Ni(NO_3)_2$

			OPC	GGBS85	SSC
$Ni(NO_3)_2$	0%	MHP (h)	11.4	13.5	14
		Peak height (mW/g)	3.87	0.71	0.48
		Total Heat Flow, 72h (J/g)	274.8	76.7	50.9
	0.1%	MHP (h)	7.9	8.8	11.4
		Peak height (mW/g)	3.88	0.70	0.47
		Total Heat Flow, 72h (J/g)	208.6	64	37.5
	0.5%	MHP (h)	7.6	8.2	8.8
		Peak height (mW/g)	3.8	0.69	0.24
		Total Heat Flow, 72h (J/g)	196.1	58.3	40.3
	2%	MHP (h)	6	8.6	32.9
		Peak height (mW/g)	3.6	0.71	0.25
		Total Heat Flow, 72h (J/g)	186.2	78.1	41.5

IV.2.4 Impact of cadmium

The samples of the hydraulic binders mixed with cadmium nitrate are presented in Table IV.8:

Table IV.8 Samples prepared for the cadmium impact investigation on the early hydration of the binders

	$Cd(NO_3)_2$		
	0.1%	**0.5%**	**2%**
100%OPC	0.1%CdOPC	0.5%CdOPC	2%CdOPC
85%GGBS/15%OPC	0.1%CdGGBS85	0.5%CdGGBS85	2%CdGGBS85
85%GGBS/14%Ca_2SO_4/1%OPC	0.1%CdSSC	0.5%CdSSC	2%CdSSC

IV.2.4.1 100%OPC formulation

The heat release during the calorimetry measurements of the 100%OPC formulation mixed with 0.1%, 0.5% and 2% $Cd(NO_3)_2$ is set out in Fig. IV.29. For the cadmium-doped OPC mixtures, there is trend of accelerated hydration for all dosages. With the increase of the cadmium salt dosage, the acceleration effect becomes more noticeable. However, the heat release decreases to some extent gradually with the increase of cadmium nitrate. The MHP of 0.1%CdOPC occurs at 7.7 h, of 0.5%CdOPC at 6.4 h, and finally of 2%CdOPC at 4 h but with the lowest heat rate of 3.2 mW/g and with a much lower value of the total heat release at 72 h.

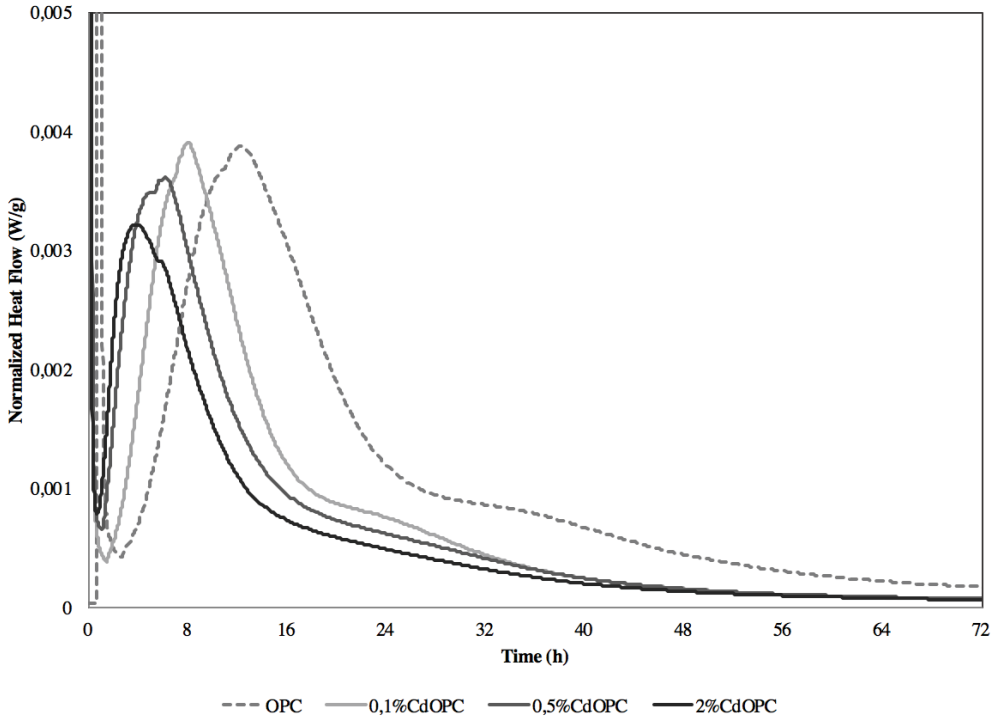

Fig. IV.29 Isothermal calorimetry of 100%OPC with addition of 0,1%$Cd(NO_3)_2$, 0,5%$Cd(NO_3)_2$, 2%$Cd(NO_3)_2$

X-ray diffractograms of the OPC formulation mixed with cadmium nitrate at different dosages show a uniform evolution of the hydration products after 24 hours, as well as after 7 days of storage (Fig. IV.30, Fig. IV.31). The only difference that stands out on the graph is the slight increase in ettringite intensity for the 2%CdOPC mixture.

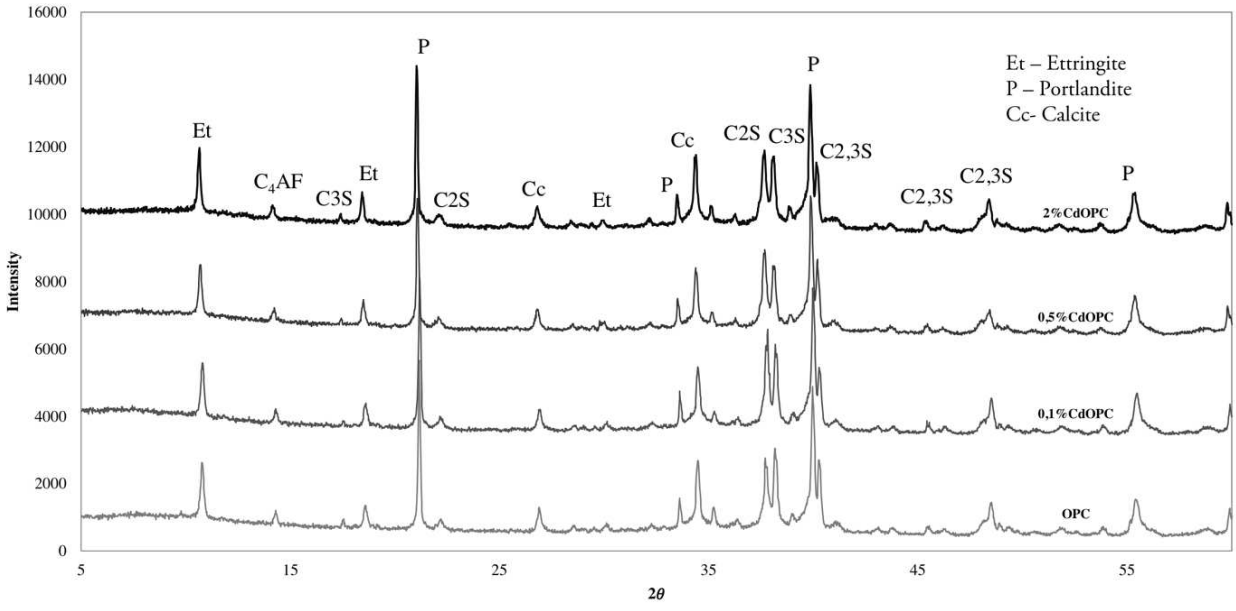

Fig. IV.30 XRD analysis of 100%OPC with addition of 0,1%$Cd(NO_3)_2$, 0,5%$Cd(NO_3)_2$, 2%$Cd(NO_3)_2$ after 24 hours of storage

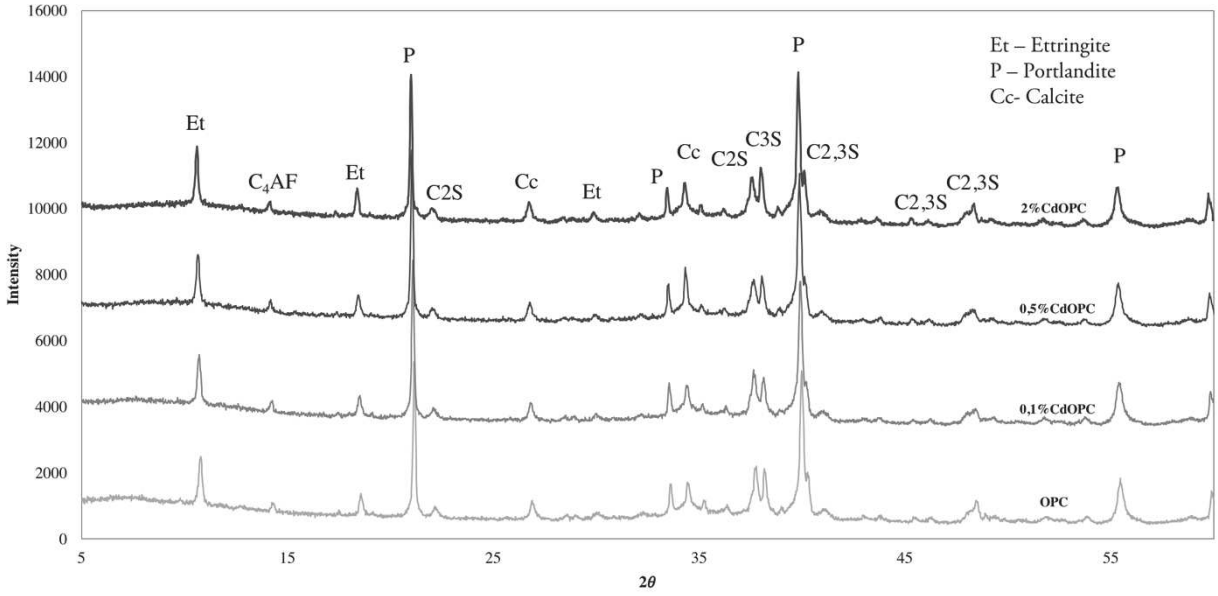

Fig. IV.31 XRD analysis of 100%OPC with addition of 0,1%$Cd(NO_3)_2$, 0,5%$Cd(NO_3)_2$, 2%$Cd(NO_3)_2$ after 7 days of storage

IV.2.4.2 85%GGBS/15%OPC formulation

Cadmium nitrate at 0.1% and 0.5%, once mixed with GGBS85, shortened the induction period (Fig. IV.32). Therefore, the MHP for 0.1%CdGGBS85 occurred at 10.2 h and for 0.5%CdGGBS85 occurred even earlier at 8.2 h. At the same time the heat rate corresponding to the pozzolanic reaction of GGBS was lower for both dosages ~ 0.6 mW/g, but the pre-peak of the acceleration stage related to Portland cement hydration remained higher than that of the control sample, producing stronger exothermic reactions. The introduction of 2% $Cd(NO_3)_2$ retarded the hydration of the mixture with the MHP (occurring at 18.8 h) and produced half the heat of the control mixture, with the acceleration period starting and ending after more time had elapsed. However, this retardation effect is much less severe compared to the effect of copper and zinc.

After 24 h of hydration, the GGBS85 formulation with and without cadmium addition shows the precipitation of portlandite, ettringite, and calcite (Fig. IV.33). The ettringite phase was precipitated in almost equal amounts for all samples, but not portlandite. The low intensity of the portlandite peak in this case was measured with 0.1%CdGGBS85 and the highest peak with 0.5%CdGGBS85. After 7 days of storage the broad peak of C-S-H gel was identified for all samples (Fig. IV.34). The ettringite phase almost disappeared in the case of 0.5%CdGGBS85 and the appearance of monocarboaluminate was detected. A considerable amount of AFm (C_4AH_{13}) was formed in 0.1%CdGGBS85 after 7 days of storage. Portlandite remains stable for all samples. Thus, this time the hydration was less impacted compared to when the other metals were added at 2%wt.

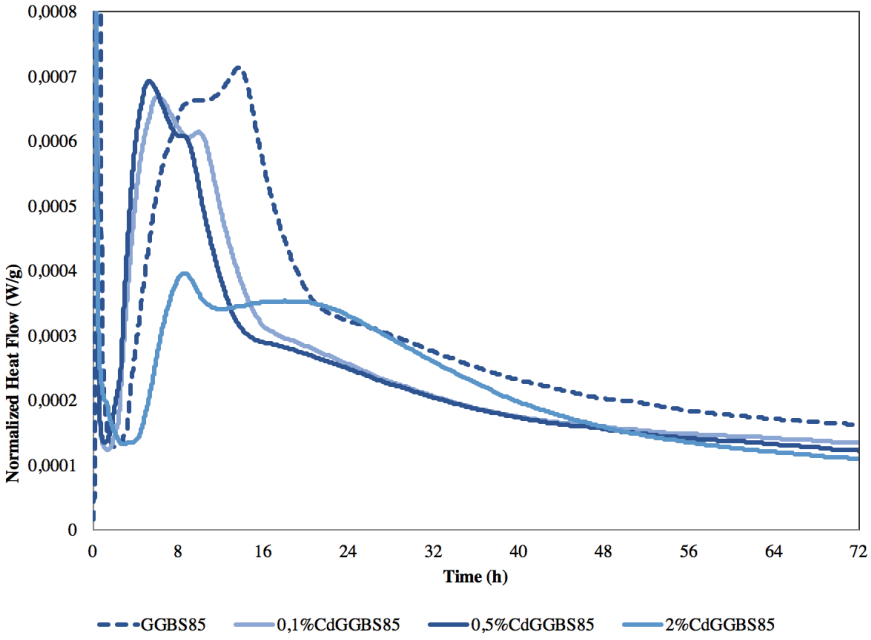

Fig. IV.32 Isothermal calorimetry of 85%GGBS/15%OPC with addition of 0,1%$Cd(NO_3)_2$, 0,5%$Cd(NO_3)_2$, 2%$Cd(NO_3)_2$

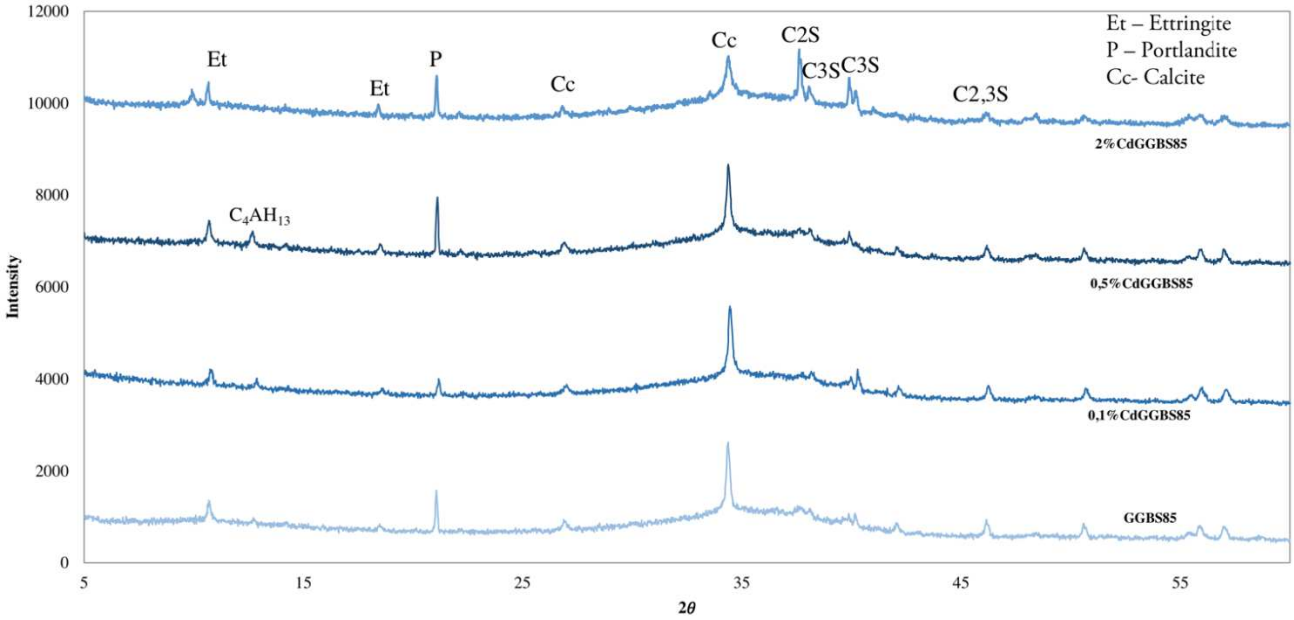

Fig. IV.33 XRD analysis of 85%GGBS/15%OPC with addition of 0,1%$Cd(NO_3)_2$, 0,5%$Cd(NO_3)_2$, 2%$Cd(NO_3)_2$ after 24 hours of storage

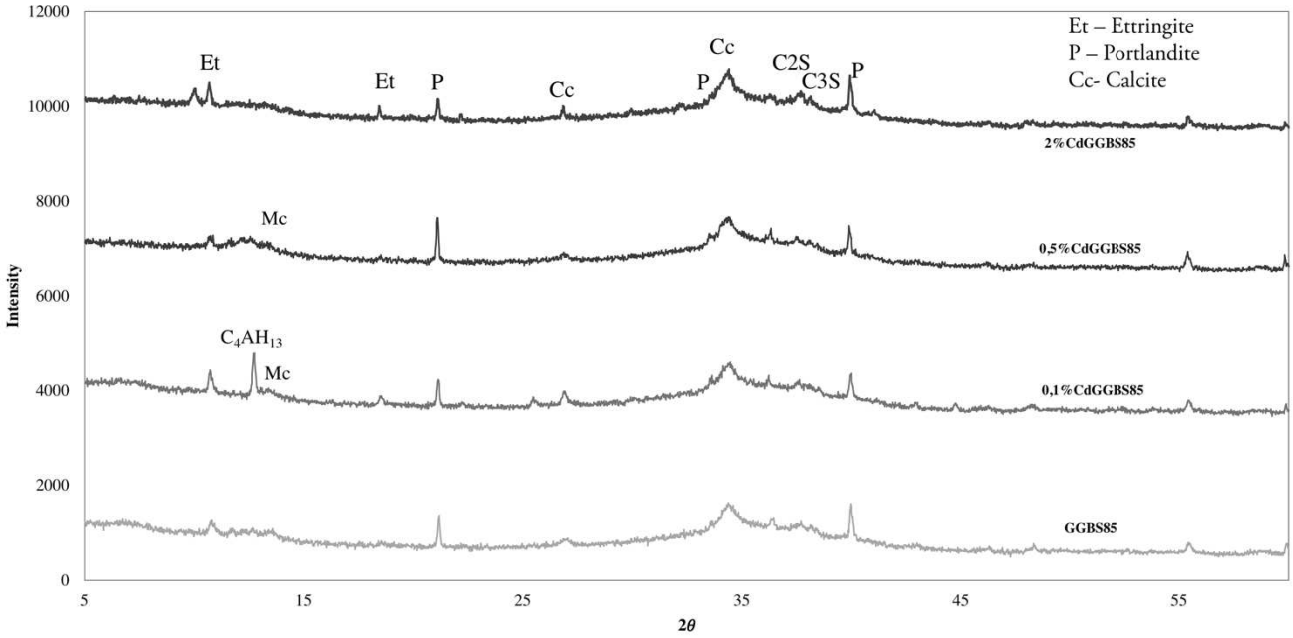

Fig. IV.34 XRD analysis of 85%GGBS/15%OPC with addition of 0,1%$Cd(NO_3)_2$, 0,5%$Cd(NO_3)_2$, 2%$Cd(NO_3)_2$ after 7 days of storage

IV.2.4.3 Supersulfated formulation

The introduction of cadmium nitrate salt into the SSC formulation had the smallest negative impact on hydration compared to the other metals according to the calorimetry measurements (Fig. IV.35). For the 0.1%CdSSC mixture, the MHP occurs after 13.5 h meaning a slight acceleration of the hydration with a higher heat rate of 0.52 mW/g. With a further increase in the content of cadmium nitrate, the occurrence of the main peak of SSC was retarded, but not completely annihilated as in the presence of copper or zinc. The MHP of 0.5%CdSSC and 2%CdSSC emerged after 19.6 h and 32.9 h, respectively.

The evolution of hydrates of the supersulfated formulation with and without cadmium addition are presented in Fig. IV.36 and Fig. IV.37. This time even at 2%wt of $Cd(NO_3)_2$ the ettringite phase was detected after 24 h of storage, but with lower intensity than for the other samples. An increase in intensity of the ettringite peak was observed for 0.5% $Cd(NO_3)_2$ at 24 h. Interestingly, all samples present a uniform development of the hydration phases at 7 days of storage, in contrast to the supersulfated formulation mixed with zinc, copper, and nickel salts (Fig. IV.37).

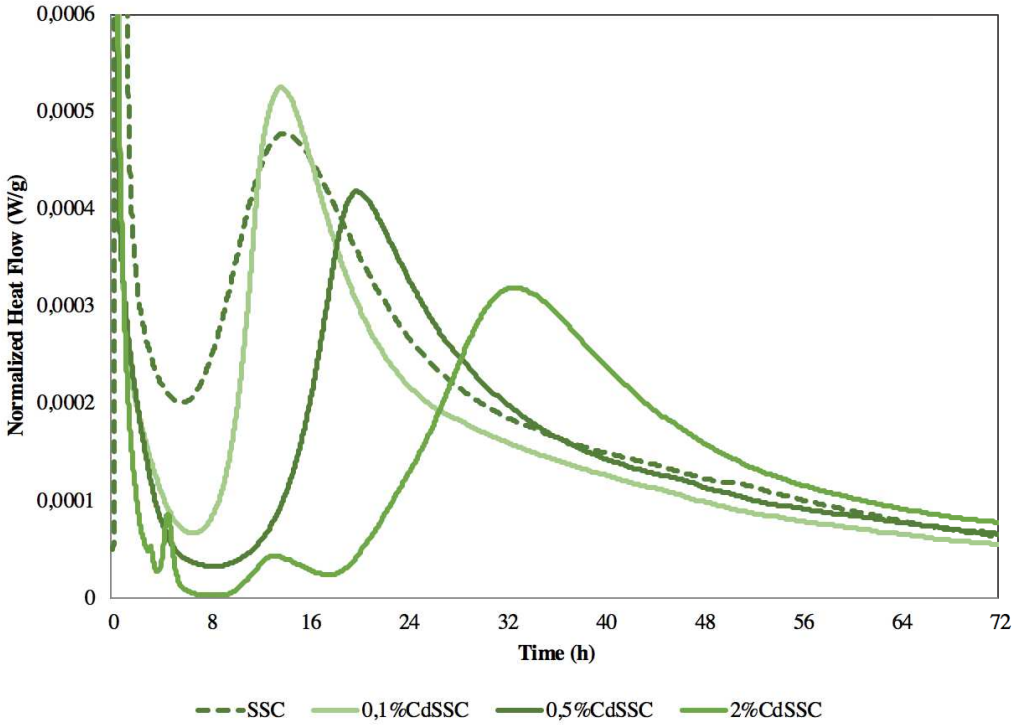

Fig. IV.35 Isothermal calorimetry of the Supersulfated formulation with addition of 0,1%$Cd(NO_3)_2$, 0,5%$Cd(NO_3)_2$, 2%$Cd(NO_3)_2$

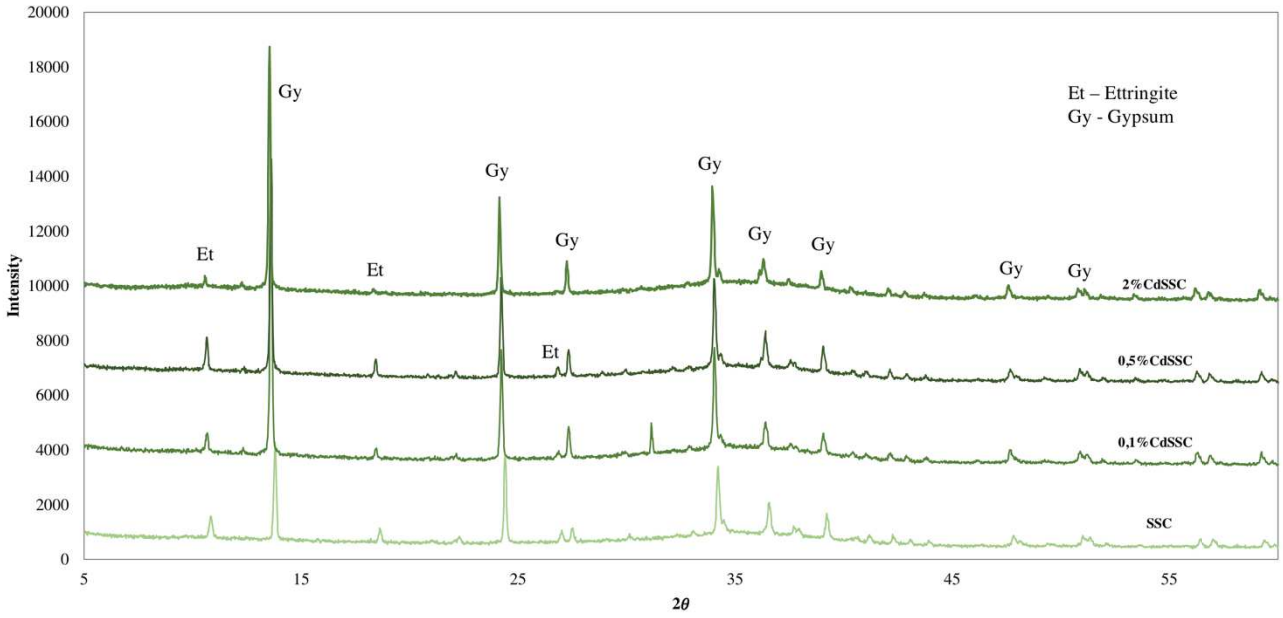

Fig. IV.36 XRD analysis of the Supersulfated formulation with addition of 0,1%$Cd(NO_3)_2$, 0,5%$Cd(NO_3)_2$, 2%$Cd(NO_3)_2$ after 24 hours of storage

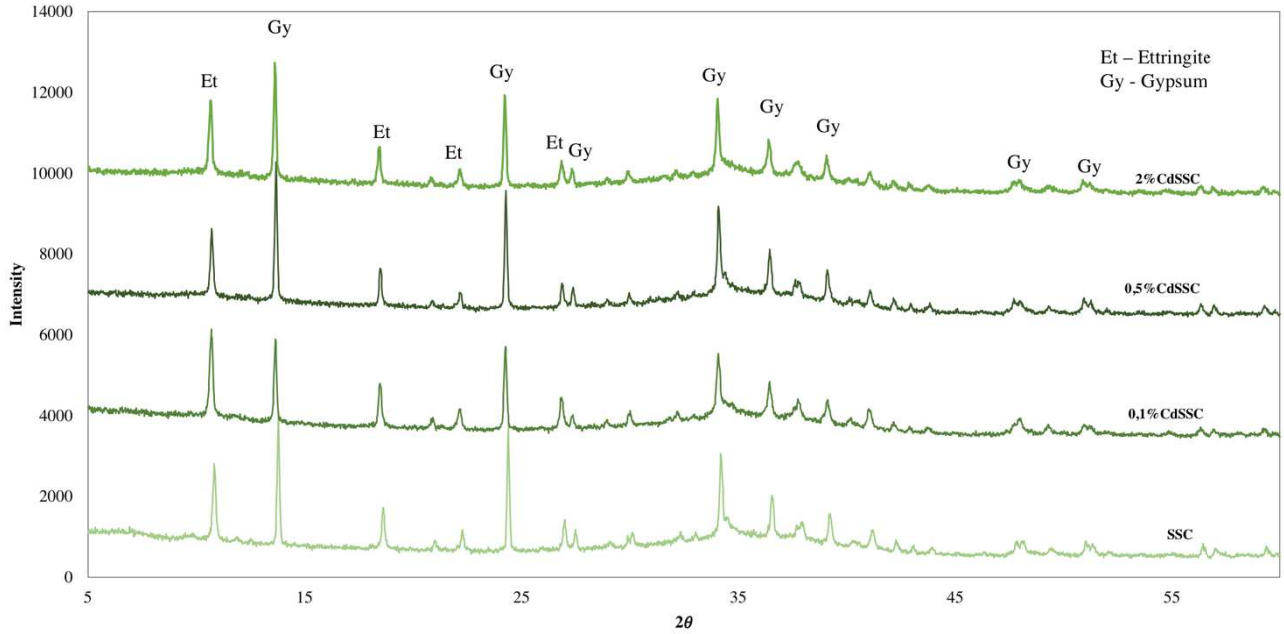

Fig. IV.37 XRD analysis of the Supersulfated formulation with addition of 0,1%$Cd(NO_3)_2$, 0,5%$Cd(NO_3)_2$, 2%$Cd(NO_3)_2$ after 7 days of storage

IV.2.4.4 Discussion

The introduction of Cd in the considered binders accelerated the main hydration reactions for OPC and GGBS85 and did not have a negative effect on the hydration of the SSC formulation. Data from several studies suggests that cadmium in cement systems will precipitate in the form of cadmium hydroxide following earlier hydration (pH>12.5), or cadmium carbonate (pH 9-11) (Achternbosch et al., 2003; Halim et al., 2004). The XANES spectra confirm the previous findings regarding the formation of cadmium hydroxides in the OPC formulation (see Chapter V). It seems that $Cd(OH)_2$ exists as distinct particles in the cementitious matrix. (Halim et al., 2004; McWhinney & Cocke, 1993) observed independent cadmium compounds such as cadmium oxides, hydroxides, and carbonates within the C-S-H of cement. The acceleration effect of cadmium on the three considered formulations may be explained by the formation of cadmium hydroxide. They may potentially provide additional sites for the nucleation of C-S-H. (Cartledge et al., 1990) suggested that the physical inclusion of $Cd(OH)_2$ in C_2SH may occur and even the acceleration of C-S-H gel precipitation by the presence of cadmium hydroxides could take place. The compressive strength developed by the cement samples mixed with 2% cadmium nitrate in the study of (Gineys et al., 2010) shows a slight decrease in strength after 2 days, but similar values were reported after 28 days of storage for the reference OPC sample and the Cd-doped sample.

At the same time, the formation of highly stable CdS in the GGBS-based formulations was detected in this study with an important prevalence of this cadmium compound due to the presence of sulfurs in GGBS (see Chapter V).

Cadmium ions present the lowest negative impact on the hydration of the binders

compared to the other considered heavy metals. It can thus be concluded that cadmium precipitates in the form of simple hydroxides in Portland cement solutions and in the form of sulfurs within GGBS-based binders. It does not block the surfaces of C_3S and C_2S and it does not interact with the calcium ions necessary for hydrate formation.

Table IV.9 Summary for the hydration heat rate results of OPC, GGBS85 and SSC mixed with $Cd(NO_3)_2$

			OPC	GGBS85	SSC
$Cd(NO_3)_2$	0%	MHP (h)	11.4	13.5	14
		Peak height (mW/g)	3.87	0.71	0.48
		Total Heat Flow, 72h (J/g)	274.8	76.7	50.9
	0.1%	MHP (h)	7.7	10.2	13.5
		Peak height (mW/g)	3.89	0.61	0.52
		Total Heat Flow, 72h (J/g)	192.5	71.1	41.4
	0.5%	MHP (h)	6.4	8.2	19.6
		Peak height (mW/g)	3.59	0.6	0.42
		Total Heat Flow, 72h (J/g)	180.9	67.7	38.4
	2%	MHP (h)	4	18.8	32.9
		Peak height (mW/g)	3.2	0.35	0.32
		Total Heat Flow, 72h (J/g)	151.5	60.8	33.8

IV.2.5 Zeta Potential of the binders in the presence of HM

IV.2.5.1 100%OPC formulation

Figure IV.38 reveals the changes in the zeta potential evolution of the 100%OPC binder mixed with the four considered heavy metal salts. The control sample gives positive values from 6 to 8 mV over 80 min (the full test duration). The positive values of the plain Portland cement sample arise from an increase in the concentration of calcium ions (Ca^{2+}) from Portland cement's anhydrous minerals adsorbed onto the negative surfaces of the silanol groups during hydration. A marked decrease in zeta potential can be seen in the presence of the zinc and copper salts. The values for 0.5%CuOPC at the beginning of the measurements are around 3.5 mV and they increase to 5.6 mV during the test. Zeta potential measured for the OPC binder mixed with the zinc solution presents slightly higher values, but they are still lower than the reference sample – from 4.2 mV to 6.9 mV. Meanwhile, the OPC formulation in the presence of nickel shows a considerable increase in zeta potential in contrast to the behaviour reported for copper and zinc. With the introduction of nickel, the values show an evolution of the zeta potential from 4.3 mV to 9 mV over the duration of the test.

Finally, OPC in the cadmium salt solution exhibits almost the same zeta potential evolution as the control sample. The trends measured in the conductivity analysis are quite similar to those of the zeta potential (Fig. IV.39). The conductivity of the samples increases gradually over time, except for the sample with 0.5%$Cu(NO_3)_2$ which remains almost stable. Zinc nitrate lowered the conductivity of the solution as well, compared to the reference sample. At the same time, the dissolution rate of the OPC binder in the presence of nickel nitrate increased.

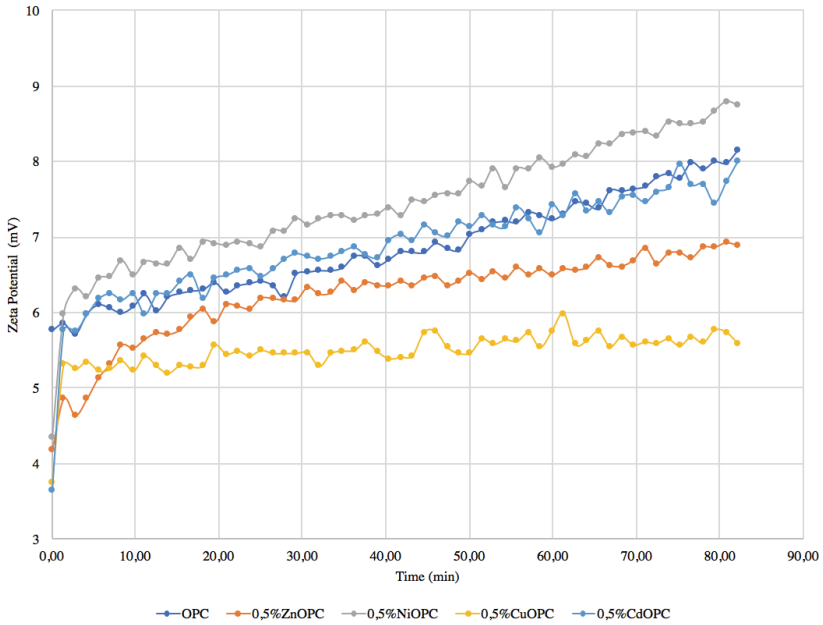

Fig. IV.38 Zeta potential measurements of the 100%OPC formulation doped with 0,5% of HM nitrates salts (Zn, Ni, Cu, Cd)

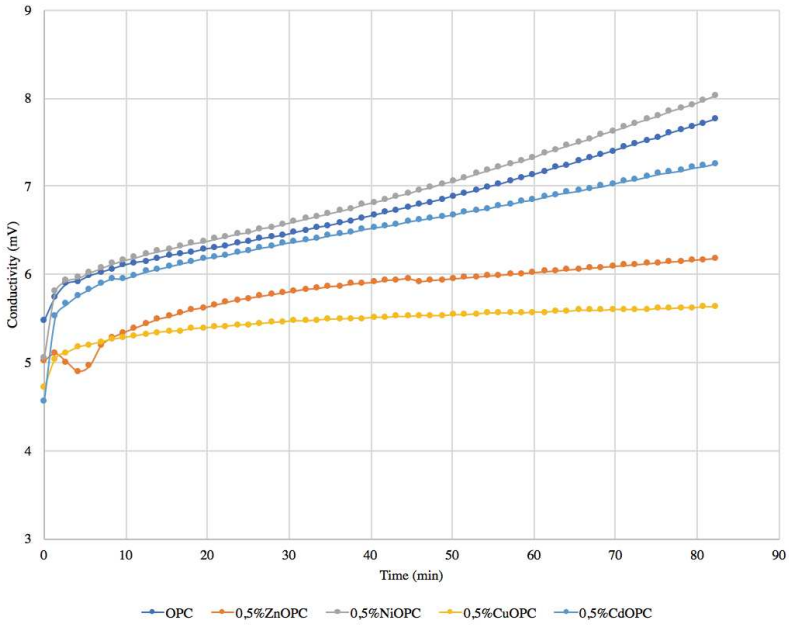

Fig. IV.39 Conductivity of the 100%OPC formulation doped with 0,5% of HM nitrates salts (Zn, Ni, Cu, Cd)

In regard to the pH values presented in Fig. 4.40, all samples exhibit a highly alkaline pH, even when considering the low concentration of the cement. The values are pretty dispersed, but in general a decrease in pH can be noted for all samples over time. Nickel and cadmium nitrates showed the greatest pH values, followed by zinc and copper, and finally the reference sample.

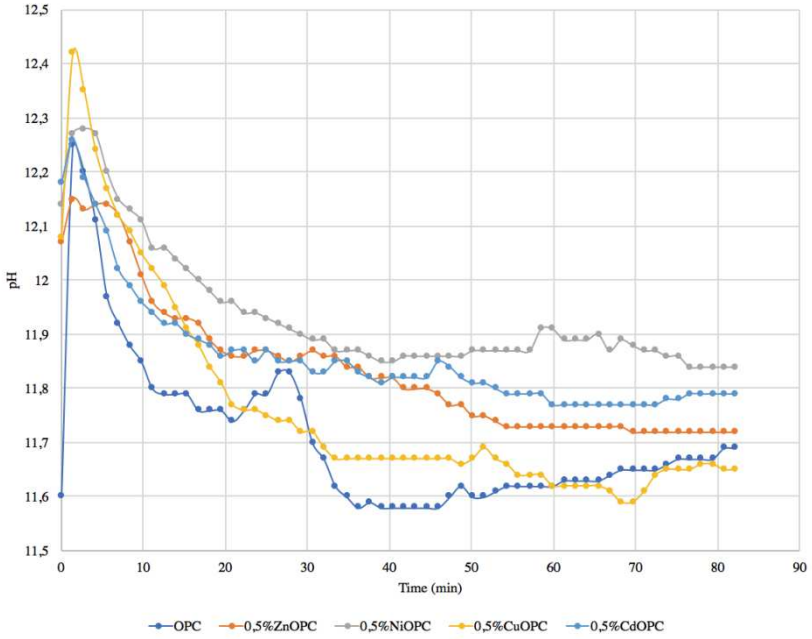

Fig. IV.40 pH of the 100%OPC formulation doped with 0,5% of HM nitrates salts (Zn, Ni, Cu, Cd)

IV.2.5.2 85%GGBS/15%OPC

The zeta potential evolution for the 85%GGBS/15%OPC formulation in demineralized water and in four heavy metal nitrate solutions is presented in Fig. IV.41. The values on the graph are noticeably lower than those of the OPC formulation but are still positive. What is interesting in the figure is the general trend in changes in zeta potential of the control sample when mixed with the heavy metal salts. This trend is fairly similar to the effect of the same considered heavy metals for the plain OPC binder. The zeta potential values of the reference formulation (GGBS85) were decreased under the influence of zinc and, especially, copper nitrate. The final value of zeta potential (after 80 min) for the reference formulation is 3.3 mV. Zinc lowered this value to 2.5 mV and copper to 1.8 mV. Unlike the effect of zinc and copper nitrates, cadmium and nickel present a growth in zeta potential. Nickel shows an increase from 1.24 mV to 4.4 mV and cadmium from 1.8 mV to 4 mV compared to the evolution of the reference formulation (from 1.4 mV to 3.3 mV) over the duration of the experiment. The conductivity and pH of GGBS85 with and without the presence of the heavy metal salts are reported in Fig. IV.42 and IV.43. The lowest pH is attributed to the reference

formulation and all heavy metal salts slightly increased the pH of the solutions. The zinc sample has the lowest pH of all the metal salt samples and the lowest conductivity values. The highest conductivity was measured for 0.5%NiGGBS85.

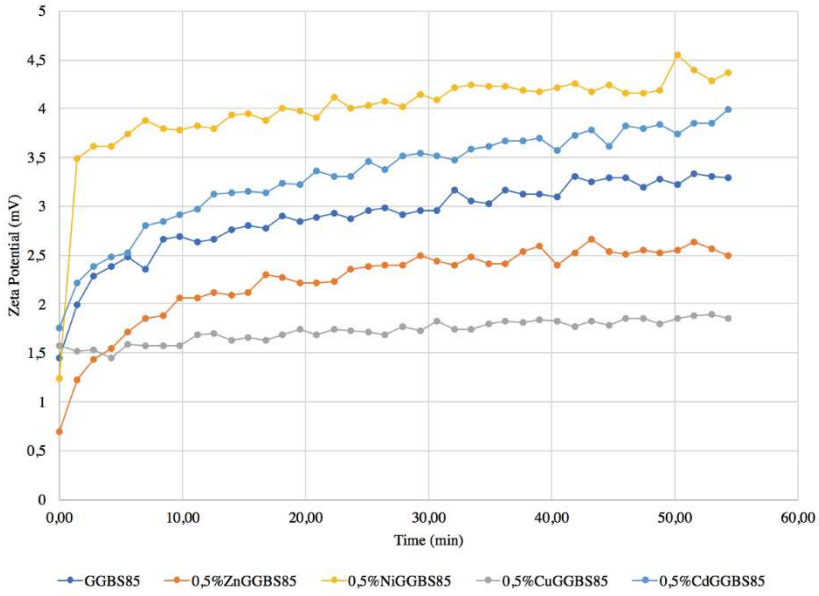

Fig. IV.41 Zeta potential measurements of the 85%GGBS/15%OPC formulation doped with 0,5% of HM nitrates salts (Zn, Ni, Cu, Cd)

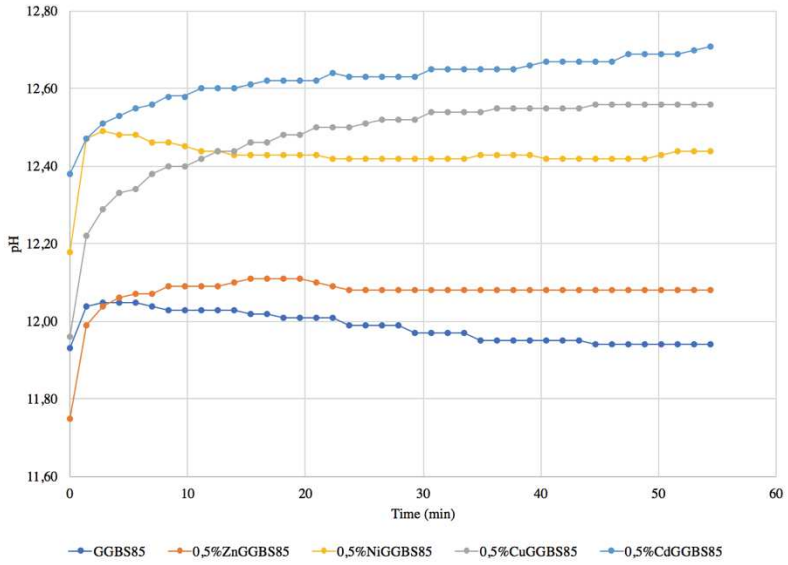

Fig. IV.42 pH of the 85%GGBS/15%OPC formulation doped with 0,5% of HM nitrates salts (Zn, Ni, Cu, Cd)

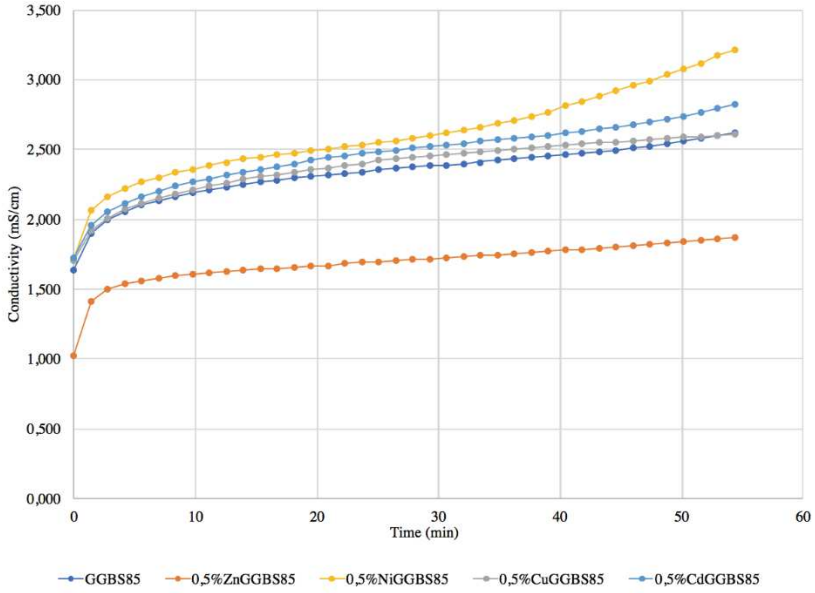

Fig. IV.43 Conductivity of the 85%GGBS/15%OPC formulation doped with 0,5% of HM nitrates salts (Zn, Ni, Cu, Cd)

IV.2.5.3 Discussion

The presented results of the evolution of zeta potential, pH, and conductivity of two binders – 100%OPC and 85%GGBS/15%OPC, introduced to pure water and four heavy metal solutions, reinforce the assumptions made about the mechanisms of the impact of heavy metals on the hydration kinetics of the binders discussed previously in this chapter.

The main observations from the study suggest that at the considered dosages, copper, and zinc will mainly have a retarding effect on hydration, while nickel and cadmium will accelerate the reactions produced during the early hydration process, or not have a noticeable impact.

The zeta potential of both binders is governed by the high pH development as well the high ionic strength, especially in case of Portland cement. At the very beginning of the contact between the cement grains with water, there are alkalis (Na^+, K^+), sulfates, and free lime (CaO) in the solution from the first minutes. After, Ca^{2+} and OH^- are released into solution from C_3A and C_3S due to hydrolysis (Lowke & Gehlen, 2015). Therefore, it can be supposed that the adsorption of calcium and sulfate ions on the cement's surface plays an important role for the zeta potential evolution. Regarding the higher calcium concentration for the plain OPC formulation compared to the GGBS-based formulation, the adsorption of divalent calcium cations will produce more positively charged surface demonstrated by higher zeta potentials.

Zeta potential can be influenced by the size and type of an ion, as well as by the ionic strength of the solution (Yukselen-Aksoy & Kaya, 2016). There are many published studies on the behaviour of metal cations in highly alkaline media (Hunter, 1992;

Weeks et al., 2008; Yukselen & Kaya, 2002). Regarding the results obtained after the calorimetry, XRD, and zeta potential measurements, it can be supposed that some heavy metal species will act in the alkaline solution following reactions 32 and 33 (Weeks et al., 2008):

$$M \rightarrow M(OH)_2 \qquad \textit{(in the presence of } OH^- \textit{ ions)} \quad (32)$$

$$M \rightarrow CaM_2(OH)_x \cdot yH_2O \qquad \textit{(in the presence of excess } OH^- \textit{ and } Ca^{2+} \textit{ ions)} \quad (33)$$

As was discussed previously, there is a strong possibility of the formation of the complex calcium salts $CaZn_2(OH)_6.2H_2O$ in the presence of zinc nitrate and $Ca_2(OH)_4.4Cu(OH)_2{\cdot}H_2O$ in the presence of copper nitrate. These reactions can explain the lowering of the zeta potential values measured here for 0.5%ZnOPC, 0.5%CuOPC, 0.5%ZnGGBS85 and 0.5%CuGGBS85. The lack of calcium ions due to the precipitation of complex salt species with Zn and Cu will delay the dissolution of the anhydrous phases and the precipitation of calcium hydroxides and C-S-H.
It can therefore be assumed that the reason why there is mostly an acceleration effect of the early reactions in the presence of nickel and cadmium (expressed here as an increase in zeta potential and conductivity) is that these heavy metals precipitate mostly as simple species (e.g. hydroxides) in the binder solutions without disturbing the availability of calcium for the main hydrate formation. Ni and Cd accelerate the hydration through increasing surface deprotonation probably due to additional seeds formation. In the case of nickel, the additional formation of Ni-Al double layer hydroxides contributes to the accelerated hydration.

IV.2.6 Conclusions

The effect of the heavy metals considered here at the chosen concentrations gives an insight into the importance of considering these variables for the choice or the correct adjustment of the binder used for the Solidification/Stabilization process of polluted sediments. Heavy metal cations may strongly affect the early hydration kinetics. The results provide some explanations for the delaying mechanisms observed in sediment-binder systems.

The results of the study can be categorized into two main groups according to the effect of the considered heavy metals on the hydration kinetics at early age:

- Copper and zinc mostly retarded the hydration of the OPC, GGBS85, and SSC formulations. It can be concluded that zinc and copper will precipitate in the form of complex calcium hydroxide compounds and retard hydration through the lack of calcium ions. Therefore, the extended induction period corresponds to the equilibrium of the system with a low dissolution rate of the anhydrous phases of

the binders. The key parameter of the retardation effect of Cu and Zn is lowered calcium activity in the binder solutions and the low dissolution rate of the binders.

- Ni and Cd ions demonstrated a different behaviour by accelerating the systems, or not dramatically impacting the hydration pathway. These heavy metals instead form simple hydroxides in the cement systems. The formation of Ni-LDH can be expected, providing additional seeds for hydration. The precipitation of CdS in the GGBS-based formulations takes place according to the EXAFS results (presented in the next chapter). Therefore, the calcium ions remain available for the formation of hydration products. Both metals increased the surface charge, inducing higher dissolution rates for the minerals.

Heavy metals affected the binders' early hydration following the order SSC>GGBS85>OPC (Table IV.10).

Table IV.10 The effect of the considered heavy metals on the early hydration of the hydraulic binders (N – No effect, A – Accelerated, D – Delayed, I – Inhibited)

Heavy metal in form of nitrate salt	(%)	OPC	GGBS85	SSC
Cu	0,1	N	D	D
	0,5	A	I	I
	2	D	I	I
Zn	0,1	A	A	D
	0,5	D	D	I
	2	D	I	I
Ni	0,1	A	A	A
	0,5	A	A	D
	2	A	A	I
Cd	0,1	A	A	A
	0,5	A	A	D
	2	A	D	D

- The supersulfated formulation was shown to have the greatest sensitivity to the addition of the heavy metal nitrates. The most negative impact on the hydration was observed with the addition of copper and zinc. The ettringite formation of SSC was completely annihilated and only gypsum formation was observed. These findings provide an understanding of the lack of strength produced for the supersulfated formulation mixed with the Dublin sediment.
- GGBS85 was also significantly affected by the presence of copper and zinc as the hydration was considerably retarded. The slow emergence of hardening (~1-2 weeks) for the sediment samples in the GGBS85 formulation can be explained by the presence of heavy metals such as copper and zinc in significant amounts.

- The weakest perturbation rate at the early stages of hydration in the presence of heavy metals was observed for the Portland cement binder. This goes in accordance with the relatively fast hardening (a few days) of the samples of the Dublin sediment mixed with Portland cement.

IV.3 ^{27}Al and ^{29}Si NMR spectra of the 'hydraulic binders-heavy metals' system. Long term hydration

IV.3.1 Introduction

As can be concluded from this chapter, the interaction of heavy metals with GGBS-based binders causes, in some cases, a significant retardation in the formation of the main hydration products compared to the Portland cement binder.
Most of the hydrated phases in GGBS-based binders are amorphous. Therefore, NMR spectroscopy is particularly well suited to quantify these phases and observe the changes in their morphology and abundance induced by the incorporation of heavy metals. The major phase in the case of the GGBS-based binder is C-A-S-H, which is the calcium silicate hydrate (C-S-H) gel phase containing aluminum. (Dong et al., 2019) in his study of the gel structure of C-S-H in a pure Portland cement system and a GGBS-OPC system observed an increase in C-A-S-H gel with an increase of the hydration rate.

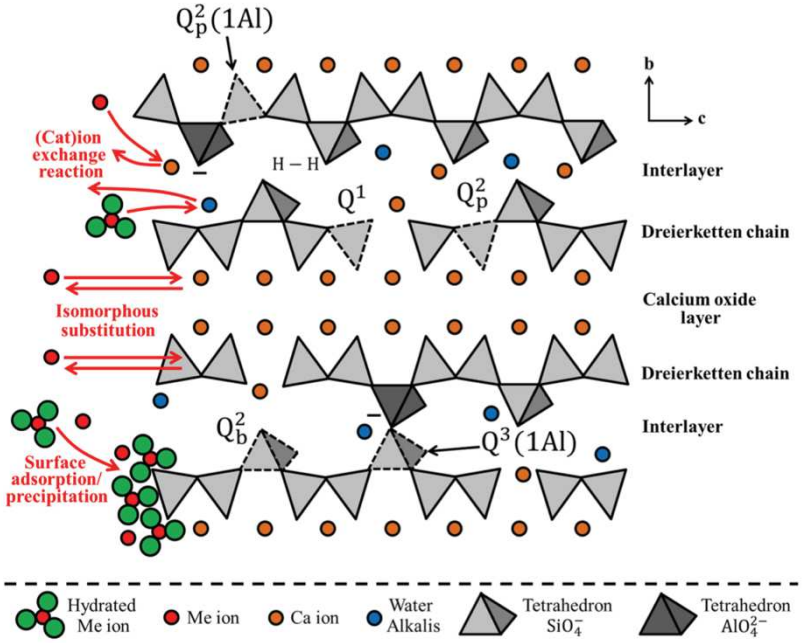

Fig. IV.44 Schematic structure of C–A–S–H with potential immobilization effects indicated in red. $Q^n_{p,b}$(mAl): Q=SiO_4 tetrahedron, n = number of neighbouring SiO_4 tetrahedra, m = number of neighbouring AlO_4 tetrahedra, p = pairing position, b = bridging position; —: negative charge; H–H: hydrogen bridge bond (from (Baldermann et al., 2019))

The substitution of Al for Si in tetrahedral sites occurs often with increasing GGBS content (Richardson & Groves, 1997). (Wang & Scrivener, 2003) also reported the incorporation of aluminium in the silicate chains of C-S-H gel in alkali-activated slag, whereas a lower Al/Si ratio was observed for the Portland cement system.
Thus, in addition to the possible fixation of heavy metals by the substitution of Ca^{2+} ions in C-S-H , the possible incorporation of heavy metals into the C-A-S-H structure is also possible to compensate for the charge deficits occurring due to substitution of Si by Al. (Baldermann et al., 2019) reported several pathways for the removal of heavy metals during C-A-S-H formation. Among them there are isomorphous substitution in octahedral and tetrahedral positions, ion exchange in the interlayer sites, and potentially surface (ad)sorption, and surface precipitation (Fig. IV.44).
At the same time, the AFm phases are also known to be responsible for heavy metal immobilization. For example, the sodium carbonate activated GGBS system produces the hydrotalcite-like phases known to have a strong removal capacity for heavy metals, exceeding those of OPC systems (B. Li et al., 2019). (Yang et al., 2020) demonstrated a strong uptake of Pb^{2+}, Cu^{2+}, and Cr^{3+} in the AAS due to the hydrotalcite phase.
Thus, in the NMR investigation an attempt was made to evaluate the impact of the presence of heavy metals on the Al environment of the three different binder systems. The main objectives of the NMR analysis were to observe the changes induced in the hydrates formation at 1 and 4 months of storage when heavy metals are introduced in the mixtures.

IV.3.2 Considered samples

The binders considered for the NMR experiments are: 100%OPC, 85%GGBS/15%OPC, as well as 100%GGBS/10%Na_2CO_3. In the case of OPC alone, potentially little incorporation of Al in the C-S-H phase takes place, knowing that it is rapidly consumed in ettringite and AFm. On the other hand, the slag is richer in Al and it is therefore incorporated in large quantities in C-A-S-H. Even greater substitution of Al for Si in the C-A-S-H phase can be expected for the AAS binder.
Two heavy metals with different ionic radii were considered: Zn and Cd (Table IV.11). The heavy metals were incorporated into the binders in the form of soluble nitrate salts and the NMR analysis was carried out after 1 and 4 months of storage.

Table IV.11 Considered samples for the NMR experiment

Samples	$Zn(NO_3)_2$ (%wt binder)	$Cd(NO_3)_2$ (%wt binder)
OPC (100%OPC)	0; 2%	
GGBS85 (85%GGBS/15%OPC)		
AAS (100%GGBS/10%Na_2CO_3)		

IV.3.3 ^{27}Al NMR spectra of the OPC system in the presence of Cd and Zn

The ^{27}Al MAS NMR spectra of the hydrated ordinary Portland cement mixed with heavy metal salts are presented in Fig. IV.45.

The 4-coordinated (tetrahedral) aluminum signals can be clearly seen on the spectra in the region of 60-80 ppm. As previously said (III.3.3.3), the ^{27}Al MAS spectrum of OPC is composed of a signal with a center of gravity at 86 ppm, attributed to Al incorporated in dicalcium silicate (C_2S) / tricalcium silicate (C_3S) and a second signal with center of gravity at 81 ppm corresponding to Al in tricalcium aluminate (C_3A) (the tetracalcium aluminoferrite phase is generally unobservable) (Skibsted et al., 1993). This broad peak ranging from 60 to 80 ppm could probably be attributed to Al(IV) in C-A-S-H, occurring during the hydration of the OPC binder and the incorporation of Al into C-S-H gel. In the range of 6-coordinated (octahedral) aluminium, three sharp signals can be distinguished at 13, 10, and 4 ppm assigned respectively to aluminium in ettringite, AFm, and a third aluminate hydrate (TAH) (Andersen et al., 2006).

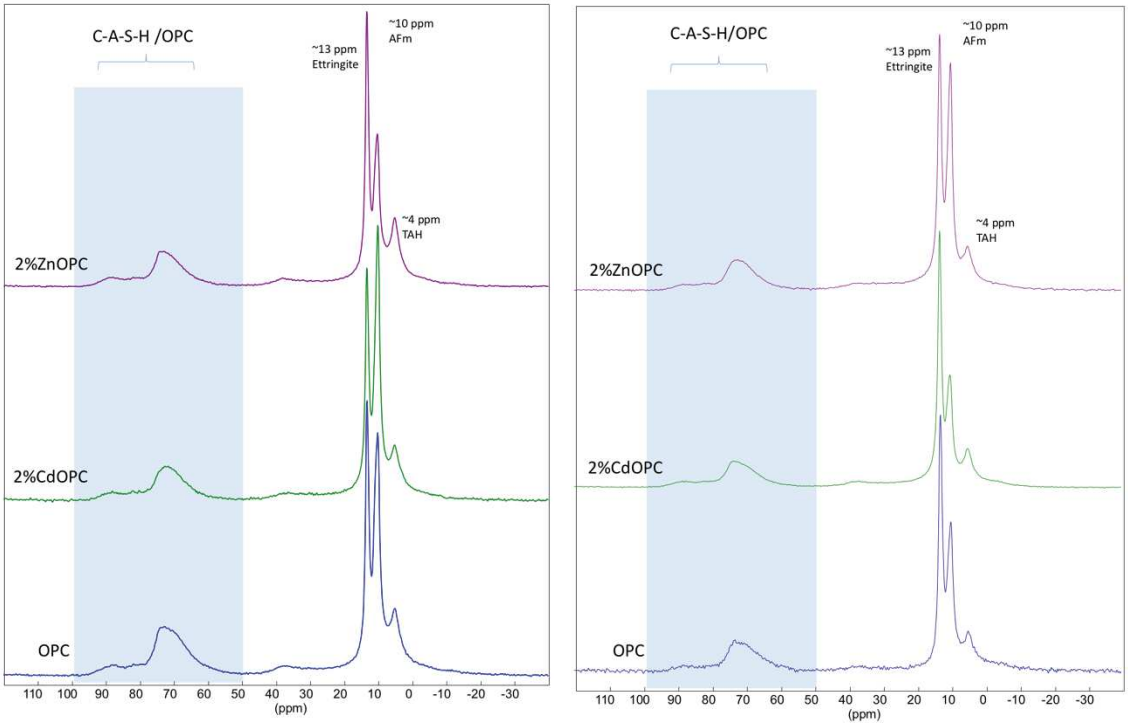

Fig. IV.45 ^{27}Al NMR spectra of OPC, 2%ZnOPC, 2%CdOPC after 1 month (left) and 4 months (right)

Regarding the C-A-S-H region for the samples containing heavy metals (2%CdOPC and 2%ZnOPC), there is no significant difference in the appearance of the resonances that can be reported. At first glance, the samples with and without zinc incorporation present almost the same chemical and structural evolution over time in the Al(IV) region. The C-S-H structure is almost unchanged as well as silicate chain length, as was already observed by (Pomiès et al., 2001) after the cadmium incorporation.

IV.3.4 ^{27}Al NMR spectra of the GGBS85 system in the presence of Cd and Zn

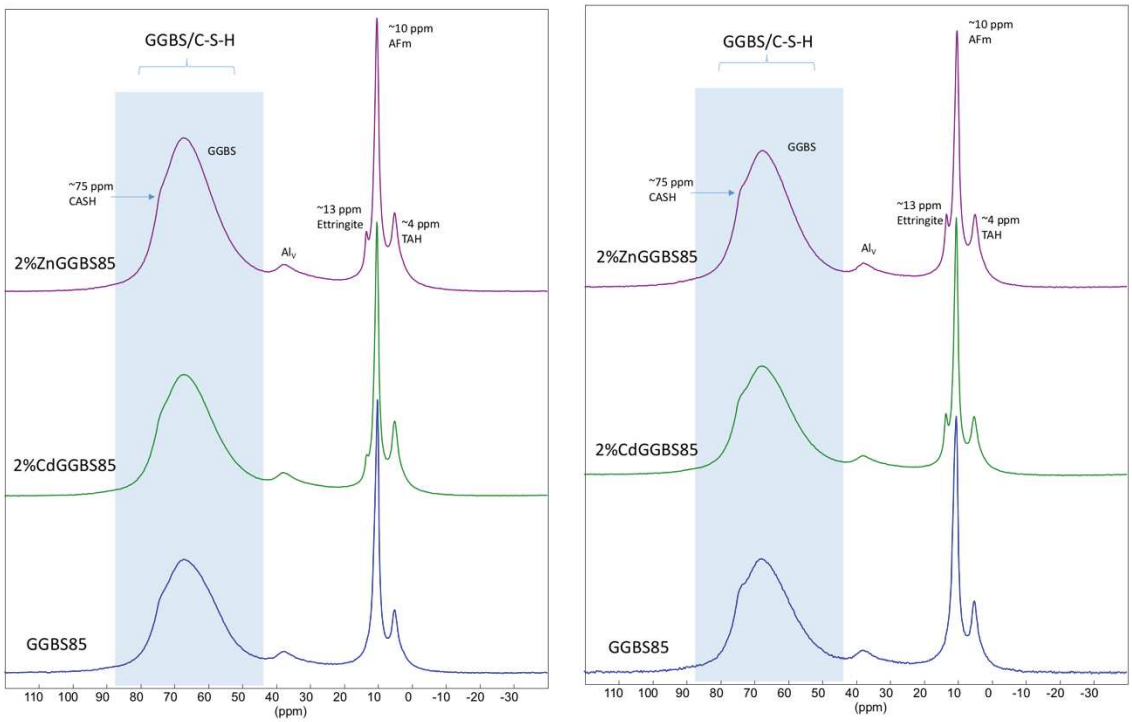

Fig. IV.46 ^{27}Al NMR spectra of GGBS85, 2%ZnGGBS85, 2%CdGGBS85 after 1 month (left) and 4 months (right)

The results obtained from the ^{27}Al NMR analysis of the GGBS-based formulation activated with Portland cement (GGBS85) and for the mixtures 2%CdGGBS85 and 2%ZnGGBS85 are compared in Fig. IV.46.

The region of the 4-coordinated aluminum displays a broad resonance ranging from 50 to 80 ppm. Regarding the high slag content (85%wt) this resonance is mainly attributed to the AlO_4 tetrahedra of a depolymerized amorphous slag framework (Neuville et al., 2008). No signal corresponding to OPC is detectable on these spectra due to its low amount and its dissolution. On the contrary, the shoulder at around 75ppm revealed the formation of C-A-S-H gel. According to the signal observed for C-A-S-H in the case of the pure OPC system (cf. Fig. IV. 45) another contribution should overlap with the GGBS signal. The shoulder at 75 ppm becomes slightly sharper in the case of GGBS85 between 1 and 4 months of storage, probably showing a more significant incorporation of Al into the C-S-H structure. No significant differences can be found for Al in tetrahedral coordination in 2%ZnGGBS85 and 2%CdGGBS85 in the region of C-A-S-H.

In the Al[VI] range, signals previously assigned to ettringite, AFm, and TAH are found. However, the proportion of ettringite is clearly different from the case of pure OPC. For the GGBS85 formulation, no ettringite is detectable both after 1 and 4 months of storage, whereas this phase was detected via XRD analysis at early age, after 24h and 7 days of storage (Fig. IV.5, IV.6). It can be concluded that AFt was transformed

into monosulfoaluminate (AFm). In the cases of 2%ZnGGBS85 and 2%CdGGBS85, a slight signal due to ettringite is observed and a more pronounced peak of ettringite occurs for the GGBS85 formulation in the presence of cadmium between 1 and 4 months of storage (cf. Fig. IV.46). (Tashiro et al., 1979) reported the acceleration effect of ettringite crystal growth when some heavy metals were added to the mix of synthesized C_3A and $Ca_2SO_4.2H_2O$. (Tumidajski & Thomson, 1995) studied the impact of CdO on the hydration of $3CaO.Al_2O_3$ and concluded that cadmium ions promote the precipitation of cubic hydrated phases. Thus, it can be supposed that the enhanced formation of AFt and AFm type phases occurs for the GGBS85 system in the presence of cadmium and zinc.

IV.3.5 ^{27}Al NMR spectra of the AAS system in the presence of Cd and Zn

The sodium carbonate activation of the blast furnace slag was adopted for the NMR study due to the potential capacity of binding heavy metals within developed hydrates. The dense C-A-S-H gel structure of AAS systems is known to have a good adsorption efficiency for the heavy metal stability (Deja, 2002; Yang et al., 2020). The hydrotalcite phase (Mg-Al LDH) is one of the main phases precipitated through Na_2CO_3 activation of GGBS. Hydrotalcite can also stabilize heavy metals within its structure of positively charged brucite-like sheets with its charge-balanced secondary anionic layer.
The ^{27}Al MAS NMR spectra of alkali activated slag (AAS) in the presence of 2%wt of zinc (2%ZnAAS) and cadmium nitrate salts (2%CdAAS) are shown in Fig. IV.47.
As was mentioned earlier, the broad peak ranging from 50 to 80 ppm is mainly due to the 4-coordinated Al from the anhydrous GGBS framework. This signal overlaps Al(IV) which is the part of the C-A-S-H gel phase developed at 1 and 4 months of storage. However, unlike the two other binder systems (OPC and GGBS85), the sharp peak at ~75 ppm assigned here to Al in the C-A-S-H frame of the AAS is more intense. After 1 month of storage, this peak is clearly visible for the AAS sample and for the 2%CdAAS sample. Nevertheless, zinc incorporated in the AAS system considerably retarded the appearance of the C-A-S-H peak. It can be also considered regarding the 6-coordinated Al within the AFm phase structure that hydrotalcite in 2%ZnAAS precipitated in a smaller amount compared to AAS and 2%CdAAS. Therefore, it can be concluded that cadmium causes a lesser impact on hydrate formation after 1 month of storage compared to zinc. Despite this retardation effect of zinc after 1 month of storage, the NMR spectra of all the samples after 4 months of hydration demonstrate a similar evolution of the hydrates.

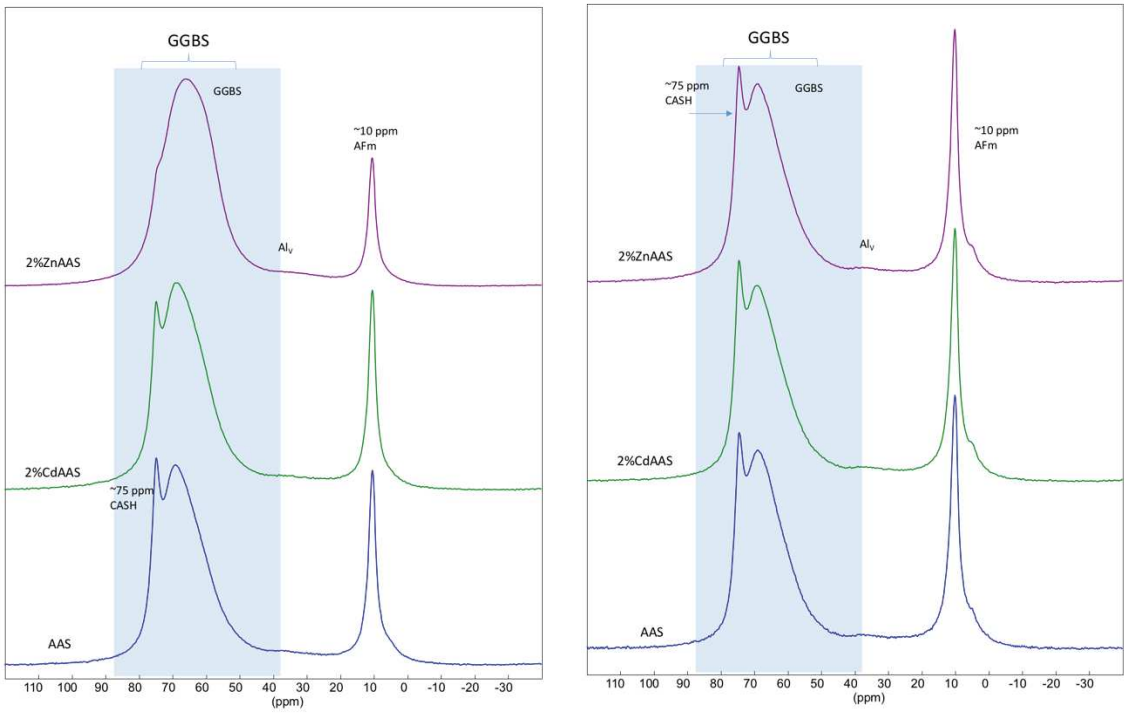

Fig. IV.47 Al NMR spectra of AAS, 2%CdAAS, 2%ZnAAS after 1 month (left) and 4 months (right)

In order to distinguish the MAS spectra of aluminum close to ^{1}H atoms, a new series of ^{1}H-^{27}Al CP-MAS experiments were carried out only for the pure sample of AAS and 2%ZnAAS. This method is particularly useful for identifying hydrous alumina within the samples and in this case to more closely inspect the effect of zinc on the hydration product development.

The CP-MAS signals (dotted lines) are compared to the ^{27}Al spectra (full lines) in Fig. IV.48. The CP-MAS signals of AAS after 1 and 4 months as well as those of 2%ZnAAS after 4 month show that the Al(IV) signals of Al in C-A-S-H are complex and exhibit at least two components, including the sharp signal at 75ppm. This shape was already observed in the case of the pure OPC system (cf. Fig. IV.45). Interestingly, the ^{1}H-^{27}Al CP-MAS signal of the C-A-S-H phase after 1 month of storage is significantly different for the sodium carbonate activated GGBS in the presence of zinc A noticeable retardation is observed, expressed as very low peak in the region from 50 to 80. However, the 4-month hydration rate of both samples is similar.

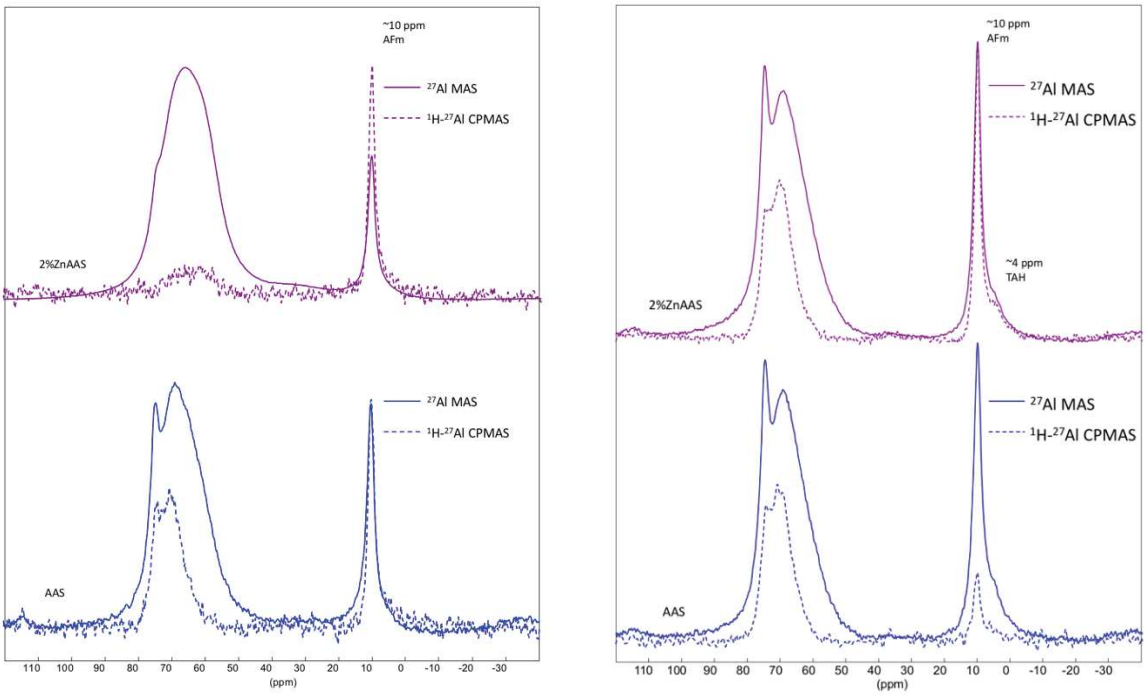

Fig. IV.48 ^{27}Al MAS and ^{1}H-^{27}Al CP-MAS spectra of AAS and 2%ZnAAS samples after 1 month (left) and 4 months (right)

IV.3.5.1 ^{29}Si NMR and ^{1}H-^{29}Si spectra of the AAS system in the presence of Zn

Regarding the evidence of the impact of the addition of zinc nitrate on the reactivity of the AAS system, and especially on the formation of C-A-S-H phase, a ^{29}Si MAS NMR analysis was performed in order to provide a deeper understanding of the hydrates evolution of the sample doped with zinc nitrate.

During the hydration of cements, C-S-H with different degrees of silicate polymerization is precipitated. Therefore, ^{29}Si NMR is largely applied to study the hydration of different cement materials. Si in cements is present in four-fold coordination with the Si-O unit's chemical shift occurring from -60 to -120 ppm. The degree of polymerization of C-S-H can be presented in terms of "Q_n" with Q as silicon bonded to four oxygen atoms and n=0 to 4 corresponding to the number of bonding oxygen, namely oxygen bonded to another forming atom (Si, Al, B, etc…).

Figure IV.49 provides the spectrum of the ^{29}Si environment in the anhydrous GGBS as well as the ^{29}Si MAS and ^{1}H-^{29}Si CPMAS spectra for the sodium carbonate activated slag with and without zinc addition.

The anhydrous GGBS sample presents a broad signal with a centre at around -75 ppm with an extension from -65 ppm to -90 ppm. It corresponds to the overlapping of Q^1(0Al), Q^2(0Al), and Q^2(1Al) units and is coherent with a depolymerized silicate structure. The spectrum of the AAS system presents the ^{29}Si signal of the residual unaltered GGBS but reveals also Q^1 and Q^2 chain units within the C-A-S-H phase with the predominance of Q^2 suggesting long polymerized silicate chains. On the other hand, 2%ZnAAS shows a completely different evolution, which can be clearly seen on

the spectrum obtained with the ^{1}H-^{29}Si CP-MAS experiment. After 1 month of hydration, the spectrum of 2%ZnAAS is still dominated by the signal of the unreacted slag, but a broad signal centred at around -93 ppm and ranging from -85 to -105 ppm corresponding to silicon in vicinity with proton is also observed (signal also observed by CP-MAS). The chemical shift range corresponds to more polymerized silicon species, namely Q^3 (0Al) or Q^4(mAl) units as reported by (C. Li et al., 2010). This signal could be attributed to a polymerized silicon gel on the surface of the GGBS grains in which a Zn-Si interaction may take place and act as passivation layer. This layer can explain the hindered formation of C-A-S-H. At the same time, it can be clearly seen from ^{29}Si MAS and ^{1}H-^{29}Si CPMAS experiments of 2%ZnAAS after 4 months of storage that the formation of C-A-S-H is then unblocked. (Qian et al., 2003) demonstrated in his study the same retardation effect of 2%$Zn(NO_3)_2$ after 28 days of storage for the AAS samples. He concluded in his study that the formation of the insoluble zinc silicate gel and calcium zincate retard the precipitation of C-S-H.

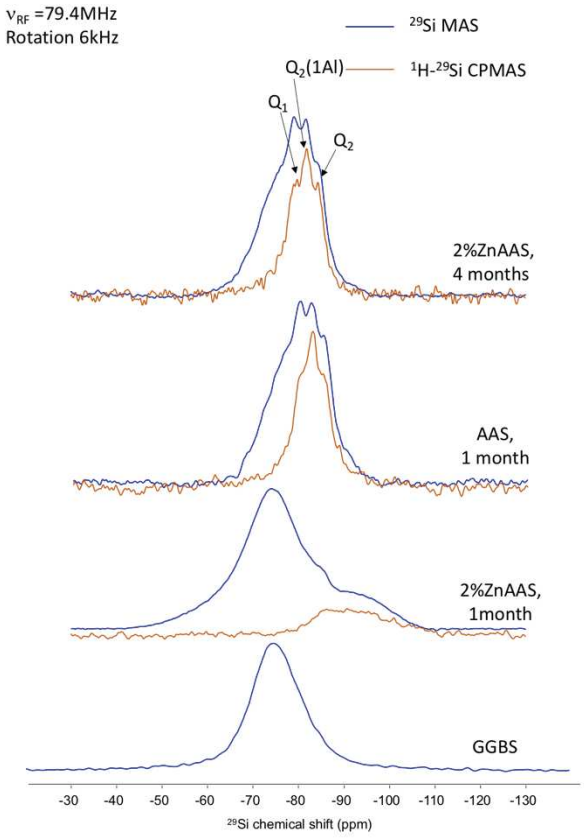

Fig. IV.49 ^{29}Si MAS and ^{1}H-^{29}Si CPMAS spectra of the anhydrous GGBS, AAS and 2%ZnAAS samples after 1 month and 4 months of storage

IV.3.5.2 Conclusions

The results of the ^{27}Al NMR study demonstrated the impact of Zn and Cd on the formation of hydration products of the OPC and GGBS-based formulations. However,

it was difficult to observe direct evidence of the effect of Zn or Cd on the Al environment within the C-A-S-H phase, except for the samples of sodium carbonate activated GGBS (in particular the retardation impact of zinc). ^{1}H-^{27}Al CP-MAS and ^{1}H-^{29}Si spectra were particularly useful to obtain further in-depth information on the mechanisms of the delayed C-S-H precipitation in the AAS system doped with zinc – the formation of a zinc silicate gel on the surface of GGBS grains seems to be detected on the spectra.

Bibliography

Achternbosch, M., Bräutigam, K. R., Hartlieb, N., Kupsch, C., Richers, U., Stemmermann, P., & Gleis, M. (2003). Heavy metals in cement and concrete resulting from the co-incineration of wastes in cement kilns with regard to the legitimacy of waste utilisation. https://doi.org/10.5445/IR/270055717

Andersen, M., Jakobsen, H., & Skibsted, J. (2006). A new Aluminium-Hydrate Species in Hydrated Portland Cements Characterized by 27Al and 29Si MAS NMR Spectroscopy. Cement and Concrete Research - CEM CONCR RES, 36, 3–17. https://doi.org/10.1016/j.cemconres.2005.04.010

Baldermann, A., Landler, A., Mittermayr, F., Letofsky-Papst, I., Steindl, F., Galan, I., & Dietzel, M. (2019). Removal of heavy metals (Co, Cr, and Zn) during calcium–aluminium–silicate–hydrate and trioctahedral smectite formation. Journal of Materials Science, 54(13), 9331–9351. https://doi.org/10.1007/s10853-019-03541-5

Bazzoni, A. (2014). Study of early hydration mechanisms of cement by means of electron microscopy. https://doi.org/10.5075/epfl-thesis-6296

Bazzoni, A., Ma, S., Wang, Q., Shen, X., Cantoni, M., & Scrivener, K. L. (2014). The Effect of Magnesium and Zinc Ions on the Hydration Kinetics of C3S. Journal of the American Ceramic Society, 97(11), 3684–3693. https://doi.org/10.1111/jace.13156

Cartledge, F. K., Butler, L. G., Chalasani, D., Eaton, H. C., Frey, F. P., Herrera, E., Tittlebaum, M. E., & Yang, S. L. (1990). Immobilization mechanisms in solidifiction/stabilization of cadmium and lead salts using portland cement fixing agents. Environmental Science & Technology, 24(6), 867–873. https://doi.org/10.1021/es00076a012

Chen, Q. Y., Hills, C. D., Tyrer, M., Slipper, I., Shen, H. G., & Brough, A. (2007). Characterisation of products of tricalcium silicate hydration in the presence of heavy metals. Journal of Hazardous Materials, 147(3), 817–825. https://doi.org/10.1016/j.jhazmat.2007.01.136

Chen, Q. Y., Tyrer, M., Hills, C. D., Yang, X. M., & Carey, P. (2009). Immobilisation of heavy metal in cement-based solidification/stabilisation: A review. Waste Management, 29(1), 390–403. https://doi.org/10.1016/j.wasman.2008.01.019

Deja, J. (2002). Immobilization of Cr6+, Cd2+, Zn2+ and Pb2+ in alkali-activated slag binders. Cement and Concrete Research, 32(12), 1971–1979. https://doi.org/10.1016/S0008-8846(02)00904-3

Dong, Y., Feng, C., Zhao, Q., & Liang, X. (2019). Study on the Structure of C-S-H Gels of Slag–Cement Hardened Paste by 29Si, 27Al MAS NMR. Applied Magnetic Resonance, 50(12), 1345–1357. https://doi.org/10.1007/s00723-019-01152-6

Fernández Olmo, I., Chacon, E., & Irabien, A. (2001). Influence of lead, zinc, iron (III) and chromium (III) oxides on the setting time and strength development of Portland cement. Cement and Concrete Research, 31(8), 1213–1219. https://doi.org/10.1016/S0008-8846(01)00545-2

Garg, N., & White, C. E. (2017). Mechanism of zinc oxide retardation in alkali-activated materials: An in situ X-ray pair distribution function investigation. Journal of Materials Chemistry A, 5(23), 11794–11804. https://doi.org/10.1039/C7TA00412E

Gineys, N., Aouad, G., & Damidot, D. (2010). Managing trace elements in Portland cement – Part I: Interactions between cement paste and heavy metals added during mixing as

soluble salts. Cement and Concrete Composites, 32(8), 563–570. https://doi.org/10.1016/j.cemconcomp.2010.06.002

Halim, C. E., Amal, R., Beydoun, D., Scott, J. A., & Low, G. (2004). Implications of the structure of cementitious wastes containing Pb(II), Cd(II), As(V), and Cr(VI) on the leaching of metals. Cement and Concrete Research, 34(7), 1093–1102. https://doi.org/10.1016/j.cemconres.2003.11.025

Hekal, E. E., Kishar, E. A., Mohamed, M. R., Mahmoud, M. K., & Mohamed, B. A. (2012). Inertization of lead by using blended cement pastes. HBRC Journal, 8(3), 153–158. https://doi.org/10.1016/j.hbrcj.2012.10.001

Hodson, M. (2004) Heavy metals—geochemical bogey men?, Environmental Pollution 129 (2004) 341–343

Hunter, R. J. (1992). Charge Reversal of Kaolinite by Hydrolyzable Metal Ions: An Electroacoustic Study. Clays and Clay Minerals, 40(6), 644–649. https://doi.org/10.1346/CCMN.1992.0400603

Komarneni, S., Breval, E., Roy, D. M., & Roy, R. (1988). Reactions of some calcium silicates with metal cations. Cement and Concrete Research, 18(2), 204–220. https://doi.org/10.1016/0008-8846(88)90005-1

Li, B., Zhang, S., Li, Q., Li, N., Yuan, B., Chen, W., Brouwers, H. J. H., & Yu, Q. (2019). Uptake of heavy metal ions in layered double hydroxides and applications in cementitious materials: Experimental evidence and first-principle study. Construction and Building Materials, 222, 96–107. https://doi.org/10.1016/j.conbuildmat.2019.06.135

Li, C., Sun, H., & Li, L. (2010). A review: The comparison between alkali-activated slag (Si+Ca) and metakaolin (Si+Al) cements. Cement and Concrete Research, 40(9), 1341–1349. https://doi.org/10.1016/j.cemconres.2010.03.020

Lowke, D., & Gehlen, C. (2015). Effect of Pore Solution Composition on Zeta Potential and Superplasticizer Adsorption. 12.

Lu, L., Xiang, C., He, Y., Wang, F., & Hu, S. (2017). Early hydration of C3S in the presence of Cd2+, Pb2+ and Cr3+ and the immobilization of heavy metals in pastes. Construction and Building Materials, 152, 923–932. https://doi.org/10.1016/j.conbuildmat.2017.07.026

Mahedi, M., Cetin, B., & Dayioglu, A. Y. (2019). Leaching behavior of aluminum, copper, iron and zinc from cement activated fly ash and slag stabilized soils. Waste Management, 95, 334–355. https://doi.org/10.1016/j.wasman.2019.06.018

McWhinney, H. G., & Cocke, D. L. (1993). A surface study of the chemistry of zinc, cadmium, and mercury in portland cement. Waste Management, 13(2), 117–123. https://doi.org/10.1016/0956-053X(93)90003-F

Neuville, D. R., Cormier, L., Montouillout, V., Florian, P., Millot, F., Rifflet, J.-C., & Massiot, D. (2008). Amorphous materials: Properties, structure, and durabilityStructure of Mg- and Mg/Ca aluminosilicate glasses: 27Al NMR and Raman spectroscopy investigations. American Mineralogist, 93(11–12), 1721–1731. https://doi.org/10.2138/am.2008.2867

Nicoleau, L., Schreiner, E., & Nonat, A. (2014). Ion-specific effects influencing the dissolution of tricalcium silicate. Cement and Concrete Research, 59, 118–138. https://doi.org/10.1016/j.cemconres.2014.02.006

P. Aïtcin and R. Flatt. (2016). Science and Technology of Concrete Admixtures. Elsevier. https://doi.org/10.1016/C2015-0-00150-2

Pomiès, M.-P., Lequeux, N., & Boch, P. (2001). Speciation of cadmium in cement Part I. Cd2+ uptake by C-S-H. Cement and Concrete Research, 7.

Qian, G., Sun, D. D., & Tay, J. H. (2003). Immobilization of mercury and zinc in an alkali-activated slag matrix. Journal of Hazardous Materials, 101(1), 65–77. https://doi.org/10.1016/S0304-3894(03)00143-2

Richardson, I. G., & Groves, G. W. (1997). The structure of the calcium silicate hydrate phases present in hardened pastes of white Portland cement/blast-furnace slag blends. 10.

Scheidegger, A. M., Wieland, E., Scheinost, A. C., Dähn, R., & Spieler, P. (2000). Spectroscopic Evidence for the Formation of Layered Ni–Al Double Hydroxides in Cement. Environmental Science & Technology, 34(21), 4545–4548. https://doi.org/10.1021/es0000798

Scrivener, K., Ouzia, A., Juilland, P., & Kunhi Mohamed, A. (2019). Advances in understanding cement hydration mechanisms. Cement and Concrete Research, 124, 105823. https://doi.org/10.1016/j.cemconres.2019.105823

Skibsted, J., Henderson, E., & Jakobsen, H. J. (1993). Characterization of calcium aluminate phases in cements by aluminum-27 MAS NMR spectroscopy. Inorganic Chemistry, 32(6), 1013–1027. https://doi.org/10.1021/ic00058a043

Tashiro, C., Oba, J., & Akama, K. (1979). The effects of several heavy metal oxides on the formation of ettringite and the microstructure of hardened ettringite. Cement and Concrete Research, 9(3), 303–308. https://doi.org/10.1016/0008-8846(79)90122-4

Taylor. (1997). TAYLOR (1997)—Cement-Chemistry—2nd Edition. Passei Direto. https://www.passeidireto.com/arquivo/18595148/taylor-1997-cement-chemistry-2nd-edition

Tumidajski, P. J., & Thomson, M. L. (1995). Influence of CdO on the early hydration of 3CaO.Al2O3. Cement and Concrete Research, 25(8), 1679–1690. https://doi.org/10.1016/0008-8846(95)00164-6

Vespa, M., Dähn, R., Grolimund, D., Wieland, E., & Scheidegger, A. M. (2006). Spectroscopic Investigation of Ni Speciation in Hardened Cement Paste. Environmental Science & Technology, 40(7), 2275–2282. https://doi.org/10.1021/es052240q

Viallis-Terrisse, H., Nonat, A., & Petit, J.-C. (2001). Zeta-Potential Study of Calcium Silicate Hydrates Interacting with Alkaline Cations. Journal of Colloid and Interface Science, 244(1), 58–65. https://doi.org/10.1006/jcis.2001.7897

Wang, S.-D., & Scrivener, K. L. (2003). 29Si and 27Al NMR study of alkali-activated slag. Cement and Concrete Research, 33(5), 769–774. https://doi.org/10.1016/S0008-8846(02)01044-X

Weeks, C., Hand, R. J., & Sharp, J. H. (2008). Retardation of cement hydration caused by heavy metals present in ISF slag used as aggregate. Cement and Concrete Composites, 30(10), 970–978. https://doi.org/10.1016/j.cemconcomp.2008.07.005

Yang, T., Zhang, Z., Zhang, F., Gao, Y., & Wu, Q. (2020). Chloride and heavy metal binding capacities of hydrotalcite-like phases formed in greener one-part sodium carbonate-activated slag cements. Journal of Cleaner Production, 253, 120047. https://doi.org/10.1016/j.jclepro.2020.120047

Yoon, H. N., Seo, J., Kim, S., Lee, H. K., & Park, S. (2020). Characterization of blast furnace slag-blended Portland cement for immobilization of Co. Cement and Concrete Research, 134, 106089. https://doi.org/10.1016/j.cemconres.2020.106089

Yukselen, Y., & Kaya, A. (2002). Zeta Potential of Kaolinite in the Presence of Alkali, Alkaline Earth and Hydrolyzable Metal Ions. 14.

Yukselen-Aksoy, Y., & Kaya, A. (2016). The Zeta Potential of a Mixed Mineral Clay in the Presence of Cations. 1(1), 8.

Chapter V. Stabilization of heavy metals using GGBS-based hydraulic binders

V.1 Introduction

The Solidification/Stabilization method for dredged sediments remediation can be very effective for the immobilization of inorganic contaminants. Its importance has increased over recent years due to prosperous results produced with this cost-effective technology and the increasing interest of researchers to use alternative cementitious materials. Ground granulated blast furnace slag can be a good binder option to enhance the mechanical and leaching performances of treated sediments. The results of the leaching tests conducted as part of the work presented in this chapter are promising for the use of GGBS. In order to gain an understanding of the efficiency of GGBS for the stabilization of heavy metals and demonstrate the benefits of using this binder, this chapter provides some explanations of the mechanisms involved in the process of reduced mobility of inorganic contaminants.

According to (Kabata-Pendias & Pendias, 2001), the most important properties of soils affecting the release and bioavailability of trace elements are: E_h (redox potential)-pH profile, CEC (cation exchange capacity), salinity, organic matter type and content, water, temperature, and microbiota and mezobiota activities. Each component of the sediment system can contribute to the accumulation of trace elements and reduce their mobility and toxicity for marine organisms. In order to characterize the heavy metal repartition using different extraction methods, sediments are usually fractioned according to the most important phases responsible for the bioavailability of HM: clays, organic matter, carbonates, sulfides, and oxides. Consequently, when environmental changes occur or some sort of disturbance of the system takes place (e.g. dredging of harbor sediments), the remobilization of contaminants may occur as a result of desorption or the chemical transformation of contaminants into more mobile and toxic forms (Eggleton & Thomas, 2004).

This work focused on the efficiency and the chemical impact of treating heavy metals contaminated port sediments with two different hydraulic binders: OPC and GGBS-based binders. The efficiency of the stabilization step was evaluated by the means of leaching tests performed on the raw form of the sediment and the treated material with binders after given curing periods. In the meantime, the impact on the chemistry of the pollutants was evaluated by means of sequential extraction and X-ray Adsorption Near-Edge Structure (XANES). The sequential extraction enabled, through the application of four selective dissolution steps, for the determination of which component/phase of the sediments were withholding a given heavy metal, whether before or after treatment with the binders. Eventually, XANES measurements indicated, for a limited number of pollutants, their initial chemical speciation within the sediment matrix and how that speciation evolved with the introduction of the different binders.

V.2 Batch leaching test

The leaching test was carried out on the range of samples at two storage periods (after 1 and 3 months) just after the compressive strength tests. Heavy metals such as As, Cd, Cr, Cu, Zn, Ni, Pb, and Hg were analyzed by the ICP-MS technique after the leaching procedure. The amount of the leached heavy metals was measured for the raw Dublin sediment as well as for the sediment treated with two types of binders – the reference condition (100% Portland cement) and GGBS-based binders.
The considered binder formulations for the leaching test were added at 150 kg/m^3 to the Dublin sediment (Table V.1.):

Table V.1. Composition of the binders used for the leaching test

	Composition
D1	100% OPC
D2	50%OPC+50%GGBS
D3	15%OPC+85%GGBS
D4	1%OPC+85%GGBS+14%Ca_2SO_4
D5	95%GGBS+5%Na_2CO_3
D6	95%GGBS+5%$MgSO_4$
D7	95%GGBS+5%MgO

It should be mentioned that certain formulations are only taken into account in this chapter concerning the stabilizing effect of GGBS for the immobilization of inorganic contaminants. The results of the compressive strength demonstrated that formulations D4, D5 and D6 did not provide the necessary strength as required by the Dublin port project. Good leaching performance is not sufficient for the future application of treated dredged material. The compressive strength must be taken into account to make an optimal choice of a binder. However, these formulations are part of a discussion in this chapter and can potentially be optimized to give the necessary strength.

V.2.1 Leaching test Results

The leaching test results are reported in Fig. V.1.
The leachability of the heavy metals from the non-treated sediment (D0) is rather low. This suggests that they should be present in rather stable compounds.
As can be seen, most of the considered heavy metals are efficiently immobilised with the addition of the binders, especially chromium, zinc, lead, and arsenic (except for D5). On the other hand, Cu and Ni are destabilized in the presence of the binders. It is apparent from the graph that a clear trend of decreasing leached heavy metals can be observed when the level of OPC substitution with GBBS increases. For example, the D1 formulation increased by approximately 13 times the amount of copper in the leachate solution after 28 days (389 μg/L) and almost doubled copper leaching

(697μg/L) after 3 months of storage whereas D3, with the highest GGBS replacement rate, slightly lowered copper leaching compared to D0.

Other types of GGBS activation have also effectively stabilized various types of heavy metals in the Dublin sediment. D4 and D6 were the most effective in copper stabilization. They significantly decreased (~10 times) the leaching of copper after 28 days of storage. However, D4 presents the same leaching level of Cu as the raw sediment at 3 months. The D6 formulation remains the most effective for the immobilization of copper after 3 months of storage. MgO activation (D7) demonstrated a low rate of leached copper (6.4 μg/L) at 28 days, however after 3 months of storage the copper detected in the leachate solution increased significantly (227 μg/L).

Turning now to the other heavy metals one by one, the value of nickel leached from the raw sediment was 20 times less than for the sediment treated with the pure OPC binder which presents the highest destabilization impact: 11.5 μg/L for D0 and 175 μg/L at 28 days for D1. D2 with an OPC:GGBS ratio of 1 was also proved to be ineffective at nickel stabilization with the value 10 times greater than nickel leached from the non-treated sediment. D3, with the highest GGBS replacement of Portland cement, and D7 demonstrated almost the same leaching performance with a nickel leaching value of 50 μg/L. The most effective formulations to immobilize nickel are D5 and D6. They decreased the leaching rate of nickel after 28 days and 3 months of storage. D4, the supersulfated mix, doubled the leaching of nickel.

Lead was effectively immobilized with all of the considered binders. The value of leaching from the raw sediment was 13.8 μg/L. The most instable metal in the Dublin sediment matrix is zinc. At the same time, zinc was well stabilized with all binders, especially after 3 months of storage. Cadmium and mercury were below the detection limit and were not destabilized in the presence of the binders. Chromium was effectively stabilised with almost all the binders at 28 days except for D5 and D7. Nevertheless, after 3 months of storage the leaching of chromium appeared for D3 and D7 and with the maximum occurring in D1.The amount of leached chromium in all cases is still less than was leached from the raw sediment.

Overall, the results reported in Fig. V.1 indicate that the supersulfated mixes (D4, D6) have the lowest destabilization effect, although they did not provide any strength (Fig. III.1). Taken together, these results suggest that there is a correlation between the effective stabilization of heavy metals and the increase in the amount of slag when replacing OPC. The dissolution of metal species is correlated and highly dependent upon the pH, therefore the next section is concerned with the pH of each binder.

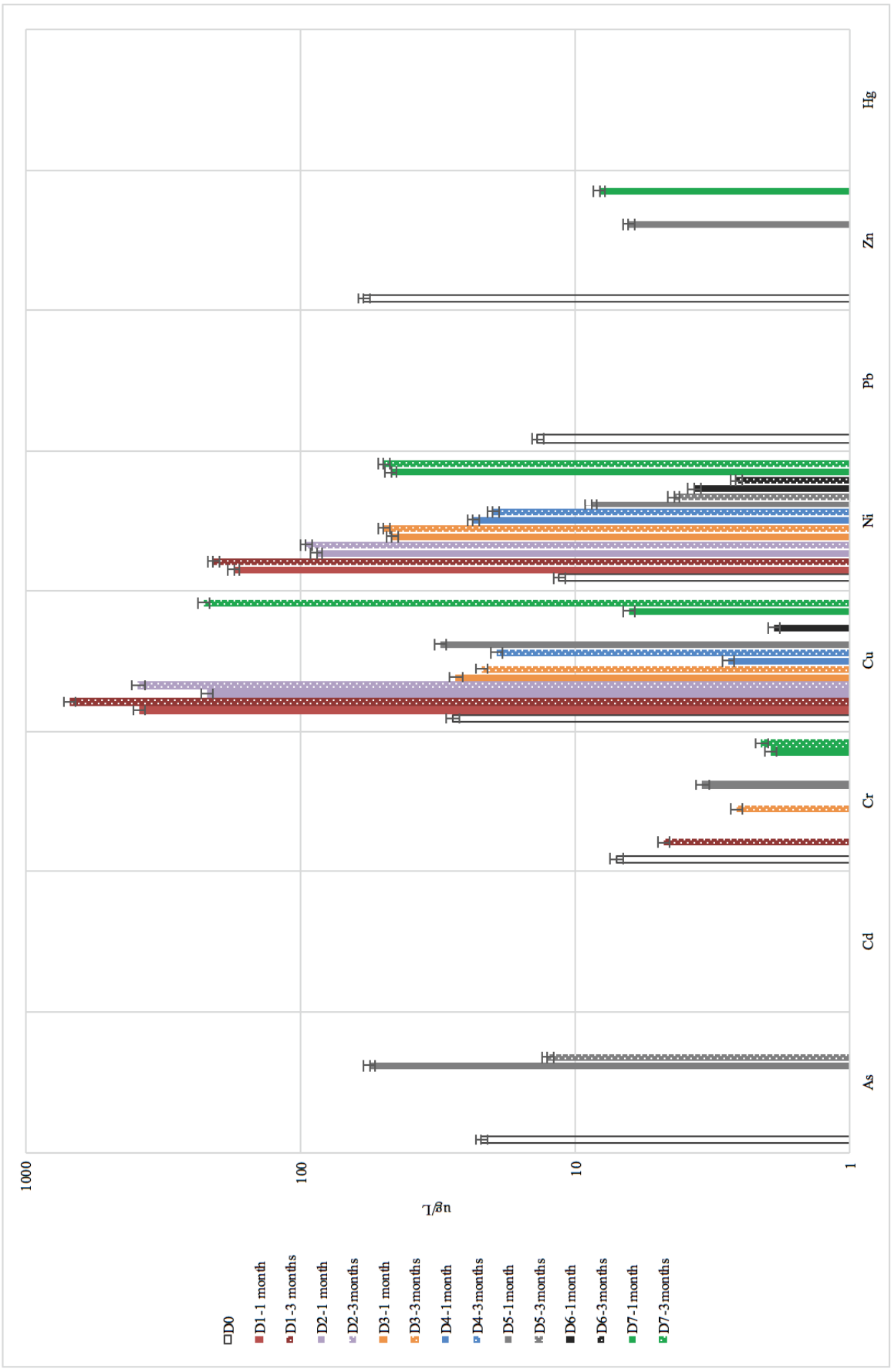

Fig. V.1. Leaching test results after 1 and 3 months of storage

V.2.2 pH measurements

The pH, as one of the main factors affecting the leaching behaviour of metals, was measured accurately at the end of each leaching procedure (Fig. V.2).

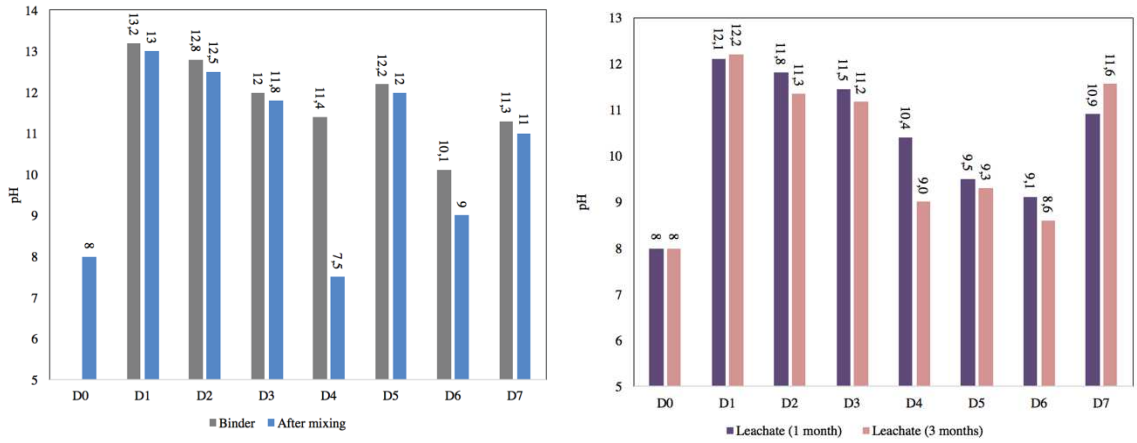

Fig. V.2 pH evolution of the binders-sediments mixtures: pure binders' pH and the sediment pH immediately after mixing with the binding agents (left); pH of leachates (right)

As was discussed in Chapter I (§ I.6.8.2) based on the literature review, most heavy metals are stable around neutral pH and can be highly destabilized in the strongly acidic or basic pH range. Fig. V.2 shows the trend of the pH decreasing with increasing amounts of GGBS depending on the type of the activation. The highest pH was obtained with the D1 formulation. The pH of the leachates of D1 were pretty similar after 1 and 3 months and was around 12.2. When the replacement rate of Portland cement with GGBS increases, the overall pH of the formulations decreases. This trend was already reported by many authors. (Eguchi et al., 2019) replaced OPC with GGBS with replacement rates from 50% to 90% and showed that the pH decreased progressively for GGBS pastes with the lowest value obtained with 90% GGBS. The composition of pore solutions in terms of ionic concentrations was reported by (Bertolini, 2014) for the different binders, mortars, and concrete and the lowest pH values were measured for blended cements. For example, the $[OH^-]$ concentration of 80%GGBS/20%OPC mortar paste was reported to be 170 mmol/L comparing to the OPC mortar with a $[OH^-]$ concentration of 391 mmol/L. The pH produced by D3 is around 12 for the binder paste and around 11.8 immediately after mixing with the Dublin sediment. Moreover, the leachate pH of D3 is about 11.5 after 1 month of storage and even lower after 3 months of storage, with a value of 11.2. As can be seen on the graph, the values of pH for the D2 samples with an OPC:GGBS ratio of 1 are situated between D1 and D3.

Finally, for D1, D2, and D3 the measured pH values are strongly correlated with the leaching rate of copper and nickel presented in Fig. V.1. The high pH of OPC destabilizes copper and nickel. The substitution of cement by GGBS makes it possible to decrease the pH and thus to decrease the destabilization of these metals in a

proportional way. The pH can be a primary explanation for the increased leaching of Cu and Ni metals in OPC environments.
The supersulfated activation also allows for a decrease in pH. The lowest pH was obtained with D4, which presents a pH around 11.4 and produces a pH of the sediment-binder mixture around 8. This may explain the highest stability and the lowest leaching rate of trace elements in the presence of this formulation. The pH of the D4 leaching solution increased to 10.4 at 1 month and then decreased to 9. A correlation between low pH with effective stabilization of metals can be also observed for D6, which is the most effective immobilizing agent among all the considered binders. The pH of the D6 binder's paste was around 10 decreasing to the value of 9 after interaction with the sediment matrix. The leachate's pH measurements gave values of around 9 after 1 month and 3 months of storage.
The carbonate activation of GGBS, denoted as D5, had a low pH of 9 following the leaching test. This decrease in pH over time can be explained by the lack of rapid hydration of the sediment-binder mixture and potential carbonation.
Finally, D7 demonstrated a paste pH of around 11.3 and 11 for the sediment-binder mix. The D7 leachate samples show a different trend compared to the other formulations; they exhibit an increase in pH between 1 and 3 months of storage. This increase corresponds to the hydration of GGBS and the appearance of mechanical strength. It can be supposed that this pH rise may potentially induce the leaching of some trace elements such as Cr, Ni, Zn, and Cu.
Taken together, these results suggest that there is an association between the pH produced during the hydration period of the treated sediment with the stabilizing agents and heavy metal stability. The next section provides experimental evidence of the pH-dependent leaching of HM from the Dublin sediment.

V.2.3 Impact of a strongly acidic and basic pH on the stability of HM in the Dublin sediment

In order to evaluate the impact of pH on the mobility of heavy metals species in the Dublin port sediment, the leaching test was performed according to the same procedure as on the raw sediment (NF EN 12457-2), however this time the initial pH of the leaching water was modified. Three types of leaching solution were used during the leaching procedure:

- Demineralized water;
- Acidic solution with 0.1M HCl (pH≈3);
- Highly alkaline solution prepared by using 1M of NaOH (pH=13.5).

The results of the leaching test after 24 hours of continuous rotation of the Dublin sediment sample with three different types of leaching water are presented in Fig. V.3.

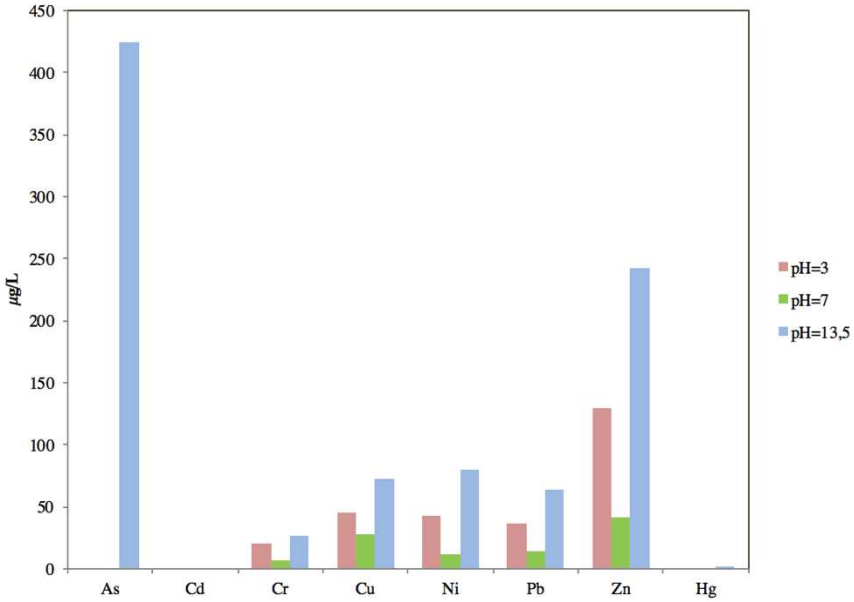

Fig. V.3 Impact of different leaching solutions on the stability of HM in the Dublin sediment

The data in this graph demonstrate evidence for the role of pH as one of the key parameters in controlling the mobility of trace elements. The lowest leaching rate was obtained with demineralized water as a leaching solution, confirming the relative stability of most heavy metals near neutral pH. Cr, Cu, Ni, Pb, and Zn exhibit similar overall trends – these metals are leached at all pH ranges with the minimum values at neutral pH and the maximum values at strongly alkaline pH. The use of the acidic solution for the leaching test increased the amount of leached metals by two to three times compared to the neutral pH.

The impact of the highly alkaline NaOH solution can be considered as the most aggressive medium with regard to the stability of heavy metals and can be correlated with certain leaching results for the sediment-binder mixtures presented in the previous section, in particular in the case of the mobility of copper and nickel. What stands out in the graph is the high rate of arsenic leaching when the highly basic solution was applied as a leaching water. It can be seen that the arsenic was not disturbed in the case of demineralized water and the acid leaching solution, but it was highly impacted by the NaOH solution. Finally, a small amount of mercury was leached into the highly alkaline medium despite the stability of this metal in the case of the introduction of the binders, when its amount was below the detection limit.

V.2.4 Discussion

The relative stability of heavy metals at neutral pH and increased mobilization of these metals at strongly acidic and basic pH reveal their amphoteric nature.

Numerous studies have reported a great impact of the pH factor in controlling the leaching behaviour of organic and inorganic species. (Mahedi et al., 2019) observe the minimum concentration of Al, Cu, and Zn near a neutral pH and an increasing

concentration in the range of acidic and basic pH. Thus, the authors provide a statement that the pH and the total concentration of metals play a crucial role in the stability of HM. Indeed, (Cetin et al., 2012) indicate in their study that Portland cement contributes to the increase in pH in the case of the activation of GGBS or fly ash and that it is responsible for the leaching of trace elements from the soil. The same correlation can be observed in the case of the Dublin sediment for the increased leaching of copper and nickel with an increase in the quantity of Portland cement. The high pH promotes the formation of metal hydroxides, carbonates, or hydrous oxides. The behaviour of metal amphoteric hydroxides can be determinative in the S/S system with high Portland cement ratio. Above a specific pH level with an excess of hydroxide ions in the interstitial solution, certain metal cations are transformed into complex anions. This can explain the beneficial use of GGBS, producing a pH lower than that of Portland cement.

V.2.4.1 Oxyanions metals

Arsenic and chromium detected in the Dublin sediment present a group of oxyanions. They are negatively charged species containing oxygen. These species vary depending on the pH and the redox potential of the environment. Examples of arsenic and chromium oxyanions are chromate, dichromate, arsenite, and arsenate (Bone et al., 2004). (Cornelis et al., 2008) indicate that the leached amount of oxyanion metals may be higher than in the case of cationic species due to their high solubility in alkaline waste.

In sediment pore water, arsenic occurs in two main soluble species (arsenite (AsO_3^{3-}) and arsenate (AsO_4^{3-})) in both oxic and anoxic environments (Smrzka et al., 2019). In sediments under sulfur-reducing conditions, arsenic has a strong affinity to interact with sulfides. The most abundant species are thioarsenites and thioarseniates as dissolved species or in solid Fe/As sulfides form (Wang et al., 2018).

It is known that As(III) is more mobile and toxic than As(V). (Paria & Yuet, 2006) reported in his review that oxidation of As(III) to As(V) is favourable to decrease the leaching of arsenic through the formation of more stable compounds to obtain effective precipitation with calcium or iron. Lime, cement, or pozzolanic material added to soils contaminated with arsenic may form Ca-As precipitates such as $Ca_3(AsO_4)_2$ or $CaHAsO_3$. The formation of these compounds may explain the stability of arsenic in all of the binders used for the Dublin sediment stabilization, except the carbonate activation (D5). At the same time, there is a possible explanation for the increased mobility of arsenic in the presence of carbonates. Oxyanions such arsenic may simply compete with other anions in the sediment-binder system such as carbonates (CO_3^{2-}), sulfates (SO_4^{2-}), and chlorides (Cl^-) as well as with high amounts of OH^-. It can be supposed that the sodium carbonate introduction to activate GGBS and the pH rise induced the desorption of arsenic oxyanions into the pore solution. The same effect can be observed in the case of NaOH solution with high OH^- concentration (Fig. V.3).

Another mechanism for immobilizing arsenic is the formation of ettringite in the pure cement systems or in GGBS/OPC. The incorporation of arsenates occurs through the replacement of sulfates in the ettringite structure (Fig. V.4).

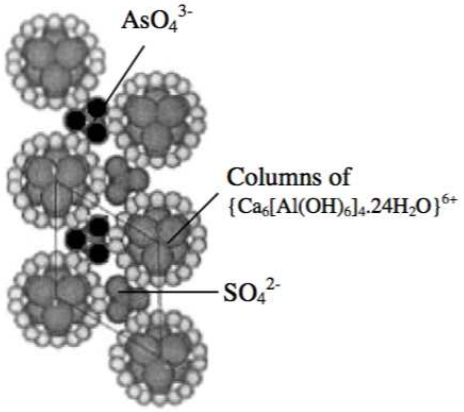

Fig. V.4 Arsenic incorporation in Ettringite (Myneni et al., 1997)

Hydrotalcite-like minerals ($Mg_6[Al(OH)_6]_2CO_3.4H_2O$) were demonstrated to be able to stabilize oxyanions such as arsenate (Doušová et al., 2003). They act like an adsorbent having a permanent positive charge. Hydrotalcite is one of the often-formed phases in GGBS-based binders.

Regarding chromium behaviour in solution, this metal also forms anionic species and is known to change its valence under different redox conditions. The most toxic and mobile is Cr^{6+} which appears in the form of the chromate oxyanion CrO_4^{2-} in the leaching solution of waste stabilized with Portland cement due to its low sorption to the cement phases (Achternbosch et al., 2003). The prior reduction in Solidification/Stabilization processes of Cr^{6+} to Cr^{3+} may be required because of the stability and low solubility of reduced species e.g. in the form of Cr(III) oxides or hydroxides at high pH. According to (Allan & Kukacka, 1995), GGBS-based binders provide a favourable reducing environment to transform Cr^{6+} to Cr^{3+} and ensure further stabilization of the chromium salts due to the formation of stable, inert, and highly insoluble Cr(III) complexes. (Cornelis et al., 2008) also reported the strong reduction capacities of GGBS and mentioned the possible low leaching of Cr(III) in GGBS environments in the form of $Cr(OH)_4^-$.

Numerous studies have attempted to explain the immobilization mechanisms of chromium wastes blended with hydraulic binders. Thereby, considering the high pH produced during the S/S process, the Cr(III) solubility is controlled by the stability of $Cr(OH)_3$. The replacement of Al^{3+} by Cr^{3+} can also be mentioned as a chemical incorporation mechanism (Glasser, 1997). (Stephan et al., 1999) demonstrated the formation of $Ca_4Al_6O_{12}CrO_4$ (valence +6) and $Ca_6Al_4Cr_2O_{15}$ (valence +3) at the beginning of C_3A hydration with the latter being a more stable compound. (Q. Y. Chen et al., 2007) demonstrated the formation of double hydroxides with calcium and Cr(III) in pure C_3S paste; $Ca_2Cr(OH)_7{\cdot}3H_2O$ was detected.

The incorporation of CrO_4^{2-} into the ettringite structure due to the substitution for SO_4^{2-} is known (Guo et al., 2017; Karamalidis & Voudrias, 2009). The mechanism is similar to arsenic incorporation as illustrated in Fig. V.4. However, the sulfatic ettringite is more stable and the reversible leaching of chromium oxyanions may occur. Therefore, the incorporation of oxyanions may be questionable in mixed systems compared to the pure paste systems due to the presence of chlorides, sulfates, and carbonates. (Cornelis et al., 2008) also reported the possible precipitation of Cr(III) hydrotalcite.
The results of the leaching test indicate the highest leaching rate for chromium for the pure OPC binder (D1) after 3 months of storage. The possible explanation may be the disappearance of ettringite over time as demonstrated by the XRD analysis (Fig. III.6). The leaching of chromium in the presence of the sulfatic formulation D4 is likely to be due to chromium oxyanions competing with sulfates.

V.2.4.2 Cationic heavy metals

Regarding the behaviour of trace elements in sediments and their sources in sedimentary pore waters, (Smrzka et al., 2019) combined cadmium, nickel, copper, and zinc in the group with similar pathways from organic and inorganic sediments phases. According to this review, Cu and Ni are strongly complexed by organic matter (Fig. V.5) in sediments or are adsorbed onto manganese oxides. Therefore, the disturbance of organic matter will induce the transport of copper (~90%) into the sediment pore water as a part of dissolved organic matter complexes. As stated by (Bruland, 1989) zinc, copper, nickel, and cadmium form strong complexes with DOC in marine sediments. Consequently, their leaching profiles may reflect some similarities in their behaviour.
Regarding the results of the leaching test for the Dublin sediment mixed with different binders, copper and nickel showed similar trends. The high leachability of these elements in the presence of the binders can be explained by their affinity to the organic matter. As was reported in Chapter III from the pyrolysis and ^{13}C NMR results, Portland cement induced a higher degradation level of the Dublin sediment organic matter compared to the GGBS-rich binder.
(Mckinley et al., 2001) observed the same trend in the leaching behaviour of copper and nickel in soils stabilized with the addition of hydrated lime. He reported an increased leaching level of Cu and Ni from the treated samples compared to the untreated samples. The measured high concentration of these elements is related to the presence of $Ca(OH)_2$ as a stabilizing agent and therefore with an increase in pH inducing the dissolution of organic matter. (Mckinley et al., 2001) also reported a high level of dissolved organic matter in the leachates after treatment and associated the Cu, Cd, and Ni high leaching levels with their complexation by DOM. (Hale et al., 2012) also established the relation of high copper leaching at high pH with the use of cement or $Ca(OH)_2$ in soils with significant organic matter content. The difficulties in the stabilization of copper were related to the high DOM concentration in the treated

samples (4 times higher than in the untreated samples) and with copper associated with DOM. Probably, there is place for the same mechanism of leaching to be produced in the case of the Portland cement treatment of the Dublin sediment regarding the high pH produced during the hydration process. The high pH is likely to attack the Dublin sediment organic matter, especially in the case of D1, D2 and D7 with the latter increasing over time.

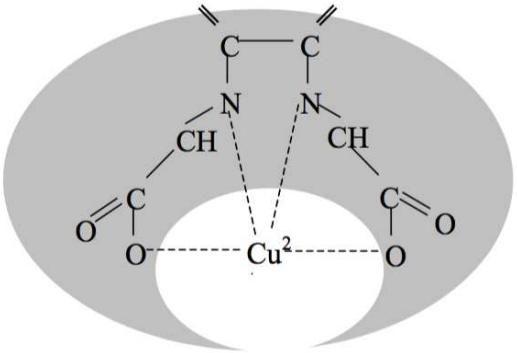

Fig. V.5 Complexation occurring between copper ion and organic substrate (after (Yong et al., 1992))

What is interesting about the leaching results of copper (Fig. V.1) is the good performance of D5 after 3 months of storage compared to the other formulations. Data from several studies suggest that copper in the alkaline medium in the presence of carbonates ions will react with carbonates to form $Cu_2CO_3(OH)_2$,known as malachite (Achternbosch et al., 2003). In the review by (Q. Y. Chen et al., 2009), the immobilization mechanism through precipitation of heavy metals as carbonates is also mentioned and in some cases is more favoured over hydroxides. In order to confirm the effectiveness of carbonates for copper stabilization, 2%wt of Na_2CO_3 was added to the D3 formulation and the leaching test was carried out after a few days of storage. As can be seen on the graph (Fig. V.6), copper was very effectively stabilized with the addition of sodium carbonate. However, further analysis of the precipitated phases and the long-term effectiveness of this mix should be carried out.

Previous research has established that in the pure cement systems copper will precipitate as $Cu(OH)_2$ during the early hydration period. Also reported in the literature was the formation of double hydroxides ($Ca_2(OH)_4.4Cu(OH)_2{\cdot}H_2O$) as was discussed in the previous chapter (Achternbosch et al., 2003; Q. Y. Chen et al., 2007). The incorporation of Cu^{2+} in C-S-H gel has been demonstrated. (Q. Y. Chen et al., 2007) reported the higher polymerization rate of copper and zinc doped C_3S samples compared to the samples without heavy metals after 1 year of storage. (Gineys et al., 2010) also supposes that copper and lead are trapped in the silica tetrahedral of the C-S-H gel during OPC hydration or by substituting Ca^{2+} in the C-S-H structure. The formation of CuO or $CuO.3H_2O$ can be also expected in pure cement systems (Roy & Cartledge, 1997). In the review of (Kogbara, 2014) OPC-GGBS mixes are shown to be

more effective for copper stabilization compared to the pure Portland cement systems or to OPC-PFA mixes.

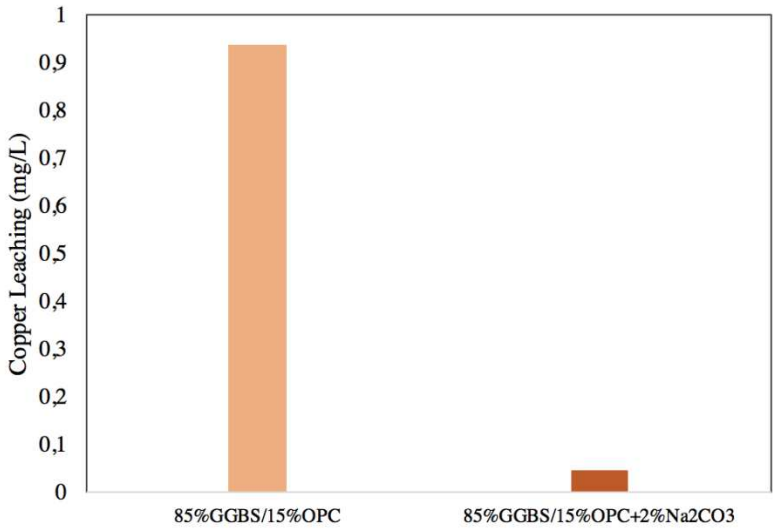

Fig. V.6 Carbonates effect on the copper stabilization. Leaching results

The results of the leaching test of zinc showed that it was effectively stabilized with all binders. Zinc in alkaline solution exists as $ZnO2^{2-}$ in dissolved form. The stability of this element in the highly alkaline pH range is ensured by zincite (ZnO) and $Zn(OH)_2$ formation controlling the leaching of zinc (Bone et al., 2004), (Mahedi et al., 2019). The formation of $ZnCO_3$ can also be expected under some specific conditions.
Data from several sources have identified the retardation effect of zinc on Portland cement hydration due to the formation of double hydroxides ($CaZn_2(OH)_6.2H_2O$) or calcium zincate, expected to be more stable than simple hydroxides (Q. Y. Chen et al., 2007; Gineys et al., 2010). (Gineys et al., 2010) observed mostly $Zn(OH)_2$ in the intergranular porosity of the OPC paste.
Zinc ions can be also embodied into the C-S-H structure. (Ziegler et al., 2001) provided results indicating the immobilization of Zn in the amorphous C-S-H structure in the interlayer region or adsorption in the form of hemimorphite ($Zn_4Si_2O_7(OH)_2 \cdot H_2O$) or γ-$Zn(OH)_2$ onto C-S-H. The substitution of Ca^{2+} by Zn^{2+} may also occur during AFt, AFm, and C-S-H formation. Resuming the possible ways of zinc stabilization, it can be supposed that this metal can be effectively stabilized within hydrates in the Dublin sediment-hydraulic binder mixes with increasing age of treated material.

One of the highly disturbed heavy metals in the presence of almost all types of the considered binders is nickel. It exists in dissolved form as Ni^{2+} at neutral pH and becomes $HNiO^{2-}$ in highly alkaline media. The leachability of nickel in the presence of binders is governed by the precipitation of $Ni(OH)_2$ with relative stability over the pH range of 9-11. Therefore, the decrease in pH with the substitution of Portland cement with GGBS may be the reason for the reduced leaching of nickel. Furthermore, as was

indicated in the case of Cu, the affinity of nickel to the organic matter in the Dublin sediment may also explain the highest leaching of Ni in the presence of the OPC binder.

Nickel and cadmium hydroxides may also become physically encapsulated in the C-S-H gel (Q. Y. Chen et al., 2009). At the same time, one of the largely discussed potential immobilization mechanisms of Ni in cement systems is the precipitation of Ni-Al LDH (Scheidegger et al., 2000; Vespa et al., 2006). The minor metastable compounds which can be formed in the presence of carbonates is $NiCO_3$.

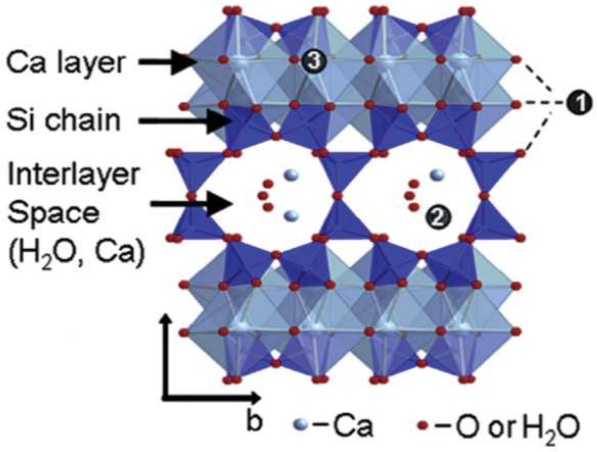

Fig. V.7 The approximate structure of C-S-H and the potential positions occupied by heavy metals (Vespa et al., 2014)

Another toxic element which has been effectively stabilized with all binders is lead, despite its amphoteric behaviour resulting in a high leaching rate when the NaOH solution was applied as a leaching solution to the Dublin sediment. The complexation of lead with organic matter may take place in sediments, with carbon-lead covalent bonding (Bone et al., 2004). The adsorption of Pb on kaolinite and illite clays is known (Yong et al., 1992). The successive stabilization of lead contaminated kaolin soils was reported using a GGBS/MgO binder with the formation of hydrocerussite ($Pb_2(CO_3)_2(OH)_2$) (Wu et al., 2018).

The most likely precipitates controlling Pb solubility in the early ages after the cement treatment is $Pb(OH)_2$ (Hale et al., 2012). However, soluble plumbite species may occur when the pH increases above12, which are highly mobile (PbO_2H^-). It can be supposed that this species occurred during the leaching test with the NaOH solution. The precipitation of carbonate or sulfate salts with Pb can take place at lower pH (<11) (Cocke et al., 1989). The occurrence of Pb mixed salts in OPC binders was mentioned as a retarding mechanism for mechanical strength development (Cartledge et al., 1990).

Table. V.2 Reported ion substitution in Ettringite (Q. Y. Chen et al., 2009)

Ca^{2+} site	Al^{3+} site	SO_4^{2-} site
Sr^{2+}	Cr^{3+}	CO_3^{2-}
Ba^{2+}	Si^{4+}	Cl^-
Pb^{2+}	Fe^{3+}	OH^-
Cd^{2+}	Mn^{3+}	CrO_4^{2-}
Co^{2+}	Ni^{3+}	AsO_4^{3-}
Ni^{2+}	Co^{3+}	NO_3^-
Zn^{2+}	Ti^{3+}	SO_3^{2-}

The prevalence of sorption processes over the substitution of heavy metals for Ca due to the formation of C-S-H in cement systems has been discussed in the literature (Park & Batchelor, 1999). However, (Gineys et al., 2010) discusses the possibility of substitution of calcium ions by lead in cement hydrates due to their similar ionic size. The lead silicate Pb_2SiO_4 was identified when fly ash treatment was applied to the contaminated soils (Moon & Dermatas, 2006). The pozzolanic reaction produced over the hydration period of the binder-soil mixes favouring Pb silicate precipitation with Si-O-Pb bonds is considered in several studies (Moulin et al., 1999). (Lasheras-Zubiate et al., 2012) indicated the precipitation of different types of silicates – plumalsite ($Pb_4Al_2(SiO_3)_7$), $Pb_2SiO_4.xH_2O$, and alamosite ($PbSiO_3$).

The leaching results showed that the amount of leached cadmium is situated below the detection limit. Cadmium demonstrates an amphoteric geochemical behaviour and can be leached as CdO_2^{2-} in highly alkaline environments with a pH greater than 12.5. Several studies investigated the formation of $Cd(OH)_2$. The precipitation of this compound is accompanied by a drop in pH at the early hydration stage (Malviya & Chaudhary, 2006). (J. Zhang et al., 2008) also demonstrated in his study that the solubility of cadmium is controlled by Cd hydroxide compounds in geopolymeric binders. The formation of cadmium carbonates ($CdCO_3$) can also be expected to occur during cement treatment. (Halim et al., 2004) observed the presence of both $Cd(OH)_2$ and $CdCO_3$ as discrete particles within the cement system. A number of studies reported the precipitation of otavite ($CdCO_3$) which controls the leaching of Cd when the pH of the treated matrix goes down (Y. Zhang et al., 2016), (Achternbosch et al., 2003). The formation of Cd hydroxyl-species which have a negative impact on the hydration of binders was also discussed in the literature (Weeks et al., 2008). The reactions require the consumption of calcium, hydroxide ions, and heavy metals to produce complex salts ($CaCd(OH)_4$). This reaction retards C-S-H nucleation by consuming calcium ions. The incorporation of cadmium into C-S-H gel is more likely to be due to the physical encapsulation. At the same time, the formation of $CaCd_2(OH)_4$ on the C-S-H surface was mentioned by (Yousuf et al., 1995).

In view of all that has been mentioned so far, one may conclude that the GGBS-based binders introduced into the Dublin sediment demonstrated better stabilization capacities for HM. However, the leaching results provide no information to explain the

mechanisms of such behaviour of the GGBS-based systems. Therefore, in the following sections XAS and sequential extraction approaches have been employed to deliver a more in-depth understanding of the stabilization process of the Dublin sediment.

V.3 XAS Investigations

V.3.1 Speciation of Zn and Cu in the raw Dublin sediment and the sediment mixed with the binders

XAS (X-ray Absorption Spectroscopy) as an element-specific and highly sensitive Synchrotron-based technique was applied to the raw sediment and the sediment treated with three different types of binding agents. The selected formulations are D1, D3, and D4. Very little was found in the literature on the question of changes in speciation of heavy metals after the introduction of hydraulic binders in hazardous waste systems. The present experiment was designed to determine the effect of the binders on Cu and Zn speciation in the Dublin sediment matrix. Sediment-binder samples aged for three months were considered.

V.3.1.1 Zinc speciation

Only three samples are considered for Zn: raw sediment (D0), Portland cement blended sediment (D1), and 85%GGBS/15%OPC blended sediment (D3). The XAS signals of the samples are compared in Fig. V.8.

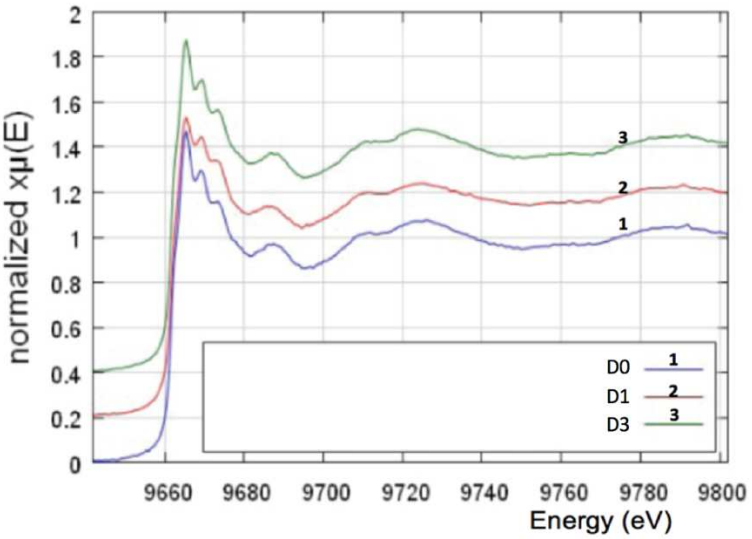

Fig. V.8 XAS spectra of the three different samples considered

The EXAFS part of the XAS signal is identical for the 3 samples considered. This indicates that the short-range atomic environment of Zn within the three samples is the same. The relatively high amplitude of the EXAFS oscillations indicates that the structure is crystalline (at least at short range (4- 5 atoms)). One may be tempted to use X-ray diffraction to characterize this structure. However, this would be a difficult task due to the very low content of this Zn-based phase. XRD is much less sensitive than XAS, which is element specific.

The XANES of the sediment and D3 are identical. This indicates that there is no modification of the chemical environment of Zn in the presence of the high content GGBS binder. In the D1, the Zn K-edge XANES is only slightly modified, but this suggests an actual change of the chemical environment of Zn when the sediment is embedded in this binder. Indeed, the ratio between the first peak corresponding to the white line and the second peak is smaller compared to the case of the two other samples.

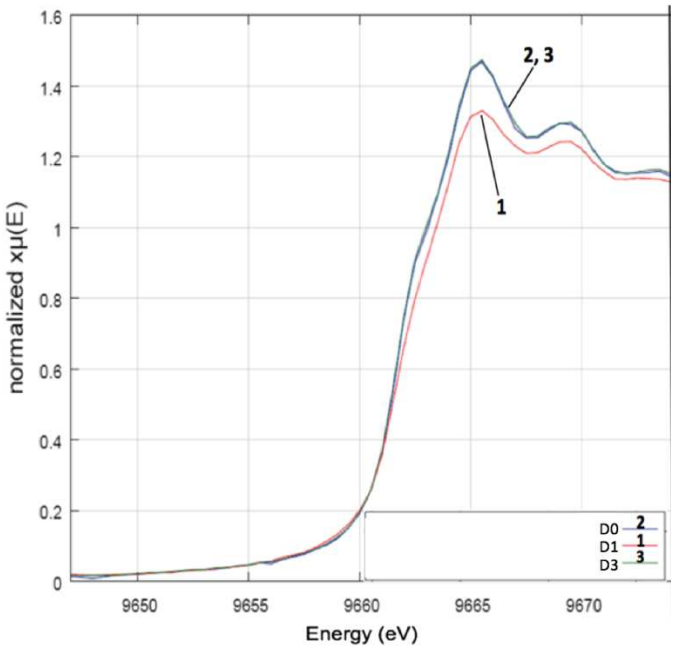

Fig. V.9 Zn K-edge XANES spectra of the samples considered

By qualitatively comparing the XAS results shown here with those of reference compounds reported in the literature (Lützenkirchen-Hecht et al., 2014), it can be concluded that the Zn in these samples is not in oxide, nor hydroxide, nor sulfide form, as one may expect since these compounds are highly stable.
In Fig. V.9 the XANES part of the three samples are reported. These results are very similar to those of zinc chromate spinels at different Zn/Cr molar ratios and annealing temperatures reported in (Tian et al., 2015). Note that the XANES of the sediment and that of the sediment embedded in the GGBS binder are indistinguishable from each

other. The signals are very similar, suggesting that Zn in the sediments are very likely to be mainly in zinc chromate form.
The pre-edge shoulder corresponds to the transition 1S→3d. The shoulder almost disappears in the presence of Portland cement. This suggests a transition from tetrahedral to octahedral coordination type of Zn (Tian et al., 2015). The presence of Portland cement also impacts the pro-edge features similar to the value of the Zn/Cr molar ratio.
The probable presence of Zn-chromate in the sediment may explain the high level of chromium found in the sediment as determined with XRF. Zn-chromate has been largely used as primer in boat paints. This compound is highly stable and may accumulate over time in port sediments.

V.3.1.2 Copper speciation

The figure below (Fig. V.10) represents the K-edge XANES spectra of Cu in four different samples: plain sediment (D0), sediment blended with Portland cement (D1), sediment blended with 85%GGBS/15%OPC (D3) and a sediment blended with a supersulfated binder (D4).
It can be noted that the chemical environment of Cu is not modified when the sediment is embedded in the GGBS-based binder. On the other hand, there is a significant change of the speciation of Cu in the presence of Portland cement.

Fig. V.11 shows the XANES spectra of typical Cu-compound references (data kindly supplied by Søren Kristiansen from Aarhus University, Denmark). The available reference data do not match the whole XANES spectra. However, based on these references it can be supposed the precipitation of $CuSO_4$ in the case of OPC-based treatment. The closest XANES reference signals for the other samples can be found in (Kumar et al., 2013). The XANES signal of the supersulfated sample is very close to that of cuprous sulfide (Cu_2S) (Kumar et al., 2013). The XANES of the sediment and the 85%GGBS/15%OPC blended sediment may be a combination of those of cuprous sulfide and cupric sulfide (CuS).

At first glance the presence of these sulfide compounds is rather intriguing. Yet a possible explanation may be put forward. Indeed, copper sulfate was widely used as an antifouling agent in boat paints for a long time. Under anaerobic conditions the eventual presence of sulfate-reducing bacteria (SRB), which breath sulfates reducing them to sulfides, may actually lead to the transformation of cupper sulfates to cuprous (or cupric) sulfides. This phenomenon should take place in a similar manner as reported in (S. Chen et al., 2014) regarding the issue of corrosion of copper in seawater due to SRB, leading to the formation of a biofilm, which is mainly composed of cuprous sulfide.

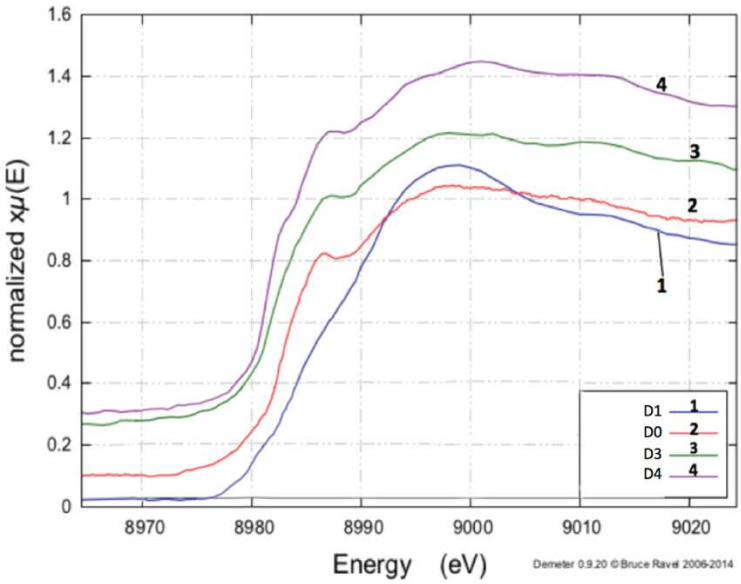

Fig. V.10 Cu K-edge XANES spectra in the different samples considered

Regarding the mainly reducing environment providing by GGBS-based binders, the sulfide compounds remain stable when embedded in GGBS binders during Solidification/Stabilization treatment. At the same time, Portland cement probably significantly changes the redox potential of the sediment matrix increasing the mobility of Cu; it is known that inorganic sulfurs may undergo oxidation during S/S treatment. Further measurements are required to provide more information about the chemical speciation of the heavy metals in the sediment matrix and to evaluate the changes implemented due to the reactions produced over the hydration period of the binders within the sediment system.

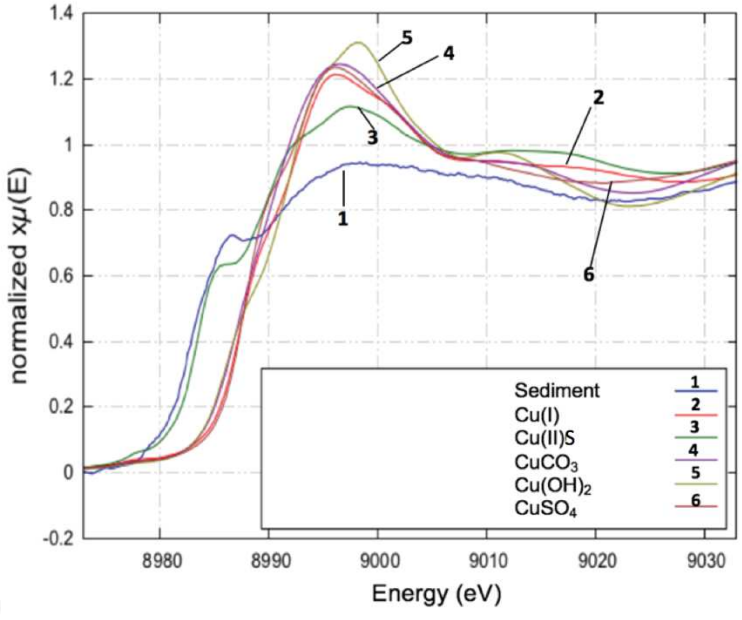

Fig. V.11 Cu K-edge XANES spectra of various Cu-compound references

V.3.2 Speciation of Ni and Cd in the binders

This time in order to simplify the polluted sediment-binding agent systems, XAFS experiments were conducted on the pure hydrated binders mixed with cadmium and nickel chloride salts. This permitted avoiding interaction with sediment constituents or with other types of heavy metals. The investigation of Ni and Cd speciation was carried out for OPC and GGBS-based binders.
Three hydraulic binders were considered: Portland cement (OPC), blended cement with 50% of Ground Granulated Blast-Furnace Slag and 50% of Portland cement (GGBS50), and the Supersulfated cement with 85% of GGBS, 14% of sulfates ($CaSO_4$) and 1% of Ordinary Portland cement (SSC). In these pastes metal salt concentrations of anhydrous cadmium $CdCl_2$ and nickel $NiCl_2$ were added separately at 0.5% (Table V.3). The metal salts were dissolved in demineralized water before being mixed with the binders.

Table V.3 Samples prepared for the zinc impact investigation

	0.5%wt $CdCl_2$	**0.5%wt $NiCl_2$**
100%OPC	0.5%CdOPC	0.5%NiOPC
50%GGBS/50%OPC	0.5%CdGGBS50	0.5%NiGGBS50
85%GGBS/14%Ca_2SO_4/1%OPC	0.5%CdSSC	0.5%NiSSC

V.3.2.1 Cadmium speciation

K-edge XANES spectra for cadmium added to the different hydraulic binders containing 0.5% $CdCl_2$ are presented in Fig. V.12. It can be found from the results that cadmium is expected to be present solely in the (II) oxidation state in the studied binders. The spectra differ from each other due to differences in coordination geometry and ligand forms of the absorber atom. The presence of GGBS leads to the decrease in the amplitude of the XANES oscillations. The K-edge XANES spectra of cadmium for individual cadmium compounds and the studied matrixes 0.5%CdOPC, 0.5%CdGGBS50 and 0.5%CdSSC are given in Fig. V.13, Fig. V.14, and Fig. V.15 respectively. The spectrum for 0.5%CdOPC is quite consistent with that of $Cd(OH)_2$ whereas the spectra for the matrixes with GGBS are quite similar to that of CdS. Moreover, the similarity with the CdS spectrum increases with the GGBS content.

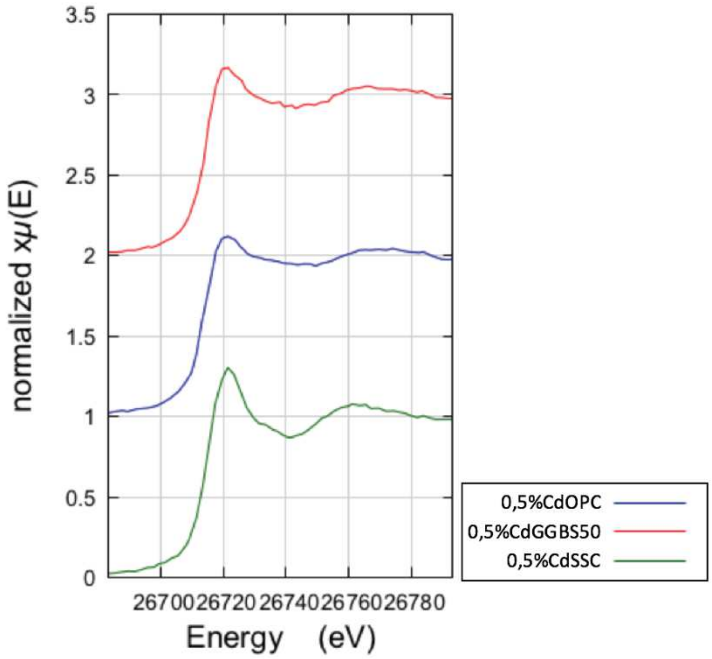

Fig. V.12 Average XANES spectra for cadmium in hydraulic binders

Based on these first observations, it seems that the main species of cadmium is $Cd(OH)_2$ in the hydrated Portland cement and CdS in the hydrated matrix containing a high GGBS content. This difference in behaviour is partially linked to the initial sulfur content of the anhydrous compounds and the pH of the interstitial solution. Indeed, cadmium hydroxide forms at high pH. As already mentioned, cadmium in cementitious materials is also present in other forms such as CdO and $CdCO_3$. Indeed, cadmium is rarely present as a single compound, it often has more than one phase.

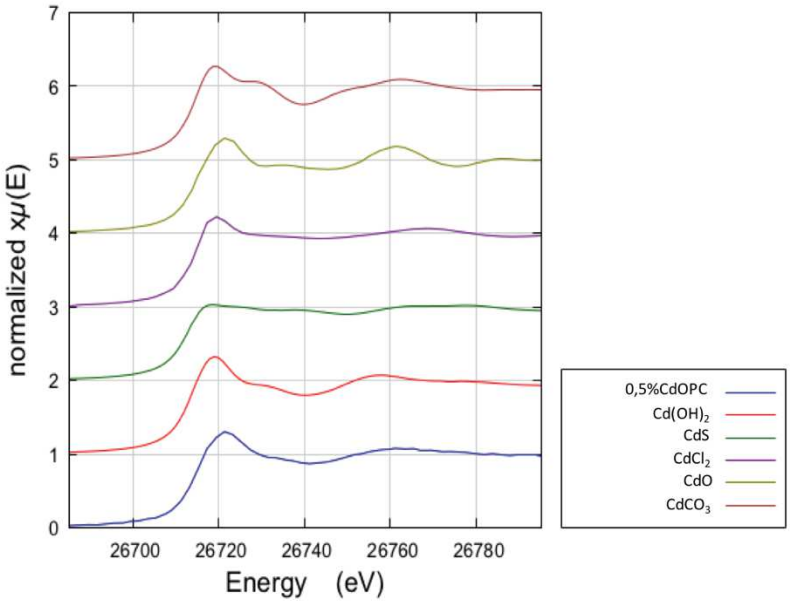

Fig. V.13 XANES spectra for cadmium in OPC and individual compounds

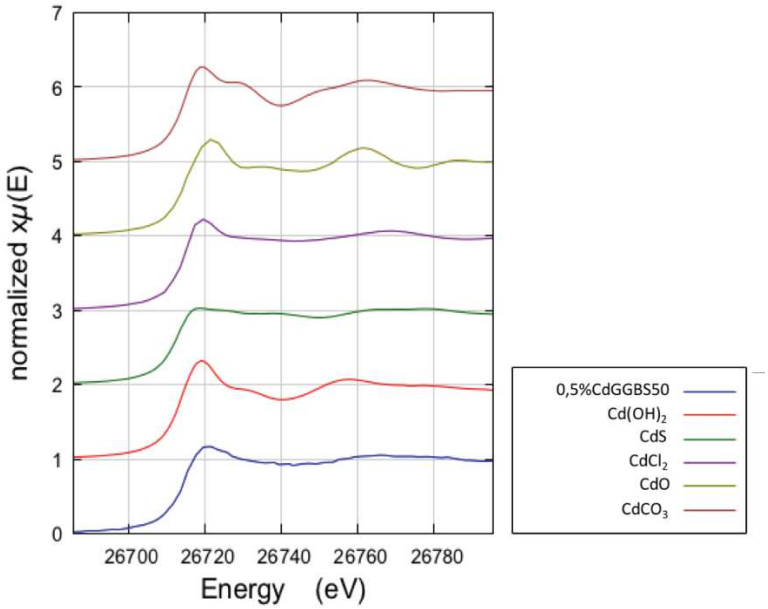

Fig. V.14 XANES spectra for cadmium in GGBS50 and individual compounds

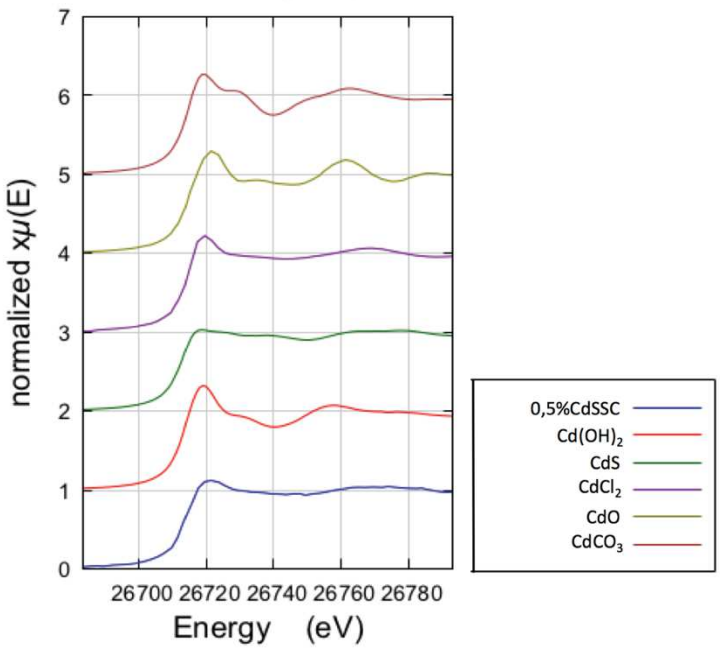

Fig. V.15 XANES spectra for cadmium in SSC and individual compounds

The type and the proportion of cadmium species in the cementitious matrix are determined by means of the EXAFS signal fingerprints of individual cadmium compounds based on the k²-weighted EXAFS functions (Fig. V.16). These results confirm the previous observations. The main compounds are $Cd(OH)_2$ for 0.5%CdOPC and CdS for 0.5%CdGGBS50 and 0.5%CdSSC. The large content of CdS is also confirmed by the sample colour (yellowish colour) as observed by (McWhinney & Cocke, 1993), (Fig. V.17). It is from these observations that the sulfur from the blast-

furnace slag can be presumed to react principally with cadmium. The added cadmium salt ($CdCl_2$) is the second product present in the studied binders. In spite of the care taken to avoid carbonation, $CdCO_3$ is the third compound identified for 0.5%CdOPC and 0.5%CdSSC. This is in agreement with (McWhinney & Cocke, 1993) which found an increase in the surface carbonate formation in the metal-ion doped cement. This may be due to the presence of cations directly or indirectly inducing the formation of greater quantities of surface carbonate species. A small content of CdS has already been detected in 0.5%CdOPC as well as a small amount of $Cd(OH)_2$ in 0.5%CdGGBS50 and 0.5%CdSSC. Finally, the compound identified in the lowest amount is CdO for 0.5%CdOPC and 0.5%CdGGBS50. It is not detected in 0.5%CdSSC. These results show that the addition of cadmium salt during the hydration process of cementitious matrices allows for the formation of new precipitates.
In order to examine the cadmium immobilization in three binder systems, the leaching tests were performed on the cementitious matrices with 0.5% of $CdCl_2$.

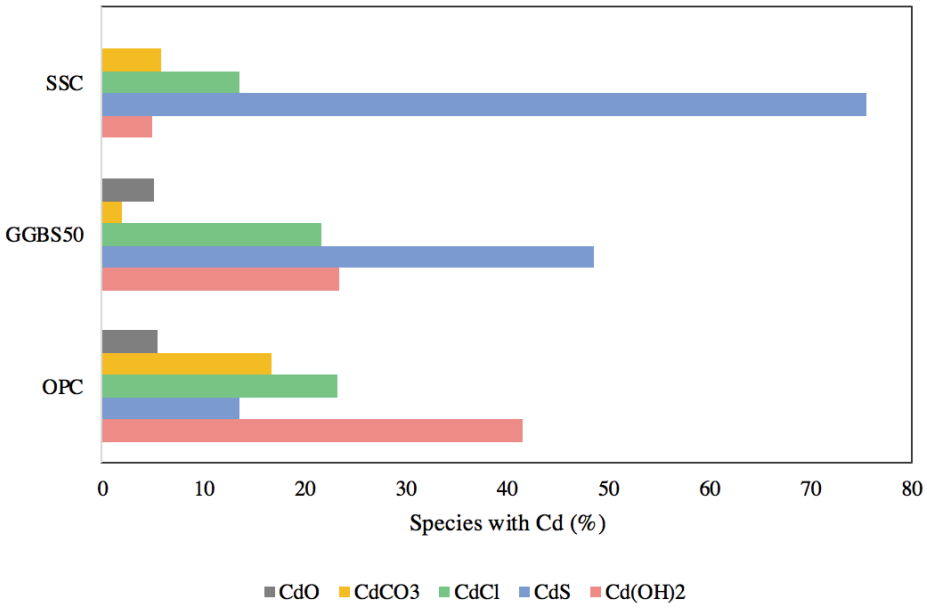

Fig. V.16 Proportion of cadmium species determined from k²-weighted EXAFS signal

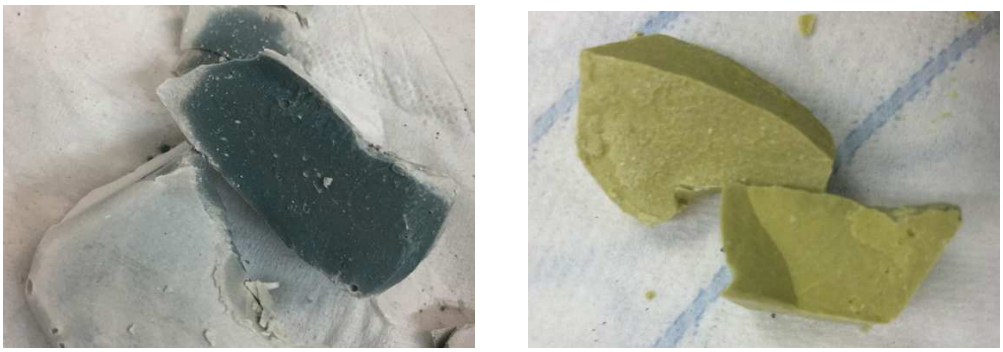

Fig. V.17 Difference in colour for SSC (left) and 0,5%CdSSC (right) after 7 days of storage

V.3.2.2 Cadmium Leaching

Figure V.18 presents the leached cadmium content for the three studied mixtures after 24 hours. The values are 8.41 μg/L, 2.6 μg/L and 0.16 μg/L for 0.5%CdOPC, 0.5%CdGGBS50 and 0.5%CdSSC respectively. For all mixtures, the cadmium leaching is low. This can be partially explained by the cadmium speciation as $Cd(OH)_2$ and CdS have low solubility. However, the addition of blast-furnace slag improves the cadmium immobilization capacity and this increases with the blast-furnace slag content. The benefit of GGBS can be explained by its larger content of C-S-H allowing a physical immobilization by cadmium sorption on its surface area (Gougar et al., 1996) and by the lower pH of its interstitial solution. Indeed, (Kogbara & Al-Tabbaa, 2011) found that the cadmium leaching is lower for a pH value between 10.8 and 12.2. The very low value of leached cadmium content for 0.5%CdSSC can be related to its lower pH and to the formation of a supplementary hydration product (ettringite) favourable to fix heavy metals (Peysson et al., 2005), (Berardi et al., 1998). Indeed, a cationic substitution can occur with Ca^{2+} in the crystal lattice (Albino et al., 1996). These results are also in agreement with other studies (Peysson et al., 2005) showing that calcium sulfoaluminate cement containing phosphogypsum (20-30%) has a good cadmium retention capacity.

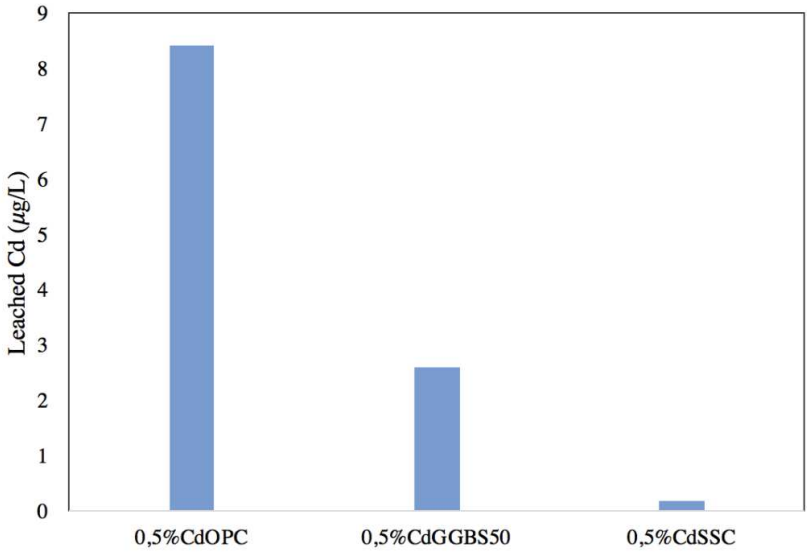

Fig. V.18 Content of leached cadmium after 28 days of storage

V.3.2.3 Nickel speciation and leaching results

The investigation of nickel speciation and its local chemical environment was determined using the same technique and procedure as for cadmium. Figure V.20 exhibits K-edge XANES spectra of Ni in the three binding systems: 0.5%NiOPC, 0.5%NiGGBS85, and 0.5%NiSSC. From the spectra of the formation of Ni-Al Layered Double Hydroxides phase can be detected. Nickel is also present as a minor

compound as $Ni(OH)_2$ as can be seen in the EXAFS region spectra of the plain Portland cement formulation and with 50% substitution by GGBS (Fig. V.20). However, this compound is not present in the Supersulfated formulation doped with nickel, which contains only the Ni-Al LDH phase. It can be concluded from the results that Ni-Al LDH is the main controlling phase of nickel immobilization in the cement systems for all considered formulations. Moreover, the results are in agreement with (Scheidegger et al., 2000; Vespa et al., 2006) who studied the hydrated cement system in the presence of Ni. (Vespa et al., 2006) highlighted the importance of Al availability from the beginning of the hydration process and observed the formation of Ni Al-LDH from the first hours of hydration.

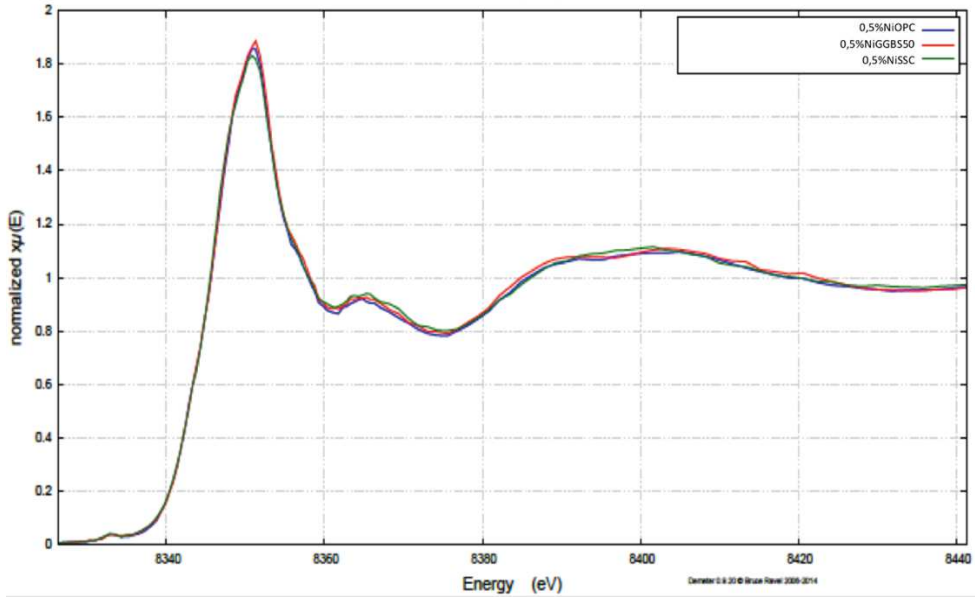

Fig. V.19 K-edge XANES spectra of 0,5%NiOPC, 0,5%NiGGBS85 and 0,5%NiSSC

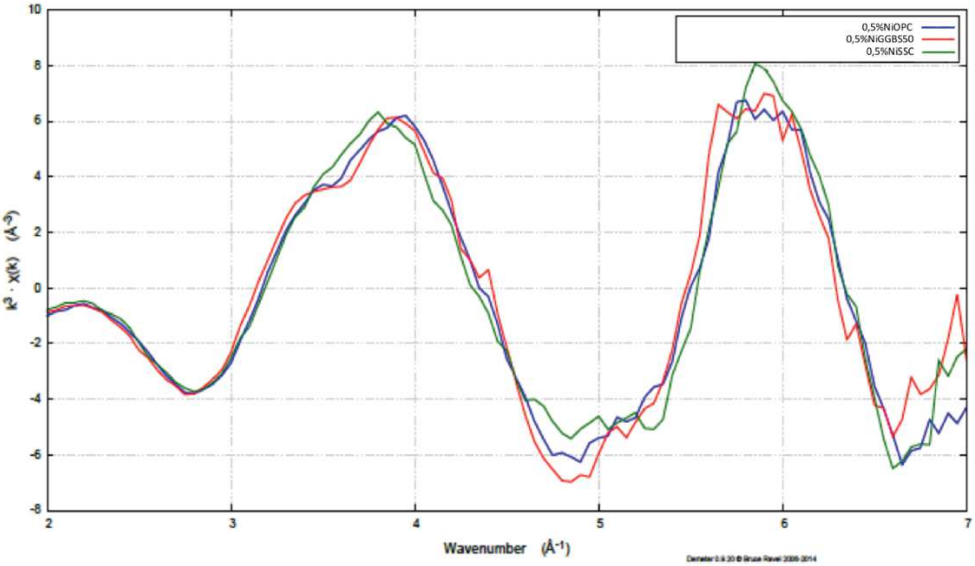

Fig. V.20 K-edge XANES spectra of 0,5%NiOPC, 0,5%NiGGBS85 and 0,5%NiSSC

The leaching test was carried out after 28 days of storage for the 0.5%NiOPC, 0.5%NiGGBS85 and 0.5%NiSSC formulations doped with 0.5% $NiCl_2$ (Fig.V.21). The highest leaching rate of nickel was measured for the Portland cement formulation. With replacement of 50%OPC by GGBS the amount of leached nickel decreased significantly to the very low value of 0.01μg/L. The Supersulfated formulation provides the highest nickel immobilization rate with nickel amount below the detection limit.
As was discussed previously, the availability of nickel is governed partially by the solubility of $Ni(OH)_2$. Thus it can be supposed that in the case of 100% Portland cement, the nickel hydroxide species will solubilize due to the high pH produced within this formulation. The low nickel leaching with 50% GGBS can be explained by the lower pH of this mixture. It can be also expected that the highest amount of Ni-Al LDH formation will occur due to the higher amount of aluminum available over the hydration period. The Supersulfated formulation gives the lowest pH and it appears that Ni remains stable within the Ni-Al LDH phase in GGBS-based systems.

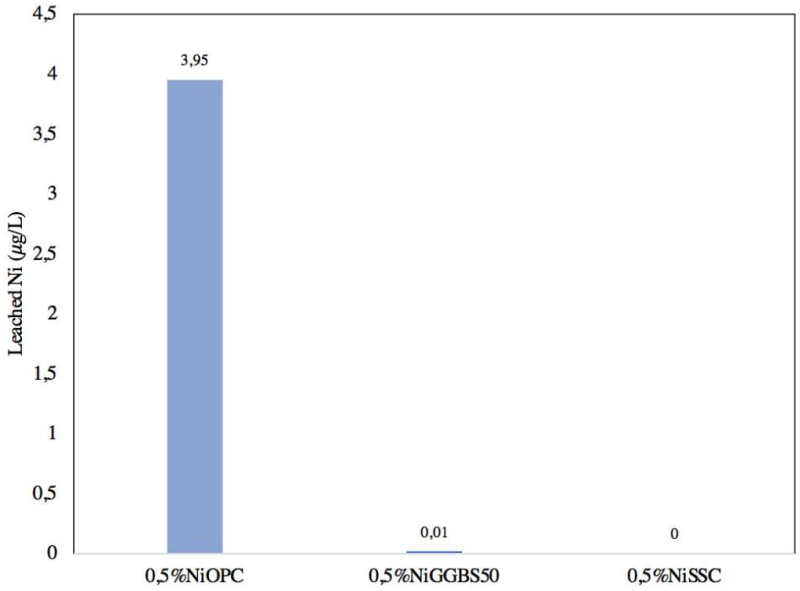

Fig. V.21 Content of leached nickel after 28 days of storage

V.4 Sequential Extractions of HM from the Dublin sediment with and without hydraulic binders' addition

This work focused on the chemical impact of two different hydraulic binders (OPC (D1) and a GGBS-based binder (D3)) on the partitioning of heavy metals in the Dublin sediment. The sequential extraction enabled, through the application of four selective dissolution steps, the determination of which component/phase of the sediments were withholding a given heavy metal whether before or after treatment with the binders.

V.4.1 Untreated sediments samples

Chemical fractionation of trace metals in untreated sediments from three different locations in the port of Dublin (D0 (A), D0 (B) and D0 (C)) was determined by means of the sequential extraction protocol described in § II.2.1.5.2.2.
As a reminder, Fraction 1 corresponds to the Exchangeable/Carbonate phase, Fraction 2 to the reducible fraction, Fraction 3 to the oxidisable fraction, and finally Fraction 4 corresponds to the remaining metals associated to refractory materials such as clays.
In this part chromium, copper, nickel, zinc, lead, and cadmium were evaluated. The results are presented in Table V.4.

Table V.4. Sequential extractions of HM and recovery percentages for the untreated sediments samples

		Fraction 1 (%)	Fraction 2 (%)	Fraction 3 (%)	Fraction 4 (%)	Recovery (%)
Cr	**D0 (A)**	0.1	6.2	15	79.1	*97*
	D0 (B)	0.1	6.6	14	79.7	*99*
	D0 (C)	0.3	8.1	18	74.1	*100*
Cu	**D0 (A)**	3.5	46.5	35.3	14.6	*100*
	D0 (B)	4.0	45.0	35.7	15.2	*102*
	D0 (C)	4.3	45.1	41.2	9.4	*100*
Ni	**D0 (A)**	7.4	13.5	25.3	53.9	*86*
	D0 (B)	7.1	15.0	20.1	57.8	*91*
	D0 (C)	10.4	16.3	22.7	50.7	*88*
Pb	**D0 (A)**	0.5	51.7	38.7	9.1	*101*
	D0 (B)	0.5	61.8	27.8	9.9	*106*
	D0 (C)	1.7	52.6	34.0	11.8	*106*
Zn	**D0 (A)**	3.9	4.8	73.2	18.2	*100*
	D0 (B)	4.4	4.9	74.0	16.7	*102*
	D0 (C)	3.8	3.2	64.9	28.1	*95*
Cd	**D0 (A)**	12.8	7.7	64.1	15.4	*105*
	D0 (B)	12.2	4.9	68.3	14.6	*114*
	D0 (C)	6.8	3.4	58.2	31.5	*107*

Between the three different samples of contaminated sediments, HM sequential extractions did not show significant differences, despite the significant differences in their total amounts obtained after the Total Attacks (II.2.1.5.1).
Firstly, it was noted that the HM considered in this study can be separated into three pairs. The first pair that gathers chromium and nickel showed large contents in Fraction 4, representing respectively more than 75% and 50%. The second pair made of copper and lead is mostly included in Fraction 2 and Fraction 3. Copper showed a repartition around 45% in F2 and more than 35% in F3, while lead was shared between 30-35% in F3 and more than 51% in F2. The sequential extraction experiments highlighted that the third pair, concerning zinc and cadmium, was in its vast majority concentrated in the organic matter phase (Fraction 3) with levels around 70% and 60% respectively.

In all cases, with the exception of cadmium, it was also noted that the most soluble phase, associated with the carbonate fraction (F1), represented the lowest fraction of retrieved contaminants. This confirms that sediments dried under air results in the presence of low labile percentage of trace metals, although some acid volatile sulfides (representing an efficient scavenging phase for trace metals) have been re-oxidised. However, it also confirms that metals included in F2 and F3 may be available in case of some redox biogeochemical transformations.
Recovery is calculated as the ratio between the cumulated mass proportions of a given trace metal obtained at the end of the four step sequential extraction divided by the amount of the same heavy metal obtained in the protocol of the total attack. Regarding the recovery ratios calculated for each sample of sediments and each metal, the calculated values were all close to 100% showing the relatively high effectiveness of the sequential extraction protocol compared to the total attack. Variations in recovery ratios observed in the table were associated to the intrinsic variability of each extraction protocol (total and/or sequential).
Finally, considering the limited differences between the three samples of untreated sediments, in the following part, sequential extraction values of the mix noted D0 (untreated sediment) correspond to the average values over the three samples, for each individual fraction and HM considered.

V.4.2 Impact of the addition of hydraulic binder on the fractionation of HM

In order to investigate the impact of both stabilizing agents, OPC and GGBS-based, on the fractionation of HM in the Dublin sediments, two formulations considered for the mechanical strength testing and the leaching test were chosen for the sequential extraction analysis: D1 and D3.
Figure V.22 summarizes the results obtained from the sequential extraction protocol.
Chromium was altered when both hydraulic binders were added to the contaminated sediments. Mostly, it was seen that the treatment with the binders increased significantly the proportion contained in F1 (from 0.2% to 20-30%) while negatively impacting the proportions of the three other fractions. The F4 fraction, where the trace metal is considered to be associated with clay minerals, remained the predominant fraction for chromium despite the hydraulic binder addition. It was eventually noted that the pure OPC treatment (D1) had a stronger impact on all fractions proportions than the GGBS-rich binder (D3).
Similarly, the impact of the hydraulic binder addition in the sediments showed an important increase of Cu in the most soluble phase (F1) and a progressive reduction of the other phase proportions. While fractions F2 and F3 were the main identified environment for copper association, F1 became the predominant fraction after the treatment. As for chromium, treatment with pure OPC (D1) had a stronger impact on the fraction distribution than D3.

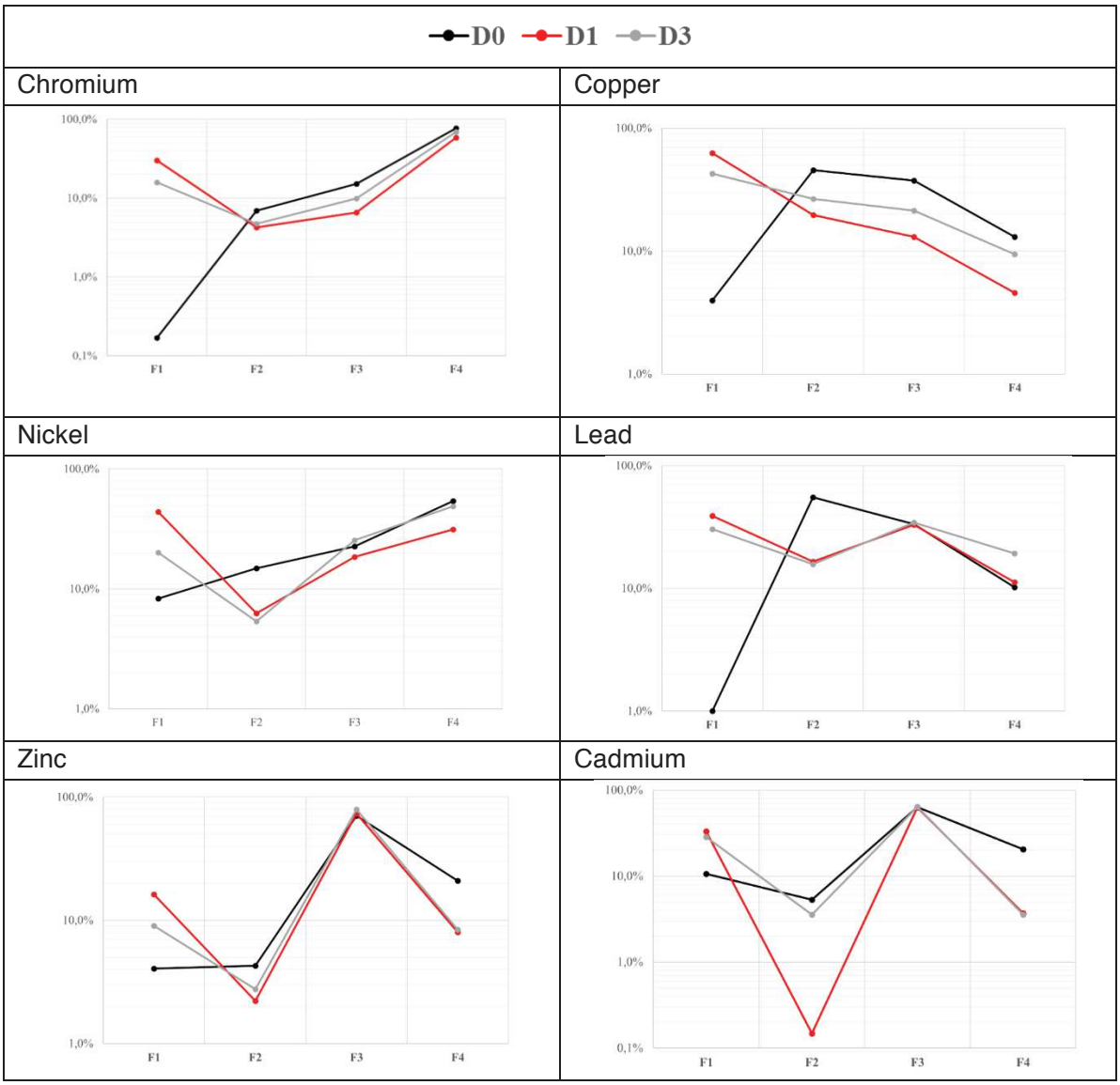

Fig. V.22 Sequential extractions of heavy metals from the mixes D0, D1 and D3

As for Cr and Cu, addition of the hydraulic binders led to a significant increase of Ni in the F1 proportion from 8% (D0) to 20% (D3) to more than 40% (D1). In the meantime, F2 showed the most significant decrease, dividing by more than two the proportion measured through sequential extraction (from 14% to 6%). It was eventually noted in the case of nickel that the higher increase in F1 when using OPC-based treatment was also compensated by a decrease in F4 (from 54% to 30%).

In the case of lead, the treatment with hydraulic binders led to a strong switch in proportions between fractions 1 and 2. The “highly soluble” fraction (F1) increased from 1% to 20-30% when binders were added while the reducible fraction (F2) was decreased from more than 50% to around 15%. Other fractions (F3 and F4) were not significantly impacted by the addition of hydraulic binders.

Concerning zinc, the major fraction remained identical before and after the treatment, *i.e.* the fraction where the metal was expected to be associated with organic matter

(F3). In all cases its value remained above 70% of the total measured proportions. As for the others heavy metals, the addition of the binders led to a strong increase of fraction F1 (from 4% to 10-15%), a slight decrease in fraction F2 (from 4% to 2%) and eventually a strong decrease in clay associated phase (F4), going from over 20% to roughly 8%.
Finally, regarding cadmium, the addition of hydraulic binders reduced the proportion associated with fraction F4 and equivalently increased the proportion associated with fraction F1. In the particular case of OPC-based treatment (D1), a very low value was noted for fraction F2.

V.4.3 Discussion

Chromium and Nickel - The results of the leaching test showed a relatively good stabilization of chromium with both stabilizing agents and with the GGBS-based binders acting better than the OPC-based binder. The occurrence of chromium mainly in the residual fraction (~77,7%) of D0 suggests the low mobility of this trace element due to the incorporation into the lattices of aluminosilicates phases as well as its non-anthropogenic origin (Audry et al., 2006). Chromium was also found in the reducible (Cr_{F2}=7%) and oxidisable (Cr_{F3}=15,2%) fractions; it can partition to solids such as Fe-Al oxides or remain in the organic matter phase. Under anoxic conditions chromium(VI) can be reduced by sulfides, iron(II) species, organic material, and bacteria to form, for instance, stable $Cr(OH)_3$ compounds (Rifkin et al., 2004), (Gorny et al., 2016). Therefore, $Cr(OH)_3$ simple hydroxide presence can be expected in Fractions 2 and 3.
The noticeable changes in chromium association can be observed after the binding agents' addition. The occurrence of Cr in the exchangeable/carbonate fraction was observed for D1 and D3, with a more noticeable Cr presence in Fraction 1 for the Portland cement formulation ($D1(Cr)_{F1}$ = 30%, $D3(Cr)_{F1}$ = 16%). The OPC-based formulation impacted more significantly the oxidisable fraction as well as the residual fraction of chromium. Therefore, it can be supposed that Portland cement increased the labile fraction of chromium more considerably than GGBS by mainly affecting the organic matter and clay components within the Dublin sediment. It should be mentioned that this toxic element was found also in Portland cement (36 mg/kg) and in GGBS (12 mg/kg), therefore the contamination of the system by the binders should be taken into account.
Nickel was found in all fractions in D0, the dominant phase being in the residual fraction (55%). This metal is likely to be incorporated into aluminosilicate minerals within the Dublin sediment. The high portion of Ni presents an approximately equal distribution between reducible and oxidisable fractions meaning that this metal is associated with iron and manganese oxides, sulfides, as well as organic matter and pyritic compounds. Nickel bound to carbonates, probably under solid dilutions, represents only ~ 9%.
Nickel is one of the elements that was demonstrated to be significantly destabilized during the leaching test, especially in the presence of the Portland cement formulation.

The sequential extraction results show the significant migration of Ni with stabilizing agents in comparison to its initial distribution between the sediment fractions. The Exchangeable/Carbonates nickel fraction of D0 shows an increase with the addition of hydraulic binders. Both D1 and D3 reduced almost two times the reducible fraction of nickel bound to manganese/iron oxides. The most important alteration rate of oxidisable (Fraction 3) and residual aluminosilicates (Fraction 4) can be observed with addition of Portland cement.
These findings are consistent with the leaching test and XANES investigations. The high pH of the Portland cement induces the desorption of nickel from sediment components and the formation of Ni hydroxides that are soluble at high pH.

Copper and Lead - Significant contamination of the Dublin sediment by copper was demonstrated by the total attack procedure. Copper and lead show a similar fractionation tendency in the raw Dublin sediment. An almost equal partition of Cu and Pb between Fractions 2 and 3 can be observed. Previous studies have investigated the association of Cu with Fe and Mn oxide weathered minerals (Silveira et al., 2006) as well as with organic matter through the formation of Cu-Organic complexes solubilized by the H_2O_2 extraction step (Audry et al., 2006; Lestari et al., 2018). Audry et al. (2006) also proposed the possible occurrence of copper in sulfide phases, for example the formation of $CuFe_2S$. These results further confirmed the presence of CuS within the Dublin sediment as it was detected by XANES spectra. Finally, the carbonate fraction contains ~4% copper.
Pb is also mainly associated with the organic matter phase and sulfides and with amorphous Fe/Mn oxides. Filgueiras et al. (2002) reported a high degree of adsorption of copper and lead by the organic matter through the complexation or bioaccumulation processes. The formation of PbS and to a much lesser extent $PbSO_4$, is likely to occur. The residual fraction recovered for Cu and Pb in the Dublin sediment was rather low,13 % and 10 % respectively.
Both stabilizing agents induced the migration of Cu to the most labile Fraction 1: $D0(Cu)_{F1}$ = 4 %, $D1(Cu)_{F1}$ = 63%, $D3(Cu)_{F1}$ = 42%. As can be seen the most noticeable migration rate was caused by Portland cement. The proportion of copper associated with organic matter/pyritic compounds considerably decreased in the presence of hydraulic binders: by 23% for the OPC-based formulation and by 14% in the case of the GGBS-based formulation. As was discussed previously, the high pH produced in the case of the Portland cement formulation disturbs more significantly the Dublin sediment compounds such as organic matter, clays, or Fe-Mn oxides. Due to the pH increase, the formation of $Cu(OH)_2$ is possible. The changes in the chemical environment of Cu in the presence of the OPC formulation was investigated by the XANES experiment (V.3.1.2). The formation of the less stable $CuSO_4$ was observed due to the oxidation of CuS. Finally, copper was extremely mobile in the presence of Portland cement and it was leached 13 times more than from the raw sediment. This high rate of contamination of the sediment and the important mobility rate of Cu can

be also related to the presence of the high amount of Cu in Portland cement. Further investigations are required.

Regarding Pb redistribution after the mixture of the Dublin sediment with two binders, the considerable enrichment of the labile exchangeable/carbonates fraction occurs from the reducible fraction, especially for D1. It can be thus supposed that lead combined with hydrous oxides of manganese or iron was desorbed from this fraction under the binders' action. The oxidisable fraction of lead in the sediment was only slightly altered by the binders. The unexpected increase for the lead portion in the residual fraction in the case of D3 may arise from the formation of highly stable lead silicates as was mentioned previously. In contrast the predominant labile lead species for D1 and D3 could include carbonates, sulfates, hydroxides, as well as mixed calcium salts.

Zinc and Cadmium - According to the leaching results, zinc was well stabilized with all binders, especially after 3 months of storage. As was already mentioned, zinc and cadmium demonstrated similar distribution profiles in the Dublin sediment. Moreover, these metals exhibited an atypical behaviour compared for instance to the reference values where the majority of Cd and Zn occur in the most mobile Fraction 1 and 2 (BCR-701, 2001). In the present study the highest percentage of cadmium and zinc was found in Fraction 3 with 71% and 64% respectively. This high proportion of Cd and Zn associated with the oxidisable fraction can be explained by the binding to the pyritic compounds (ZnS and CdS being solubilized during the second step of the sequential extraction) as well as the formation of Zn- and Cd-organic matter complexes. Similar behaviour of cadmium and zinc can be explained by similarities in their chemistry such as electronegativities, ionic structures, and ionization energies (Fuge et al., 1993). Binding of Cd and Zn to reducible and carbonate fractions remains relatively low (~10%), whereas in other sediments, these HM are characterized by high mobility (see for instance (Billon et al., 2001), (Boughriet et al., 2007)). Residual zinc and cadmium accounted for around 21%. Primary aluminosilicate minerals play an important role in Zn retention (Silveira et al., 2006). It should be mentioned that zinc chromate compound was detected in the Dublin sediment after XANES investigation. Therefore, the unusual behaviour of zinc may be explained by the presence of this highly stable compound.
Both stabilizing agents altered the reducible and residual fractions of zinc in the sediment by reducing them twofold. However, the predominant oxidisable Zn fraction seems to be unaffected and even enriched in the case of D3.
Cadmium is one of the main contaminants in the Dublin sediment. Its concentration significantly increased in Fraction 1, especially for D1. The GGBS-based binder also increased the proportion of cadmium in the exchangeable/carbonate fraction but to a lesser extent than the OPC-based formulation. It can be assumed that the hydraulic binders caused the migration of cadmium mainly from the reducible and residual

fractions. Portland cement also caused a higher alteration of cadmium associated with Fraction 3. The higher alteration rate of the organic matter by Portland cement, as demonstrated Chapter III, can explain the reduced percentage of cadmium in Fraction 3 and its migration to Fraction 1. As was already mentioned earlier, the formation of $CdCO_3$ or $Cd(OH)_2$ as well as $CaCd_2(OH)_4$ can be expected in the presence of hydraulic binders (§IV.5.4). $Cd(OH)_2$ was probably the dominant species for the OPC-based formulation and the formation of CdS in the presence of GGBS is expected as confirmed by the XANES investigation. CdS is known to be extracted in the second stage (Fraction 2). The leaching test demonstrated a good stability of cadmium with both binders.

V.4.4 Conclusions

The selective extraction procedure can be an effective method to assess the distribution of heavy metals before and after treatment with hydraulic binders. The results were validated according to the recovery calculations. Despite variations in the contaminant content at three different locations in the port of Dublin, sequential extraction has shown that the chemical speciation/distribution is roughly the same among all samples. The treated samples show a significant redistribution of toxic elements in certain cases under modified environmental conditions after the introduction of the hydraulic binders. It concerns particularly the OPC binding agent which has considerably increased the proportion of F1 fraction compared to GGBS treatment. It should be mentioned, that both binders add significant concentrations of HM. Therefore, the contamination of the system by the binders is possible, especially by Portland cement, which has very high concentrations of Cu, Ni, Zn, Cr.

V.5 Conclusions

To summarize this chapter of the leaching results and potential mechanisms of heavy metals immobilization using different hydraulic binders, some main conclusions can be drawn:

- The partitioning of contaminants in different fractions of the Dublin sediment is roughly the same among three different locations considered for dredging operations according to the sequential extraction analysis.
- Concerning the untreated samples, the contaminants are rather stable and their leaching from the sediments is quite low compared to the total quantity of these elements. This indicates that the sediment under its current conditions tends to stabilize pollutants. Probably, under natural conditions, these sediments are anoxic and trace metals are well stabilized by the reduced sulfur pool, which is partially oxidized during the dredging and drying process.

- Almost all of the toxic elements were fairly well stabilized with binding agents after the S/S treatment, except for Cu and Ni.
- OPC is the most disturbing binding agent for the contaminants distribution. The sequential extraction method demonstrated the highest migration level of contaminants to the Exchangeable/Carbonate fraction in the presence of the OPC formulation compared to the GGBS-based binder. XANES results revealed a modified chemical environment of Cu and Zn after the treatment with OPC compared to the raw Dublin sediment and GGBS-treated samples;
- It seems that pH is one of the main parameters controlling the leaching behaviour of trace elements. The pH measurements showed that the 100% Portland cement formulation developed the highest pH during the treatment which can disturb the Dublin sediment constituents serving as a sink for the considered heavy metals. Heavy metal hydroxide compounds can solubilize with the pH increasing above 12.5.
- The most effective stabilizers were the supersulfated formulations which develop the lowest pH.
- GGBS-based binders were shown to be the least destabilizing solution. XANES results of Cu and Zn speciation show the undisturbed state of these elements after GGBS-based treatment.
- The presence of sulfides as a minor element (<1%) in GGBS can provide an additional advantage of its use due to the possible precipitation of sulfide species which have a very low solubility rate under alkaline conditions (Fig. V.23).

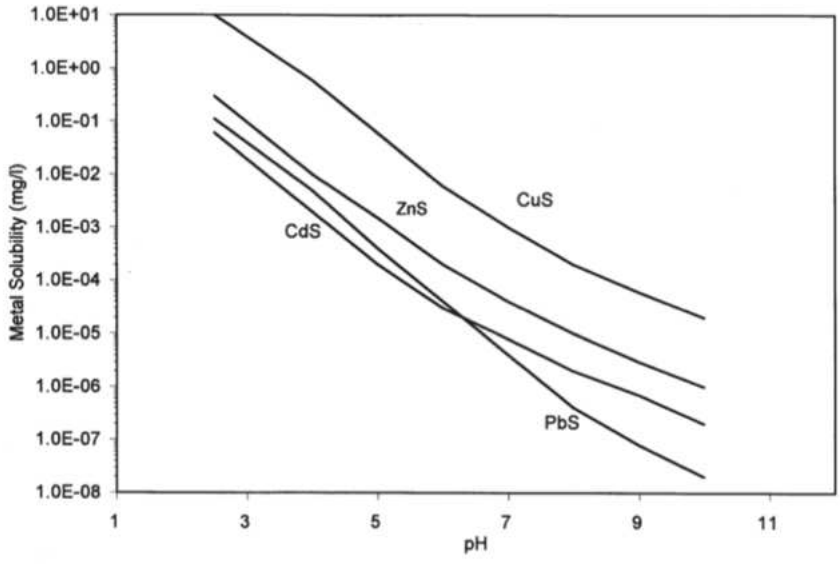

Fig. V.23 Metal sulfide solubility *vs* pH (Conner & Hoeffner, 1998)

- It seems that GGBS produces a denser material over time due to the formation of mostly amorphous phases, as demonstrated Chapter III. The potential incorporation of mobilized pollutants in the hydrated phases of the GGBS-

based binders can take place. The lower amount of calcium in GGBS/OPC blends compared to OPC promotes the formation of C-A-S-H with a lower Ca/Si ratio providing additional sites for trace metals as charge compensators of aluminium. Hydrotalcite LDH-like phases are also effective in immobilizing pollutants and are known to be precipitated with a high GGBS content.

Bibliography

Achternbosch, M., Bräutigam, K. R., Hartlieb, N., Kupsch, C., Richers, U., Stemmermann, P., & Gleis, M. (2003). Heavy metals in cement and concrete resulting from the co-incineration of wastes in cement kilns with regard to the legitimacy of waste utilisation. https://doi.org/10.5445/IR/270055717

Albino, V., Cioffi, R., Marroccoli, M., & Santoro, L. (1996). Potential application of ettringite generating systems for hazardous waste stabilization. Journal of Hazardous Materials, 51(1), 241–252. https://doi.org/10.1016/S0304-3894(96)01828-6

Allan, M. L., & Kukacka, L. E. (1995). Blast furnace slag-modified grouts for in situ stabilization of chromium-contaminated soil. Waste Management, 15(3), 193–202. https://doi.org/10.1016/0956-053X(95)00017-T

Audry, S., Blanc, G., & Schäfer, J. (2006). Solid state partitioning of trace metals in suspended particulate matter from a river system affected by smelting-waste drainage. Science of The Total Environment, 363(1–3), 216–236. https://doi.org/10.1016/j.scitotenv.2005.05.035

BCR-701. (2001, July 17). The certification of the extractable contents (mass fractions) of Cd, Cr, Cu, Ni, Pb and Zn in freshwater sediment following a sequential extraction procedure: BCR-701. [Website]. Publications Office of the European Union. http://op.europa.eu/en/publication-detail/-/publication/02c41803-8f6d-41f2-a73d-c47225ff8c6e

Berardi, R., Cioffi, R., & Santoro, L. (1998). Matrix stability and leaching behaviour in ettringite-based stabilization systems doped with heavy metals. Waste Management, 17(8), 535–540. https://doi.org/10.1016/S0956-053X(97)10061-7

Bertolini, L. (2014). Corrosion of Steel in Concrete: Prevention, Diagnosis, Repair, 2nd Edition | Wiley. Wiley.Com. https://www.wiley.com/en-us/Corrosion+of+Steel+in+Concrete%3A+Prevention%2C+Diagnosis%2C+Repair%2C+2nd+Edition-p-9783527331468

Billon, G., Ouddane, B., & Boughriet, A. (2001). Artefacts in the speciation of sulfides in anoxic sediments. Analyst, 126(10), 1805–1809. https://doi.org/10.1039/B104704N

Bone B. D., Barnard L H., Boardman D. I., Carey P. J., Hills C. D., Jones H. M., MacLeod C. L., Tyrer M., (2004) Review of scientific literature on the use of stabilisation/solidification for the treatment of contaminated soil, solid waste and sludges

Boughriet, A., Proix, N., Billon, G., Recourt, P., & Ouddane, B. (2007). Environmental Impacts of Heavy Metal Discharges from a Smelter in Deûle-canal Sediments (Northern France): Concentration Levels and Chemical Fractionation. Water, Air, and Soil Pollution, 180(1), 83–95. https://doi.org/10.1007/s11270-006-9252-5

Bruland, K. W. (1989). Complexation of zinc by natural organic ligands in the central North Pacific. Limnology and Oceanography, 34(2), 269–285. https://doi.org/10.4319/lo.1989.34.2.0269

Cartledge, F. K., Butler, L. G., Chalasani, D., Eaton, H. C., Frey, F. P., Herrera, E., Tittlebaum, M. E., & Yang, S. L. (1990). Immobilization mechanisms in solidifiction/stabilization of cadmium and lead salts using portland cement fixing agents. Environmental Science & Technology, 24(6), 867–873. https://doi.org/10.1021/es00076a012

Cetin, B., Aydilek, A. H., & Guney, Y. (2012). Leaching of trace metals from high carbon fly ash stabilized highway base layers. Resources, Conservation and Recycling, 58, 8–17. https://doi.org/10.1016/j.resconrec.2011.10.004

Chen, Q. Y., Hills, C. D., Tyrer, M., Slipper, I., Shen, H. G., & Brough, A. (2007). Characterisation of products of tricalcium silicate hydration in the presence of heavy metals. Journal of Hazardous Materials, 147(3), 817–825. https://doi.org/10.1016/j.jhazmat.2007.01.136

Chen, Q. Y., Tyrer, M., Hills, C. D., Yang, X. M., & Carey, P. (2009). Immobilisation of heavy metal in cement-based solidification/stabilisation: A review. Waste Management, 29(1), 390–403. https://doi.org/10.1016/j.wasman.2008.01.019

Chen, S., Wang, P., & Zhang, D. (2014). Corrosion behavior of copper under biofilm of sulfate-reducing bacteria. Corrosion Science, 87, 407–415. https://doi.org/10.1016/j.corsci.2014.07.001

Cocke, D., Ortego, J. D., McWhinney, H., Lee, K., & Shukla, S. (1989). A model for lead retardation of cement setting. Cement and Concrete Research, 19(1), 156–159. https://doi.org/10.1016/0008-8846(89)90078-1

Conner, J. R., & Hoeffner, S. L. (1998). A Critical Review of Stabilization/Solidification Technology. Critical Reviews in Environmental Science and Technology, 28(4), 397–462. https://doi.org/10.1080/10643389891254250

Cornelis, G., Johnson, C. A., Gerven, T. V., & Vandecasteele, C. (2008). Leaching mechanisms of oxyanionic metalloid and metal species in alkaline solid wastes: A review. Applied Geochemistry, 23(5), 955–976. https://doi.org/10.1016/j.apgeochem.2008.02.001

Doušová, B., Machovicˇ, V., Koloušek, D., Kovanda, F., & Ák, V. D. (2003). Sorption of As(V) Species from Aqueous Systems. 17.

Eggleton, J., & Thomas, K. V. (2004). A review of factors affecting the release and bioavailability of contaminants during sediment disturbance events. Environment International, 30(7), 973–980. https://doi.org/10.1016/j.envint.2004.03.001

Eguchi, K., Kato, Y., & Katpady, D. N. (2019). Study on physical property and durability of concrete with high content of blast furnace slag. Life-Cycle Analysis and Assessment in Civil Engineering: Towards an Integrated Vision - Proceedings of the 6th International Symposium on Life-Cycle Civil Engineering, IALCCE 2018, 561–566. https://tus.elsevierpure.com/en/publications/study-on-physical-property-and-durability-of-concrete-with-high-c

Filgueiras, A. V., Lavilla, I., & Bendicho, C. (2002). Chemical sequential extraction for metal partitioning in environmental solid samples. Journal of Environmental Monitoring, 4(6), 823–857. https://doi.org/10.1039/b207574c

Fuge, R., Pearce, F. M., Pearce, N. J. G., & Perkins, W. T. (1993). Geochemistry of Cd in the secondary environment near abandoned metalliferous mines, Wales. https://doi.org/10.1016/S0883-2927(09)80006-1

Gineys, N., Aouad, G., & Damidot, D. (2010). Managing trace elements in Portland cement – Part I: Interactions between cement paste and heavy metals added during mixing as soluble salts. Cement and Concrete Composites, 32(8), 563–570. https://doi.org/10.1016/j.cemconcomp.2010.06.002

Glasser, F. P. (1997). Fundamental aspects of cement solidification and stabilisation. Journal of Hazardous Materials, 52(2–3), 151–170. https://doi.org/10.1016/S0304-3894(96)01805-5

Gorny, J., Billon, G., Noiriel, C., Dumoulin, D., Lesven, L., & Madé, B. (2016). Chromium behavior in aquatic environments: A review. Environmental Reviews, 24(4), 503–516. https://doi.org/10.1139/er-2016-0012

Gougar, M. L. D., Scheetz, B. E., & Roy, D. M. (1996). Ettringite and C S H Portland cement phases for waste ion immobilization: A review. Waste Management, 16(4), 295–303. https://doi.org/10.1016/S0956-053X(96)00072-4

Guo, B., Liu, B., Yang, J., & Zhang, S. (2017). The mechanisms of heavy metal immobilization by cementitious material treatments and thermal treatments: A review. Journal of Environmental Management, 193, 410–422. https://doi.org/10.1016/j.jenvman.2017.02.026

Hale, B., Evans, L., & Lambert, R. (2012). Effects of cement or lime on Cd, Co, Cu, Ni, Pb, Sb and Zn mobility in field-contaminated and aged soils. Journal of Hazardous Materials, 199–200, 119–127. https://doi.org/10.1016/j.jhazmat.2011.10.065

Halim, C. E., Amal, R., Beydoun, D., Scott, J. A., & Low, G. (2004). Implications of the structure of cementitious wastes containing Pb(II), Cd(II), As(V), and Cr(VI) on the leaching of metals. Cement and Concrete Research, 34(7), 1093–1102. https://doi.org/10.1016/j.cemconres.2003.11.025

Kabata-Pendias, A., & Pendias, H. (2001). Trace elements in soils and plants (3rd ed). CRC Press.

Karamalidis, A. K., & Voudrias, E. A. (2009). Leaching and Immobilization Behavior of Zn and Cr from Cement-Based Stabilization/Solidification of Ash Produced from Incineration of Refinery Oily Sludge. Environmental Engineering Science, 26(1), 81–96. https://doi.org/10.1089/ees.2007.0040

Kogbara, R. B. (2014). A review of the mechanical and leaching performance of stabilized/solidified contaminated soils. Environmental Reviews, 22(1), 66–86. https://doi.org/10.1139/er-2013-0004

Kogbara, R. B., & Al-Tabbaa, A. (2011). Mechanical and leaching behaviour of slag-cement and lime-activated slag stabilised/solidified contaminated soil. Science of The Total Environment, 409(11), 2325–2335. https://doi.org/10.1016/j.scitotenv.2011.02.037

Kumar, P., Nagarajan, R., & Sarangi, R. (2013). Quantitative X-ray Absorption and Emission Spectroscopies: Electronic Structure Elucidation of Cu2S and CuS. Journal of Materials Chemistry. C. https://doi.org/10.1039/C3TC00639E

Lasheras-Zubiate, M., Navarro-Blasco, I., Fernández, J. M., & Álvarez, J. I. (2012). Encapsulation, solid-phases identification and leaching of toxic metals in cement systems modified by natural biodegradable polymers. Journal of Hazardous Materials, 233–234, 7–17. https://doi.org/10.1016/j.jhazmat.2012.06.028

Lestari, Budiyanto, F., & Hindarti, D. (2018). Speciation of heavy metals Cu, Ni and Zn by modified BCR sequential extraction procedure in sediments from Banten Bay, Banten Province, Indonesia. IOP Conference Series: Earth and Environmental Science, 118, 012059. https://doi.org/10.1088/1755-1315/118/1/012059

Lützenkirchen-Hecht, D., Müller, L., Hoffmann, L., & Wagner, R. (2014). Analysis of engine motor oils by X-ray absorption and X-ray fluorescence spectroscopies. X-Ray Spectrometry, 43(4), 221–227. https://doi.org/10.1002/xrs.2543

Mahedi, M., Cetin, B., & Dayioglu, A. Y. (2019). Leaching behavior of aluminum, copper, iron and zinc from cement activated fly ash and slag stabilized soils. Waste Management, 95, 334–355. https://doi.org/10.1016/j.wasman.2019.06.018

Malviya, R., & Chaudhary, R. (2006). Factors affecting hazardous waste solidification/stabilization: A review. Journal of Hazardous Materials, 137(1), 267–276. https://doi.org/10.1016/j.jhazmat.2006.01.065

Mckinley, J. D., Thomas, H. R., Williams, K. P., & Reid, J. M. (2001). Chemical analysis of contaminated soil strengthened by the addition of lime. Engineering Geology, 60(1–4), 181–192. https://doi.org/10.1016/S0013-7952(00)00100-9

McWhinney, H. G., & Cocke, D. L. (1993). A surface study of the chemistry of zinc, cadmium, and mercury in portland cement. Waste Management, 13(2), 117–123. https://doi.org/10.1016/0956-053X(93)90003-F

Moon, D. H., & Dermatas, D. (2006). An evaluation of lead leachability from stabilized/solidified soils under modified semi-dynamic leaching conditions. Engineering Geology, 85(1–2), 67–74. https://doi.org/10.1016/j.enggeo.2005.09.028

Moulin, I., Stone, W. E. E., Sanz, J., Bottero, J.-Y., Mosnier, F., & Haehnel, C. (1999). Lead and Zinc Retention during Hydration of Tri-Calcium Silicate: A Study by Sorption Isotherms and 29Si Nuclear Magnetic Resonance Spectroscopy. Langmuir, 15(8), 2829–2835. https://doi.org/10.1021/la981062u

Myneni, S. C. B., Traina, S. J., Logan, T. J., & Waychunas, G. A. (1997). Oxyanion Behavior in Alkaline Environments: Sorption and Desorption of Arsenate in Ettringite. Environmental Science & Technology, 31(6), 1761–1768. https://doi.org/10.1021/es9607594

Paria, S., & Yuet, P. K. (2006). Solidification–stabilization of organic and inorganic contaminants using portland cement: A literature review. Environmental Reviews, 14(4), 217–255. https://doi.org/10.1139/a06-004

Park, J.-Y., & Batchelor, B. (1999). Prediction of chemical speciation in stabilized/solidified wastes using a general chemical equilibrium model II: Doped waste contaminants in cement porewaters. Cement and Concrete Research, 29(1), 99–105. https://doi.org/10.1016/S0008-8846(98)00181-1

Peysson, S., Péra, J., & Chabannet, M. (2005). Immobilization of heavy metals by calcium sulfoaluminate cement. Cement and Concrete Research, 35(12), 2261–2270. https://doi.org/10.1016/j.cemconres.2005.03.015

Rifkin, E., Gwinn, P., & Bouwer, E. (2004). Chromium and Sediment Toxicity. 5.

Roy, A., & Cartledge, F. K. (1997). Long-term behavior of a portland cement-electroplating sludge waste form in presence of copper nitrate. Journal of Hazardous Materials, 52(2–3), 265–286. https://doi.org/10.1016/S0304-3894(96)01812-2

Scheidegger, A. M., Wieland, E., Scheinost, A. C., Dähn, R., & Spieler, P. (2000). Spectroscopic Evidence for the Formation of Layered Ni–Al Double Hydroxides in Cement. Environmental Science & Technology, 34(21), 4545–4548. https://doi.org/10.1021/es0000798

Silveira, M. L., Alleoni, L. R. F., O'Connor, G. A., & Chang, A. C. (2006). Heavy metal sequential extraction methods—A modification for tropical soils. Chemosphere, 64(11), 1929–1938. https://doi.org/10.1016/j.chemosphere.2006.01.018

Smrzka, D., Zwicker, J., Bach, W., Feng, D., Himmler, T., Chen, D., & Peckmann, J. (2019). The behavior of trace elements in seawater, sedimentary pore water, and their

incorporation into carbonate minerals: A review. Facies, 65(4), 41. https://doi.org/10.1007/s10347-019-0581-4

Stephan, D., Maleki, H., Knöfel, D., Eber, B., & Härdtl, R. (1999). Influence of Cr, Ni, and Zn on the properties of pure clinker phases Part II. C3A and C4AF. Cement and Concrete Research, 7.

Tian, S., Wang, S., Wu, Y., Gao, J., Xie, H., Li, X., Yang, G., Han, Y., & Tan, Y. (2015). The real active sites over Zn–Cr catalysts for direct synthesis of isobutanol from syngas: Structure-activity relationship. RSC Advances, 5(108), 89273–89281. https://doi.org/10.1039/C5RA17289F

Vespa, M., Dähn, R., Grolimund, D., Wieland, E., & Scheidegger, A. M. (2006). Spectroscopic Investigation of Ni Speciation in Hardened Cement Paste. Environmental Science & Technology, 40(7), 2275–2282. https://doi.org/10.1021/es052240q

Vespa, M., Dähn, R., & Wieland, E. (2014). Competition behaviour of metal uptake in cementitious systems: An XRD and EXAFS investigation of Nd- and Zn-loaded 11Å tobermorite. Physics and Chemistry of the Earth, Parts A/B/C, 70–71, 32–38. https://doi.org/10.1016/j.pce.2014.01.001

Weeks, C., Hand, R. J., & Sharp, J. H. (2008). Retardation of cement hydration caused by heavy metals present in ISF slag used as aggregate. Cement and Concrete Composites, 30(10), 970–978. https://doi.org/10.1016/j.cemconcomp.2008.07.005

Wu, H.-L., Jin, F., Bo, Y.-L., Du, Y.-J., & Zheng, J.-X. (2018). Leaching and microstructural properties of lead contaminated kaolin stabilized by GGBS-MgO in semi-dynamic leaching tests. Construction and Building Materials, 172, 626–634. https://doi.org/10.1016/j.conbuildmat.2018.03.164

Yong, R. N. Y., Mohamed, A. M. O., & Warkentin, B. P. (1992). Principles of Contaminant Transport in Soils. /paper/Principles-of-Contaminant-Transport-in-Soils-Yong-Mohamed/12a530c0d1e4512490b6919540590bd3bc0fb27e

Yousuf, M., Mollah, A., Vempati, R. K., Lin, T.-C., & Cocke, D. L. (1995). The interfacial chemistry of solidification/stabilization of metals in cement and pozzolanic material systems. Waste Management, 15(2), 137–148. https://doi.org/10.1016/0956-053X(95)00013-P

Zhang, J., Provis, J. L., Feng, D., & van Deventer, J. S. J. (2008). Geopolymers for immobilization of Cr6+, Cd2+, and Pb2+. Journal of Hazardous Materials, 157(2–3), 587–598. https://doi.org/10.1016/j.jhazmat.2008.01.053

Zhang, Y., Cetin, B., Likos, W. J., & Edil, T. B. (2016). Impacts of pH on leaching potential of elements from MSW incineration fly ash. Fuel, 184, 815–825. https://doi.org/10.1016/j.fuel.2016.07.089

Ziegler, F., Scheidegger, A. M., Johnson, C. A., Dähn, R., & Wieland, E. (2001). Sorption mechanisms of zinc to calcium silicate hydrate: X-ray absorption fine structure (XAFS) investigation. Environmental Science & Technology, 35(7), 1550–1555. https://doi.org/10.1021/es001437+

General Conclusions

The aim of the present research was to develop an appropriate GGBS (ground granulated blast-furnace slag) -based formulation for the Solidification/Stabilization (S/S) treatment of contaminated sediments from the Dublin Port, Ireland. The port authorities require an improvement in the engineering properties of the dredged material for its reuse in the Alexandra Basin Redevelopment (ABR) Project. One of the main concerns regarding the reuse of dredged material (DM) is the presence of toxic trace metals within the sediment matrix. Consequently, the stabilization of contaminants is also critical. From the economical point of view, the amount of the binder was fixed at 150 kg per cubic meter of sediment with the sediment having a density of 1400 kg/m^3 and a water content of 45% after the dewatering process. Regarding the low amount of binder and high water content in the system, as well as the complex nature of the sediment, the selection of an appropriate S/S binding agent to achieve the required properties of the final material was challenging. Therefore, this study has explored the mechanisms that govern the evolution of the mechanical properties of the GGBS-treated sediment, as well as the mechanisms of the stabilization of pollutants within the newly formed solidified system.

First, the results of the physical and chemical analysis of the Dublin sediment (D0) were obtained in order to characterize its nature and then to investigate the main parameters governing mechanical strength development, and mobility of HM. The study compares the physicochemical parameters of D0 with the sediment which originated from the Gothenburg Port (G0) to assess the efficiency of the solidification process using a GGBS-based formulation in different cases. Physical analysis showed a difference in particle size, with the Dublin sediment having a finer texture compared to G0 and also a lower density. The mineralogy of both sediments was explored using XRD analysis. A mostly clayey nature was detected for the Dublin sediment, with a significant amount of calcite and quartz. The Gothenburg sediment mainly contains siliceous minerals. The XRD analysis of the clay fraction showed that illite is the main clay phase of both sediments. The samples were also characterized in terms of Cation Exchange Capacity (CEC), Total Organic Carbon (TOC), and organic matter content as important parameters controlling heavy metal (HM) mobility and mechanical changes. The results indicated much greater values for the Dublin sediment.

During the next stage of the project the uniaxial compressive strength of the treated Dublin sediment was tested from 1 to 6 months of storage for the range of GGBS-based formulations and the Portland cement (OPC) formulation (D1) as reference introduced into the sediment at 150 kg/m^3. An important decrease in uniaxial compressive strength (UCS) of the reference mix was measured between 3 and 6 months of storage. At the same time, the investigation of strength development demonstrated the improvement in long-term strength when the OPC binder was

partially replaced by GGBS. Based on the UCS results, the most efficient GGBS-based formulation with the highest proportion of granulated slag was 85%GGBS/15%OPC (D3). An absence of strength was observed for the supersulfated mixes and carbonate activation of GGBS. Adding these binders to the sediment produced a low pH, which is not sufficient for the hydration process. Therefore, at this stage of the project, D3 was chosen as the optimal GGBS-based formulation for the S/S process and compared to the widely-used OPC binder D1. The XRD analysis of D1 demonstrated a significant decrease in the intensity of the main crystalline OPC phases after 1 month of storage – portlandite, ettringite and C_4AHx. In addition, the test for assessing the volumetric variations of the mixtures demonstrated a greater shrinkage rate for the OPC formulation compared to D3. The microstructure investigation revealed the denser microstructure of the GGBS-based sample D3 compared to the more porous and inhomogeneous medium of D1. Therefore, the results of the compressive strength were attributed to the hydration phases development in both mixtures over time as well as to the microstructure evolution.

The following part of the solidification study assessed the impact of the same formulations on the engineering behaviour of the Dublin and Gothenburg sediments. This time the binder content was 300 kg/m^3. The results demonstrated a steady increase in strength for the GGBS formulation from 1 to 6 months of storage, with higher values for the Dublin sediment. Unlike the GGBS formulation, OPC mixed with the sediments showed a stagnation in strength development, with greater values for the Gothenburg sediment. It was concluded that the granulometry and CEC values play an important role in the sediments/soils solidification process. The results of the OPC treatment of both sediments confirmed earlier findings – a finer sediment structure provides lower strength due to a higher CEC. However, an opposite trend was observed for the GGBS-based samples. This led to the conclusion that the higher content of organic matter (OM) and clay in the Dublin sediment provides a good capacity for water storage necessary for long term hydration of GGBS. XRD analysis demonstrated that due to the addition of the binding agents, the peaks of clay minerals (illite and montmorillonite) decreased over time due to the high pH of the mixtures and pozzolanic reactions produced over time.

The study thus suggested that the interaction of binding agents with the clay fraction is one of the important parameters for strength development. Therefore, the illitic clay was mixed with both binders to assess UCS and microstructure evolution. The results showed the same trend of UCS as in the case of sediments – a considerable increase over time for the GGBS-based formulation and a stagnation/slight degradation for the OPC samples. The investigation of hydration products did not provide a clear vision of the mechanisms responsible for hydration. At the same time, the microstructure investigation revealed the flocculated state of the OPC-based formulation and a more

homogenous and dense microstructure of the GGBS-based sample. It was then concluded that the repartition of hydrates plays an important role in the strength development in such dilute systems, in particular the flocculation/dispersion phenomenon. The impact of the interstitial solution of the binding agents on the clay particle arrangement was investigated through zeta potential and rheology. The higher flocculation rate in the presence of Portland cement was confirmed due to the greater calcium content. This leads to the more open and porous structure of the clay fabric, or of the sediment in this case.

Taken together, these findings suggest that for the solidification of sediment/soil systems with a low amount of binding agent, flocculation/dispersion is a crucial indicator. To evaluate the role of a more dispersed state of the sediment matrix, two types of dispersing agents were introduced into the Dublin sediment before treatment with the OPC and GGBS-based formulations. Indeed, the UCS was twice as much for both formulations in the case of the dispersed state of the sediment prior to S/S treatment.

The current study found that the organic matter of the Dublin sediment was impacted in the presence of hydraulic binders with a significant alteration of carbohydrates, amino-sugars, and nitrogen compounds as demonstrated by ^{13}C NMR and the reconstruction of OM via Py-GC-MS. The alteration rate of OM compounds was greater for the OPC-based formulation compared to the GGBS-based treated Dublin sediment. This more significant perturbation of OM in the presence of OPC can be explained by the higher pH produced during S/S treatment. The delay in hydration of the OPC and GGBS-based binders with the addition of humic acids was assessed separately using calorimetry measurements. A significant retardation/annihilation was observed from 5%wt dosage. Thus, these experiments provide evidence of the important role of organic matter as part of a complex sediment matrix. The changes in environmental factors (pH, ionic concentration, etc.) of the sediment due to the addition of binding agents can have a considerable impact on organic matter and consequently on the evolution of mechanical properties, as well as on the migration of contaminants having a great affinity for OM.

Another question in this study was to assess the impact of trace metals on the early hydration of the treated sediments. Three types of binding agents – OPC, GGBS/OPC and the supersulfated formulation – were mixed with Zn, Cu, Cd, and Ni in the form of nitrate salts at 0.1%wt, 0.5%wt and 2%wt. The observations of early hydration demonstrated widely different effects for the introduced metal ions; copper and zinc greatly retarded or even annihilated the hydration pathway, whereas nickel and cadmium mostly accelerated or had no impact on the precipitation of hydrates. The hydration of the GGBS-based formulations was greatly affected by Cu and Zn compared to OPC, especially the supersulfated mix. These results further support the

hypothesis that calcium depletion occurs due to the formation of Cu and Zn complex calcium salts (e.g. calcium zincate), therefore the formation of hydrates is delayed. Unlike copper and zinc, nickel and cadmium form hydroxide species (or layered double hydroxide (LDH), sulfides) without calcium consumption. These findings partially explain the longer hydration period for the sediments treated with GGBS-based binders.

The last part of this study investigates the mechanisms of stabilization of trace metals of the Dublin after S/S treatment sediment using GGBS-based binders. First, the results of the leaching test showed a relatively low leaching rate of HM from the untreated sediment and the increased mobility of trace metals after the use of hydraulic binders, especially copper and nickel. The leaching test has shown that with an increase in the amount of GGBS, the level of leached HM decreased significantly compared to the OPC-based treatment. The most performant formulations were supersulfated mixes. This study has found that the crucial parameter controlling the mobility of trace metals is pH. OPC provided the highest pH after being mixed with the sediment with the highest leaching rate of HM, whereas the supersulfated formulations developed the lowest pH. Moreover, X-ray absorption spectroscopy (XAS) analysis of the Dublin sediment with and without the addition of binding agents revealed changes in the chemical environment of Cu and Zn after OPC addition. The speciation of zinc in the raw sediment is very close to the highly stable zinc chromate used as a primer in marine paints. GGBS activated by a small amount of OPC did not impact the chemical environment of Zn, while the Portland cement formulation changed its coordination number. In the same way, copper's oxidation state was changed with the addition of Portland cement, but not with the formulations with the high proportion of GGBS. The presence of cuprous sulfide and cupric sulfide was detected in the raw sediment and for the GGBS treated sediment.

XAS analysis was also performed for Ni and Cd, introduced into the pure OPC and GGBS-based binders in form of chlorides. The results for Cd have shown the precipitation of $Cd(OH)_2$ in the case of the OPC binder and the more stable CdS in the case of GGBS formulations due to the presence of sulfurs in GGBS. Hydroxide species of nickel was also detected for the OPC binder and 50%GGBS/50%OPC after $NiCl_2$ addition, with the majority being the Ni-Al Layered Double Hydroxides phase. It can be concluded that the formation of these compounds governs the mobility of Cd and Ni in sediment-binder systems in practice.

Finally, the method of sequential extraction was applied to the Dublin sediment before and after the addition of the OPC and GGBS-based formulations. The Dublin sediment from three different locations within the Alexandra Basin was subjected to the analysis and the results demonstrated a similar distribution of trace metals between the main

fractions. After the hydraulic binders' introduction, a different partitioning of HM was observed with migration to the less stable fractions (Exchangeable/Carbonates fractions), especially in the case of Portland cement.

This work has contributed to the understanding of the main parameters that govern the evolution of the mechanical strength of the Dublin sediment treated with GGBS-based binders as well as the stabilization of contaminants. The findings of this study have a number of practical implications for the ABR project as well as in the field of the Solidification/Stabilization remediation practice.

Perspectives

This research has raised numerous questions in need of further investigation.

Specifically, the following issues were identified regarding solidification:

- The issue of different sediments having different natures depending on their origin and composition could be explored further in terms of the applicability of a GGBS-based formulation developed in the current study to successfully treat different types of dredged materials. The extensive uniaxial compressive strength (UCS) and leaching testing program with practical implications can be adopted for the samples from different dredged locations.
- One question raised by the study of the solidification process of sediments is the addition of dispersants to improve the engineering behaviour of the mixtures. More research is needed using a wider range of dispersing agents as well as sediments from other locations. Evaluation and improvement of the use of dispersants on the industrial scale can be proposed according to market needs.
- Another important question that remains to be answered is the durability of GGBS-treated sediments. The compressive strength results demonstrated a significant increase in the performance of the GGBS-based mixtures over 6 months of storage as well as a good stability of heavy metals after treatment. However, the potential risks of environmental, chemical, or physical attacks (e.g. freeze/thaw) should be examined.

For the stabilization of contaminants, the following items merit further investigation:

- Further experimental study is needed to assess the effect of GGBS-based treatment on the stabilization of organic contaminants which are of a great

concern for many harbours areas (i.e. PCB, PAH, TBT). The existing solutions for the stabilization of organic contaminants (oxidation, various adsorbents) can be potentially combined with GGBS-based formulations.

- A further in-depth study is required to investigate the interaction of additional types of heavy metals with GGBS-based binders to better understand their impact on early hydration and to explain the long term immobilization of HM. As was shown in Chapter V, the XAS experiment can be very useful in observing the formation of new precipitates and the incorporation of HM into hydrates.
- The total attack of OPC and GGBS revealed a considerable amount of heavy metals, especially in the case of Portland cement. Further research needs to be done to establish whether trace metals in binders are responsible for leaching after S/S treatment and to investigate the stability of these HM compounds before and after the hydration process.

Due to the increasing demand for alternative 'low carbon' binders for different construction fields, the following perspectives can be proposed:

- Further research could be conducted to develop an efficient and economically viable "zero Portland cement" binder with low environmental impact for the Solidification/Stabilization treatment of dredged material.
- Different types of supplementary cementing materials could be used today to reduce the carbon footprint. Further, it is possible to thermally activate sediments due to their significant clay content. Once activated, the sediment can replace a certain amount of clinker in certain products to reduce CO_2 emissions.

Annex A

Stabilization of the Dublin sediment contaminated by Tributyltin (TBT). Leaching test results

Organotin compounds have been introduced into the aquatic environment over the past decades from various industries and agriculture. Tributyltin (TBT) has been widely used as an anti-fouling agent on ships, but its use is currently limited in many countries. At the same time, some organotin compounds are still present in waterbodies at concentrations that are very toxic to the aquatic ecosystem.

TBT (tributyltin), MBT (monobutyltin) and DBT (dibutyltin) are initially present in Dublin sediment at 205, 78.9 and 34.3 μ(Sn)/kg, respectively. The presence of DBT is usually linked to the degradation of TBT by microbial activity and/or photochemical reactions in sediments. These values are consistent with the conclusion of some authors who establish that the TBT degradation occurs in stages with the loss of butyl group (Furdek et al. 2016). In this study, the Solidification/Stabilization method using a hydraulic binder for sediments valorization is considered because of technical, environmental and economic benefits. On this way, Granulated ground blast-furnace slag (GGBS) based binders is used as stabilizing agent in immobilizing butyltins compounds (Gutsalenko T. et al., 2018).

The hydraulic binders considered consisted of mixtures of Portland cement (OPC) and slag (GGBS) from ECOCEM. Three different hydraulic binders were mixed with sediments. The mixtures are reported in Table A.1. F1 correspond to the Portland cement (OPC) binder, F2 and F3 are Portland cement-Granulated ground blast furnace slag (GGBS) mixtures at two different GGBS contents. Initially, the binder is mixed with water with at w/b ratio 0.45. Samples F1 and F2 are obtained by mixing 150 kg of total binder with 1 m^3 of sediment, the F3 sample was prepared at 175kg/m^3.

The considered samples in this study are presented in Table A.1.

Table A.1. Sediment-Binder mixtures

Mixture	Binder content (%)	
	Cement	GGBS
F1	100	0
F2	50	50
F3	15	85

Procedure

The monolithic leaching test for tributyltin (TBT) from the Dublin sediment treated with different binding agents was performed according to C1308-08.
This test method provides procedures for measuring the leaching rates of elements from a solidified matrix material and allows for the determination of the leaching trajectories of specific contaminants as a function of the cumulative mass flux over a cumulative period.

Fig. A.1 TBT leaching test

The method applied in this study measures the release of a component from a cylindrical solidified waste specimen into water. Thus, the samples were prepared using special cylindrical molds with dimensions 40x40mm in order to respect a diameter-to-height ratio of 1:1. Leaching containers made of glass were used during this test in order to prevent any possible reactions with the leachant, leachate, or specimen. The top of the container was fit tightly to minimize evaporation (Fig. A.1). The leachant volume used for each interval was 10×the surface area of the specimen, or 600 ml for each sample.
After each time increment (0, 0.25, 1, 2.25, 4, 9, 16, ... days) the leachates were sent for analysis by gas chromatography. The mass and dimensions of the specimens as well as the pH of the leachates were recorded.

Results

The TBT leaching test were conducted on the sediment-binder mixes, the results are presented in Fig. A.2. TBT, MBT and DBT are quite efficiently immobilized with all the binders.

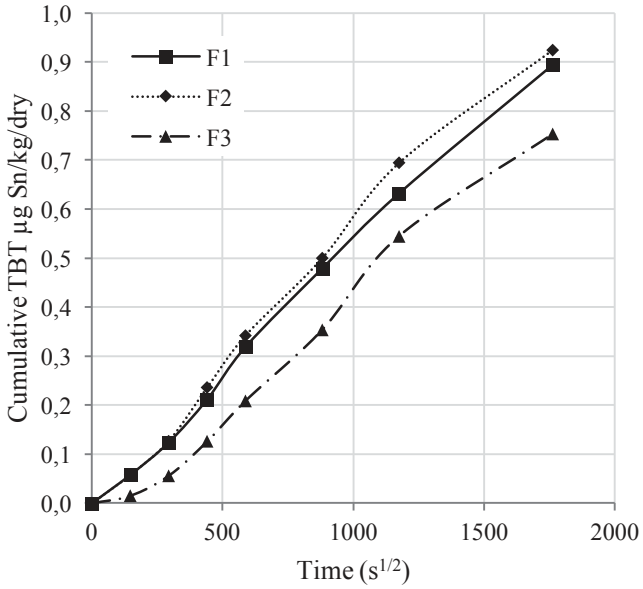
1,0
0,9
0,8
0,7
0,6
0,5
0,4
0,3
0,2
0,1
0,0
Cumulative TBT µg Sn/kg/dry
F1
F2
F3
0
500
1000
1500
2000
Time (s1/2)

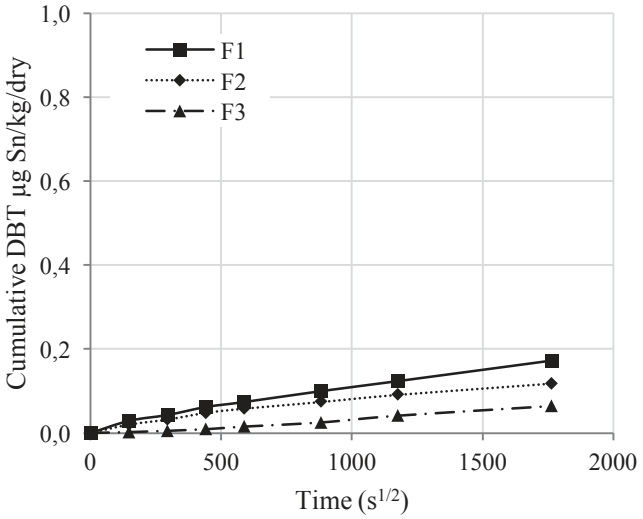
1,0
0,8
0,6
0,4
0,2
0,0
Cumulative DBT µg Sn/kg/dry
F1
F2
F3
0
500
1000
1500
2000
Time (s1/2)

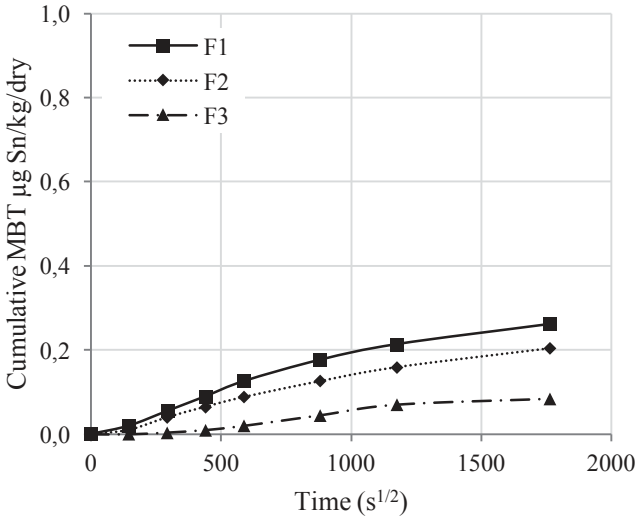
1,0
0,8
0,6
0,4
0,2
0,0
Cumulative MBT µg Sn/kg/dry
F1
F2
F3
0
500
1000
1500
2000
Time (s1/2)

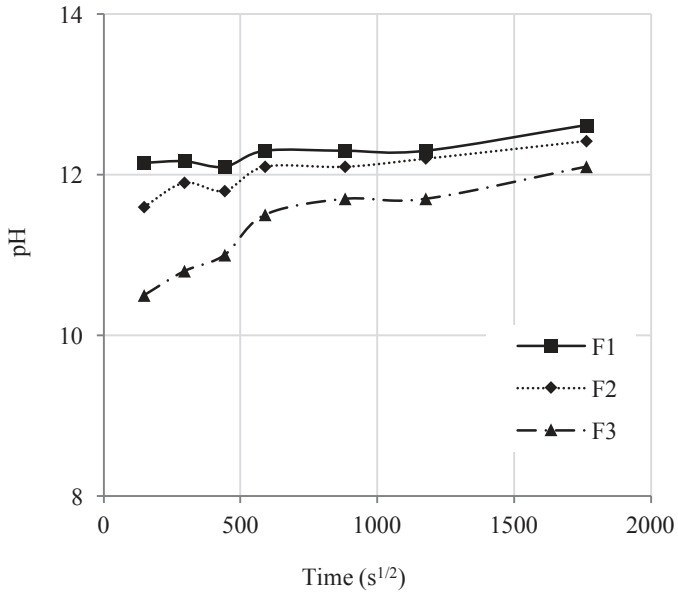

Fig. A.2 Leaching measurements of TBT, MBT and DBT and pH of the considered leachates

The compounds could stay strongly adsorbed to clays minerals, oxides and hydroxides, and organic material. It can be noticed that the destabilizing effect decreases when the level of OPC substitution with GBBS increases. These trends seem to be related to the pH of the samples (Fig. A.2). The highest pH is obtained with the OPC based sample F1 (around 12.5). Overall the pH decreases when increasing the fraction of GGBS. The lowest pH is obtained with F3. The effect of pH on TBT or DBT adsorption was already studied by (E. Burton, 2004 and M. Hoch, 2003) and showed a destabilization at low and high pH. From pH = 6, neutral species are present: TBT(OH), $MBT(OH)_3$ and $DBT(OH)_2$ (Fang et al. 2012). The adsorption of TBT, MBT and DBT on adsorbent surfaces would therefore be predominated by a hydrophobic adsorption mechanism (Hoch, Alonso-Azcarate, and Lischick, 2002). However, the gap between pHs for the different mixes is decreasing over time whereas the concentration gap of pollutant increasing. Therefore, pH does not seem to be the only parameter influencing the leachability of TBT and its derivatives. Further studies are required in order to get a deeper understanding of the mechanisms governing TBT immobilization using S/S method. Summing up, with regard to the leachability of TBT and its derivatives over time, the values are very weak. The values are the lowest using high percentage of GGBS in binder.

Bibliography

C1308-08 - Standard Test Method for Accelerated Leach Test for Diffusive Releases from Solidified Waste and a Computer Program to Model Diffusive, Fractional Leaching from Cylindrical Waste Forms1.

Burton E. D., Phillips I. R., and Hawker D. W., Sorption and Desorption Behavior of Tributyltin with Natural Sediments, Environ Sci Technol 38 (2004), 6694–6700

Gutsalenko T., Bourdot A., Seymour P., Frouin L., Solidification/Stabilization of port sediments contaminated by heavy metals and TBT using slag-based binders, SynerCrete'18 International Conference (2018)

Hoch M., Alonso-Azcarate J., and Lischick M., Assessment of adsorption behavior of dibutyltin (DBT) to clay-rich sediments in comparison to the highly toxic tributyltin (TBT), Environ Pollut 123 (2003), 217–227

Hoch M., Alonso-Azcarate J., Lischick M. (2002), Adsorption behavior of toxic tributyltin to clay-rich sediment under various environmental conditions, Environmental Toxicology and Chemistry, 21: 1390–1397.

Furdek M., Mikac N., Bueno M., Tessier E., Cavalheiro J., Monperrus M. (2016), Organotin persistence in contaminated marine sediments and porewaters: In situ degradation study using species-specific stable isotopic tracers, Journal of Hazardous Materials, 307: 263–273.

Fang L., Borggaard O.K., Christensen J.H., Holm P.E., Hansen H.C.B. (2012), Adsorption of mono- and dibutyltin by a wheat charcoal: PH effects and modeling, Chemosphere, 89: 863–868.

List of Figures

List of Tables

université PARIS-SACLAY

ÉCOLE DOCTORALE
Sciences mécaniques et énergétiques, matériaux et géosciences (SMEMAG)

Titre : Solidification/Stabilisation des sédiments portuaires à l'aide des liants hydrauliques à base de laitier de haut-fourneau

Mots clés : laitier de haut-fourneau, sédiment pollué, métaux lourds, Solidification/Stabilisation

Résumé : L'accumulation des sédiments sur les littoraux se créée à partir des processus physiques, chimiques et biologiques. Les activités anthropiques participent fortement à l'augmentation du taux de sédimentation. Elles sont également une source de contaminants chimiques notamment des métaux lourds qui sont un risque pour l'environnement aquatique et la santé publique. Afin de dégager les voies de navigation, des opérations régulières de dragage dans les grands ports industriels sont réalisées et produisent autour de 100-200 millions m^3/an de déblais de dragage contaminés. Il peut donc être nécessaire de traiter ces sédiments, notamment par Solidification/Stabilisation (S/S).

L'étude actuelle s'intéresse plus particulièrement à la valorisation de sédiments provenant de Dublin (Irlande) pour une réutilisation potentielle comme matériaux de remplissage dans le cadre du projet de réaménagement du bassin d'Alexandra (ABR). Les sédiments contaminés en métaux lourds, doivent être stabilisés par la technologie de S/S au moyen d'un liant hydraulique. Cette recherche propose l'utilisation du laitier de haut-fourneau (LHF) comme agent liant alternatif au ciment Portland largement utilisé. L'objectif de cette étude est donc de développer un liant à base de LHF pour fournir un comportement mécanique requis pour une utilisation ultérieure du nouveau matériau en s'intéressant à comprendre les mécanismes ayant un rôle dans la solidification du sédiment traité mais également la stabilisation des métaux lourds.

Les sédiments traités par liants hydrauliques à base de LHF ont fait l'objet d'un suivi de la résistance à la compression en comparaison à des sédiments traités par liant à base d'OPC. Le traitement au LHF activé par une petite quantité d'OPC a démontré une augmentation significative de la résistance au fil du temps, tandis que celle du traitement à l'OPC a montré une dégradation des propriétés mécaniques. Dans le but d'expliquer les résultats obtenus, des études de suivi de la formation des hydrates, de retrait et de microstructure ont été menées. En outre, les interactions avec les différents liants de la fraction argileuse, de la matière organique et des métaux lourds, qui constituent les sédiments de Dublin étudiés, ont été évaluées séparément et au moyen de milieux simplifiés. La thèse met en évidence par l'étude de l'impact de la fraction argileuse que le phénomène de dispersion/floculation est un des principaux mécanismes responsables de l'évolution des propriétés mécaniques du sédiment traité. L'étude des interactions entre la matière organique avec les liants montre une dégradation de certains composés organiques au cours de temps et ce d'autant plus avec l'OPC. Enfin, certains métaux lourds impactent par un retard ou une accélération significative de l'hydratation des liants considérés.

La mobilité des métaux lourds du sédiment de Dublin après le traitement S/S a été examiné en utilisant un test de lixiviation standardisé. L'augmentation de la proportion de LHF induit une diminution de la quantité de métaux lourds lixiviés. En effet, l'analyse par extraction séquentielle a permis de suivre la distribution des métaux lourds parmi les principales fractions de sédiments avant et après traitement. L'emploi de LHF permet une réduction de la migration des métaux dans la fraction la moins stable après le traitement S/S. Dans le but d'explorer les mécanismes de stabilisation, en particulier les changements dans l'environnement chimique des métaux lourds (état d'oxydation/numéro de coordination etc.), la spectroscopie d'absorption aux rayons X s'est avérée être une technique pertinente. Ainsi, il a été observé que l'environnement chimique du Cu et du Zn n'a pas été modifié dans le cas des liants à forte teneur en LHF.

Title: Solidification/Stabilization of harbor sediments using GGBS-based hydraulic binders

Keywords: GGBS, contaminated sediment, heavy metals, Solidification/Stabilization

Abstract: The accumulation of sediment particles in coastal areas arises from physical, chemical, and biological processes. Anthropogenic activities dramatically increase the sedimentation rate. Sediments may contain chemical contaminants including heavy metals (HM) and are consequently a risk to the aquatic environment and human health. Regular dredging of important shipping lanes in large industrial ports is required and this produces around 100-200 million m^3 of contaminated dredged material per year. Therefore, proper treatment of the contaminated sediments is necessary, with Solidification/Stabilization (S/S) remediation technology at the forefront.

The current study is specifically interested in the treatment of sediment originating in the Dublin Port for its potential reuse as a fill material for the Alexandra Basin Redevelopment (ABR) Project. The sediment is contaminated with heavy metals and must be stabilized by S/S technology using a hydraulic binder. This research proposes the use of ground granulated blast furnace slag (GGBS) as an alternative binding agent to the widely used Portland cement. The objective of this study is therefore to develop an appropriate GGBS-based binder to provide the required engineering properties for further reuse of the newly formed solidified material by focusing on understanding the mechanisms having a role in the solidification of the treated sediment, but also in the stabilization of heavy metals.

The compressive strength of the range of GGBS-based formulations was assessed with the UCS test and compared to the OPC-based treatment. GGBS activated by a small amount of Portland cement demonstrated a considerable increase in strength over time while that of only OPC showed a degradation of mechanical properties. To explain the obtained results, XRD, shrinkage, and microstructure investigations were conducted. In addition, the interaction of the binders with the clay fraction, organic matter, and trace metals, which were found in the studied Dublin sediments, was assessed separately through simplified models. The study of the clay fraction highlights that the phenomenon of dispersion/flocculation is one of the main mechanisms responsible for the evolution of the mechanical properties of the treated sediment. The findings from the organic matter study show a decrease of the content of some organic compounds over time, with the greatest impact observed via treatment with Portland cement. Moreover, certain heavy metals have an impact by delaying or significantly accelerating the hydration of the considered binders.

The mobility of heavy metals in the treated Dublin sediment was examined using a standard leaching test. It was found that with an increase in the proportion of GGBS, the amount of leached HM decreased. Moreover, sequential extraction analysis was shown to be effective in studying the distribution of trace metals among the main sediment fractions before and after treatment. The use of GGBS as a stabilizing agent allows a decrease of the migration of heavy metals into the less stable fraction after S/S treatment. X-ray Adsorption Spectroscopy (XAS) was demonstrated to be a useful technique to explore the stabilization mechanisms, in particular changes in the chemical environment of HM (oxidation state, coordination number, etc.). It was observed that the chemical environment of Cu and Zn was not modified in the case of binders with high GGBS content.